AN INVESTIGATION OF DAYLIGHTING PERFORMANCE IN SIDELIT SPACES

by

Zhe Kong

A Dissertation Submitted in

Partial Fulfillment of the

Requirements for the Degree of

Doctor of Philosophy

in Architecture

at

The University of Wisconsin-Milwaukee

August 2018

ABSTRACT
AN INVESTIGATION OF DAYLIGHTING PERFORMANCE IN SIDELIT SPACES

by

Zhe Kong

The University of Wisconsin-Milwaukee, 2018
Under the Supervision of Professor D. Michael Utzinger

The positive influence of daylight on people's work and well-being has been confirmed in many studies. However, excessive daylight causes discomfort glare, which decreases work productivity, impairs occupants' vision, and may even cause headaches. Substantial studies explored glare by correlating physical lighting measurements and subjective evaluations. With the development of High Dynamic Range (HDR) image techniques, dynamic changes of daylighting distributions can be effectively captured. Consequently, more studies paired HDR image techniques with subject evaluations to explore glare. However, studies merely relying on field measurements are not only time-consuming and labor-intensive but may also disturb occupants. To address these problems, this dissertation proposed the method of integrating three research tools, HDR image techniques, simulations, and questionnaire surveys, to investigate daylight glare. Using sidelit spaces across five buildings as the example, this dissertation aimed to demonstrate the accuracy of simulation results and the correlations between subject occupant evaluations and physical lighting data derived from both field measurements and simulation results.

This dissertation is comprised of three sections. The first section focused on field measurements. Over 200 HDR images across five buildings were taken and analyzed using select visual discomfort metrics. The results showed that daylight glare probability (DGP) outperformed the other visual discomfort metrics in terms of identifying intolerable and imperceptible glare. The second section utilized these HDR images to calibrate four of the five buildings' Radiance models. The relative RMSE of simulated vertical eye illuminance

under both the Perez all-weather sky model and the hybrid photo-radiometer sky model were 23.7% and 21.2%, respectively. The frequencies of accurate glare prediction under both sky models were 93.9% and 95.5%, respectively. The results indicated that Radiance models with precise geometries and material properties can accurately represent the real lighting environments. Finally, the third section paired questionnaire surveys with both the HDR image technique and simulations to investigate daylight qualities within an open-plan office. The study found that taller windows, proximity to windows, and facing towards windows caused severe glare. By removing workstation partitions and arranging seating orientations perpendicular to the windows, the renovated layout design increased occupant satisfaction with their daylighting environments and tolerance for daylight glare. The last section demonstrated the effectiveness of integrating the three tools in lighting studies and the importance of interior layout and furniture designs in terms of daylight glare reduction.

© Copyright by Zhe Kong, 2018
All Rights Reserved

To my Dear Parents and Grandma

TABLE OF CONTENTS

1 INTRODUCTION 1
1.1 BENEFITS OF DAYLIGHT 1
1.2 RESEARCH OBJECTIVES 2
1.3 SCOPE AND LIMITATIONS 3
1.4 DISSERTATION OVERVIEW 4
2 LITERATURE REVIEW 6
2.1 LIGHTING RELATED FACTORS 6
2.1.1 Illuminance-based Visual Discomfort Metrics 6
2.1.2 Luminance-based Visual Discomfort Metrics 7
2.1.3 Combined Visual Discomfort Metrics 13
2.2 NON-LIGHTING INFLUENTIAL FACTORS 14
2.2.1 Contextual Factor – Outside Views 14
2.2.2 Individual Factors 15
2.3 SUBJECTIVE ADAPTATION TO LIGHTING ENVIRONMENTS 16
2.3.1 Adaptation Theory 16
2.3.2 Adaption to Lighting Environments 18
2.4 RESEARCH TOOLS 19
2.4.1 HDR Image Techniques 19
2.4.2 Simulations 20
2.4.3 Interview and Questionnaire Survey 25
2.4.4 Integration of Three Tools 25
2.5 RESEARCH GAPS 26
2.5.1 Comparison of Visual Discomfort Metrics 26
2.5.2 Validation of the HPR Sky Model 26
2.5.3 Utilization of Three Tools 27
3 FIVE BUILDINGS INTRODUCTION 28
3.1 COLUMBIA ST. MARY'S HOSPITAL 30
3.1.1 Building Overview 30
3.1.2 Studied Spaces 31
3.2 CHRISTOPHER CENTER LIBRARY 33
3.2.1 Building Overview 33

3.2.2 Studied Spaces 34
3.3 ALDO LEOPOLD FOUNDATION CENTER 35
3.3.1 Building Overview 35
3.3.2 Studied Spaces 36
3.4 HAMMEL, GREEN & ABRAHAMSON INC. 37
3.4.1 Building Overview 37
3.4.2 Studied Spaces 38
3.5 SCHOOL OF ARCHITECTURE AND URBAN PLANNING 41
3.5.1 Building Overview 41
3.5.2 Studied Spaces 42
3.6 CONCLUSION 43
4 FIELD MEASURMENT OF LIGHTING DISTRIBUTIONS 44
4.1 RESEARCH OBJECTIVES 44
4.2 RESEARCH QUESTION 44
4.3 METHODOLOGY 44
4.3.1 Data Collection 45
4.3.2 Data Post-Processing 47
4.3.3 Data Analysis 49
4.4 RESULTS 50
4.4.1 Lighting Distributions at CSM 50
4.4.2 Lighting Distributions at CCL 52
4.4.3 Lighting Distributions at ALF 54
4.4.4 Lighting Distributions at HGA 58
4.4.5 Lighting Distributions at AUP 60
4.4.6 Five Buildings Summary 63
4.5 DISCUSSION 71
4.5.1 Impacts of Daylighting Buffer Zones 71
4.5.2 Inconsistency of Visual Discomfort Metrics 72
4.6 LIMITATIONS 74
4.7 CONCLUSION 75
5 SIMULATED LUMINANCE MAPS WITH ACCURATE GLARE PREDICTION . 76
5.1 RESEARCH OBJECTIVES 76
5.2 RESEARCH QUESTION 76
5.3 METHODOLOGY 76

5.3.1 Vertical Eye Illuminance Validation 76
5.3.2 Daylight Simulation 77
5.3.3 Data Analysis 80
5.4 RESULT 82
5.4.1 Validation of vertical eye illuminance 82
5.4.2 CSM Simulations under CIE and Perez Skies 82
5.4.3 AUP Simulations under Perez Skies 85
5.5 DISCUSSION 86
5.5.1 Application and Limitations of CIE Skies 87
5.5.2 Accuracy and Limitations of Perez Skies 87
5.5.3 Causes of Simulation Discrepancies 88
5.6 CONCLUSION 89
6 EVALUATION OF SKY MODEL ACCURACY 90
6.1 RESEARCH OBJECTIVES 90
6.2 RESEARCH QUESTION 90
6.3 METHODOLOGY 90
6.3.1 Interior daylight luminance distributions 90
6.3.2 Exterior sky luminance distribution 92
6.3.3 Simulation 96
6.3.4 Data Analysis 97
6.4 RESULTS OF HORIZONTAL HPR SKIES 98
6.4.1 Validation of diffuse sky components 98
6.4.2 Global Horizontal Illuminance 99
6.4.3 Visual Comparison of Skies and Interior Daylight Distributions 102
6.4.4 Comparison of Visual Discomfort Metrics 103
6.5 RESULTS OF VERTICAL HPR SKIES 106
6.6 DISCUSSION 107
6.7 CONCLUSION 109
7 A POE STUDY OF DAYLIGHTING QUALITIES 110
7.1 RESEARCH OBJECTIVES 110
7.2 RESEARCH QUESTIONS 110
7.3 METHODOLOGY 110
7.3.1 Interview 110
7.3.2 Questionnaire 111

7.3.3 Participants 112
7.3.4 Annual Glare Simulations 113
7.3.5 Data Analysis 114
7.4 RESULTS 115
7.4.1 Interviews Summary 115
7.4.2 Descriptive Data 116
7.4.3 Individual Different Attitudes 118
7.4.4 Environmental Variations 121
7.4.5 Annul DGP Simulations 124
7.5 DISCUSSION 127
7.5.1 Individual Variability 127
7.5.2 Daylight Quality in Original Tiers 128
7.5.3 Daylight Quality in Renovated Tier 129
7.5.4 Benefits of Integrating Three Tools 131
7.6 CONCLUSION 132
8 OCCUPANT ADAPTATION TO LIGHTING ENVIRONMENTS 134
8.1 RESEARCH OBJECTIVES 134
8.2 RESEARCH QUESTIONS 134
8.3 METHODOLOGY 134
8.3.1 Subjective Interview and Questionnaire 134
8.3.2 Objective Lighting Distributions 135
8.4 RESULTS & DISCUSSION 135
8.4.1 Descriptive Data 135
8.4.2 Causes of Glare 137
8.4.3 Contextual Factors 138
8.4.4 Effects of Adaptive Behaviors 141
8.5 CONCLUSION 145
9 CONCLUSION 147
9.1 CONCLUSIONS 147
9.2 DISCUSSION 150
9.2.1 Spatial Proportion 150
9.2.2 Interior Design Incorporation 151
9.3 FUTURE WORK 153
9.3.1 Individual Variability in Glare Perception 153

9.3.2 Dynamic Daylight Glare Prediction 153
9.3.3 Subjective Adaption towards Lighting Environments 154
REFERENCES 155
APPENDICES 164
APPENDIX A: HDR images and simulated luminance maps at CSM 164
APPENDIX B: Institutional Review Board Approvals 167
APPENDIX C: HGA Online Questionnaire 168
APPENDIX D: Interview Responses Summary 174
APPENDIX E: Participants' Comments on Control Systems 180
CURRICULUM VITAE 182

LIST OF FIGURES

Figure 2.1: Bird's eye view of CSM 12
Figure 3.1: The locations of the five buildings 28
Figure 3.2: The perspective view of CSM (DRI Design, n.d.) 29
Figure 3.3: Exterior view of CCL (Courtesy of D. Michael Utzinger) 29
Figure 3.4: Exterior view of ALF (Utzinger & Wasley, 2013) 29
Figure 3.5: Exterior view of HGA 29
Figure 3.6: Exterior view of AUP (Courtesy of Jing Hong) 29
Figure 3.7: Bird's eye view of CSM 31
Figure 3.8: CSM's surrounding environments 32
Figure 3.9: First floor layout of CSM (Kong et al., 2015) 32
Figure 3.10: Two heights of the ceilings in the common spaces (Kong et al., 2015) 33
Figure 3.11: The movable partitions introduced two months after CSM's openness to block direct sunlight 33
Figure 3.12: Bird's eye view of CCL 34
Figure 3.13: First floor layout of CCL 35
Figure 3.14: Interior view of the study area 35
Figure 3.15: Bird's eye view of ALF 35
Figure 3.16: Floor layout of ALF 37
Figure 3.17: Deep roof along the southern elevation (Utzinger & Wasley, 2013) 37
Figure 3.18: The top-side windows in the exhibit space (Utzinger & Wasley, 2013) 37
Figure 3.19: The southern corridor adjacent to the public office (Utzinger & Wasley, 2013) 37
Figure 3.20: Bird's eye view of HGA 38
Figure 3.21: Floor layout of HGA 39
Figure 3.22: Three window heights along the southwest façade 39
Figure 3.23: External overhangs 40
Figure 3.24: Occupants put up foam core boards to block sunlight 40
Figure 3.25: The original cubicle design in Tiers One, Three, and Four (left), along with the more open workstation in Tier Two (right) 40
Figure 3.26: Eight seating orientations related to the southwest façade 41
Figure 3.27: Bird's eye view of AUP 42
Figure 3.28: The trees along AUP's eastern elevation 42
Figure 3.29: Biological Department across from 42

Figure 3.30: The select offices on the second, third, and fourth floors at AUP 43
Figure 4.1: LDR images to record different ranges of luminance 45
Figure 4.2: The equipment for taking HDR images 46
Figure 4.3: The camera response curve of Canon 5D Mark II 47
Figure 4.4: The camera response curve of Canon EOS 6D 47
Figure 4.5: The HDR images taken at 5^{o} intervals to generate a vignetting correction function 48
Figure 4.6: The vignetting correction function for SIGMA f/3.5 at f/5.6.....49
Figure 4.7: Nine scenes at CSM where HDR images were taken 50
Figure 4.8: The HDR images, falsecolor images, and DGP analysis of four scenes at CSM .52
Figure 4.9: Four scenes at CCL where HDR images were taken 53
Figure 4.10: The HDR images, falsecolor images, and DGP analysis of four scenes at CCL 54
Figure 4.11: Thirteen scenes at ALF where HDR images were taken.....55
Figure 4.12: The HDR images, falsecolor images, and DGP analysis of select scenes at ALF 57
Figure 4.13: Select workstations at HGA where HDR images were taken 58
Figure 4.14: The HDR images, falsecolor images, and DGP analysis of twelve scenes at HGA 59
Figure 4.15: The select offices at AUP where HDR images were taken.....61
Figure 4.16: The HDR images, falsecolor images, and DGP analysis of five rooms at AUP.62
Figure 4.17: Students' way of occupying workstations on the overcast day (left) and sunny day (right) (Courtesy of D. Michael Utzinger) 69
Figure 4.18: Different DGP results caused by interior venetian blinds from a student's perspective 71
Figure 4.19: Glare indices profiles of 44 scenes.....73
Figure 5.1: Lighting simulation procedure 77
Figure 5.2: The layout and geometric model of the lobby and common spaces at CSM 77
Figure 5.3: The layout and geometric model of Office 326 at AUP.....78
Figure 5.4: The layout and geometric model of Office 422 at AUP.....78
Figure 5.5: The layout and geometric model of Office 479 at AUP.....78
Figure 5.6: The weather station collecting data for CSM simulations (left) (taken by Jing Hong) and the weather station collecting data for AUP simulations (right).....80
Figure 5.7: The scatter plot of vertical eye illuminance from HDR images against the measured vertical eye illuminance.....82

Figure 5.8: Falsecolor images of the HDR images and simulated luminance maps under CIE and Perez skies at CSM....83
Figure 5.9: E_v comparison under the sunny (top) and overcast skies (bottom)....84
Figure 5.10: Falsecolor images of the HDR images and simulated luminance maps under Perez sky models at AUP....85
Figure 5.11: DGP results of the HDR images and simulated luminance maps in Office 326.86
Figure 5.12: DGP results of the HDR images and simulated luminance maps in Office 422.86
Figure 5.13: DGP results of the HDR images and simulated luminance maps in Office 479.86
Figure 6.1: Three offices' locations at AUP....91
Figure 6.2: Three select offices' layouts....91
Figure 6.3: Select workstations at HGA where HDR images were taken....91
Figure 6.4: The scenes at ALF where HDR images were taken....91
Figure 6.5: The camera and photometric sensor assembled with the shading disks....92
Figure 6.6: Data collection equipment....94
Figure 6.7: The procedures of generating the HPR sky model....95
Figure 6.8: A 40^o horizontal band on the HDR images and simulations within Office 326 (two left) and HGA (two right)....97
Figure 6.9: HDR sky images for the validation study....99
Figure 6.10: Diffuse horizontal illuminance of measurements and HDR sky images....99
Figure 6.11: The profiles of GHI_{meas}, GHI_{HPR}, and GHI_{Perez} on May 17^{th} (top) and July 25^{th} (bottom)....100
Figure 6.12: The scatter plot of GHI_{HPR} against GHI_{meas} (left) and the scatter plot of GHI_{Perez} against GHI_{meas} (right)....101
Figure 6.13: E_v profiles of HDR images and simulated luminance maps under HPR and Perez skies....104
Figure 6.14: The scatter plot of COV_{HPR} against COV_{HDR} (left) and the scatter plot of COV_{Perez} against COV_{HDR} (right)....106
Figure 6.15: Falsecolor images of vertical HPR skies, interior HDR images, and simulated luminance maps at ALF....107
Figure 6.16: Various positions of camera settings in simulations in plan (left) and section (right)....108
Figure 7.1: Spatial factors on the office layout....114
Figure 7.2: Participants' ratings of daily visual discomfort....116
Figure 7.3: Participants' ratings of three causes of visual discomfort....117

Figure 7.4: Sky conditions (left) and seasonal effects (right) on visual discomfort occurrence 118
Figure 7.5: Pairwise tests of satisfaction levels with natural light (left), degree of direct sunlight on people's face and/or eyes (middle), and visual discomfort between 2 and 4 p.m. (right) among four tiers 122
Figure 7.6: Pairwise tests of direct sunlight on people's face and/or eyes (left), high contrast (middle), and direct sunlight on monitors (right) among four zones. 123
Figure 7.7: Pairwise tests of degrees of visual discomfort between 2 and 4 p.m. (left) and direct sunlight on peoples' faces and/or eyes (right) among three seating orientation groups. 124
Figure 7.8: The variation in window heights with respect to annual DGP profiles 125
Figure 7.9: The variation in workstation enclosure with respect to annual DGP profiles 125
Figure 7.10: The variation in distance between workstation and the windows with respect to annual DGP profiles 126
Figure 7.11: Effect of seating orientation on the annual DGP profiles at four workstations. 127
Figure 7.12: Mean satisfaction levels of the four tiers 131
Figure 8.1: Problems related to the interior mechoshade system 139
Figure 8.2: Pairwise tests of frequency of rotating monitor(s) between four tiers (left) and pairwise tests of frequency of erecting boards between four zones (right) 141
Figure 8.3: Luminance differences before and after including adaptive behaviors 142
Figure 8.4: DGP differences caused by adaptive behaviors 143
Figure 8.5: DGP profile variations caused by adaptive behaviors 144
Figure 8.6: The percent of E_v variations caused by adaptive behaviors 145
Figure 9.1: The objective and method structure of the dissertation 149
Figure 9.2: Spatial ratio using CSM as an example 150
Figure 9.3: The scatter plot of the ratio against annual glare duration 151

LIST OF TABLES

Table 2.1: Glare Indices summary 8
Table 2.2: Nomenclature of Glare Index equations 9
Table 2.3: Select visual discomfort metrics throughout this dissertation 14
Table 3.1: The summary of the five buildings 29
Table 4.1: Data collection schedule across the five buildings 46
Table 4.2: Summary of the analyzed HDR images 63
Table 4.3: Summary of glare analysis across the five buildings 68
Table 5.1: Select Radiance material definitions at CSM and AUP 79
Table 5.2: DGP results of the HDR images and simulations 84
Table 5.3: T-test results between the DGP of the HDR images and simulations 84
Table 5.4: Relative MBE and RMSE of Ev within three offices at AUP 87
Table 6.1: Data collection calendar across the three buildings 93
Table 6.2: Select Radiance material definitions at AUP, HGA, and ALF 96
Table 6.3: MBE_{rel} and $RMSE_{rel}$ under HPR and Perez skies 101
Table 6.4: Falsecolor images of horizontal HPR skies, interior HDR images, and simulated luminance maps across three buildings 102
Table 6.5: Statistical comparison between HPR and Perez skies 105
Table 6.6: T-test results between HPR and Perez skies 105
Table 7.1: Count of the occupants and interviewees in the office 111
Table 7.2: Interview questions 111
Table 7.3: Numeric values for 7-scale Likert questions 112
Table 7.4: Participant information 113
Table 7.5: Independent and dependent variables 114
Table 7.6: Grouped data based on the environmental factors 115
Table 7.7: Correlations between lighting environmental items 119
Table 7.8: Correlations between participants attitudes towards lighting environmental factors 119
Table 7.9: The Mann-Whitney U test of satisfaction with natural light due to individual variability 120
Table 7.10: The Mann-Whitney U test of gender differences 121
Table 7.11: Kruskal-Wallis results among tier groups 121
Table 7.12: Kruskal-Wallis results for zone group 123

Table 7.13: Kruskal-Wallis results for seating orientation group 123
Table 7.14: Annual glare duration based on three degrees at 14 workstations 126
Table 8.1: Percent of windows covered by mechoshades on the winter solstice 135
Table 8.2: Frequency of adaptive behaviors due to visual discomfort 136
Table 8.3: Correlations between the causes of visual discomfort and adaptive behaviors 137
Table 8.4: Kruskal-Wallis results among tier and zone groups 140
Table 8.5: E_v variations before and after including adaptive behaviors 142

LIST OF ABBREVIATIONS

CIE	International Commission on Illumination
COV	Coefficient of Variation
DGI	Daylight Glare Index
DGP	Daylight Glare Probability
DNI	Direct Normal Illuminance
DHI	Diffuse Horizontal Illuminance
E_v	Vertical Eye Illuminance
GHI	Global Horizontal Illuminance
HDR image	High Dynamic Range image
IBL	Image-based Lighting
LDR image	Low Dynamic Range image
LEED	Leadership in Energy and Environmental Design
IESNA	Illuminating Engineering Society of North America
POE	Post-Occupancy Evaluation
S.D.	Standard Deviation
RBE	Relative Bias Errors
RMSE	Root Mean Squared Errors
WFR	Window to Floor Ratio
WWR	Window to Wall Ratio

ACKNOWLEDGMENTS

First, I would like to express my sincere gratitude to my Committee Chair, Professor Michael Utzinger, for his patience, support, and thoughtful suggestions throughout my entire PhD program. He helps me decide daylighting designs as my research direction and opens the sustainable world before me. More importantly, he sets me a good example of being a knowledgeable and caring teacher with integrity. Second, I would like to thank Dr. Gerald D. Weisman, who introduced me the architecture research world when we met in Harbin, 2010. Dr. Weisman's support is my primary reason for pursuing a PhD degree after finishing my master's degree. I would like to acknowledge the important contributions of the rest of my Committee members. Dr. Brian Schermer has provided wisdom and guidance in the areas of subjective human research. Professor Filip Tejchman has provided steadfast guidance throughout my studies. Dr. J. Alstan Jakubiec has been generously helping me out extending back to 2011. I thank him for patiently contributing his knowledge about daylighting design and research as well as offering me a research position in Singapore.

I extend a special thank you to Dr. Mehlika Inanici from the University of Washington for personally teaching me HDR image techniques and daylight simulations. I also received invaluable suggestions and help from Chris Humann concerning the HPR sky model. I am indebted to Greg Ward and other experts from Radiance Mailing list, who answered my questions patiently and quickly.

Additionally, I also received great help from my colleagues, Layla Qarout who proof-reading my writings and always encourages me, Leyla Sanati who teaches me daylighting courses, Jing Hong who continuously provides me with weather data, along with Nasim Shareghiboroujeni and Yu (Naomi) Clark who help me take HDR images of skies.

I would like to express my gratitude to Hammel Green and Abrahamson (HGA) Milwaukee Office for offering me the research fellowship. I am very grateful to my team

members at HGA, Troy Steege, Kara Freihoefer, and Catherine Hall, for their assistant and suggestions about all the studies conducted in the HGA Milwaukee Office.

Finally, I would like to acknowledge support from my friends and family: Pastor Steven Jihn and Haichi Jihn for mentoring my belief; John Wang and Cynthia Wang for offering me a job during my difficult times; Sunny Wong and Kitty Li for taking care of my health; Brother Shau Nong Jea, Sisters Yen Ling Jea and Kuei Shen for their consistent prayer and love; and the brothers and sisters from the students' fellowship for their encouragement and consideration. I want to thank my beloved parents, Lingqiang Kong and Weijie Bi, for their enduring love, support, understanding, and sacrifice throughout my life. To my grandma Huanyun Liu, thank you for your continued love.

1 INTRODUCTION

1.1 BENEFITS OF DAYLIGHT

Taking advantage of daylight in building designs can both fulfil human needs and conserve building energy consumption. Substantial studies demonstrated that daylight has positive influence on people's task performance, comfort, and well-being (Veitch, 2001). As previous studies showed, people prefer natural lighting conditions to artificial ones while working (Bhusal et al., 2014). The existence of daylight can improve productivity and occupant satisfaction in their working environments (Boyce, Hunter, & Howlett, 2003; Elzeyadi, 2011). Natural light also satisfies people's biological needs and enhances people's circadian rhythms (Boyce et al., 2003). Boubekri et al. found that the participants who had more daylight exposure in their offices had better sleep quality, activity patterns, and quality of life (Boubekri, Cheung, Reid, Wang, & Zee, 2014). Hence, daylighting is a crucial component in Indoor Environmental Quality (IEQ) (Veitch, 2007; Kim & Dear, 2012). Additionally, daylight plays a key role in interior lighting environments due to its energy-conservative characteristic. In office buildings, for instance, artificial lights are one of the most energy-intensive end uses, accounting for 14% of the site energy (U.S. Department of Energy, 2012). Artificial lights contribute to significant amount of carbon emissions, which lead to global warming. Previous studies showed that the collaboration between electric lighting control and daylighting design could potentially save energy between 7% and 60% (M. C. Dubois & Blomsterberg, 2011; Galasiu, Newsham, Suvagau, & Sander, 2007). Therefore, harvesting natural light in indoor environments can both provide occupants with healthy environments and reduce energy consumption.

However, glare caused by daylight can easily jeopardize all these benefits of daylight. Lindsay and Littlefair found that glare was the primary motivation that cause occupants to occlude windows with blinds (Lindsay & Littlefair, 1992). Likewise, Inkarojrit found that

20% to 35% of respondents considered glare as a negative factor related to windows (Inkarojrit, 2005). Besides disconnections from outdoor views, blind occlusions also motivate occupants to turn on artificial light with the potential of increasing heating energy (M. C. Dubois & Blomsterberg, 2011; Newsham, 1994). Given the benefits of daylight in buildings and negative consequences caused by excessive daylight, this research examines daylight glare by integrating field measurements, simulations, and POE studies.

1.2 RESEARCH OBJECTIVES

The primary objective is to explore and integrate three tools that are mainly employed in lighting studies: HDR image techniques, lighting simulations, and questionnaire surveys. Each tool collects and presents lighting data from different perspectives. HDR image techniques are mainly utilized for field measurements in existing spaces; lighting simulations are commonly used to predict lighting performance of design projects; questionnaire surveys reflect occupant evaluations and subjective opinions of their lighting experience. The integration of these three tools guarantees the internal consistency of the study and enriches explanations for the conclusions.

Three sub-aims are derived from the primary objective below:

1. Compare select visual discomfort metrics in terms of identifying daylight glare across different building settings;
2. Calibrate daylight simulation results by field measurements and investigate the accuracy of the HPR sky model in terms of simulating luminance maps;
3. Integrate physical daylighting environments with occupant subjective evaluations in terms of analyzing daylighting qualities.

In order to propose the visual discomfort metric that can accurately identify daylight glare in sidelit spaces, over 200 HDR images taken in 14 sidelit spaces are analyzed by select

glare indices. Analyzing HDR images taken onsite excludes the inaccurate visual discomfort metrics and lays a foundation for the remaining studies.

Derived from the primary objective, the second sub-aim is to investigate the accuracy of the horizontal HPR sky model in terms of simulating luminance maps. As the primary lighting sources in daylight simulations, sky models play an important role in determining the accuracy of simulation results. This HPR sky model that combines physically-based solar component and HDR sky images can include subtle luminance variations and cloud distributions as well as resolve luminance overflow caused by the solar corona. The HPR sky model is tested in multiple building settings and spatial configurations to enrich its application.

The final sub-aim is to reveal indoor environmental factors and their impacts on occupants' lighting experiences through both subjective occupant assessments and objective lighting environments. One office where occupants complained about glare includes three window heights and two interior layouts. These environmental variables lead different lighting qualities to occupants. By integrating questionnaires with field measurements and climate-based simulations, this sub-aim is to identify the environmental factors that significantly influence occupants' lighting experiences and evaluate the effectiveness of the renovated design layout in terms of glare reduction.

1.3 SCOPE AND LIMITATIONS

This dissertation has the following limitations. The data collection was limited by both the weather type and seasons. Since the five studied buildings are in either Wisconsin or Indiana, this dissertation only reflects the lighting conditions under a humid continental weather. The data collection was carried out in spring, summer, and autumn. Second, the occupants within one open-plan office were carried out interview and questionnaire. These participants working at an architecture firm possessed professional knowledge and

understandings in regard to lighting designs. These participants were able to quickly comprehend questions and provide accurate feedback from their lighting experience. Therefore, further research is required to include more participants with diverse demographic information.

1.4 DISSERTATION OVERVIEW

Chapter 2 reviews the previous studies concerning visual discomfort metrics and introduces the three tools mainly used in the dissertation. First, the current consent and dissent on visual discomfort metrics are discussed. Second, this chapter reviews the environmental and individual factors that influence occupant visual discomfort evaluations with daylighting environments. Third, the studies concerning people's adaptation towards environmental discomfort are discussed. Finally, the three tools utilized in this dissertation are introduced.

Chapter 3 introduces the five buildings where all the studies in this dissertation were carried out. The spatial characteristic and daylighting design strategies utilized in the five buildings are discussed.

Chapter 4 focuses on field measurements of lighting distributions. Chapter 4 presents the HDR images taken across the five buildings. Select visual discomfort metrics are applied to the HDR images. Different daylighting design strategies and their impact on interior daylighting performance are discussed.

Chapter 5 and Chapter 6 concentrate on daylight simulations. Chapter 5 uses two buildings as an example to compare CIE sunny and overcast skies with the Perez all-weather sky model in terms of simulating luminance maps. Chapter 6 continues daylight simulations by investigating the accuracy of the HPR sky model in terms of simulating luminance maps. Six rooms across three buildings are used to enrich the application of the HPR sky model. The Perez all-weather sky model is employed as a reference. Select visual discomfort metrics

are applied to both HDR images taken on site and the simulated luminance maps. Then, the comparison of the results is made.

Chapters 7 and 8 include subjective occupant evaluations by employing interviews and questionnaires. Chapter 7 explores occupants' lighting experiences in the open-plan office. Both environmental factors and individual factors that contribute to occupants' visual discomfort and satisfaction with lighting environments are examined. Annual DGP profiles are simulated at select workstations to confirm occupant assessments. The effectiveness of redesigning interior layout in terms of glare reduction is discussed. Chapter 8 investigates individual adaptative behaviors towards lighting environments from both objective lighting data and subjective responses. Occupants' adaptive behaviors are categorized based on frequencies and kinds. Glare reduction caused by representative adaptive behaviors is simulated.

Finally, Chapter 9 provides the conclusions of this dissertation and outlines the potential research topics in the future.

2 LITERATURE REVIEW

First, this chapter introduces research concerning visual discomfort metrics and selects the visual discomfort metrics applied in this dissertation. Second, this section elaborates the contextual factors and individual factors that influence people's glare sensation. Third, the literature reviews focus on people's adaptation towards environmental discomfort, especially on lighting qualities. Then, this section presents the three tools utilized throughout the entire dissertation, HDR image techniques, lighting simulations, along with interviews and questionnaires. Finally, this chapter summarizes the research gaps.

2.1 LIGHTING RELATED FACTORS

2.1.1 Illuminance-based Visual Discomfort Metrics

Illuminance measures the total amount of luminous flux incident on a unit surface in the SI units of lux. Illuminance has been the major photometric measure in lighting design industries due to its ease of measurement and calculation. Architects and lighting designers are required to achieve certain range of illuminance values on horizontal working planes (British Standards Institution, 2002; Dilaura, Houser, Mistrick, & Steffy, 2011; Society of Light and Lighting, 2009). However, recent studies demonstrated the inability of horizontal-illuminance metrics in terms of visual discomfort prediction (K. S. Konis, 2012; K. G. Van Den Wymelenberg, 2014).

The switch of working tasks from the paper-based to the computer-based leads to different lighting environments accordingly. Due to the wide use of computers in office work, people's dominant working planes have been switched from the horizontal to the vertical. In that case, the original horizontal-illuminance based metrics cannot reflect a majority of people's lighting environments during their work. Additionally, unlike paper-based work, monitors are self-luminous objects. In other words, different lighting characteristics of

computer-based work requires different lighting design criteria to achieve comfortable lighting environments (Boyce, 2014).

Noticing the changes of working planes, researchers paid more attention to lighting studies related to computer-based work. Substantial research demonstrates a wide range of illuminance levels due to individual preference. Escuyer and Fontoynont concluded that people preferred light levels between 100 and 300 lux for computer work, and the average between 150 and 400 lux of electric light was added to daylight levels (Escuyer & Fontoynont, 2001). In Begemann et al.'s research, the illuminance levels added by electric light was much greater, between 300 and 1,200 lux (Begemann, Beld, & Tenner, 1997). Halonen and Lethovaara's study also presented the greatly varying individual preference of illuminance levels between 230 and 1,000 lux (Halonen & Lehtovaara, 1995).

Furthermore, vertical eye illuminance (E_v) has been commonly employed for visual discomfort prediction. E_v describes the amount of light falling on people's eyes. It is an important factor in Daylight Glare Probability (DGP) (Wienold & Christoffersen, 2006) formula. Painter et al. (Painter, Fan, & Mardaljevic, 2009) proposed E_v as one visual discomfort metric to predict visual discomfort from a 12-month longitudinal study. Van Den Wymelenberg also concluded the correlation between E_v and subjective responses to visual discomfort (K. Van Den Wymelenberg, 2012). Later, Jakubiec et al. proposed an integrated framework for visual discomfort prediction, which includes E_v as one of the five metrics (J. Alstan Jakubiec, Reinhart, & Van Den Wymelenberg, 2015). Compared with horizontal illuminance levels, E_v provides more accurate subjective visual discomfort prediction due to its measurement at the eye level rather than on a separate horizontal workplane.

2.1.2 Luminance-based Visual Discomfort Metrics

Luminance describes the amount of light that reflects from a surface and reaches an observer's eyes. Luminance values can directly demonstrate people's perception of lighting.

Studies showed that luminance-based visual discomfort metrics predict more accurate visual discomfort than illuminance-based ones (K. S. Konis, 2012; K. G. Van Den Wymelenberg, 2014). As this dissertation concentrates on discomfort glare caused by daylight, the section below introduces the commonly used glare indices and the methods of defining glare sources.

2.1.2.1 Glare Index

Discomfort glare describes a subjective human phenomenon in which either high luminance values or great ratios between a task and the glare source exist. Equation 2.1 (CIE, 1983) describes the factors that are related to the degree of discomfort glare, which are the ratio of size, locations, and luminance of glare sources in a field of vision compared to the background luminance (J. Jakubiec & Reinhart, 2012) .

$$\text{Glare} = \sum_{i=1}^{n} \frac{L_{s,i}^{exp}\,\omega_{s,i}}{L_b^{exp}\,P_i^{exp}} \qquad Equation\ 2.1$$

L_{si}^{exp} : Luminance of glare source (cd/m^2)
ω_{si}: Angular substances of glare source at eye (sr)
L_b^{exp}: Luminance of background (cd/m^2)
P_i^{exp}: Guth position index

In order to quantify glare likelihood from an occupant's perspective, various glare indices were derived from human experiments or previous studies. The five glare indices, Cornell Formula or Daylight Glare Index (DGI), Visual Comfort Probability (VCP), Unified Glare Rating Glare Index (UGR), Daylight Glare Probability (DGP), and Unified Glare Probability (UGP), along with their categorical rating scheme, are listed in Table 2.1.

Table 2.1: Glare Indices summary

Glare index	DGI	VCP	UGR	DGP	UGP
Imperceptible	<18	80-100	<13	<0.35	Comfort <0.5
Perceptible	18-24	60-80	13-22	0.35-0.4	Discomfort ⩾0.5
Disturbing	24-31	40-60	22-28	0.4-0.45	
Intolerable	>31	<40	>28	>0.45	

The equations to calculate DGI, DGP, UGR, and UGP are given in Equation 2.2 to Equation 2.5, respectively. The nomenclatures in the four equations are listed in Table 2.3.

$$DGI = 10 \times log_{10} 0.48 \sum_{i=1}^{n} \frac{L_{s,i}^{1.6} \omega_{pos\ s,i}^{0.8}}{L_b + (0.07 \omega_{s,i}^{0.5} L_{s,i})} \qquad Equation\ 2.2$$

$$\text{DGP} = 5.87 \times 10^{-5} E_v + 9.18 \times 10^{-5} \log_{10} 2 \left(\sum_{i=1}^{n} \frac{L_{s,i}^2 \omega_{s,i}}{E_v^{1.87} P_i^2} \right) \qquad Equation\ 2.3$$

$$UGR = 8 \times log_{10} \frac{0.25}{L_b} \sum_{i=1}^{n} \frac{L_{s,i}^2 \omega_{s,i}}{P_i^2} \qquad Equation\ 2.4$$

$$UPG = \frac{1}{(1 + \frac{2}{7}\left(10^{-\frac{1}{40}(UGR+5)}\right))^{10}} \qquad Equation\ 2.5$$

Table 2.2: Nomenclature of Glare Index equations

L_s	Luminance of glare source (cd/m2)	L_b	the average of the background luminance by excluding glare sources (cd/m2)
ω_{si}	Angular substances of glare source at eye (sr)	ω_{pos}	the solid angle of the glare source modified for its position in the field of view (sr)
E_v	Total vertical eye illuminance (lux)	P_i	Guth position index

Hopkinson generated DGI based on his earlier work and validated the glare index later in human validation studies (Hopkinson, 1972). DGI cannot be applied to the conditions where direct sunlight or interior specular reflections exists (J. Jakubiec & Reinhart, 2012). UGR was derived from the CIE Glare Index (CGI) (Einhorn, 1979) to exclude the calculation of direct sources of light for easier calculation. VCP was defined by Guth and Sylvester and utilized by IESNA (S. K. Guth, 1963; S. Guth & K., 1966). Since VCP was generated under limited condition where ceiling-mounted electric lights were used, it is not valid under daylighting environments in terms of revealing discomfort glare. Later, the development of HDR image techniques led to the generation of several glare indices. DGP (Wienold & Christoffersen, 2006) was generated from human experiments under sidelit daylighting environments. E_v in Equation 2.3 can identify glare sources when a scene is completely overlit (J. Jakubiec & Reinhart, 2012). UGP was developed based on UGR in five buildings in Australia (Hirning, Isoardi, & Cowling, 2014) and validated in six buildings in Malaysia

(Hirning, Isoardi, & Garcia-Hansen, 2017). Hirning et al. correlated occupants' comfortable and uncomfortable responses with the glare index values calculated from HDR images. Hirning et al. also integrated POE surveys with HDR image technique to conduct the research. Unlike previous glare indices, UGP groups discomfort glare into two categories: comfort and discomfort ratings.

Since these glare indices are limited by the experimental conditions, like lighting sources and available equipment for data collection, substantial studies demonstrated the significant inconsistency and inaccuracy issues of glare index results under diverse lighting environments. Jakubiec and Reinhart compared five glare indices (DGI, VCP, CGI, UGR, and DGP) in simulations and concluded that DGP yields the most plausible results under daylighting environments. DGI and UGR are valid only under the conditions without direct sunlight, while VCP produces the most deviated results from the remaining four glare indices (Jakubiec and Reinhart 2011). Suk et al. correlated the results of the same glare indices (DGI, VCP, CGI, UGR, and DGP) with subjective responses and concluded that DGP functions best at absence of glare and existence of intolerable glare (Suk, Schiler, & Kensek, 2017). Since these validation studies had similar interior spaces with sidelighting windows as the laboratories where DGP was generated, it is reasonable to reach the conclusion that DGP outperformed the other glare indices. However, Van Den Wymelenberg concluded that DGP is less able to predict subjective visual discomfort based on his laboratory experiment (K. Van Den Wymelenberg, 2012). Hirning et al. also concluded that both DGP and DGI are unable to predict discomfort glare reported by participants due to overall low E_v (Hirning et al., 2014). One agreement that previous research reaches is that single glare index predicts glare issues in low accuracy.

2.1.2.2 Methods of Glare Source Detection

There are two methods of defining glare sources in calculating glare index, absolute luminance thresholds and relative luminance thresholds (K. Van Den Wymelenberg, 2012). Similar to illuminance-based metrics, researchers have not research a consensus on either absolute luminance thresholds or relative luminance ratios to define glare sources.

Absolute luminance thresholds present the extreme luminance values in a visual field. Previous studies demonstrated a wide range of absolute luminance thresholds to define glare sources. Swedish National Board for Industrial and Technical Development (NUTEK) proposed 500, 1,000, and 2,000 cd/m^2 as the absolute luminance thresholds to control lighting comfort within a space. Dubois suggested that these luminance values should be multiplied by two if the glare source is natural light (Dubois 2001). Wienold proposed four luminance ranges to predict glare degrees: 2,000 cd/m^2 for perceptible glare, 4,000 cd/m^2 for acceptable glare, 6,000 cd/m^2 for uncomfortable glare, and 8,000 cd/m^2 for intolerable glare (Wienold & Christoffersen, 2005). Based on an experiment included 18 participants, Van Den Wymelenberg suggested that 2,000 cd/m^2 as the single best predictor of people's satisfaction in DGP analysis (K. Van Den Wymelenberg, Inanici, & Johnson, 2010). Suk and Schiler proposed 5,500 cd/m^2 as the absolute glare boundary, and the luminance values between 3,000 and 5,500 cd/m^2 as the relative glare zone (Suk, Schiler and Kensek 2013).

Relative luminance ratios are defined by N times of the average luminance of an entire scene or a given zone, like a task area or a horizontal 40^o band. In evalglare (Wienold, 2015), a software for glare analysis, five is the default number to multiply scene-based mean luminance value or task-area-based mean luminance value for glare source detention. Van Den Wymelenberg concluded that the mean luminance of the glare source, which is defined by 7 times of the mean luminance of a task area, is the most effective metric (K. Van Den Wymelenberg et al., 2010). Figure 2.1 uses two scenes to demonstrate the inconsistent results

defined by different glare indices. The first row shows one scene with intolerable glare, which was consistently defined by DGP, DGI, and UGP. The second row, however, shows conflict results defined by the three glare indices. DGP defined this scene with imperceptible glare, DGI detected this scene with perceptible glare, while UGP defined this scene with uncomfortable glare. Due to the great E_v (2,612 lux) and the existence of direct sunlight in the scene, DGP failed to provide accurate results.

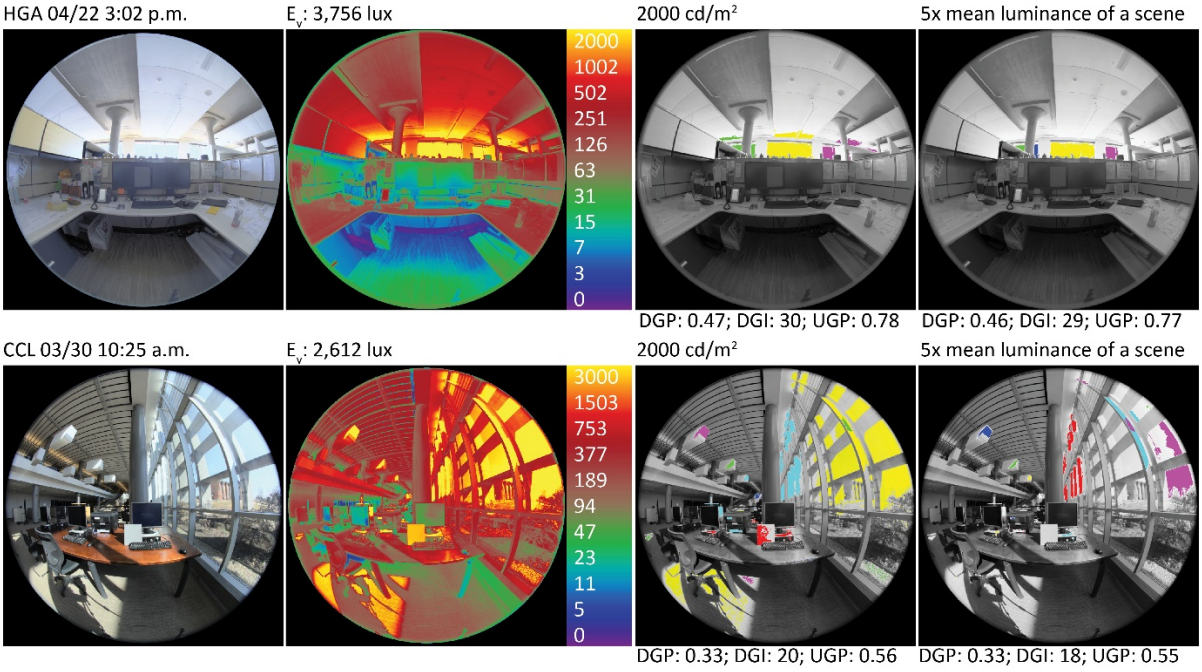

Figure 2.1: Bird's eye view of CSM

2.1.2.3 Other Candidate Metrics

In addition to glare indices introduced above, other visual discomfort metrics include representative statistics of specific areas. For instance, Van Den Wymelenberg reported that the top three visual discomfort metrics that produce the highest squared correlation coefficient with subjective responses are the standard deviation (S.D.) of window luminance, as well as the 25th and 50th percentile luminance values of the lower window area (K. Van Den Wymelenberg, 2012). Additionally, the effectiveness of the mean luminance of a horizontal 40^{o} band in terms of visual discomfort prediction has been independently validated by different studies (K. Konis, 2013; Mahić, Galicinao, & Van Den Wymelenberg, 2017; K.

Van Den Wymelenberg, 2012), which confirms previous studies' findings (Carter, 1994; Loe, Mansfiedl, & Rowlands, 1994). Consequently, Wienold included the calculation of average luminance of a 40^o horizontal band in Evalglare 2.0 (Wienold & Andersen, n.d.). Furthermore, the coefficient of variation (COV) of luminance in a 40^o horizontal band was proposed from a field study for its strong squared correlation coefficients with subjective responses and stability across multiple positions within a scene (Mahić et al., 2017)

2.1.3 Combined Visual Discomfort Metrics

Research showed that multiple factors influence people's perception of discomfort glare, and the factors vary from lighting sources to lighting intensities, from seasonal effects to time of day, from participants' gender and age to their physical states (Pierson, Wienold, & Bodart, 2017). These various unstable factors explain the reasons for consistently low coefficient of determinations (R^2) for single visual discomfort metrics to predict subjective assessments of visual discomfort (Jakubiec et al., 2015; Van Den Wymelenberg, 2012). Furthermore, more and more researchers found that using several metrics outperforms a single one in terms of predicting visual discomfort. For point-in-time analysis, Van Den Wymelenberg found that using several metrics in a multiple regression model predicted subjective visual discomfort better than a single metric alone (K. Van Den Wymelenberg, 2012). For a long-term analysis, Jakubiec and Reinhart noted that they could better resolve reported visual discomfort by using multiple visual discomfort metrics compared to using a single metric (Jakubiec & Reinhart, 2013). Later, Jakubiec et al. recommended a combination of five metrics to correctly identify 65.2% of subjective evaluations (Jakubiec et al., 2015). As previous studies demonstrated the greater accuracy of visual discomfort prediction achieved by employing several visual discomfort metrics, this dissertation selects the metrics listed in Table 2.2. All the select visual discomfort metrics have been validated in human validation studies. The reasons for selecting each metric are listed in the right column.

Table 2.3: Select visual discomfort metrics throughout this dissertation

Visual discomfort metrics	Note
Mean luminance of a 40^o horizontal band >700 cd/m^2	A 40^o horizontal band has been proposed and validated by multiple independent studies. Since this dissertation analyzes the HDR images and simulated luminance maps across five buildings with various spatial configurations and façade designs, the luminance-based metrics based on a 40^o horizontal band are selected for its view-independent characteristic.
COV of a 40^o horizontal band	
E_v >1500 lux	E_v can reveal people's visual perception since it describes the amount of light falling on people's eyes. It has been validated and commonly used by many studies as an effective metric.
DGI, DGP, and UGP	DGP and DGI are generated to identify glare caused by daylight. They have been employed and tested in many field studies. UGP is derived from field studies that integrated subjective evaluations with HDR images in daylit open-plan offices. However, UGP has not be employed by other researchers except Hirning et al.

2.2 NON-LIGHTING INFLUENTIAL FACTORS

Besides the lighting factors discussed in the previous section that influence humans glare sensation, like luminance intensities of glare sources and background reflected in glare index equations, this section concentrates on contextual factors and individual factors that have impacts on humans' degrees of glare sensation.

2.2.1 Contextual Factor – Outside Views

Studies showed that the quality of outside views play a significant role in people's sensation of daylighting glare. Tuaycharoen and Tregenza used eight images to test the relationship between participants' glare ranking and image interest. The results showed that interests in images can increase participants' tolerance for glare (Tuaycharoen & Tregenza, 2005). Later, they used real settings to further explore outside view effects. The second study demonstrated consistent conclusions and resulted in a new glare index, which subtracts the score of view interest from DGI (Tuaycharoen & Tregenza, 2007). Shin et al. used simulated views to explore the same inquiry and concluded that types of views, distances of views, and variation of luminance values of a window influence participants' glare sensation (Shin, Yun, & Kim, 2012). Their conclusions concerning view types and distance confirmed Aries et al.'s research (Aries, Veitch, & Newsham, 2010). Although there is no consent on what types of

views increase or decrease occupants' tolerance for glare, previous studies all agreed that human's glare sensation is affected by the aesthetic view factor (Jay, 1954).

2.2.2 Individual Factors

Individuals have a wide range of visual perception and preferred levels of lighting quantities. Experiments and field studies that quantified appropriate illuminance or luminance values from people's perspectives noted occupant variability (Galasiu & Veitch, 2006; J. Alstan Jakubiec & Reinhart, 2013; K. Van Den Wymelenberg, 2012). The diverse occupant variabilities also add difficulties for researchers to standardize preferred lighting levels and thresholds of glare in research. Demographic variables, like gender, age, and culture, influence people's glare sensation. Kosnik et al. demonstrated the negative effect of increasing age on visual capabilities and visual task performance (Kosnik, Winslow, Kline, Rasinski, & Sekuler, 1998). Compared with younger people, older people are more sensitive to daylight glare (Wienold, 2013). Researchers also proposed cultural background as one factor that influences people's visual discomfort. Compared to the results of a similar study in America, Subova noticed that Slovak's subjects had greater sensitivity of glare sensation (Subova, Kittler, & MacGowan, 1991). Iwata et al discovered that Japanese subjects had greater tolerance for glare than American subjects (Subova et al., 1991). Huang and Wang (Huang & Wang, 2016) developed the DGI_{China} with greater thresholds based on Chinese participants, which reinforced that Chinese people might have greater tolerance for glare than the participants in Hopkinson's study. As researchers start noticing the importance of including individual differences in visual discomfort studies, a recent research revealed that caffeine ingestion might increase participants' tolerance for glare (Kent, Altomonte, Tregenza, & Wilson, 2016).

2.3 SUBJECTIVE ADAPTATION TO LIGHTING ENVIRONMENTS

As occupants constantly interact with and adapt themselves to their immediate environments (Yang, Yan, & Lam, 2014), this section concentrates on occupants' adaptations towards lighting environments. This section starts with the concept of adaptation and related studies concerning thermal comfort and shifts to the research that explored subjective adaptations to lighting environments.

2.3.1 Adaptation Theory

Helson (1964) defined the theory of adaptation-level (AL) as "a quantitative shift in the distribution of judgmental or affective responses along a stimulus continuum, as a function of continued exposure to a stimulus" (as summarized in Wohlwill, 1974). Helson proposed an equation to quantify different stimuli effects upon AL. Although further studies are required to test Helson's quantitative theory, AL laid a foundation for further studies related to temporal and spatial interaction between all relevant stimuli (Parducci, 1965). Using Helson's AL theory, Wohlwill focused on differentiating people's adaptations from adjustments and emphasized the importance of environmental effects on people's long-range behavior changes (Sonnenfeld, 1967; Wohlwill, 1974).

Moreover, researcher are interested in people's instantons and long-term reactions towards environmental stimulations to predict building energy consumption (Brien & Gunay, 2014; Hoes, Hensen, Loomans, Vries, & Bourgeois, 2009). Nicol and Humphreys discussed subjects' adaptive behaviors to climatic conditions from field studies (Nicol & Humphreys, 1973), where the adaptation principle was expressed as: "if a change occurs such as to produce discomfort, people react in ways which tend to restore their comfort". This topic quickly spread to other environmental stimulations like lighting and acoustical aspects. Heerwagen and Diamond categorized occupants' adaptions and coping to uncomfortable stimulations of thermal, lighting, and acoustical environments into three types: environmental

alternations, changes in behavior, and psychological processes that refer to the conditions when subjects put up with or ignore the problem (Heerwagen & Diamond, 1992).

Nikolopoulou and Steemer broadened the concept of adaptation. Based on their thermal comfort studies conducted under urban space contexts, they defined three levels of adaptations: a physical level, a physiological level, and a psychological level (Nikolopoulou & Steemers, 2003). Physical adaptation refers to all the changes a person makes, either adjusting oneself or the environment, which are introduced as reactive and interactive adaptations. Physiological adaptation refers to changes in the physiological responses resulting from repeated exposure to a stimulus. Last, psychological adaptation refers to a subject's psychological understanding about a condition, including naturalness, expectations, past experience, time of exposure, perceived control, and environmental stimulation (Nikolopoulou & Steemers, 2003).

In addition to studies concerning concepts and kinds of adaptive behaviors, subtle contextual factors and environmental variables significantly influence occupant behavior (Fabi, Andersen, Corgnati, & Olesen, 2012). O'Brien and Gunay defined nine contextual factors that influence occupant behaviors: availability of personal control, accessibility of personal control, complexity and transparency of automation systems, presence of mechanical/electrical systems, views to and connection with the outdoors, interior design, experiences and foreseeable future conditions, visibility of energy use, and occupancy patterns and social constrains. These contextual factors partially explain the discrepancies between simulation results that employ oversimplified behavior models and buildings' actual energy consumption. In other words, these contextual factors can also assist in exploring occupants' rational or logic behind their decision-making procedures.

2.3.2 Adaption to Lighting Environments

Even though researchers notice the importance of occupant adaptation under lighting environments, most of the studies focused on the behavior level, especially occupants' control patterns of shading systems and artificial lights. Previous studies explored occupants' patterns of manipulating window shades (Haldi & Robinson, 2010). Some studies demonstrated that occupants tended to override electric lighting controls (Lindelöf & Morel, 2006). Keyvanfar et al summarized the adaptive behaviors from visual comfort perspective, including turning on or off electric lighting, adjusting electric lighting operative hours, using desktop lamps, adjusting desktop or task surface, changing position or direction of furniture, covering room surface, opening or closing shading devices, opening or closing windows, and so on (Keyvanfar et al., 2014). Including the theory of adaptive zone in visual discomfort prediction can decrease over 90% of glare during occupied hours based on simulation results (J. Jakubiec & Reinhart, 2012).

Although substantial research investigated occupant behavior models in terms of shading controls and artificial lighting controls, insufficient studies explores occupant adaptive behaviors in the spaces where neither shading nor artificial lighting controls are accessible to a majority of occupants. Yet, automatic controls of shading systems and artificial lights are widely utilized in commercial buildings, especially in large offices. Even manual controls of shades and artificial lights are usually inaccessible to every occupant in shared offices due to the diversity in the preferred conditions of occupants and various forms of social etiquette (Fabi et al., 2012; Sanati, 2014). In order to fill the gap, this dissertation utilizes mixed quantitative and qualitative methods to investigate occupant adaptive behaviors caused by daylight glare in a control-constrained shared office.

2.4 RESEARCH TOOLS

This section introduces the three tools utilized throughout the dissertation, HDR image techniques, simulations, along with interviews and questionnaires. As the previous section demonstrates the effectiveness of luminance-based metrics in terms of visual discomfort prediction, this section introduces the two methods of generating luminance maps for visual discomfort analysis. There are two fundamentally different ways of generating HDR images: image-taking process and simulations. The former involves taking multiple images at a fixed aperture in varying shutter speeds and then combining these images into one luminance map (M. N. Inanici, 2006). The latter refers to the combination of inputting geometries, materials, and lighting data to a simulation software to generate HDR images (Reinhard, et al., 2010). Following one of these two methods, luminance values can be extracted from the RGB channels of HDR images.

2.4.1 HDR Image Techniques

Unlike traditional Low Dynamic Range (LDR) images that provide lighting information around 2 orders of magnitude, HDR images can contain lighting information around 14 orders of magnitude (Reinhard, et al., 2010). HDR image techniques combine multiple LDR images HDR images to present accurate luminance distributions of a scene. This technique uses a camera positioned from an occupant's perspective to efficiently record both magnitudes and directs of luminous intensities perceived by an occupant (Cai, 2013). According to Inanici's validation study, HDR image techniques can capture luminance distributions with an average error of 5.8% for outdoor environments and 10.1% for daylit interior scenes (M. N. Inanici, 2006).

Despite the efficiency of data collection, HDR image techniques require strict data post-processing to guarantee the accuracy of measurements for further analysis. Jacobs explained the steps of generating a camera response curve to combine HDR images (Jacobs,

2011). The required settings for taking images under daylighting environments are: ISO 100, White Balance of daylight, and Neutral Picture Style (Mehlika N. Inanici, 2010). An HDR image captured by a fisheye lens appears falling-off luminance values from the center to the periphery, which needs a vignetting correction. Inanici introduced a method of rotating a camera at 5^{o} intervals to measure the vignetting effect of a fisheye lens at one aperture (Mehlika N. Inanici, 2010). Cauwerts et al. compared the vignetting effects with two cameras and two fisheye lenses. The research concluded that the larger an aperture, the more accentuated the luminance loss at the periphery of an image. More importantly, an accurately measured vignetting correction function can be applied in future studies, as long as the camera and the lens are identical as the previous one (Cauwerts, Bodart, & Deneyer, 2012). Jakubiec et al. recommended using f/11 for taking HDR images, which can achieve a balance between minimizing vignetting effect and lens flare (Jakubiec, Van den Wymelenberg, Inanici, & Mahic, 2016). They also suggested measuring both the vertical illuminance in front of a lens opening and luminance from a grey card for local calibrations. The measurement of vertical illuminance can test both lighting changes during image taking and luminous overflow (Jakubiec, Inanici, Van den Wymelenberg, & Mahic, 2016).

2.4.2 Simulations

This section focuses on two aspects of daylight simulations, reasons for using Radiance as the main simulation software in the dissertation and sky model selections for accurate simulation results.

2.4.2.1 Simulation Software

This research uses Radiance as the lighting simulation software. The reasons for selecting Radiance include five key points. First, Radiance (Ward & Rubinstein, 1988) generates accurate lighting results, which has been globally and independently validated (Mardaljevic J., 1997; Grynberg, 1998). Second, compared with other software, Radiance is

the most commonly used one among researchers, engineers, and designers (C. Reinhart & Fitz, 2006). Third, Radiance is a free open source software that is continuously updating. Due to its free feature, programs and functions have been developed based on Radiance. For example, DAYSIM (C. Reinhart, n.d.-b) was generated based on Radiance to generate climate-based simulations with the inclusion of people's shading controls. Fourth, Radiance has comprehensive tutorials (Ward, n.d.-c) and useful mailing lists (Ward, n.d.-d) for beginners to learn. Radiance exporters are willing to reply to people's questions. However, one disadvantage of Radiance is its script-based property. Radiance is flexible without a Graphic User Interface (GUI), which adds difficulties for non-programmers to learn. Hence, DIVA-for-Rhino (Jakubiec & Reinhart, 2011) is also recommended since it uses Radiance as the lighting calculation engine. DIVA-for-Rhino ("DIVA for Rhino," n.d.) is a Rhino plugin to simulate lighting and thermal environments as well as energy consumption. It combines DAYSIM and EnergyPlus with the inclusion of occupant's reactions as a part of the simulation.

2.4.2.2 Sky Model Selection

One concern of simulation is to what extent can simulation results be compared with field measurements. There are multiple factors that influence the resultant accuracy in daylight simulations, like building geometries, material properties, software algorithms, and sky models (M. Inanici & Hashemloo, 2016). A sky model is the primary lighting source in daylight simulations. Generic CIE sky models (CIE/ISO, 2004a, 2004b; CIE, 2014) and the Perez all-weather sky model (Perez, Seals, & Michalsky, 1993) are currently in wide use. The development of High Dynamic Range (HDR) image techniques led to another method of generating sky models, Image based sky models (Debevec, 2002; Reinhard et al., 2010).

The International Commission on Illumination (CIE) has adopted 15 standard skies ranging from clear to overcast conditions. CIE skies are mathematical models that use the

sun's zenith angles, azimuth angles, and conceptualized arbitrary sky elements to generate sky luminous intensities (CIE/ISO, 2004a, 2004b; CIE, 2014). However, there are only six types of CIE sky models available in gensky: a standard CIE clear sky with or without the sun, a standard CIE intermediate sky with or without the sun, a standard CIE overcast sky, and completely uniform cloudy sky (Ward, n.d.-a). Simple inputs of a location, given time, and selection of a sky condition can generate a CIE sky model by gensky. Due to their simple inputs, CIE sky models are commonly used in daylight simulations, especially by beginners. Previous studies concluded that CIE sky models cannot simulate accurate results. Inanici et al. concluded that CIE skies consistently underestimate interior lighting distributions (M. Inanici & Hashemloo, 2016; M. Inanici & Liu, 2016), which was confirmed by Cauwerts and Piderit (Cauwerts & Piderit, 2018). Jones and Reinhart (Jones & Reinhart, 2016) suggested using the CIE sunny sky to yield the worst glary situations, which agrees with Kong et al.'s conclusion (Kong, Utzinger, & Liu, 2015) that the CIE sunny sky can generate accurate DGP results (Wienold & Christoffersen, 2006). Limited by six sky conditions and the mathematical methods, generic CIE sky models are suitable to calculate interior daylighting performance under specific conditions or compare design alternatives (M. Inanici & Hashemloo, 2016; M. Inanici & Liu, 2016) rather than being utilized in validation studies.

The Perez all-weather sky model combines a mathematical framework with a set of coefficients stemmed from sky-scan data. It covers diverse sky conditions ranging from totally overcast to very clear (M. Inanici & Hashemloo, 2016; M. Inanici & Liu, 2016). The inputs of a location, given time, direct normal and diffuse horizontal solar irradiance, for example, generate a Perez sky in gendaylit (Delaunay, Wienold, Sprenger, & ISE, n.d.). Solar irradiance or illuminance data can be collected onsite or downloaded online. EnergyPlus provides abundant weather data that covers a variety of cities in different formats, like Typical Meteorological Year (TMY) files and Chinese Standard Weather Data (CSWD)

(EnergyPlus, n.d.). Unlike CIE sky models that can only be used in point-in-time simulations, the Perez sky model is also employed in climate-based simulations (C. Reinhart, n.d.-a). Due to the Perez sky's high level of accuracy and simplicity procedures of utilization, it has been widely used in software and methods validation studies (Mardaljevic, 1995; C. F. Reinhart & Andersen, 2006; C. F. Reinhart & Walkenhorst, 2001).

However, luminance distributions of actual skies, which involves light scatted by water and dust, are more complex than the models generated by the Perez sky model or CIE sky models. Image based sky models are capable of including the sky complexity by utilizing HDR images as the lighting source in simulations (Debevec, 2002; Reinhard et al., 2010). A horizontal HDR sky image provides lighting and cloud distributions, and a vertical HDR sky image documents a site's luminous surrounding environments.

One difficulty of capturing skies via HDR image techniques is the extreme luminance values of the solar disk. To the author's knowledge, there are two solutions. One solution is to separate the solar disk from the diffuse sky component by taking two HDR images simultaneously (Debevec, 2002; Reinhard et al., 2010). Inanici and others used f/16 with 3.0 ND filters to capture the solar disk and f/4 to capture diffuse skies. In order to avoid the underestimation of the solar corona and the overestimation of the luminance values of the remaining sky, Inanici used direct horizontal solar radiation and diffuse horizontal solar radiation to calibrate the solar corona and the remaining sky image, respectively. Then, the two HDR images were fused together. The solar corona was extracted by mksource from the fused HDR sky image. Inanici and others validated the image-based sky model through both horizontal illuminance and luminance maps. The studies concluded that the image-based sky model generate comparable simulation results when compared with the simulation results under the Perez sky model (M. Inanici & Hashemloo, 2016; M. Inanici & Liu, 2016).

The other solution to separate the solar corona from diffuse skies is to block the solar corona when taking HDR images. Chiou and Huang employed a shadow ring to block the sun from a camera sensor and complemented the blocked portion of the images in Adobe Photoshop following certain luminance gradation pattern (Chiou & Huang, 2015). Although their study concentrated on the diffuse sky component, it demonstrated the accuracy of using measured diffuse horizontal illuminance to calibrate HDR sky images without the sun (Chiou & Huang, 2015). Humann and McNeil proposed a hybrid photo-radiometer (HPR) sky model by integrating modelled physical descriptions of the sun and HDR sky images (Humann & Mcneil, 2017). Their method used only one camera to capture diffuse skies and removed the insufficiently captured solar corona with a black disk if the sun was not occluded by clouds. Then, the calibrated HDR images of diffuse skies and the solar disk generated in gendaylit were integrated as the HPR sky. As the camera sensor cannot record the light spectrum outside of the visible range (400-700nm), illuminance (lux) values for the direct and diffuse sky components rather than full spectrum irradiance (W/m^2) values were used in the HPR sky model (Humann & Mcneil, 2017).

Compared with the solution of using two cameras to separate the solar corona from the diffuse sky component, Humann and McNeil's method simplifies the procedures of data collection and post-processing. Using one camera to mainly take the diffuse sky component, their method narrows the range of exposure values and shortens the image-capture duration. Generating the solar disk in the Perez sky model, this method solves the luminance overflow caused by the sun. Furthermore, this method eliminates the need for ND filters and corrections of chromatic shift. Since their method has only been validated in a physical scale model study using illuminance values, this dissertation uses three buildings to test the accuracy of the horizontal HPR sky model in real environments.

2.4.3 Interview and Questionnaire Survey

This dissertation uses exploratory sequential mixed methods (Creswell, 2014) to collect and analyze subjective occupant assessments. With the intention of developing an effective questionnaire which can comprehensively identify daylight glare in an office, select participants are interviewed before generating a questionnaire, which is a part of the interview result. Furthermore, comments and responses to the interviews can be referred to when data is analyzed and interpreted.

2.4.4 Integration of Three Tools

Many researchers combined physical measurements and POE surveys as the dominant method to evaluate lighting environments. Before the wide use of HDR image techniques, Illuminance values on horizontal or vertical working planes were recorded to represent indoor lighting quality (Galasiu & Veitch, 2006; Veitch, Farley, & Newsham, 2002). With the development and availability of HDR image techniques, however, researchers have a more effective tool to capture large quantities of luminance values.

The combination of HDR image techniques and POE surveys has been widely utilized in evaluating indoor lighting qualities. Konis comprehensively assessed the outcomes of the retrofitted elevation of an open-plan office building in terms of daylighting quality (Konis, 2013). Hirning et al. carried out a series of studies that correlated the results of POE studies with luminance maps in open-plan offices to generate a new glare index, UPG (Hirning et al., 2014, 2017). Jin et al. utilized both HDR image techniques and POE surveys to explore occupants' comfortable lighting levels in shopping malls (Jin, Li, Kang, & Kong, 2017).

Although these studies proved the effectiveness of this combined method of assessing lighting qualities, they all limited the lighting data within the periods of data collection. Therefore, this dissertation adds simulations to this combined method. On the one hand, simulations can accurately replicate a real-world context and generate large quantities of data

at low cost. On the other hand, since HDR image techniques can only provide instantaneous luminance distributions, simulation models can extend data outside of the data collection periods for a long-term perspective.

2.5 RESEARCH GAPS

2.5.1 Comparison of Visual Discomfort Metrics

Although substantial studies explored daylight glare issues, most of them were conducted in limited building contexts. Most researchers investigated the effectiveness of visual discomfort metrics in sidelit offices (Suk et al., 2017; K. Van Den Wymelenberg et al., 2010) or derived a glare index under similar spatial contexts (Hopkinson, 1972; Wienold & Christoffersen, 2006). Hiring et al. explored occupant visual discomfort evaluations under open-plan office contexts (Hirning et al., 2014, 2017). Jakubiec and Reinhart compared glare indices through simulation results in a sidelit private office and an open-plan office (Jakubiec & Reinhart, 2012). Yet, insufficient research explores the performance of glare indices under multiple spatial contexts. This dissertation fills this gap and compares the performance of select visual discomfort metrics in diverse spatial contexts that include variations in orientation, shading system, spatial organization, and façade configuration. Rather than using simulations, all the analyzed data stem from field measurements.

2.5.2 Validation of the HPR Sky Model

Additionally, as introduced in Section 2.4.2.2, Humann and McNei's method has only been validated in a physical scale model study using illuminance values (Humann & Mcneil, 2017). In order to extend this sky model in real environments, this dissertation will utilize three buildings to explore the accuracy of the horizontal HPR sky model in terms of simulating luminance maps.

2.5.3 Utilization of Three Tools

Although a considerable amount of studies integrated POE studies with field measurements of physical lighting environments, the rare published work utilizes three tools, HDR image techniques, simulations, questionnaires and surveys, to examine interior lighting qualities. Hence, using an open-plan office as an example, this dissertation encompasses simulations in addition to the combination of HDR image techniques and POE studies to explore daylighting performance.

3 FIVE BUILDINGS INTRODUCTION

This chapter introduces the five buildings where all the studies were conducted. The five buildings are: Main Hospital of the Columbia St. Mary's Hospital (CSM), The Christopher Center Library (CCL) at Valparaiso University, The Aldo Leopold Foundation Center (ALF), The Hammel, Green, and Abrahamson Office (HGA) in Milwaukee, and the School of Architectural and Urban Planning (AUP) at the University of Wisconsin-Milwaukee. As shown in Figure 3.1, all five buildings are located in a humid continental climate, three in Milwaukee, WI, one in Baraboo, WI, and one in Valparaiso, IN. Table 3.1 summarizes these buildings' basic information.

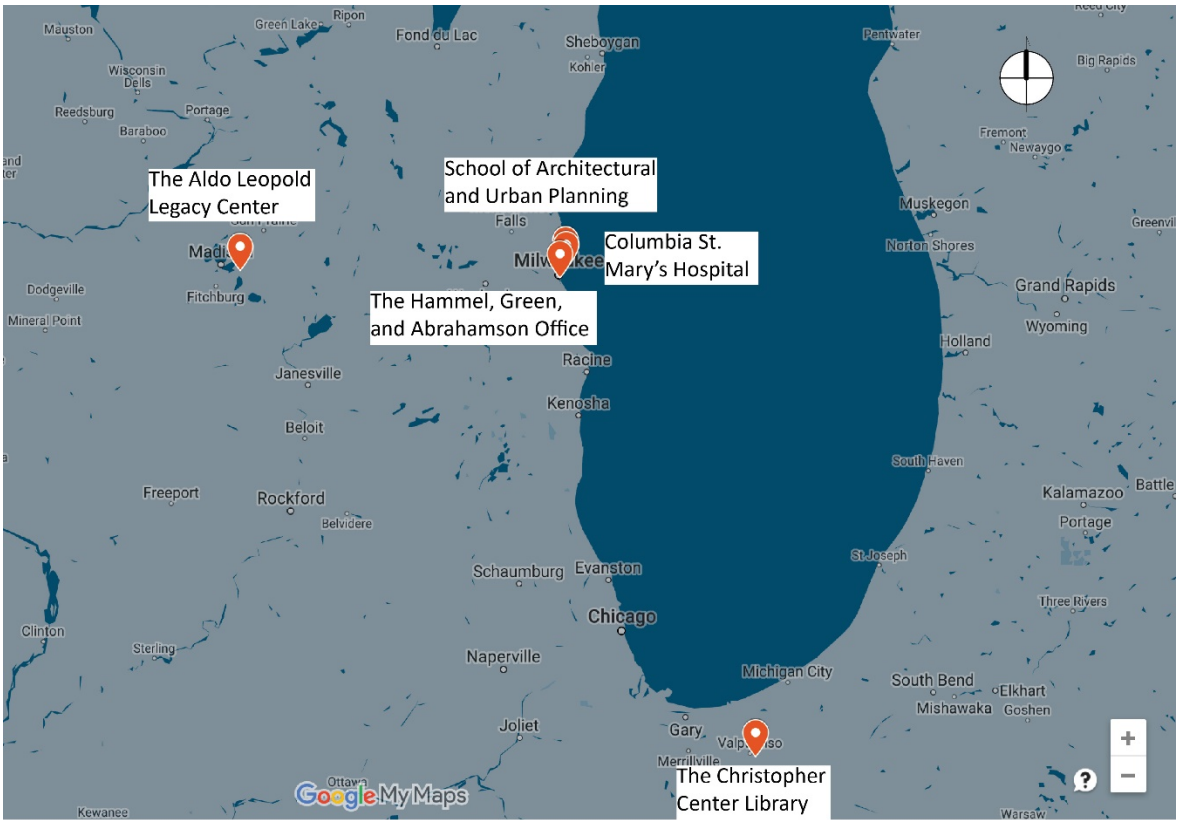

Figure 3.1: The locations of the five buildings

Table 3.1: The summary of the five buildings

Building	Abbr.	Geographic coordinate	Floor	Area (m^2)	Program	Open year	Architecture firm
The Main Hospital of Columbia St. Mary's Hospital	CSM	43.1 N, 87.9 W	Nine	77,574	Commercial facility, hospital	2010	Hellmuth, Obata + Kassabaum, Kahler Slater & Plunkett Raysich
Christopher Center Library	CCL	41.5 N, 87.0 W	Five	9,755	Educational facility	2004	Esherick Homsey Dodge & Davis
The Aldo Leopold Foundation Center	ALF	43.6 N, 89.6 W	One	1,106	Commercial facility, foundation	2007	The Kubala Washatko Architects & Oscar J. Boldt Construction
Hammel Green & Abrahamson Inc. Milwaukee	HGA	43.0 N, 87.9 W	Five	3,075	Commercial facility, office	2006	The Hammel, Green, and Abrahamson
School of Architecture and Urban Planning	AUP	43.1 N, 87.9 W	Four	13,273	Educational facility	1996	Holabird & Root Architects Engineers Planners

Figure 3.2: The perspective view of CSM (DRI Design, n.d.)

Figure 3.3: Exterior view of CCL (Courtesy of D. Michael Utzinger)

Figure 3.4: Exterior view of ALF (Utzinger & Wasley, 2013)

Figure 3.5: Exterior view of HGA

Figure 3.6: Exterior view of AUP (Courtesy of Jing Hong)

These five buildings have different daylighting performances and lighting environments, which are influenced by multiple factors like building designs, spatial configurations, and daylighting design strategies. Figure 3.2 shows the exterior view of CSM. The studied space, the two-story high lobby and common spaces, are enclosed by curtain walls without shading systems. The lack of solar control and the glazing in high transmittance led severe glare to occupants. Figure 3.3 demonstrates CCL's southern elevation. The combination of external brise soleils and internal mechoshades creates comfortable daylighting environments for occupants in the open-plan space, the study areas on the first and second floors. Figure 3.4 presents the exterior view of ALF. Different from CSM and CCL, ALF has small windows and roof overhangs that strictly control the amount of daylight penetration. As shown in Figure 3.5, HGA's southwest elevation faces the Milwaukee River. The large side windows have external overhangs and internal mechoshades to control daylight penetration. However, some occupants expressed dissatisfaction with their lighting environments. Figure 3.6 shows AUP's exterior view. AUP has windows facing all four orientations, north, south, east, and west. Interior blinds are provided for occupants to manipulate in most of the offices and classrooms.

3.1 COLUMBIA ST. MARY'S HOSPITAL

3.1.1 Building Overview

CSM is located in downtown Milwaukee, WI. As shown in Figure 3.7, CSM has the North Point Tower and Lake Michigan along its southeast. Figure 3.8 displays CSM's surrounding environments. The nine-floor Women's Hospital, located on CSM's northeast, blocks the sunlight early in the morning. One five-story office to the east of CSM belongs to the hospital campus. The rest are all residential buildings between two and four stories. Consequently, CSM has unobstructed surrounding environments. CSM is a nine-floor hospital facility that opened in October 2010. The building was designed by HOK and cost

$417 million (Ascension, 2010). The first four floors include medical, surgical, and advanced clinical specialties, while the fifth floor and above mainly contain ward departments.

3.1.2 Studied Spaces

The reasons for including CSM in the study is due to the severe glare in the lobby and common spaces. The lobby is the entrance to the hospital, where patients congregate and request information. The common spaces include registration desks and waiting areas for three departments. The lobby is an 18.3-by-14.8 meters rectangle facing southeast. The common spaces span 104.4 meters along its east-west face, while it runs 9.4 meters along the north-south axis. The common's glazing faces both south and southwest. Figure 3.9 shows the layout of the first floor with the lobby and common spaces highlighted in green. With Lake Michigan and North Point Tower outside, the lobby and common spaces are enclosed mainly by curtain walls without shading devices. In Figure 3.9, the curtain walls that face south, southeast, and southwest are circled in a pink dashed line. In the common spaces, the ceiling is 11.6 meters high with two sections extending to 21.3 meters and reaching the hospital's fourth floor (Figure 3.10).

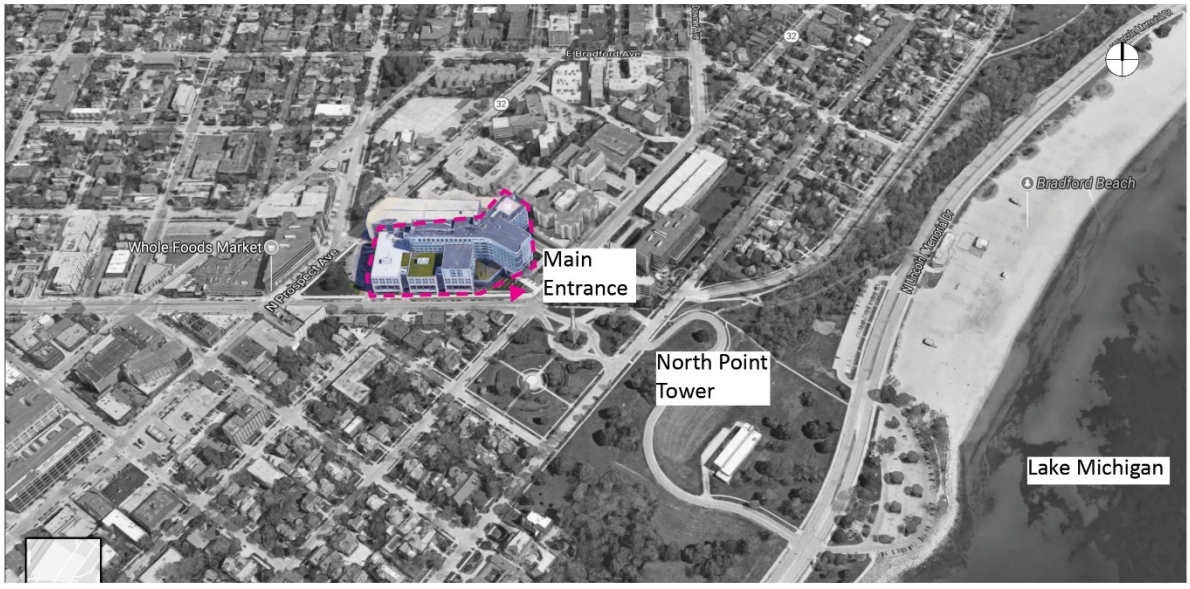

Figure 3.7: Bird's eye view of CSM

Figure 3.8: CSM's surrounding environments

Figure 3.9: First floor layout of CSM (Kong et al., 2015)

Unlike the patients' rooms, where interior mechoshades are provided for occupants, the architects failed to provide any shading device in the lobby and common spaces, which led severe glare to occupants. Two months after the hospital opened, movable partitions were introduced to the spaces. Figure 3.11 displays the movable partitions that were placed around the information desk and the registration desk. The daily and annual changes of daylight forced the staff members to move the partitions around on sunny days. What's worse, these partitions hindered patients' paths and sight, which added more difficulties to the wayfinding

systems at CSM. In order to investigate the severe visual discomfort in the lobby and common spaces, CSM were selected to conduct both field measurements and simulations.

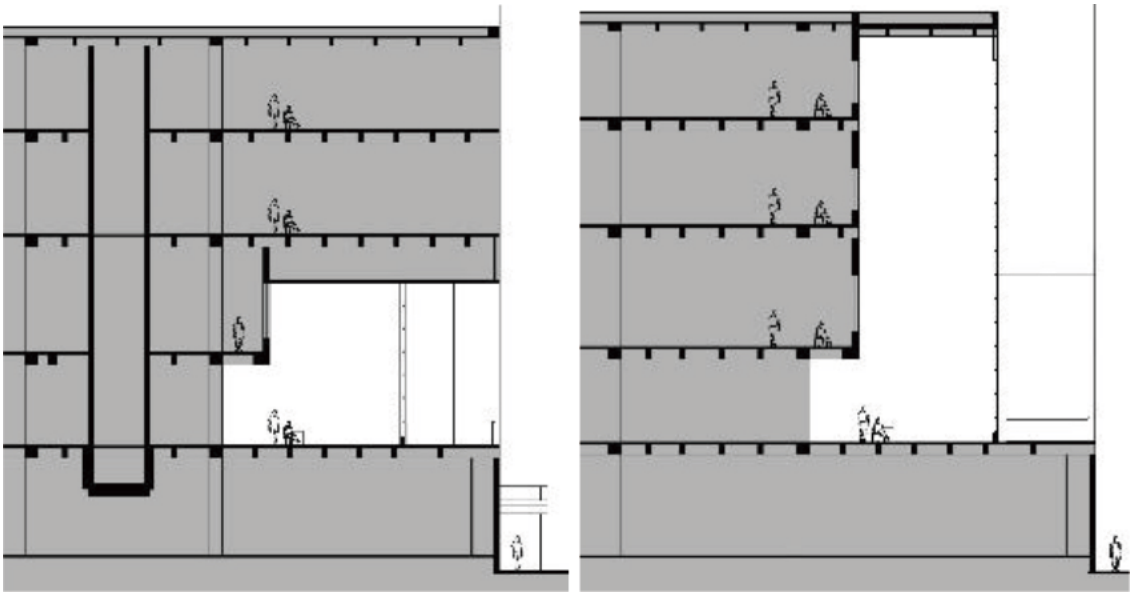

Figure 3.10: Two heights of the ceilings in the common spaces (Kong et al., 2015)

Figure 3.11: The movable partitions introduced two months after CSM's openness to block direct sunlight

3.2 CHRISTOPHER CENTER LIBRARY

3.2.1 Building Overview

CCL is the library at Valparaiso University, IN. Figure 3.12 presents CCL's surrounding environments. The three-story Chapel of the Resurrection is located along CCL's east, and the four-story Art and Science building flanks CCL's west. The library is located on the top of a slope with a parking lot at the bottom of its southern slope. No surrounding buildings cast shadows on the building's southern or eastern elevation.

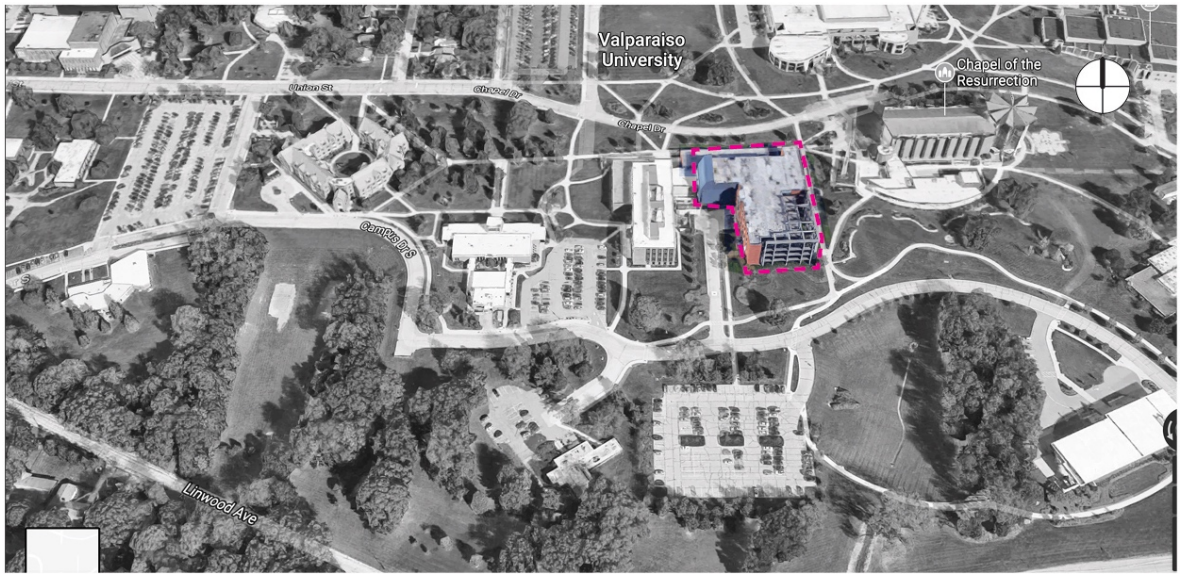

Figure 3.12: Bird's eye view of CCL

CCL is a well-designed building that won five awards covering both architecture design and interior design. The architecture firm, Esherick Homsey Dodge & Davis, followed the campus tradition of low-rise masonry structures ("Christopher Center Library Services: READ Posters: Index," n.d.). The external brise soleils flanking CCL's southern and eastern facades satisfy the aesthetic purpose and function as solar controls. In addition to the external brise soleils, CCL has internal mechoshade along the southern façade, which is automatically controlled by a solar radiometer on the roof. D. Michael Utzinger was the solar controls & daylighting consultant. The library provides diverse furniture designs and spatial programs to support faculty and students' multiple activities ("Christopher Center Library Services: READ Posters: Index," n.d.).

3.2.2 Studied Spaces

The studied space included the open study areas on the first and second floors. The study area on the first floor is a 17.3-by-36.2 meters rectangle facing south and east, while the study area on the second floor starts one bay away from the eastern elevation. Like the lobby and common spaces at CSM, the study area on the first floor at CCL is a two-story space enclosed by curtain walls. The study area is well-protected by both the exterior brise soleils and interior mechoshades. Several café tables are located along the eastern perimeter and an

open staircase to the second floor is next to the café area. All the desks are organized perpendicular to the eastern elevation. Therefore, all the monitors face either south or north. Figure 3.13 shows the first-floor layout with the study area highlighted in green. Figure 3.14 presents an interior view of the study area taken from the staircase.

Figure 3.13: First floor layout of CCL

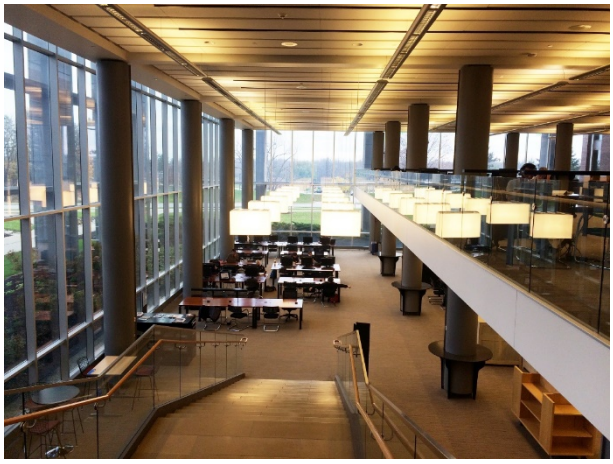

Figure 3.14: Interior view of the study area

3.3 ALDO LEOPOLD FOUNDATION CENTER

3.3.1 Building Overview

Located in Baraboo, ALF was opened in 2007 as the headquarters of the Aldo Leopold Foundation. As shown in Figure 3.15, the entire three-building campus is located on a slope and surrounded by trees. Consequently, its open surrounding environments allow for a substantial unshaded foreground.

Figure 3.15: Bird's eye view of ALF

ALF was envisioned as a net zero energy and carbon neutral building. In order to minimize the disturbance on the site, the campus was built based on the previously disturbed site on the Leopold Reserve. The main building was orientated along the east-west axis to maximize the prevailing winds and daylight. The rainwater on site was managed for natural percolation of rain garden. PV panels were placed on the roofs to offset energy consumption (Utzinger & Wasley, 2013). A portion of the construction materials were recycled from a dismantled airport. The wood was debarked on-site, air-dried, and used for construction (Qarout, 2017). ALF was designed to use 70% less energy than a comparable conventional building (Utzinger & Wasley, 2013). Consequently, ALF received the LEED Platinum and became the first certified carbon neutral building.

3.3.2 Studied Spaces

Figure 3.16 shows the layout of ALF with the studied spaces highlighted in green. The meeting room at the southwest corner was excluded since it was occupied during the data collection period. The garage was excluded because of its storage function unrelated to the research aims. The designers merge daylighting designs to various aspects of building designs to achieve comfortable daylighting environments. First, the aperture sizes are strictly designed to control the amount of daylight penetrating into spaces. Top-side windows in the exhibit space and the open office, either 0.3-by-0.3 meters or 0.6-by-0.6 meters, are evenly distributed along the southern and northern elevations (Figure 3.18). The private offices have larger windows (0.9-by-1.7 meters), since these offices face north without direct sunlight. Second, the roof overhangs, either 0.6 meters or 0.9 meters deep, collaborate with the windows to both block direct sunlight and reduce solar heat gain (Figure 3.17). Third, internal blinds are provided for the occupants in west-facing offices. Fourth, a corridor adjacent to the southern façade functions as an acoustical and solar buffer zone between the outside and the open-plan office (Figure 3.19) (Utzinger & Wasley, 2013).

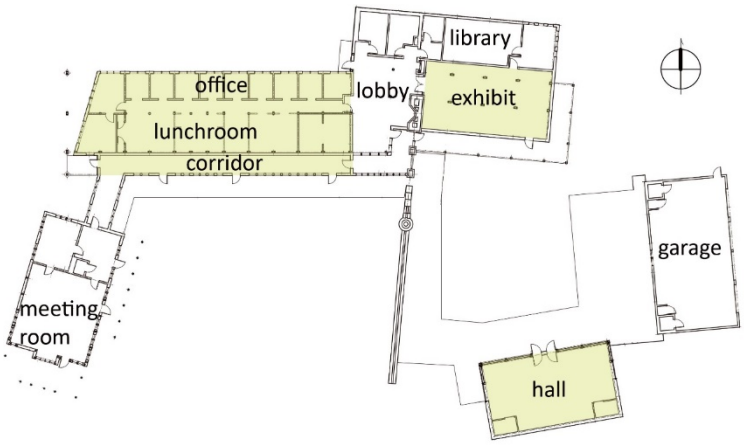

Figure 3.16: Floor layout of ALF

Figure 3.17: Deep roof along the southern elevation (Utzinger & Wasley, 2013)

Figure 3.18: The top-side windows in the exhibit space (Utzinger & Wasley, 2013)

Figure 3.19: The southern corridor adjacent to the public office (Utzinger & Wasley, 2013)

3.4 HAMMEL, GREEN & ABRAHAMSON INC.

3.4.1 Building Overview

Figure 3.20 shows the surrounding environments of HGA in downtown Milwaukee. The HGA Milwaukee Office occupies the first floor of this five-story mixed-function building by the Milwaukee River. The upper four floors are for residents. The office's main façade, the southwest façade that faces the Milwaukee River, is distant from the buildings across the river. Hence, no surrounding buildings shade the southwest facade. However, some occupants complained about the light reflected from the surrounding buildings.

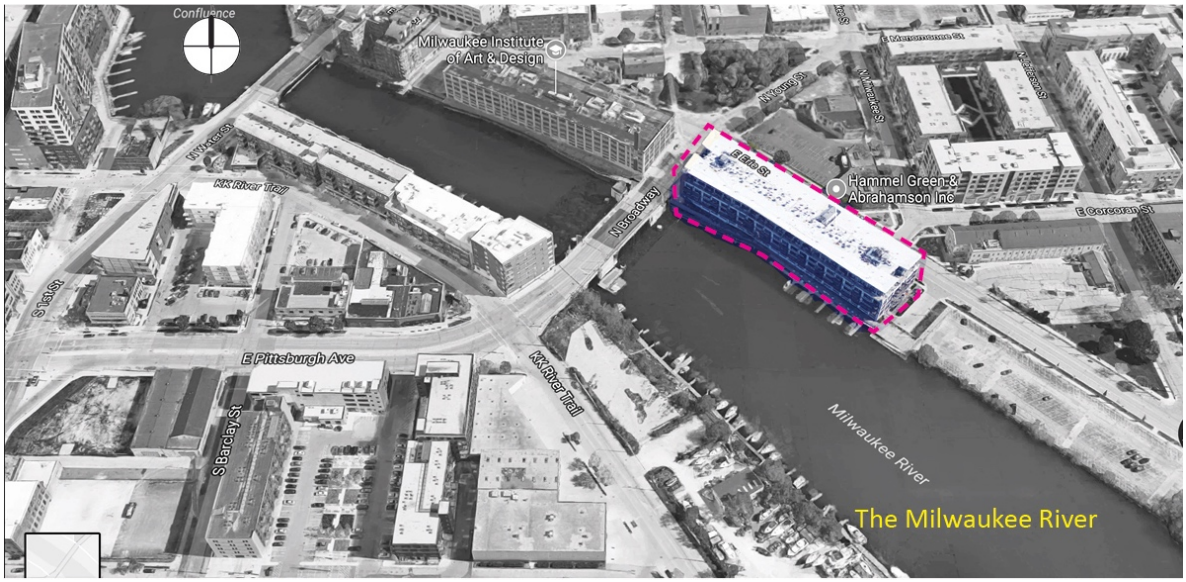

Figure 3.20: Bird's eye view of HGA

3.4.2 Studied Spaces

The office measures 95.5 meters along the southwest axis by 32.2 meters along the northeast axis. The entire office has the same ceiling height. Following the site slope, the office was designed in four tiers, with a 0.2 meters height differential between each tier. Figure 3.21 shows the layout of the office and the four tiers. As the building's southwest elevation faces the Milwaukee River, the architects designed large windows to provide outside views and daylight with occupants. There are three window heights in the office. Tier One has the greatest window height (3.6 meters), Tiers Two and Three have a lower window height (3.2 meters), and Tier Four has the lowest window height (2.8 meters). Figure 3.22 displays three window heights on the southwest facade. The office has both external and internal solar controls. The balconies on the second floor and the overhangs between the balconies block the sunlight at high angles (Figure 3.23). The interior mechoshade systems are automatically controlled by both the solar radiometers on the roof and the photometric sensors on the floor. The mechoshade control systems are divided into three groups and controlled independently by three sensors due to three window heights. In each tier, the first row of the artificial lights by the windows are controlled by a sensor located on the surface of

the middle table. When the measured horizontal illuminance is lower than 583 lux (50 fc), the artificial lights in the first row will be turned on. Otherwise, the artificial lights in the first row are off. The other artificial lights in the three rows back are automatically on between 7 a.m. and 7 p.m. during weekdays. Even though the office has both static external and movable internal shading devices, the occupants experienced visual discomfort. Staff members' methods of occupying the office indicated their dissatisfaction with daylighting environments. The occupants sitting adjacent to the southwest windows put up foam core boards along the cubicles to protect themselves and their monitors from direct sunlight (Figure 3.24). Some staff members complained that they sometimes had to wear sunglasses on sunny days while working.

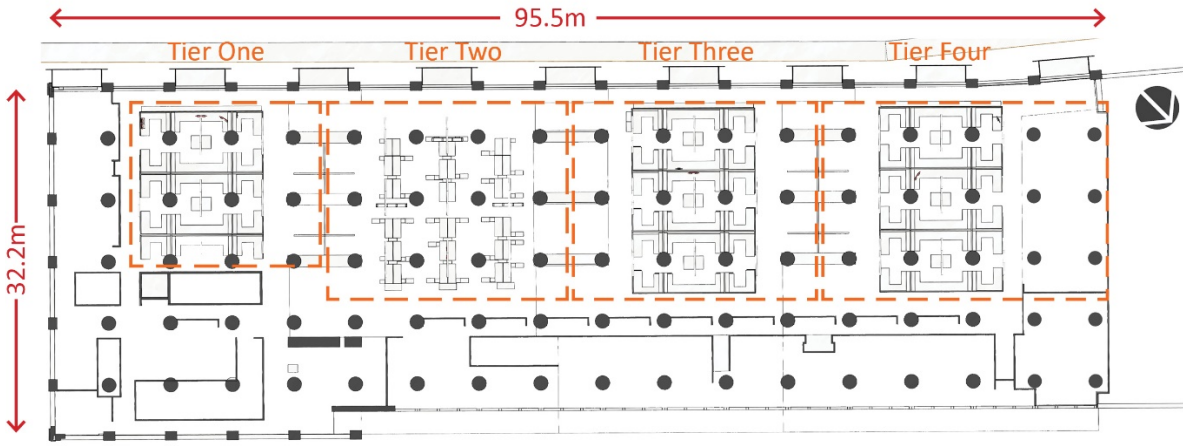

Figure 3.21: Floor layout of HGA

Figure 3.22: Three window heights along the southwest façade

Figure 3.23: External overhangs

Figure 3.24: Occupants put up foam core boards to block sunlight

Figure 3.25: The original cubicle design in Tiers One, Three, and Four (left), along with the more open workstation in Tier Two (right)

Aiming to improve staff members' satisfaction with their working environments and solve daylight glare, HGA started an office renovation project in 2016. When the study was carried out, the office had two layout designs, the original layout in Tier One, Tier Three, and Tier Four, along with the renovated layout in Tier Two. The original layout was comprised of 2.1-by-2.8 meters cubicles. Each cubicle had one or two sides enclosed by 1.3-meter opaque partitions and another side enclosed by a 1.7-meter opaque partition (Figure 3.25 (left)). All the cubicles were arranged along the office's northwest-and-southeast axis, which led to eight seating orientations (Figure 3.26). The renovated layout design in Tier Two consisted of 1.5-by-1.8 meters new workstations. Each workstation had one opaque partition reaching 1.3 meters to block the opposite staff member's sight (Figure 3.25 (right)). All the workstations were perpendicular to the southwest windows, which made all seating orientations parallel to

the windows. Compared with the original layout, the workstation areas in Tier Two were set 2.3 meters away from the windows.

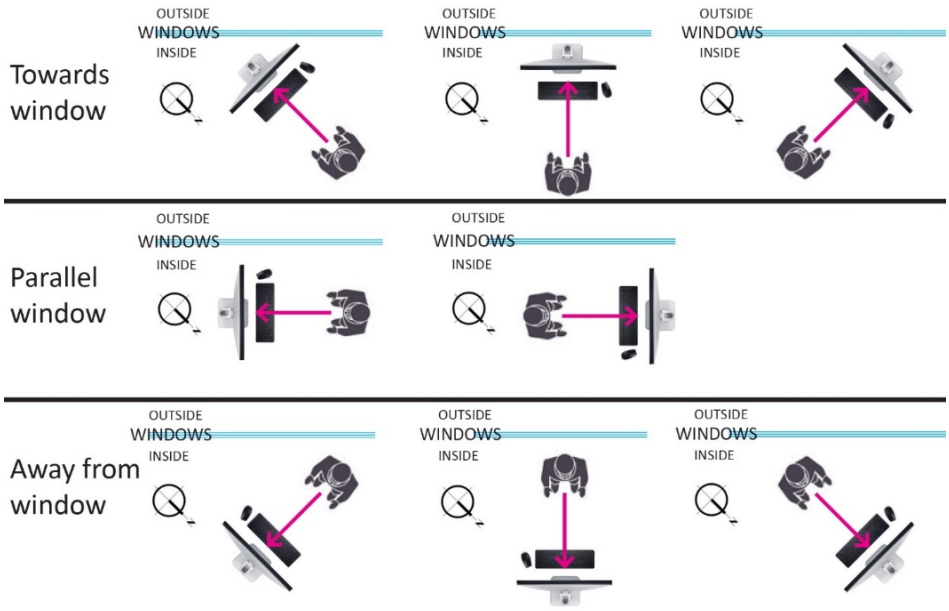

Figure 3.26: Eight seating orientations related to the southwest façade

3.5 SCHOOL OF ARCHITECTURE AND URBAN PLANNING

3.5.1 Building Overview

Figure 3.27 displays the surrounding environments of AUP at the University of Wisconsin-Milwaukee (UWM). AUP is a four-story L-shaped educational facility. It has different external environments. Deciduous trees along AUP's eastern elevation reach the third floor and block sunlight in summer (Figure 3.28). The Biological Science Department opposite AUP's southern elevation partially blocks the windows on the fourth floor and the windows below (Figure 3.29). AUP has relatively large windows in offices and studios. The rooms with the windows facing south, east, and west have interior venetian blinds for occupants to manually control.

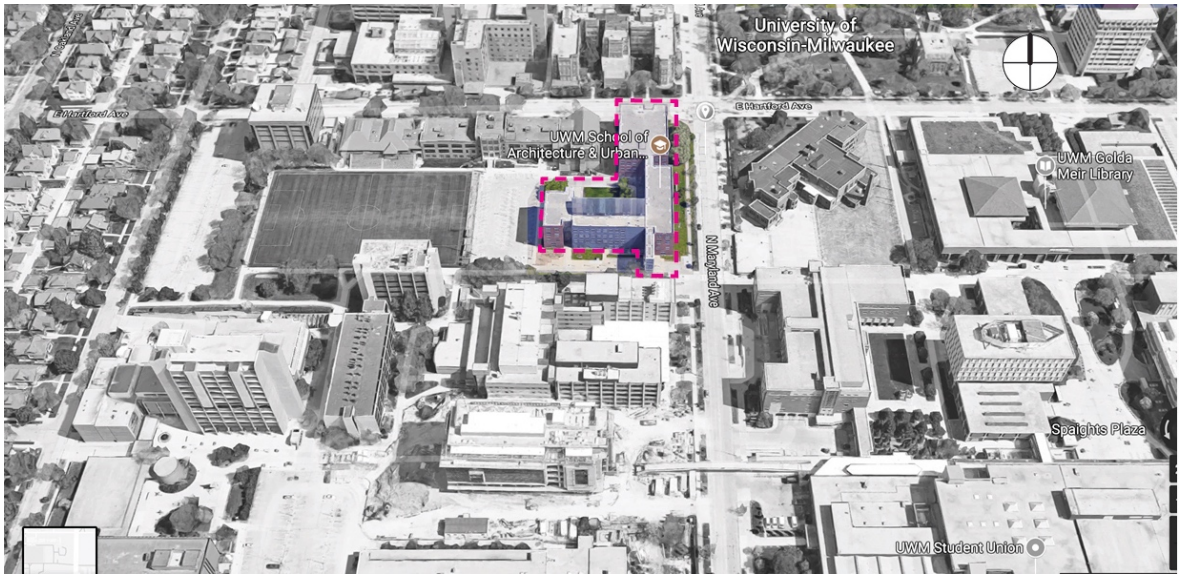

Figure 3.27: Bird's eye view of AUP

Figure 3.28: The trees along AUP's eastern elevation

Figure 3.29: Biological Department across from

3.5.2 Studied Spaces

In order to cover different environmental contexts, five offices on different floors with different orientations were selected. Two offices facing south, one on the third floor (Office 326) and the other one on the fourth floor (Office 422), were selected to reflect the impact of the Biological Science Department on interior daylighting distributions. Three other offices facing east, from the second to the fourth floors (Office 283, Office 383, and Office 479) (Figure 3.30), were selected to demonstrate varying daylighting distributions caused by the outside trees. Office 326 and Office 422 are 3-by-8 meters individual offices having one window. Office 479 is a 4.1-by-3.9 meters thesis room possessing one window. Office 283 and Office 383 are 8.1-by-7.8 meters with two windows for two faculty members.

Figure 3.30: The select offices on the second, third, and fourth floors at AUP

3.6 CONCLUSION

This chapter introduces the five buildings where all the studies in the dissertation were carried out. CSM and HGA were included due to their occupants' complaints about visual discomfort in the studied spaces. CCL was selected due to its similar façade design as CSM, where both buildings have huge curtain walls. However, the daylighting design strategies employed at CCL lead to completely different daylighting performance from CSM's conditions. AUP was chosen due to its relatively complex building contexts and the convenience for conducting research. ALF was included to broaden facade configurations and enrich daylighting design strategies utilized in building design.

4 FIELD MEASURMENT OF LIGHTING DISTRIBUTIONS

Luminance describes the amount of light that reflects from a surface and reaches an observer's eyes. HDR image techniques can efficiently capture large quantities of luminance data. This chapter presents the HDR images taken across five buildings on sunny and overcast days. Select visual discomfort metrics are applied to all the HDR images. The effectiveness of the visual discomfort metrics in terms of identifying daylight glare is compared. Related daylighting design strategies in each building are discussed.

4.1 RESEARCH OBJECTIVES

The objectives of this chapter are to analyze visual discomfort caused by daylighting in multiple sidelit spaces through the HDR image technique, to discuss the effectiveness of daylighting design strategies in terms of creating comfortable visual environments, and to compare the consistency and accuracy of different glare indices based on the HDR images taken on site.

4.2 RESEARCH QUESTION

In order to propose the effective visual discomfort metrics in terms of detecting daylight glare under diverse sidelit spaces and lay a foundation for the remaining chapters, this chapter mainly answers one question: how do the select visual discomfort metrics perform in terms of identifying daylight glare?

4.3 METHODOLOGY

This chapter used the HDR image technique to capture interior lighting distributions on sunny and/or cloudy days in the five buildings. The data were entered in evalglare (Wienold, 2015) for luminance-based analysis. Select visual discomfort metrics were calculated to examine their accuracy and consistency in revealing glare.

4.3.1 Data Collection

The images were taken by either a Canon 5D Mark II or a Canon EOS 6D with SIGMA EX DG f/3.5 fisheye lens. The camera was fixed on a Benro A1580F tripod. The ISO was 100, the White Balance was set as daylight, and the Picture Style was neutral. Ten to twelve LDR images were taken for each scene at f/5.6 with varying shutter speeds. The shutter speeds varied between 6s and 1/8000s (Figure 4.1). An 18% grey card was placed at the center of each scene. While LDR images were taken, the luminance value at the center of the grey card was recorded by a luminance meter, Gossen Starlite 2. Figure 4.2 illustrates all the equipment for taking HDR images. The HDR images were taken under both sunny and cloudy skies across three buildings (CSM, CCL, and AUP) and under sunny skies across the remaining two buildings (ALF and HGA). Each scene was taken from an occupant's perspective with the lens set at the same height of an occupant's eye level. The data collection started in October 2013 and ended in July 2017 and captured over 200 HDR images in total. The collected data covered both daily and seasonal changes of daylight. Table 4.1 summarizes the data collection periods in each building.

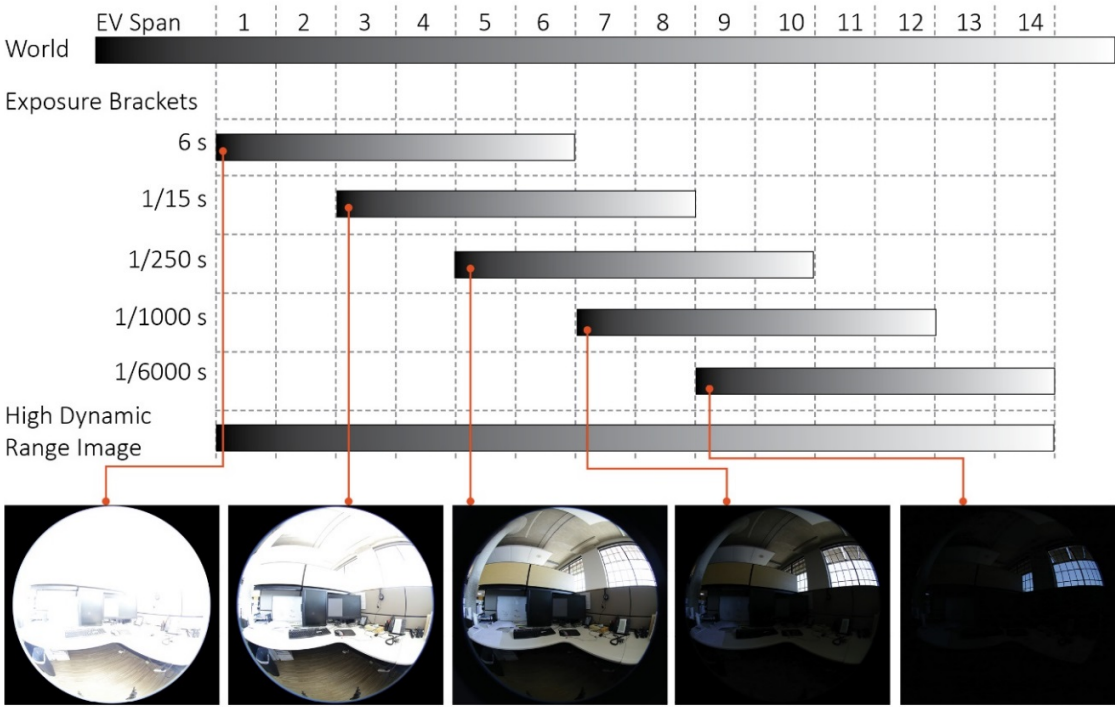

Figure 4.1: LDR images to record different ranges of luminance

Figure 4.2: The equipment for taking HDR images

Table 4.1: Data collection schedule across the five buildings

Building	Studied space	Time	Sky condition	Note
CSM	Lobby & common spaces	10/27/2013	Clear & sunny	Nine scenes were selected to cover the lighting distributions in the studied space as comprehensive as possible on both sunny and cloudy days.
		11/10/2013	Clear & sunny	
		11/17/2013	Cloudy	
		12/15/2013	Clear & sunny	
		01/05/2014	Cloudy	
CCL	Study areas	03/27/2014	Cloudy	Four scenes were selected to cover the lighting distributions in the study area on both sunny and cloudy days.
		03/30/2014	Clear & sunny	
ALF	Most of the building	05/22/2017	Clear & sunny	Twelve scenes were selected to record the lighting distributions in the spaces with different functions.
HGA	The open-plan office	03/20/2017	Cloudy & Intermediate	Artificial light and mechoshade systems on
		04/22/2017	Clear & sunny	Artificial light off and mechoshade on
		05/07/2017	Clear & sunny	Artificial light on and mechoshade on
		05/27/2017	Clear & sunny	Artificial light off and mechoshade on
		07/27/2017	Clear & sunny	Artificial light and mechoshade off
AUP	Office 326	05/17/2017	Intermediate	One scene was taken from the occupant's perspective in each office. The HDR images were taken at 20 or 30-minute intervals between 9 a.m. (local time) and 5 p.m. (local time).
		07/28/2017	Cloudy Clear & sunny	
	Office 422	05/18/2017	Intermediate	
		07/28/2017	Cloudy Clear & sunny	
	Office 283	07/25/2017	Intermediate Clear & sunny	
	Office 383	07/25/2017	Intermediate Clear & sunny	
	Office 479	07/25/2017	Intermediate Clear & sunny	

4.3.2 Data Post-Processing

LDR images were assembled in hdrgen following the extracted camera response curve. Hdrgen needs a camera response curve to accurately assemble HDR images. Each camera has a unique camera response curve. One way of extracting a camera response curve is to take twelve or more images of one scene, which includes brightness, darkness, and gradations of intensity. A camera response curve can then be extracted by photosphere and reused to generate HDR images that are taken by the same camera (Jacobs, 2011). Figures 4.3 and 4.4 present the camera response curve of Canon 5D Mark II and Canon EOS 6D respectively. A fisheye-view HDR image needs to be proceeded by both vignetting correction and calibration to guarantee the accuracy of the luminance value at each pixel (M. N. Inanici, 2006). Vignetting effect indicates the falling-off of luminance from the center to the perimeter of a fisheye lens. Vignetting correction functions

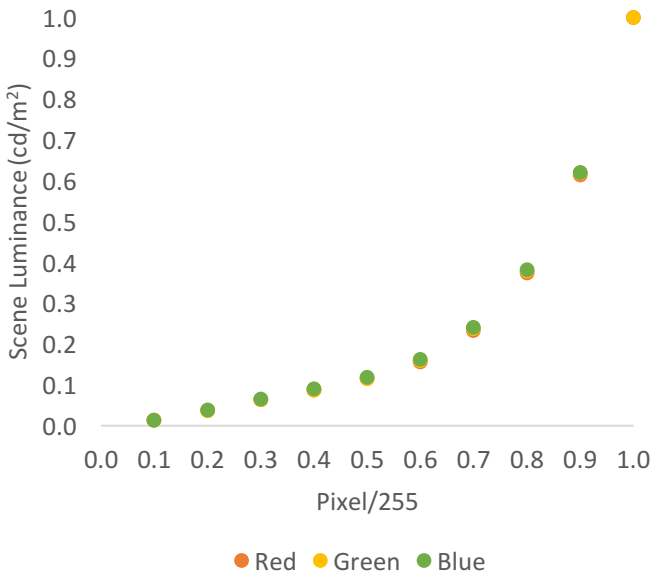

Figure 4.3: The camera response curve of Canon 5D Mark II

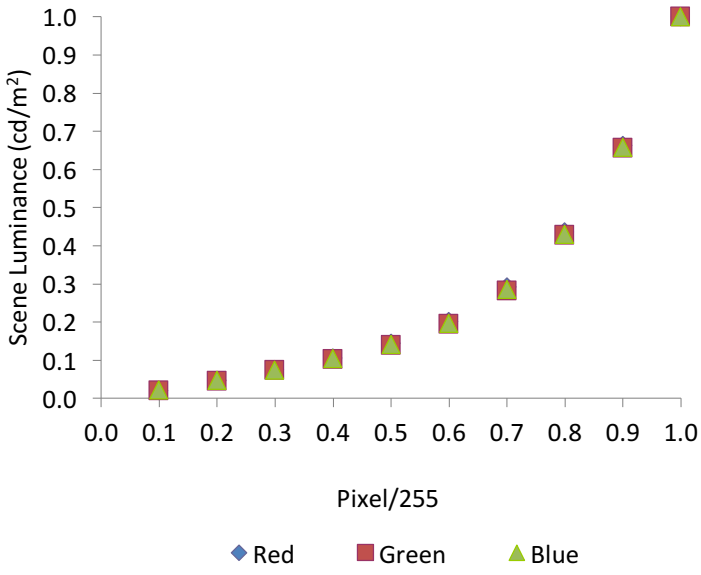

Figure 4.4: The camera response curve of Canon EOS 6D

vary according to aperture sizes and types of fisheye lens. One way of generating a vignetting correction function is to take multiple HDR images of a grey card by rotating a camera at 5° intervals from 0° to 90° under a consistent lighting environment (Inanici, 2010). Figure 4.5 shows the 19 HDR images taken at 5° intervals, and Figure 4.6 shows the vignetting correction curve of f/5.6 for the SIGMA f/3.5 fisheye lens mounted on the Canon 5D Mark II. After applying the vignetting correction function, the measured luminance values from the grey card were used to calibrate HDR images. Finally, each HDR image was decreased to 1000 x 1000 pixels for further analysis.

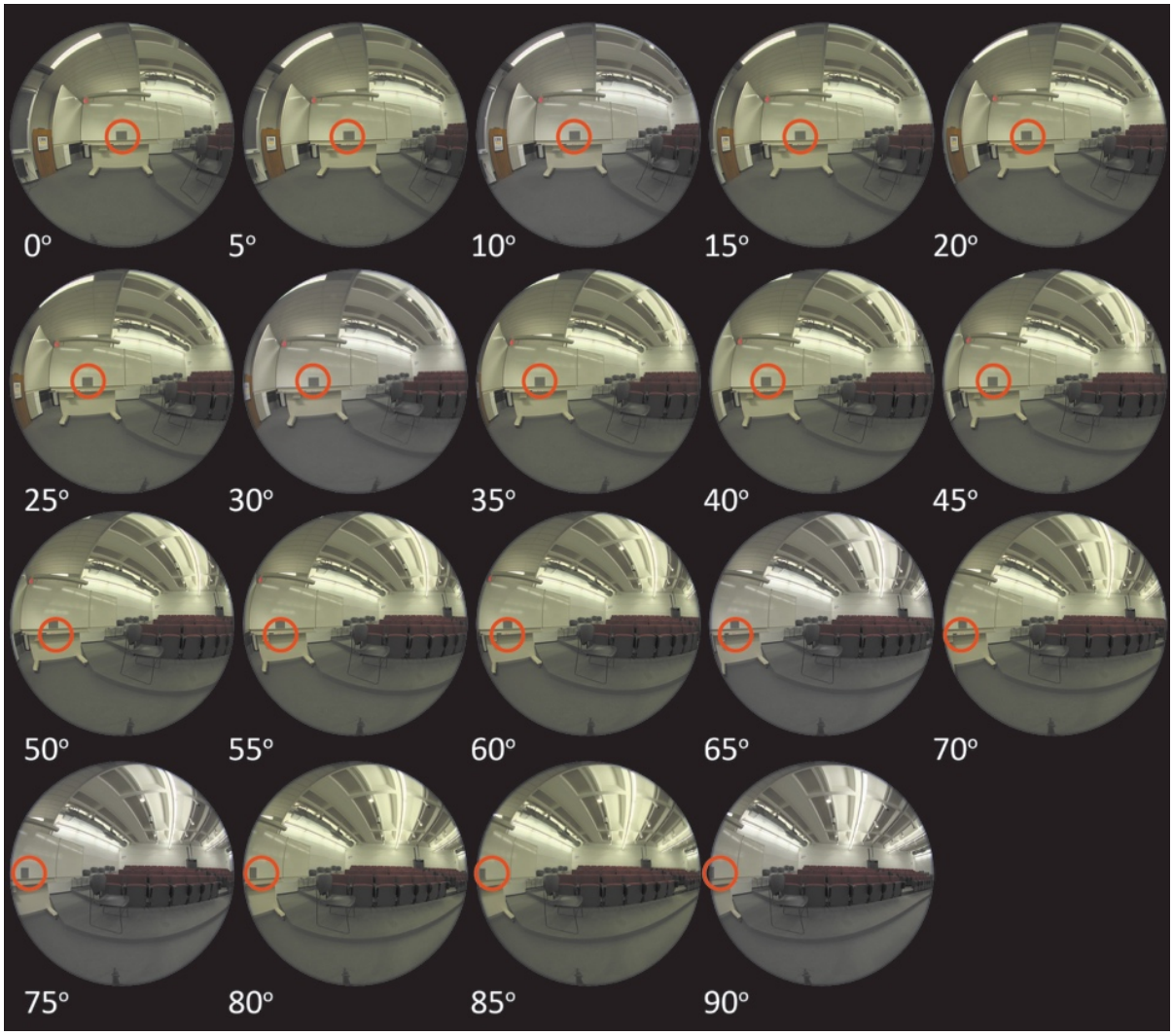

Figure 4.5: The HDR images taken at 5° intervals to generate a vignetting correction function

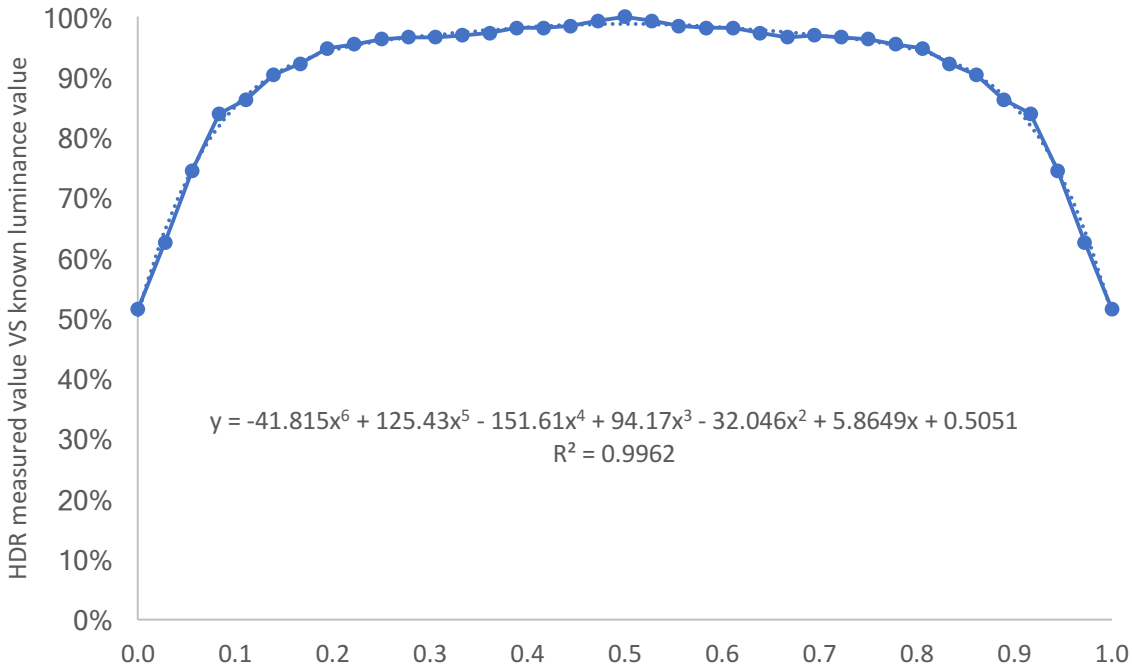

Figure 4.6: The vignetting correction function for SIGMA f/3.5 at f/5.6

4.3.3 Data Analysis

As this chapter focused on visual discomfort caused by daylight, DGP (Wienold & Christoffersen, 2006), DGI (Hopkinson, 1972), and UGP (Hirning et al., 2014, 2017) were selected to reveal different degrees of glare. DGI results were normalized by multiplying a factor of 0.01452 (J. Jakubiec & Reinhart, 2012) to convert the result range between 0 and 1. The calibrated HDR images were entered into evalglare (Wienold, 2015), a software to calculate glare indices and E_v, for glare analysis. Two methods of defining glare sources were used, predetermined absolute luminance threshold and scene-based mean luminance threshold. 2000 cd/m^2 was considered as the absolute luminance threshold (K. G. Van Den Wymelenberg, 2014), and five times of the mean luminance of a scene was regarded as the scene-based luminance threshold (Wienold, 2015). E_v of the HDR images was also calculated for comparison.

4.4 RESULTS

4.4.1 Lighting Distributions at CSM

Figure 4.7 illustrates the nine scenes where the HDR images were taken at CSM. Scenes One and Three were taken from staff members' perspectives, one at the information desk and one at the registration desk. The remaining seven scenes were taken from patients' perspectives in the waiting areas. Figure 4.8 shows the lighting distributions of four scenes on both sunny and overcast days. The top group shows the condition on sunny days, while the bottom group shows the condition on overcast days. The HDR images of all nine scenes are in Appendix A. Each scene includes the HDR images on both the sunny and cloudy days. The falsecolor images in the second-from-left column display the luminance distributions of each scene according to the color legends. For each scene, the falsecolor images demonstrate the great luminance differences between the sunny and overcast days. Greater luminance values concentrated on the glazing areas. On the sunny days, the high contrasts between the sunlight penetration and the shadows were recorded and reflected via the HDR images.

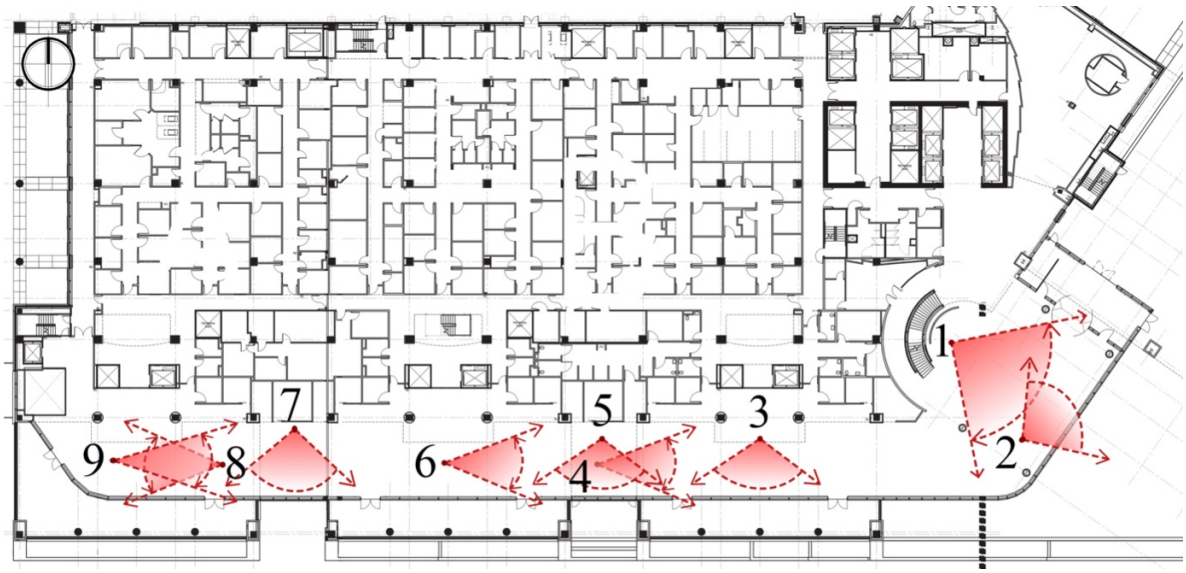

Figure 4.7: Nine scenes at CSM where HDR images were taken

The two columns on the right of Figure 4.8 present the DGP results defined by 2000 cd/m^2 and five times of the mean luminance of a scene (5X). The DGP results showed that on sunny days, each scene had disturbing or intolerable glare. On cloudy days, however, only

Scenes One and Seven had disturbing glare. Compared with the remaining seven scenes, Scenes One and Seven had a greater percent of glazing areas related to the entire HDR images, which might result in disturbing glare on the cloudy days. The DGP results indicated the cause of visual discomfort at CSM, the existence of the sun and direct sunlight on sunny days. The analysis of HDR images confirmed the occupants' complaints about the severe glare in the lobby and common spaces

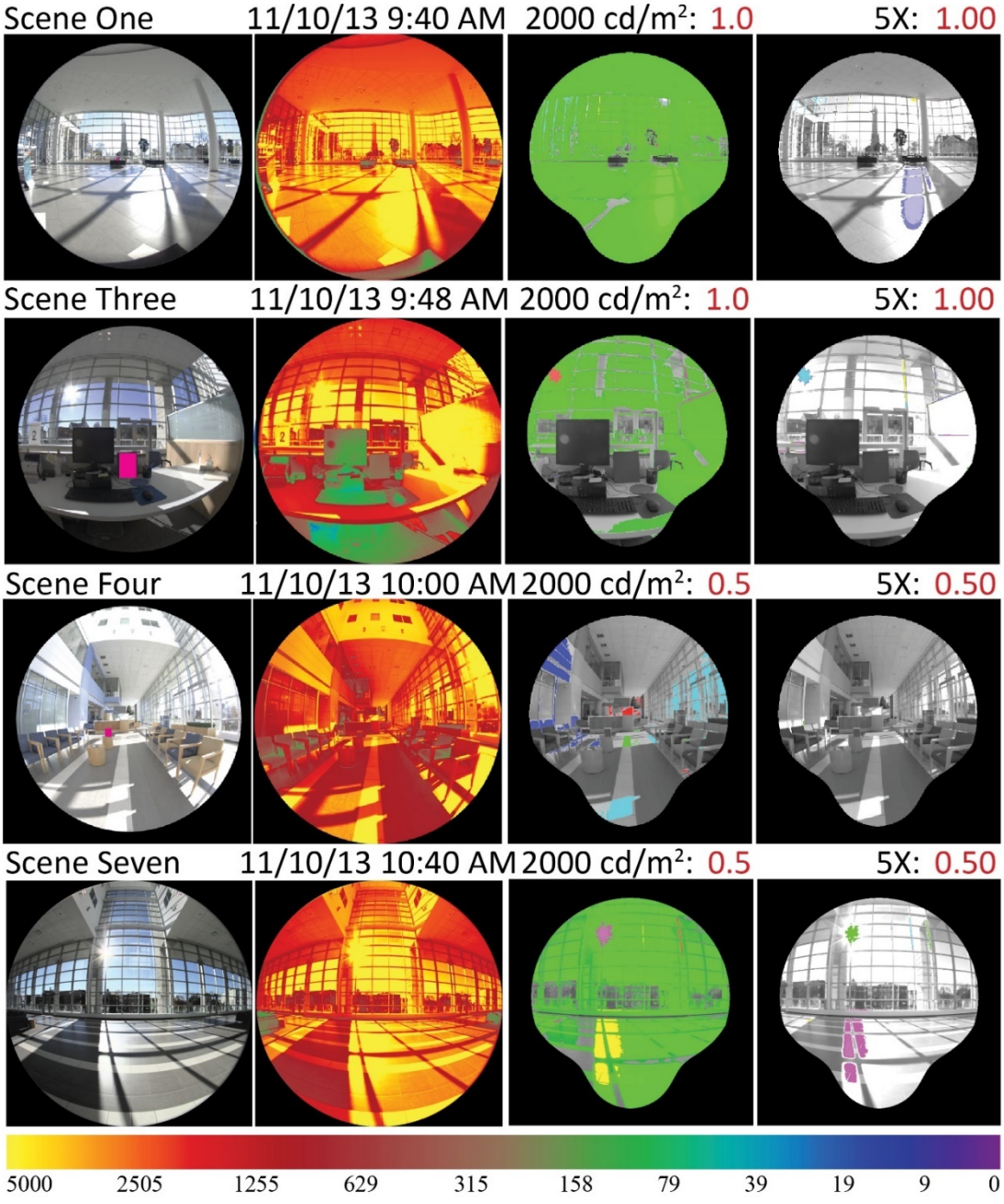

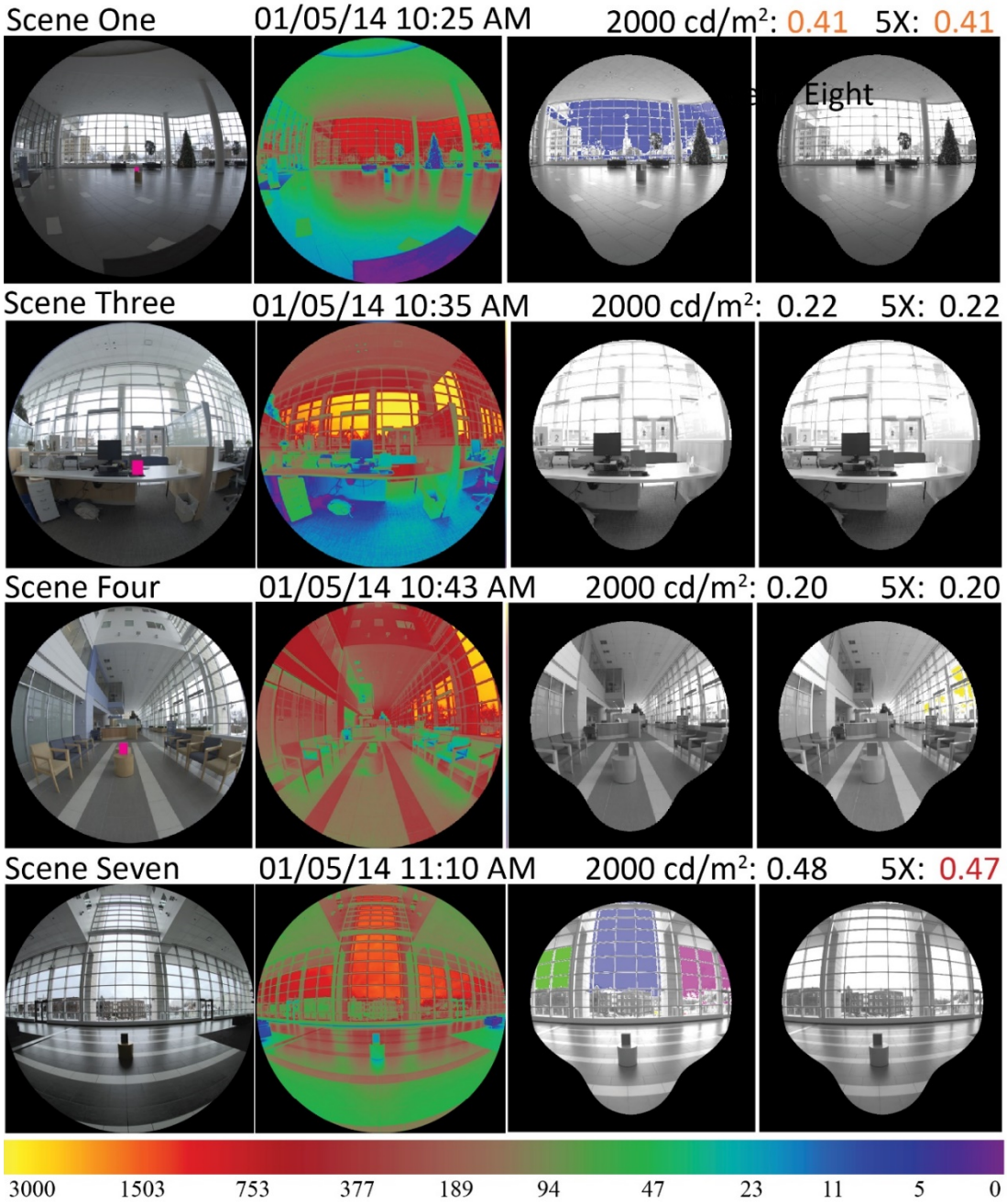

Figure 4.8: The HDR images, falsecolor images, and DGP analysis of four scenes at CSM

4.4.2 Lighting Distributions at CCL

Figure 4.9 highlights the studied areas in green and demonstrates the four scenes to take HDR images on the first and second floors. Figure 4.10 presents the HDR images, falsecolor images, and the DGP results of these four scenes. On the sunny day, the interior mechoshades on the southern elevation were fully down. On the overcast day, the mechoshades were retracted, and the artificial lights were on. On the sunny day, Scenes One,

Two, and Four presented sunlight penetration from the eastern curtain walls in the morning. The great luminance differences between the eastern and southern curtain walls, as shown in Scenes Two and Three on the sunny day, demonstrated the effectiveness of mechoshades in terms of reducing lighting intensities. Like CSM, these scenes presented great luminance differences between the sunny and cloudy days at CCL. Only Scene One on the sunny day had intolerable glare (0.72). Although Scene Four resulted in imperceptible glare (0.33), the existence of direct sunlight on task areas was identified as one cause of glare (Jakubiec & Reinhart, 2016; Kong, Utzinger, Freihoefer, & Steege, 2018). Even though the HDR images revealed the existence of glare in the study areas, no students or faculty members reported their visual discomfort experience in the spaces.

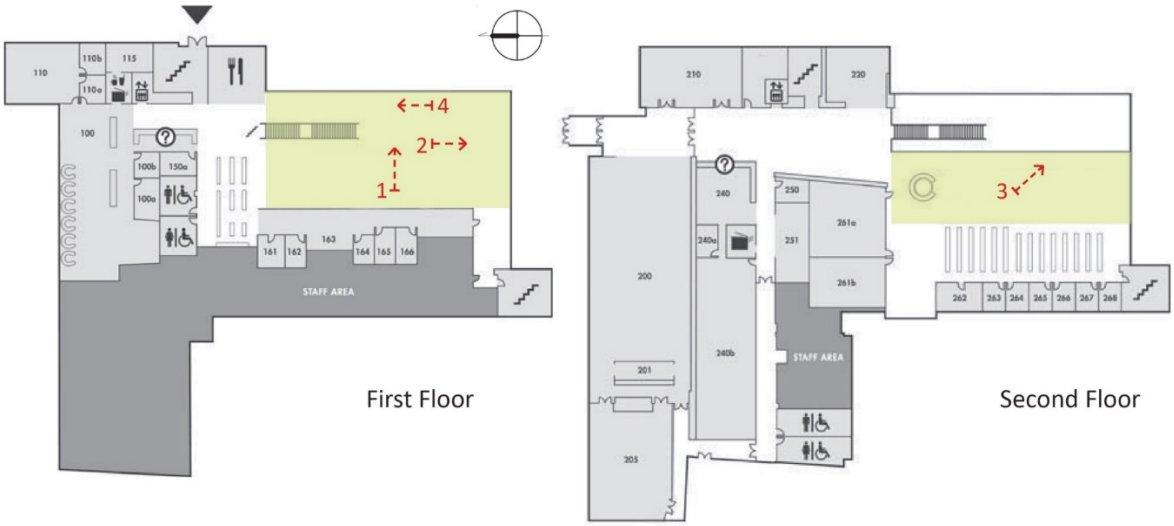

Figure 4.9: Four scenes at CCL where HDR images were taken

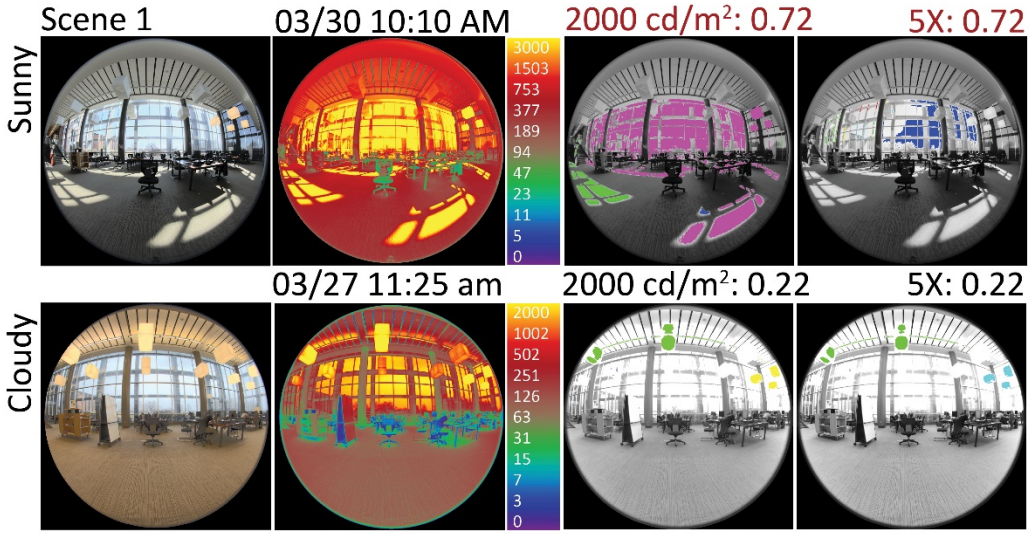

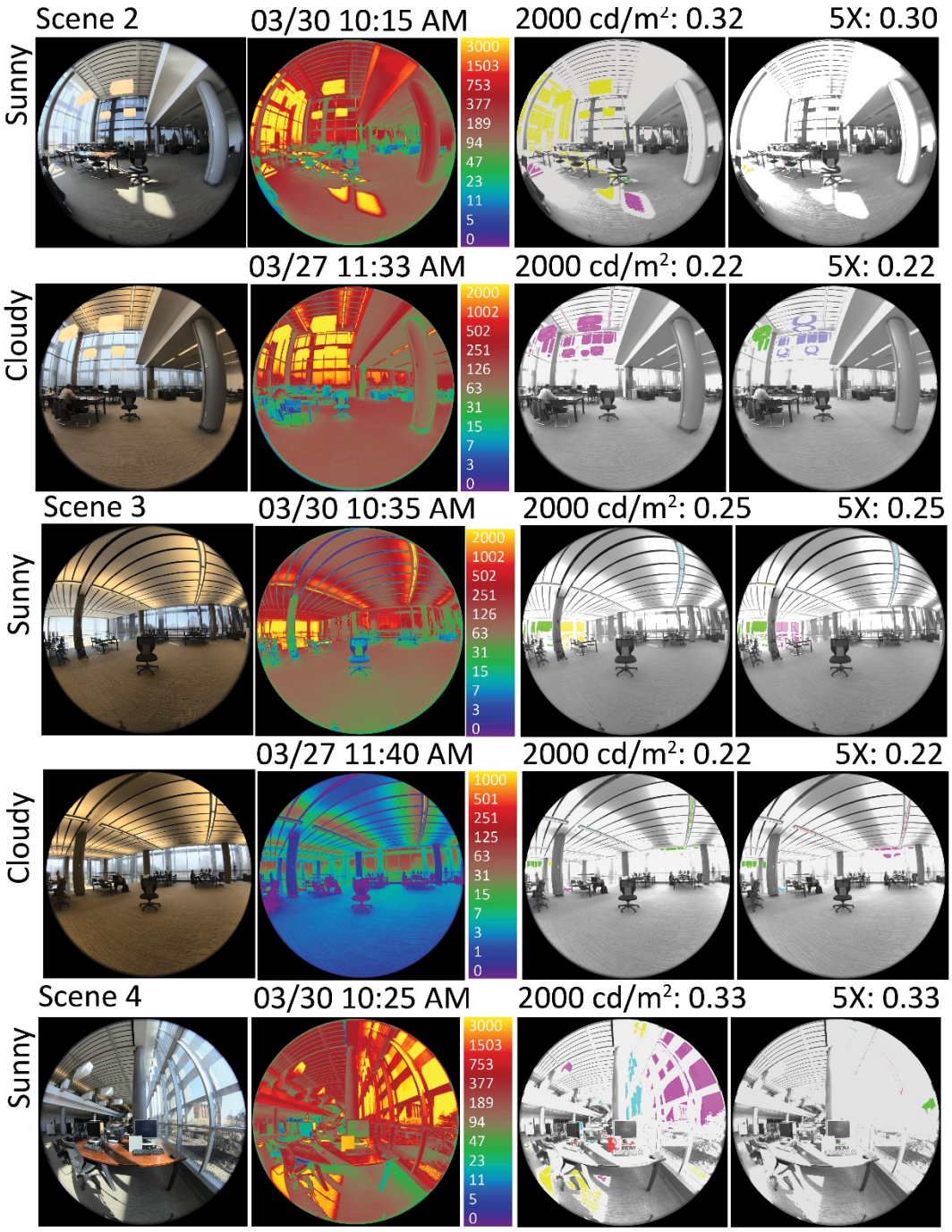

Figure 4.10: The HDR images, falsecolor images, and DGP analysis of four scenes at CCL

4.4.3 Lighting Distributions at ALF

Figure 4.11 illustrates the thirteen scenes to take HDR images at ALF. The scenes were scattered across the entire campus to cover interior lighting distributions as comprehensively as possible. The camera faced different directions in some spaces to reveal the impact of seating orientations on lighting distributions. Scenes 3.1, 3.2 and 3.3 were all captured in the north-facing private office highlighted in green with the camera pointing in

different directions. For the purpose of drawing clarity, these scene numbers were placed in three private offices in Figure 4.11. In addition to the private office, two scenes, one facing east and one facing west, were taken in the exhibit space (Scenes 4.1 and 4.2). Another two scenes, one facing west and one facing north, were taken in the private office at the southwest corner of the administration building (Scenes 8.1 and 8.2).

Figure 4.11: Thirteen scenes at ALF where HDR images were taken

Figure 4.12 shows the HDR images, falsecolor images, and DGP results of eight scenes at ALF. Scenes 1, 2.2, and 4.1 presented the lighting environments generated by the top-side windows in the open-plan office and the exhibit space. The small top-side windows (0.6-by-0.6 meters), which were evenly arranged on the northern and southern elevations, introduced diffuse daylight and created evenly distributed lighting environments. In the exhibit space, however, the top-side windows failed to provide sufficient lighting levels. Hence, the artificial lights were on as the supplementary lighting source. As shown in Scene 3.2, an occupant sitting towards the windows experienced perceptible glare that mainly

stemmed from the window. Scene 5 presented the daylighting distributions within a southern corridor. Compared with Scene 5, the luminance distributions in Scene 7 greatly decreased, which indicated the effectiveness of the southern corridor that functioned as a daylighting buffer zone. Both Scenes 6 and 8.1 reflected the daylighting qualities in west-facing spaces in the afternoon.

Scene 3.2 had perceptible glare due to the seating orientation towards the window. The other two scenes, Scenes 3.1 and 3.3 that were taken in the same office with different camera directions, had no glare. Facing westward, Scenes 6 and 8.1 had sunlight penetration during the afternoon. Nonetheless, Scene 8.1 presented a relatively comfortable visual environment without glare (0.27). One possible explanation was the trees and bushes outside the office scattered direct sunlight. Scene 5 presented imperceptible glare (0.24), which was attributed to the collaboration of 0.9 meters roof overhangs and the small windows.

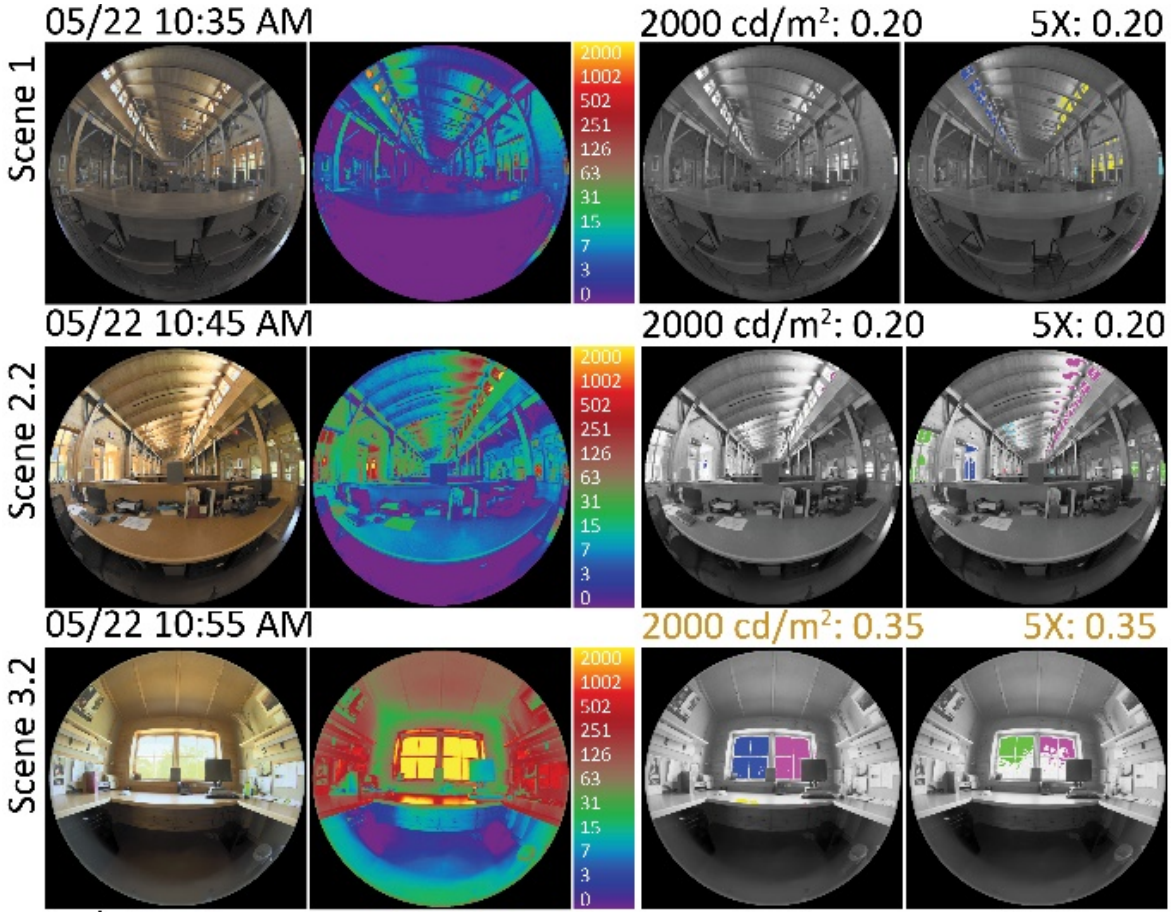

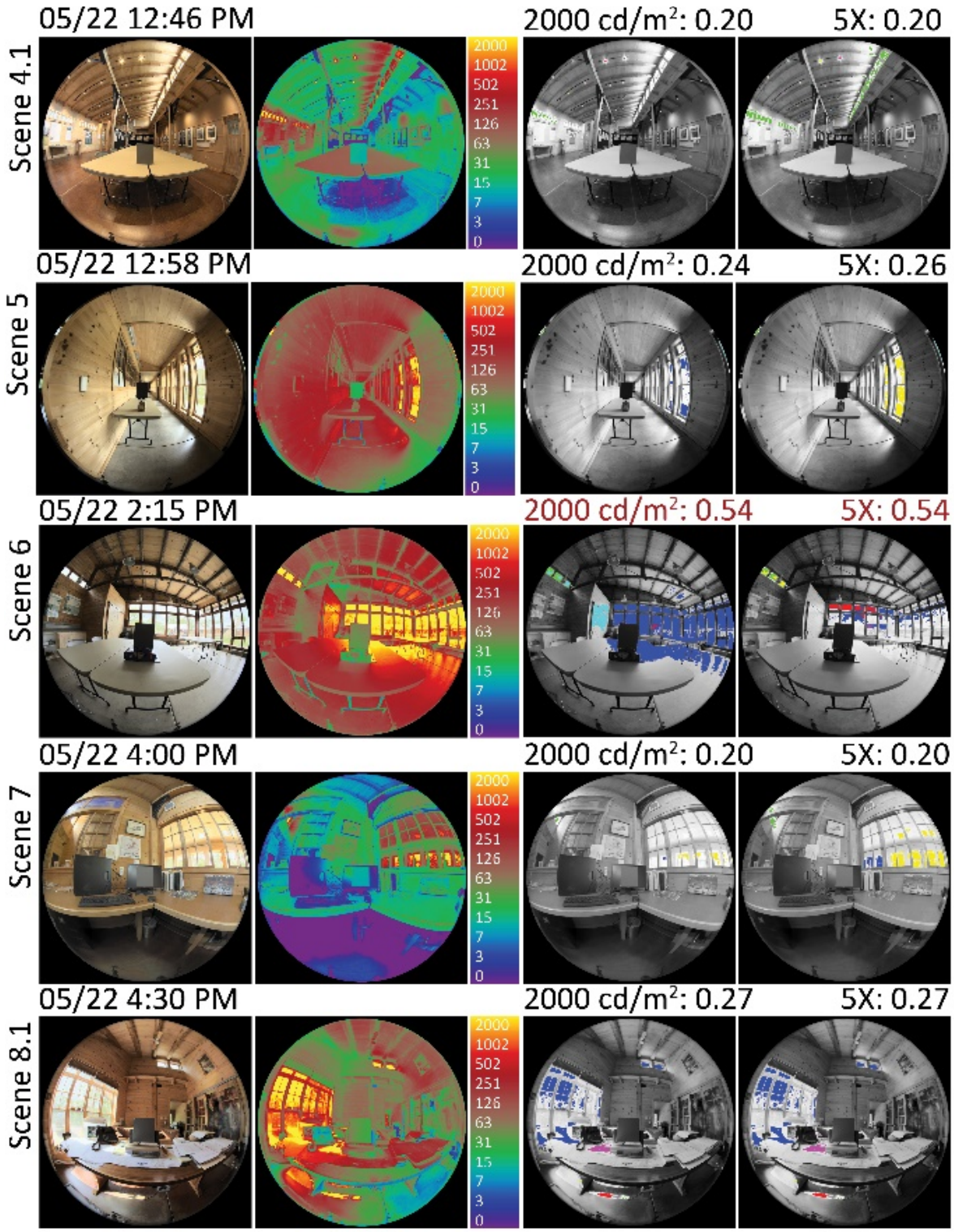

Figure 4.12: The HDR images, falsecolor images, and DGP analysis of select scenes at ALF

4.4.4 Lighting Distributions at HGA

Figure 4.13 illustrates the workstations where the HDR images were taken from occupants' perspectives. Each workstation was numbered by a combination of its tier number, row number, and alphabetical seating number. The grey bars in Figure 4.13 show the alphabetical seating numbers in Tier Two and Tier Three. For example, T1R3A represents the first workstation from the left in Tier One Row Three.

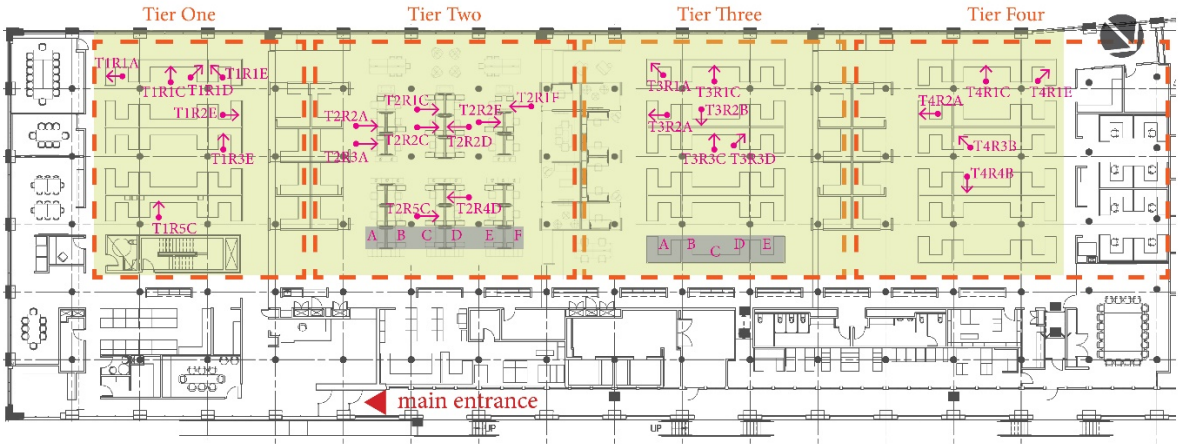

Figure 4.13: Select workstations at HGA where HDR images were taken

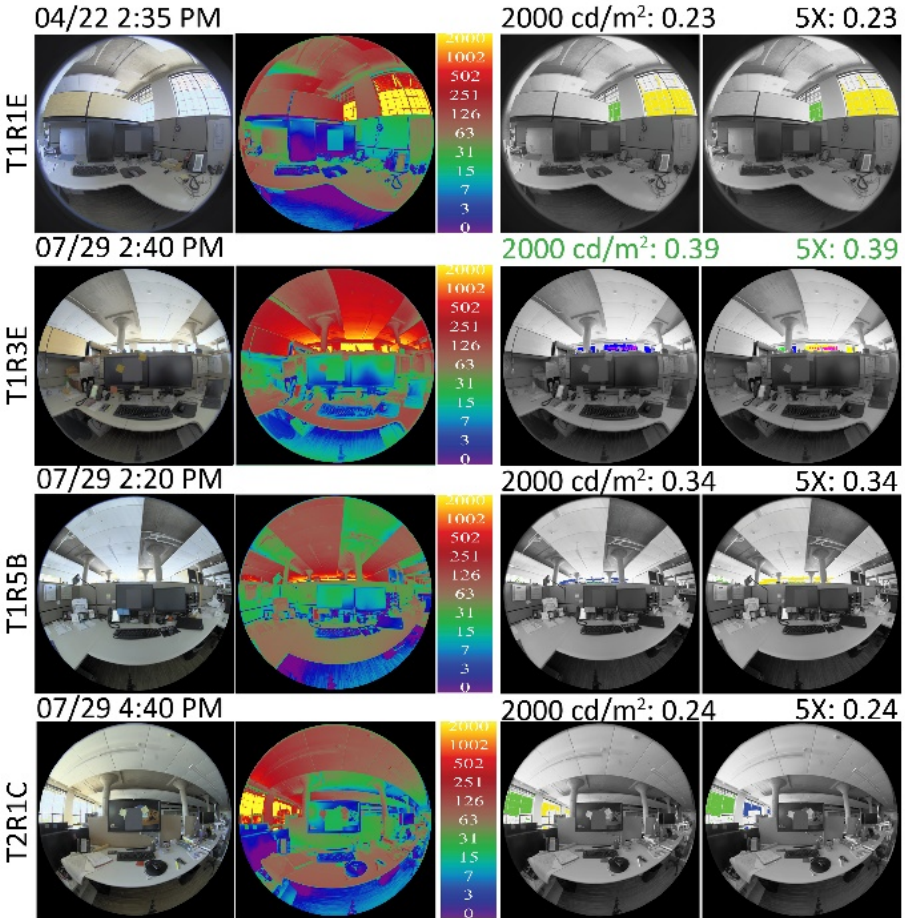

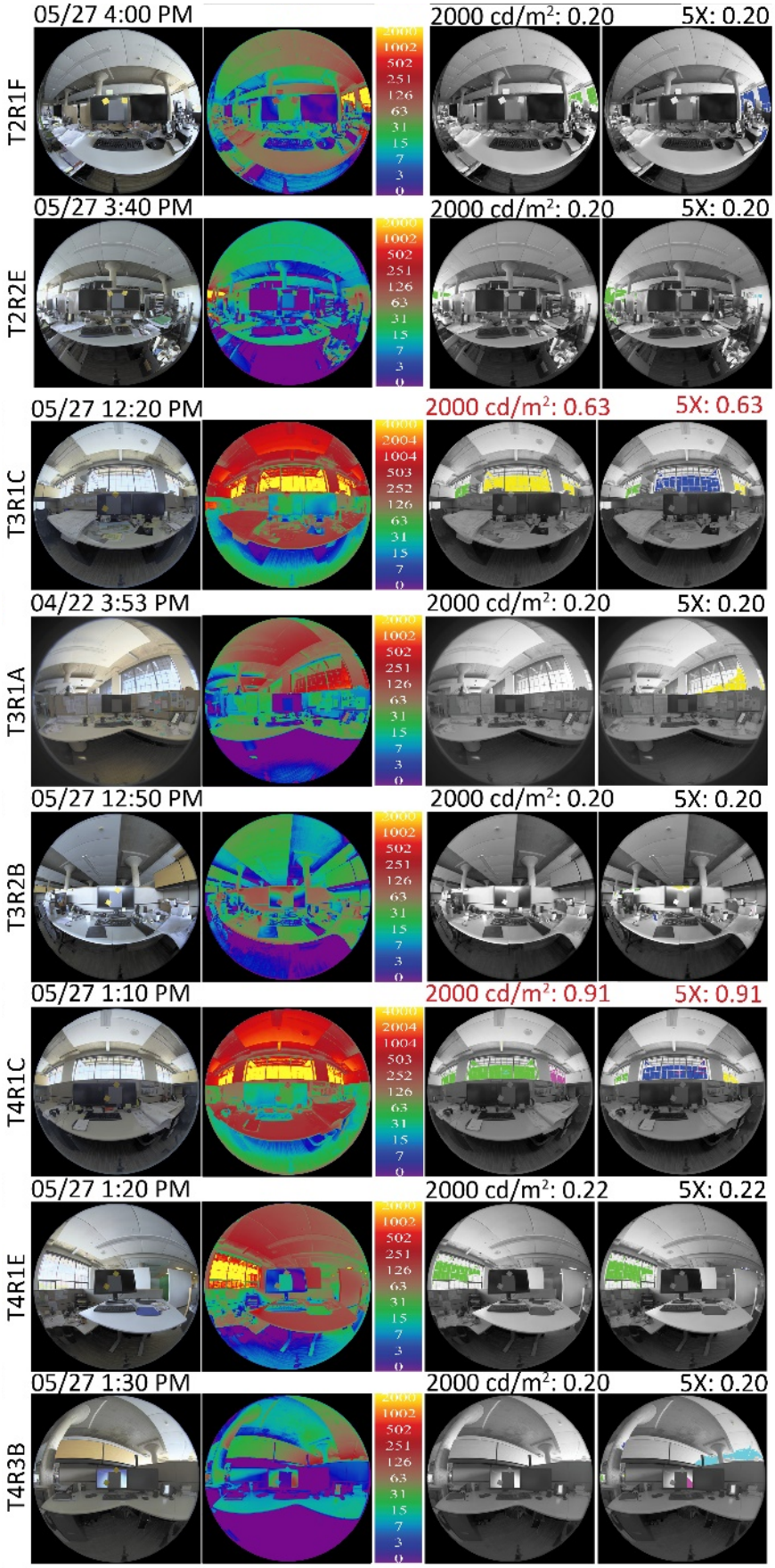

Figure 4.14: The HDR images, falsecolor images, and DGP analysis of twelve scenes at HGA

Figure 4.14 presents the HDR images, falsecolor images, and DGP analysis of twelve scenes, three scenes in each tier. Scene T1R3E and Scene T1R5B showed noticeable difference of daylighting distributions due to the distance between workstations and the southwest façade. The longer the distance between a workstation and the windows, the lower the luminance distributions. In other words, sitting closer to the windows increased the percent of glazing areas within a scene and resulted in greater luminance distributions. The seating orientation also had great impact on daylighting performance. The workstations facing towards the windows, like Scenes T3R1C and T4R1C, presented much greater luminance values than the remaining scenes. Compared with the original tiers (Tiers One, Three, and Four), the HDR images taken in Tier Two displayed much lower luminance distributions. The DGP results showed that Scenes T1R3E, T3R1C, and T4R1C had glare, which were attributed to the seating orientation. The occupants who faced towards the windows suffered from severe visual discomfort. In other words, facing towards the windows resulted in larger solid angles subtended by the windows with respect to an occupant's eyes and high risk of seeing the sun.

4.4.5 Lighting Distributions at AUP

Figure 4.15 illustrates the five offices for taking HDR images from the second to the fourth floors at AUP. Figure 4.16 displays the HDR images, falsecolor images, and the DGP analysis of the HDR images taken on both the sunny and cloudy days. Scenes One, Two, and Three, which were taken in three east-facing offices, demonstrated gradual increase of luminance on both the sunny and cloudy days. The gradually changing luminance distributions were attributed to the effects of both different floors and the outside deciduous trees. Scene One's windows on the second floor were mostly covered by leaves and presented low lighting levels. Scene Three's window on the fourth floor was above the trees and

presented greater lighting levels, while the windows in Scene Two were between the two conditions.

Additionally, the noticeable differences of luminance values between Scenes Four and Five demonstrated the effect of the blockage by the opposite buildings. Compared with Scene Four, a larger portion of the window in Scene Five on the third floor was obstructed by the Biological Department across. The DGP results showed that these five scenes barely had visual discomfort during the data collection. However, both Scenes Two and Three captured the morning sunlight falling on the desks and the monitors, which is the same condition that DGP failed to detect at CCL.

Figure 4.15: The select offices at AUP where HDR images were taken

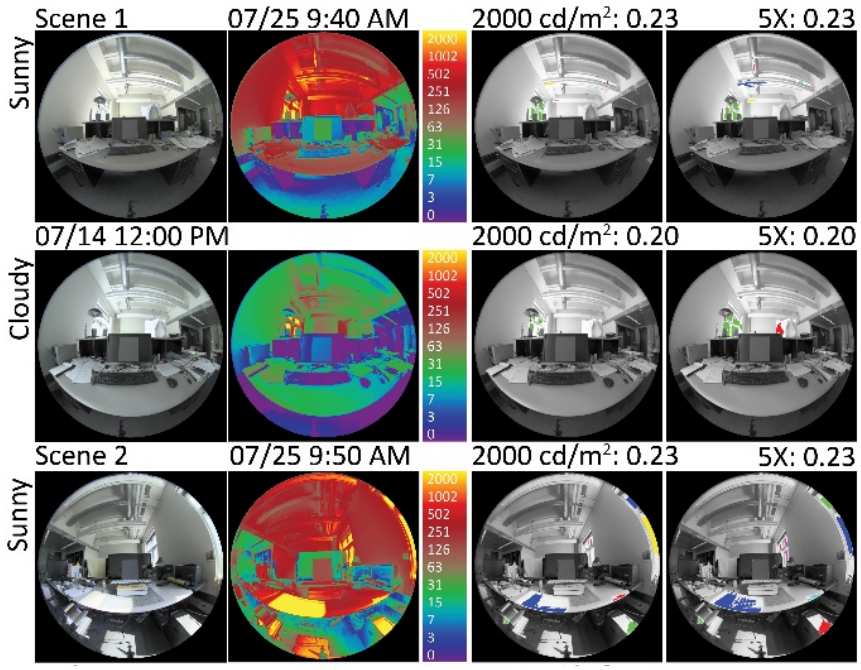

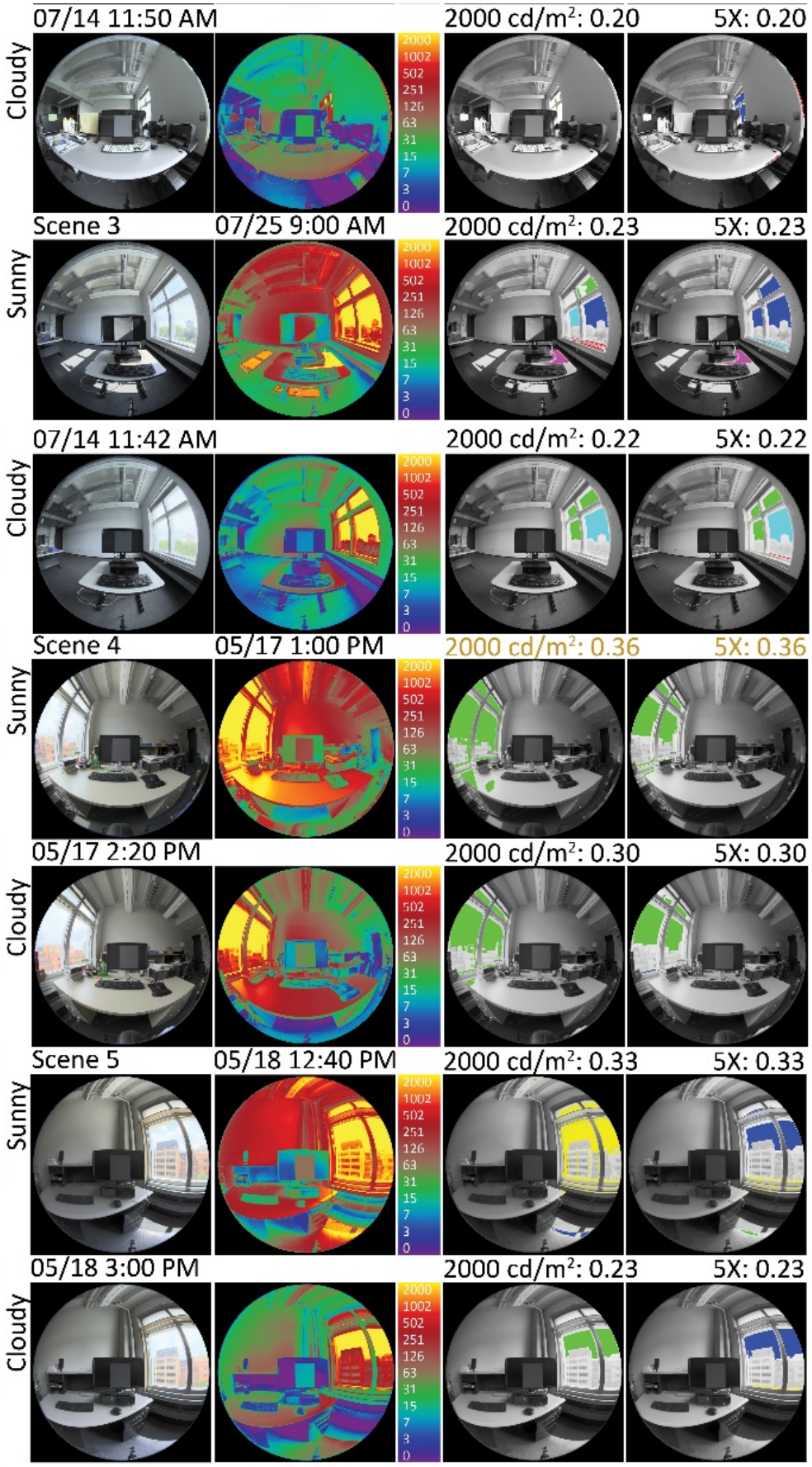

Figure 4.16: The HDR images, falsecolor images, and DGP analysis of five rooms at AUP

4.4.6 Five Buildings Summary

As shown in Table 4.2, 44 scenes were selected to represent the lighting distributions across the five buildings as comprehensively as possible. Table 4.2 includes each scene's number and the sky condition under which this HDR image was taken. "S" represents sunny days, while "C" represents cloudy days. Table 4.2 also summarizes the aperture design and shading devices of each scene, along with the camera's direction. M19 and M22 displayed the changes of luminance distributions caused by the changed positions of interior mechoshades for S19 and S22, respectively. Since CSM had extreme daylight distributions, the HDR images taken at CSM on sunny days had an individual legend in greater luminance range. Although S10, S11, S21, M19, and M22 were also taken under sunny days, the lower luminance distributions at these scenes led them to be grouped with the overcast conditions.

Table 4.2: Summary of the analyzed HDR images

Image No.	Building	Space	Camera direction	Sky	Aperture design	Thumbnail	Falsecolor image
S01	CSM	Lobby & common spaces	Southeast	Sunny	Curtain walls		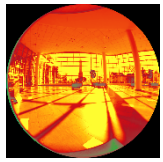
S02	CSM	Lobby & common spaces	South	Sunny	Curtain walls		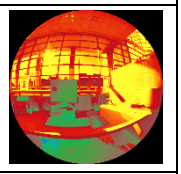
S03	CSM	Lobby & common spaces	East	Sunny	Curtain walls		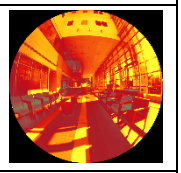
S04	CSM	Lobby & common spaces	East	Sunny	Curtain walls	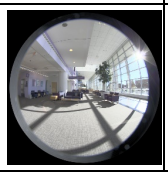	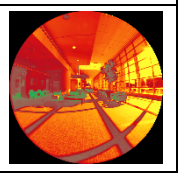
S05	CSM	Lobby & common spaces	West	Sunny	Curtain walls		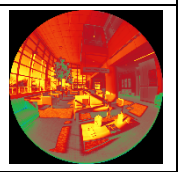
Legend		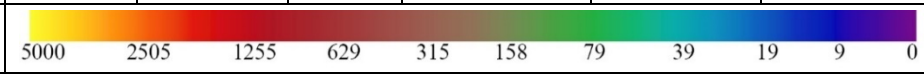					

Table 4.2: Summary of the analyzed HDR images (continued)

Image No.	Building	Space	Camera direction	Sky	Aperture design	Thumbnail	Falsecolor image
S06	CCL	Study area on the first floor	East	Sunny	Curtain walls + exterior brise soleils		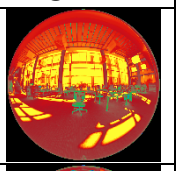
S07	CCL	Study area on the first floor	South	Sunny	Curtain walls + exterior brise soleils + interior mechoshade		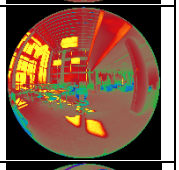
S08	CCL	Study area on the first floor	Southeast	Sunny	Curtain walls + exterior brise soleils + interior mechoshade		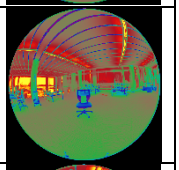
S09	CCL	Study area on the first floor	North	Sunny	Curtain walls + exterior brise soleils		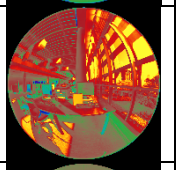
S12	ALF	North-facing private office	North	Sunny	Sidelight + 0.6 meters roof overhangs		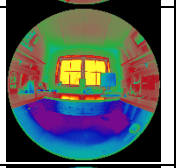
S13	ALF	Exhibit space	West	Sunny	Top sidelight + 0.6 meters roof overhangs		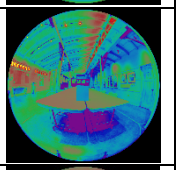
S14	ALF	Southern Corridor adjacent to the open-plan office	East	Sunny	Sidelight + 0.9 meters roof overhangs		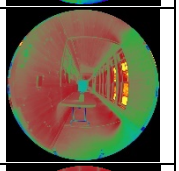
S15	ALF	West-facing meeting hall	West	Sunny	Sidelight + 0.6 meters roof overhangs		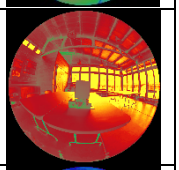
S16	ALF	South-facing open-plan office	South -east	Sunny	Secondary sidelight + 1.9 meters corridor		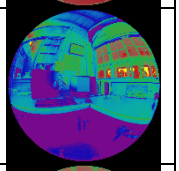
S17	ALF	West-facing private office	North	Sunny	Sidelight		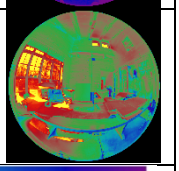
Legend		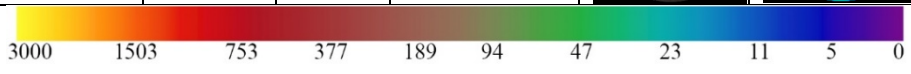 3000 1503 753 377 189 94 47 23 11 5 0					

Table 4.2: Summary of the analyzed HDR images (continued)

Image No.	Building	Space	Camera direction	Sky	Aperture design	Thumbnail	Falsecolor image
S18	HGA	Southwest-facing open-plan office	Tier One Row One South	Sunny	Sidelight + exterior overhang		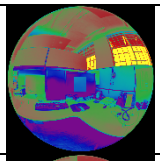
S19	HGA	Southwest-facing open-plan office	Tier One Row Three Southwest	Sunny	Sidelight + exterior overhang	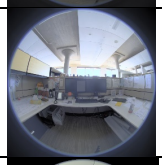	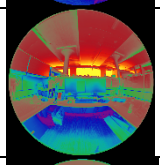
S20	HGA	Southwest-facing open-plan office	Tier Two Row One Northwest	Sunny	Sidelight + exterior overhang		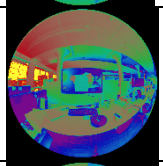
S22	HGA	Southwest-facing open-plan office	Tier Three Row Two Northeast	Sunny	Sidelight + exterior overhang		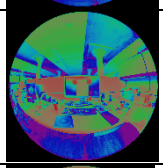
S23	HGA	Southwest-facing open-plan office	Tier Three Row One South	Sunny	Sidelight + exterior overhang		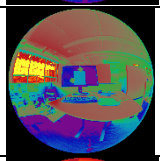
S24	HGA	Southwest-facing open-plan office	Tier Four Row One Southwest	Sunny	Sidelight + exterior overhang	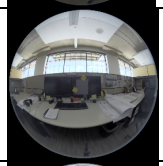	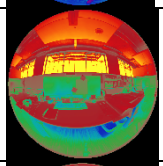
S25	AUP	East-facing Office 283	South	Sunny	Sidelight		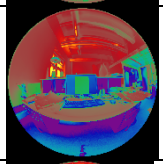
S26	AUP	East-facing Office 383	North	Sunny	Sidelight	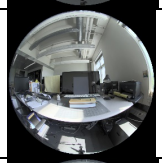	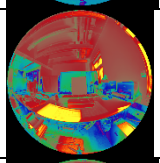
S27	AUP	East-facing Office 479	North	Sunny	Sidelight		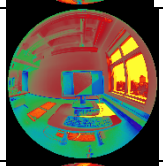
S28	AUP	South-facing Office 362	Southeast	Sunny	Sidelight		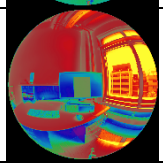
S29	AUP	South-facing Office 422	West	Sunny	Sidelight		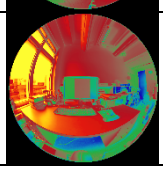
Legend		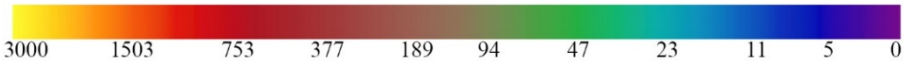					

Table 4.2: Summary of the analyzed HDR images (continued)

Image No.	Building	Space	Camera direction	Sky	Aperture design	Thumbnail	Falsecolor image
C01	CSM	Lobby & common spaces	Southeast	Cloudy	Curtain walls		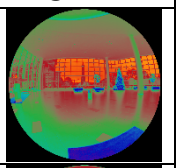
C02	CSM	Lobby & common spaces	South	Cloudy	Curtain walls		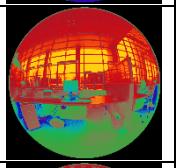
C03	CSM	Lobby & common spaces	East	Cloudy	Curtain walls	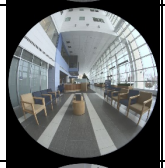	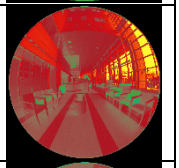
C04	CSM	Lobby & common spaces	East	Cloudy	Curtain walls		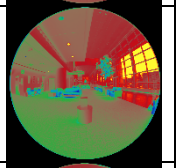
C05	CSM	Lobby & common spaces	West	Cloudy	Curtain walls		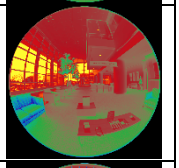
C06	CCL	Study area on the first floor	East	Cloudy	Curtain walls + exterior brise soleils		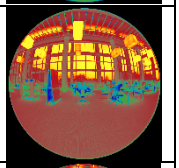
C07	CCL	Study area on the first floor	South	Cloudy	Curtain walls + exterior brise soleils		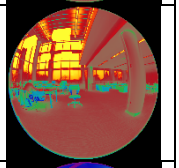
C08	CCL	Study area on the second floor	Southeast	Cloudy	Curtain walls + exterior brise soleils	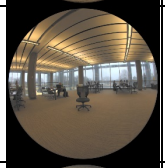	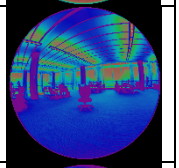
S10	ALF	South-facing open-plan office	East	Sunny	Top + middle sidelight + 0.9 meters roof overhangs		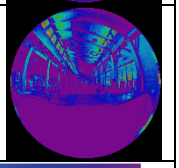
Legend		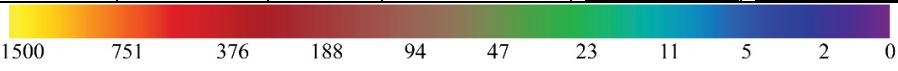					

Table 4.2: Summary of the analyzed HDR images (continued)

Image No.	Building	Space	Camera direction	Sky	Aperture design	Thumbnail	Falsecolor image
S11	ALF	South-facing open-plan office	West	Sunny	Top + middle sidelight + 0.9 meters roof overhangs		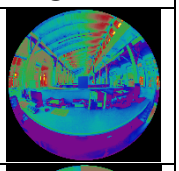
M19	HGA	Southwest-facing open-plan office	Tier One Row Three Southwest	Sunny	Sidelight + exterior overhang + interior mechoshade	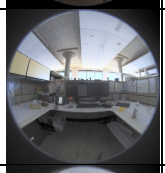	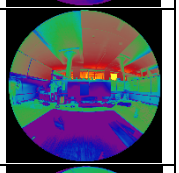
S21	HGA	Southwest-facing open-plan office	Tier Two Row Two Southeast	Sunny	Sidelight + exterior overhang	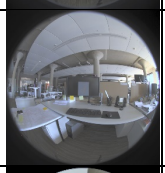	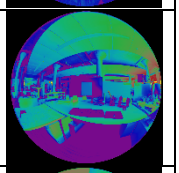
M22	HGA	Southwest-facing open-plan office	Tier Three Row Two Northeast	Sunny	Sidelight + exterior overhang + interior mechoshade		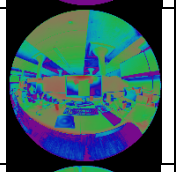
C25	AUP	East-facing Office 283	South	Cloudy	Sidelight	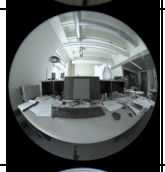	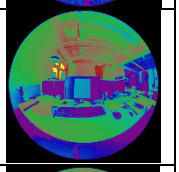
C26	AUP	East-facing Office 383	North	Cloudy	Sidelight		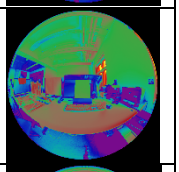
C27	AUP	East-facing Office 479	North	Cloudy	Sidelight		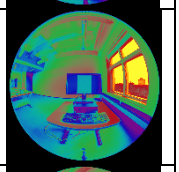
C28	AUP	South-facing Office 362	Southeast	Cloudy	Sidelight		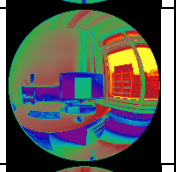
C29	AUP	South-facing Office 422	West	Cloudy	Sidelight		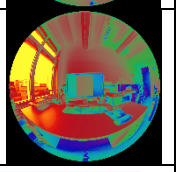
Legend		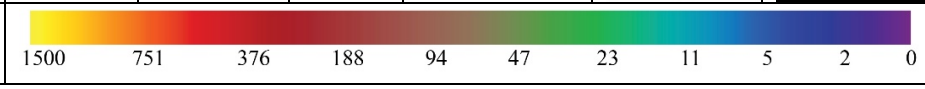					

Table 4.3: Summary of glare analysis across the five buildings

	Studied space	Scene No.	E_v	DGP	DGI	UGP	WFR (%)	WWR (%)	Glazing Trans.
CSM	Lobby & common spaces	S1	13,210	0.93	28.0	0.77			0.70
		C1	817	0.22	15.3	0.50			
		S2	15,946	0.67	22.1	0.59			
		C2	1009	0.22	6.9	0.14			
		S3	5,978	0.53	20.0	0.62			
		C3	641	0.20	8.6	0.36			
		S4	5,732	0.51	17.9	0.57			
		C4	424	0.19	10.1	0.38			
		S5	4,649	0.45	18.4	0.56			
		C5	738	0.22	15.6	0.50	78.7	72.4	
CCL	Study areas	S6	8,994	0.72	24.3	0.69	54.9	81.7	0.65
		C6	1,057	0.23	11.5	0.42			
		S7	2,276	0.31	17.2	0.55			
		C7	1,090	0.23	10.7	0.43			
		S8	854	0.25	19.3	0.58			
		C8	32	0.01	6.9	0.26			
		S9	2,612	0.33	18.2	0.55			
ALF	Open-plan office	S10	12	0.00	4.5	0.20			0.45
		S11	69	0.02	11.5	0.37			
		S16	142	0.07	14.8	0.49	10.6	21.2	
	North-facing private office	S12	3,664	0.43	26.2	0.75	17.0	23.1	
	Exhibit space	S13	137	0.06	10.6	0.34	2.5	4.5	
	Southern corridor	S14	736	0.24	18.2	0.56	37.6	26.1	
	Meeting hall	S15	8,555	0.72	27.9	0.74	44.6	34.0	
	West-facing private office	S17	1,247	0.27	20.5	0.61	27.7	22.5	
HGA	Open-plan office	S18	650	0.22	18.0	0.57			0.72
		S19	3,756	0.47	30.3	0.78			
		M19	270	0.20	17.5	0.56			
		S20	460	0.23	17.9	0.58			
		S21	29	0.01	8.1	0.30			
		S22	65	0.07	3.5	0.28			
		M22	151	0.01	7.3	0.20			
		S23	1,048	0.26	17.5	0.62			
		S24	11,985	0.92	30.8	0.80	13.5	64.1	
AUP	Office 283	S25	647	0.20	9.5	0.38			0.71
		C25	117	0.05	14.3	0.48	16.9	26.0	
	Office 383	S26	1,263	0.27	20.7	0.60			
		C26	115	0.04	11.6	0.40	16.9	26.0	
	Office 479	S27	1,847	0.29	21.3	0.62			
		C27	615	0.22	15.9	0.57	13.5	24.2	
	Office 326	S28	2,757	0.34	20.4	0.61			
		C28	644	0.21	13.6	0.52	22.7	30.1	
	Office 422	S29	3,073	0.36	18.5	0.59			
		C29	992	0.23	13.5	0.50	19.7	30.1	

Table 4.3 lists the DGP, DGI, UGR, and E_v of the 44 scenes, along with the WFR, WWR, and glazing transmittance of each studied space. Black, green, blue, and red results of DGP and DGI represent imperceptible, perceptible, disturbing, and intolerable degrees of glare, respectively. Red UGR and E_v results indicate the existence of glare, while black results mean imperceptible glare.

CSM had the greatest WFR (78.7%), the second greatest WWR (72.4%), and the glazing in high transmittance (0.7). Without any designed shading device, occupants at CSM suffered from severe visual discomfort on sunny days, which was mainly caused by direct sunlight and views of the sun. According to the occupants, the lower sun angles during the winter led to worse conditions. CCL had the second greatest WFR (54.9%) and the greatest WWF (81.7%). Contrary to CSM, CCL employed both external brise soleils and internal movable mechoshades to control glare. Although sunlight penetrated through the eastern brise soleils and caused visual discomfort, occupants had multiple choices of seating positions. Figure 4.17 presented the workstations occupied by students and faculty members on the overcast day (left) and the sunny day (right). On the overcast day, the occupied workstations scattered randomly in the study areas. On the sunny day, however, occupants selected the workstation in shadows. According to the staff members at CCL, faculty members and student were satisfied with the daylighting environments in the studied areas at CCL.

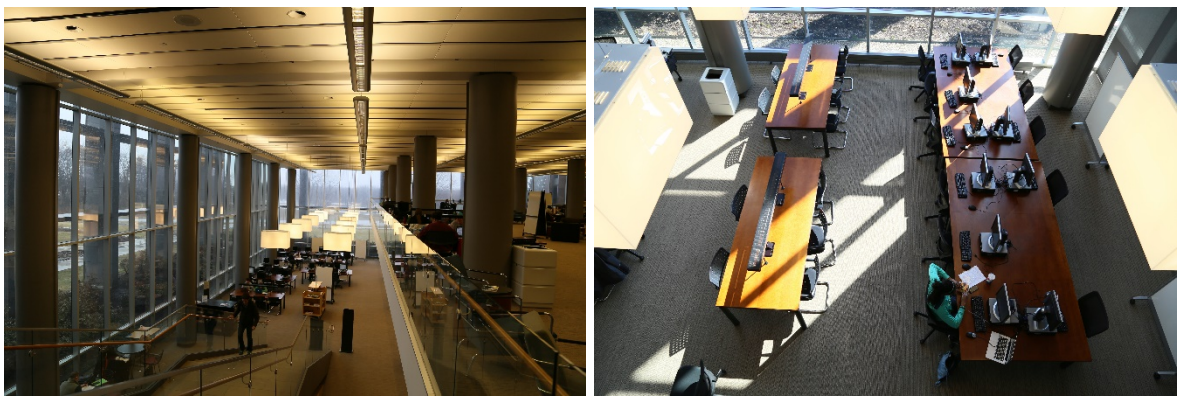

Figure 4.17: Students' way of occupying workstations on the overcast day (left) and sunny day (right) (Courtesy of D. Michael Utzinger)

ALF possessed multiple small windows in the lowest transmittance (45%), which led to relatively lower WFRs varying between 2.5% and 44.6% as well as lower WWRs varying between 4.5% and 34%. For example, the exhibit space had sixteen 0.5-by-0.6 meters top-side windows on the northern elevation and twenty 0.3-by-0.3 meters top-side windows on the southern elevation. Moreover, the roof overhangs, either 0.6 meters or 0.9 meters deep, effectively blocked direct sunlight over the summer. S10, S11, S13, and S16 reflected the glare free conditions in both the open-plan office and exhibit space. However, the strict controls of daylighting designs led to artificial lights on as the supplementary lighting source in these two rooms. Since northern windows merely introduced diffuse skylight into the offices, high contrasts between a task area and the background glazing caused visual discomfort in S12. No occupant at ALF reported any visual discomfort. Nonetheless, these daylighting design strategies restricted daylight and sometimes deprived the occupants of dynamic changes of daylight.

HGA utilized the glazing in the highest transmittance (72%) of the five buildings. It also had the greatest WWR (64.1%) of the three sidelight buildings (ALF, HGA, and AUP). Despite the exterior static overhangs and interior movable mechoshades, some staff members complained about the glare caused by daylight. DGP, DGI and E_v revealed that S19 and S24, the workstations facing the southwest windows, had visual discomfort.

Finally, the five offices at AUP had similar WFRs varying between 13.5% and 22.7% and WWRs varying between 24.2% and 30.1%. Since every office provided interior venetian blinds with occupants, no occupants reported glare. Figure 4.18 demonstrate luminance differences caused by venetian blinds in Office 326. With the venetian blinds down, the scene with perceptible glare was decreased to imperceptible glare. Rather than taking the HDR image from the faculty's perspective, it was taken from a student's perspective to demonstrate the bright window background. Furthermore, when the HDR images were taken,

the five deciduous trees outside protected a majority of direct sunlight from Office 283 and partial direct sunlight from Office 326. According to the occupants in the east-facing offices, even though these trees blocked direct sunlight in the morning, they also prevented diffused skylight in the afternoon and led to gloomy lighting environments.

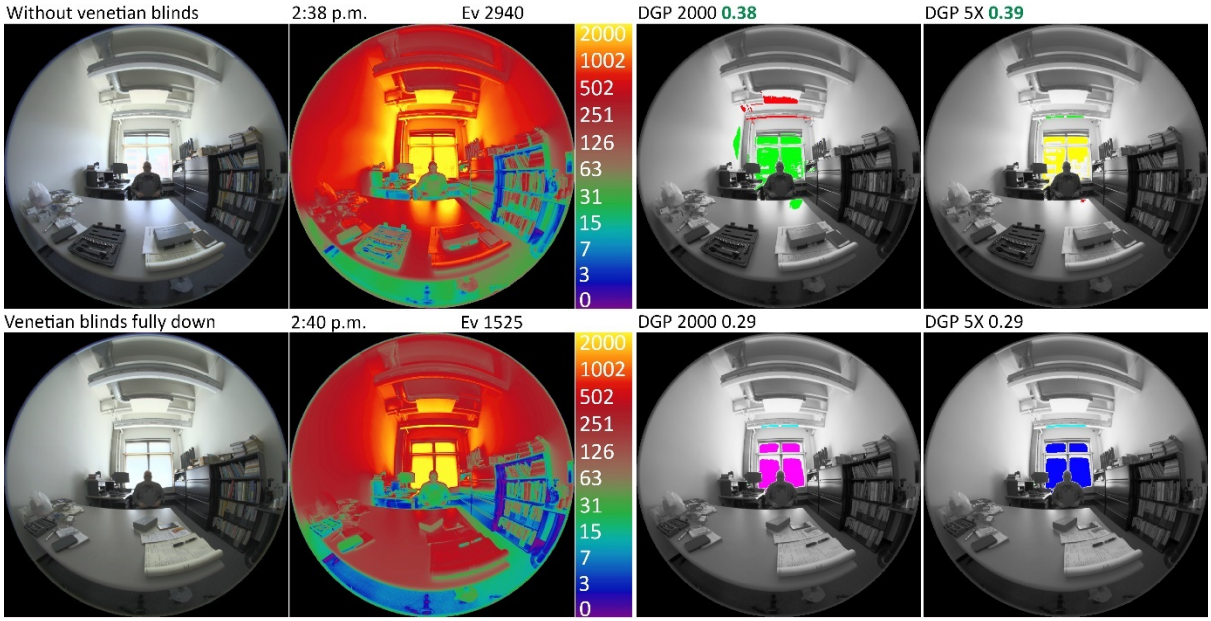

Figure 4.18: Different DGP results caused by interior venetian blinds from a student's perspective

Based on the glare analysis and occupants' feedback, CSM was the building with the most severe visual discomfort caused by daylight. CCL's lighting environments were comfortable for occupants who had flexibility in choosing seating positions. HGA had uncomfortable lighting environments for a portion of occupants, especially the ones facing towards windows or sitting close to windows. AUP had comfortable lighting environments because occupants were capable of controlling internal blinds. Finally, ALF had strictly controlled lighting environments without visual discomfort.

4.5 DISCUSSION

4.5.1 Impacts of Daylighting Buffer Zones

In addition to the aperture designs and shading devices that laid a foundation for interior daylighting environments, the analysis of these five buildings revealed the impact of daylighting buffer zones on daylighting performance.

Daylighting buffer zones were commonly employed in different forms across these buildings. Both CSM and HGA placed circulations adjacent to the facades to separate the main function areas from the glazing. By placing café tables along the eastern curtain walls, CCL generated an effective daylighting buffer zone that separated the study areas from the direct sunlight which penetrated through the eastern curtain walls. ALF had a southern corridor adjacent to the exterior southern wall, which mainly provided secondary diffuse daylight for the open office.

Although four buildings employed daylighting buffer zones in diverse forms, not every buffer zone functioned as the way it was expected to. As the curtain walls in the lobby and common spaces at CSM reached 11.6 meters high, the 3.6 meters wide circulation was insufficient to alleviate direct sunlight falling on occupants. Hence, the buffer zone at CSM had no effect of glare reduction. Conversely, enlarging the distance between the southwest windows and the workstations by 2.3 meters, the enlarging space in Tier Two at HGA successfully avoided direct sunlight falling on most of the occupants. S21 and S22 in Tier Two presented much lower E_v, DGP, and DGI results. In other words, sufficient spacing between glazing and main function areas can effectively mitigate the glare caused by direct sunlight. Furthermore, partitions improve a daylighting buffer zone's function. The wooden wall designed between the corridor and the open office effectively blocked direct sunlight. Compared with the lighting distributions within the corridor (S14), the open office presented much lower lighting distributions (S10, S11, and S16). Different effects of these buffer zones across the four buildings demonstrate that a buffer zone can alleviate daylight glare but cannot compensate for errors in daylighting designs.

4.5.2 Inconsistency of Visual Discomfort Metrics

Figure 4.19 demonstrates the results of DGP, normalized DGI, UGP, and E_v of all 44 scenes. The left vertical axis presents DGP, DGI, and UGP results, while the right vertical

axis presents E_v in lux. The results were separated based on sky conditions, buildings, and then organized based on E_v from great to low values. The profiles of normalized DGP in the red line and UGP in the grey line had similar trend. The profiles of DGP and E_v also had similar trend. Given that the formula of DGP includes E_v as an important element, the change of E_v greatly influences DGP results.

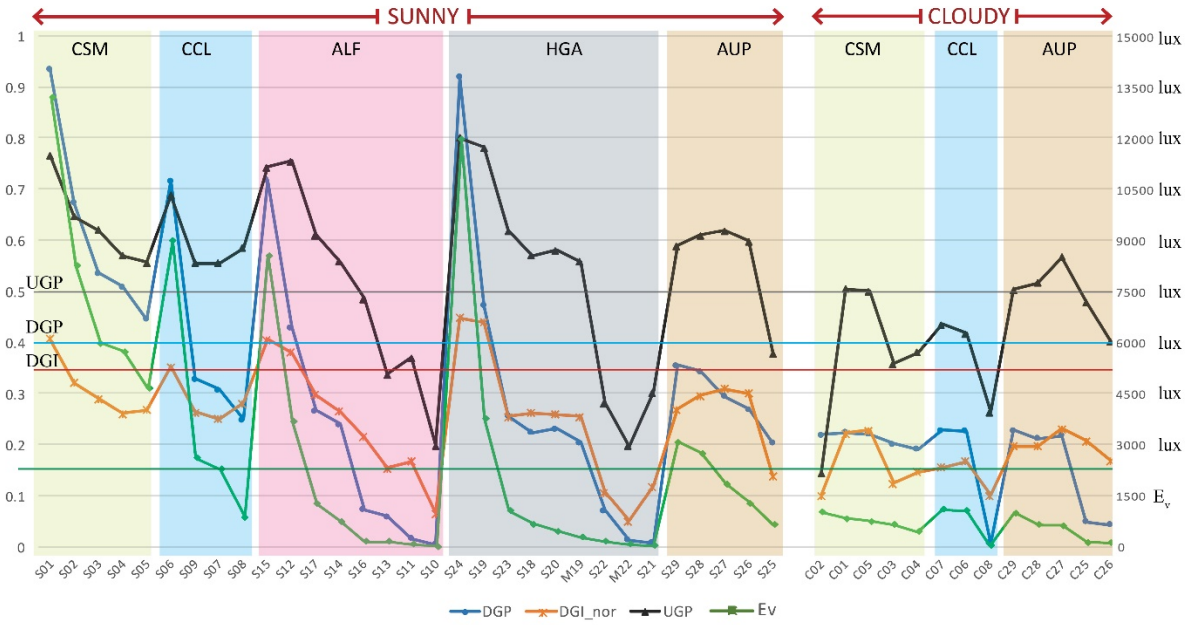

Figure 4.19: Glare indices profiles of 44 scenes

The four metrics employed in this chapter demonstrated inconsistency in terms of identifying visual discomfort, which is in line with previous studies' conclusions (Jakubiec et al., 2015). Compared with DGP, DGI underestimated ten of 29 scenes under sunny days in terms of glare degrees, five of which included sunlight penetration in the scenes. For example, DGP defined all five scenes at CSM as intolerable glare, while DGI detected perceptible or disturbing glare. On the other hand, DGP failed to identify visual discomfort issues in five scenes (S7, S9, S17, S26, S27) where direct sunlight fell on monitors and/or desks. However, both DGI and UGP presented relatively consistent results of these five scenes. Furthermore, UGP overestimated seven scenes (C1, C5, M19, S20, C27, C28, and C29), five of which were taken under cloudy conditions, and one of which had mechoshade down. Both DGI and UGR are more sensitive to detect the scenes with lower degrees of

visual discomfort, like S14, S17, S18, S26, S27, and S28. Unlike the previous studies that was either conducted through simulations (Jakubiec & Reinhart, 2012) or in one sidelight office (Van Den Wymelenberg, 2012), this chapter investigated the inconsistency of glare indices across different buildings. Through the field measurements, this chapter broadened the variety of building contexts and enriched interior spatial configurations. The inconsistent results of DGP, DGI, UGP, and E_v showed the necessity of employing multiple metrics to reveal visual discomfort caused by different factors, such as direct sunlight, reflections on monitors, or high contrast between a task area and the background (Jakubiec & Reinhart, 2012). The glare analysis comparisons of 44 scenes indicated that DGI underestimated most of the scenes with intolerable glare, especially under the condition where the sun was visible. UGP overestimated some scenes with imperceptible glare under either sunny or cloudy sky conditions. DGP was capable of revealing glare with intolerable or imperceptible glare. However, DGP failed to detect most of the scenes with disturbing or perceptible glare, which were mostly identified by DGI.

4.6 LIMITATIONS

Although this chapter presented all the HDR images together, it demonstrated the author's procedure of learning and modifying the HDR image technique from 2012. Luminous overflow occurred during the early data collection, especially at CSM, the first building for practicing the HDR image technique. Seven of the nine scenes at CSM included the sun in the HDR images. As glare at CSM was too severe, DGP still detected intolerable glare of all these seven scenes at CSM. However, the luminance values in real world at CSM should be greater. S6 at CCL and S15 at ALF presented luminous overflow with the E_v over 5,000 lux (Jakubiec et al., 2016). This error can be solved by measuring the vertical illuminance in front of a lens before and after taking LDR images, which was employed while taking HDR images at HGA.

4.7 CONCLUSION

This chapter presents the field measurement of lighting distributions via the HDR image technique across five buildings. Within the five buildings, ALF created well-controlled daylighting environments for occupants; AUP provided controls of interior blinds with occupants to reduce glare; CCL generated comfortable daylighting environments by offering both solar controls and multiple seating positions for occupants; HGA limited occupants' controls over their lighting environments and resulted in glare for a portion of occupants; finally, CSM had the most severe glare with the lack of shading devices of the curtain-wall façade.

The comparison of glare analysis across five buildings demonstrated the consistent problem of DGP, DGI, and UGP. Due to the overestimation of UGP, the following studies exclude UGP. This chapter recommends integrating DGP, DGI, with E_v to detect glare in sidelit spaces. E_v functions as a testing factor. The scenes with E_v values greater than 1,000 lux and the existence of direct sunlight should be examined by DGI, since DGP failed to detect most of the disturbing and perceptible glare scenes that DGI identified.

Apart from capturing luminance values within existing spaces, HDR image techniques can also be utilized to calibrate simulation models. Unlike HDR images that only provide instantaneous lighting data, simulations produce lighting data for existing or design projects in a long term, like Useful Daylight Illuminances (UDI) (Nabil & Mardaljevic, 2006) and Daylight Autonomy (DA) (C. F. Reinhart, Mardaljevic, & Rogers, n.d.; C. F. Reinhart & Walkenhorst, 2001) calculations. The following chapter presents the procedure of simulating accurate luminance maps under CIE and Perez sky models.

5 SIMULATED LUMINANCE MAPS WITH ACCURATE GLARE PREDICTION

This chapter introduces another method, simulations, to generate HDR files that provide luminance values at pixel levels. The procedures of generating Radiance models for daylight simulations are elaborated. Two buildings, CSM and AUP, are used as the example. The HDR images taken in both buildings, which were processed glare analysis in the previous chapter, were continuously utilized in this chapter. Two commonly used sky models, Generic CIE sky models and Perez all-weather sky model, are employed in simulations. In order to explore the accuracy of these two sky models, falsecolor images, DGP, and E_v are calculated as the criteria. Finally, the causes of discrepancies in simulation are discussed.

5.1 RESEARCH OBJECTIVES

The objectives of this chapter are to elaborate the typical flow of simulating luminance maps, to compare the accuracy of CIE sunny and overcast skies with the Perez all-weather sky model in terms of visual discomfort prediction, and to investigate the accuracy of the Perez all-weather sky model with the weather data measured onsite.

5.2 RESEARCH QUESTION

This chapter mainly answers one question: compared with field measurements, how accurate are simulated luminance maps generated by Radiance models?

5.3 METHODOLOGY

5.3.1 Vertical Eye Illuminance Validation

An independent validation study was conducted to compare measured E_v and E_v calculated from interior HDR images. HDR images were taken in Office 326 on May 22nd when the LI-210R photometric sensor placed besides the camera was recording vertical illuminance. The procedures of taking HDR images were introduced in Chapter Three.

5.3.2 Daylight Simulation

A model for lighting simulations is comprised of three parts: a geometric model, material properties, and lighting sources (sky models for daylight simulations). Figure 5.1 illustrates the three components and the simulation flow. Rhino was used to build geometric models. Other software like Revit and Sketchup are also applicable. When modelling a building or a space, the objects should be organized in different layers based on their material properties. After setting a view, either Generic CIE skies or Perez all-weather skies are applied to generate a luminance map.

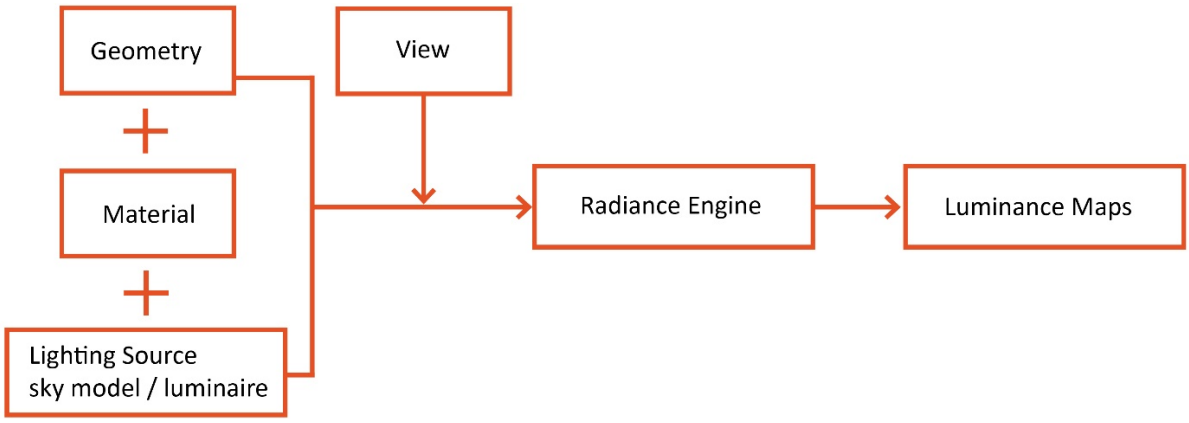

Figure 5.1: Lighting simulation procedure

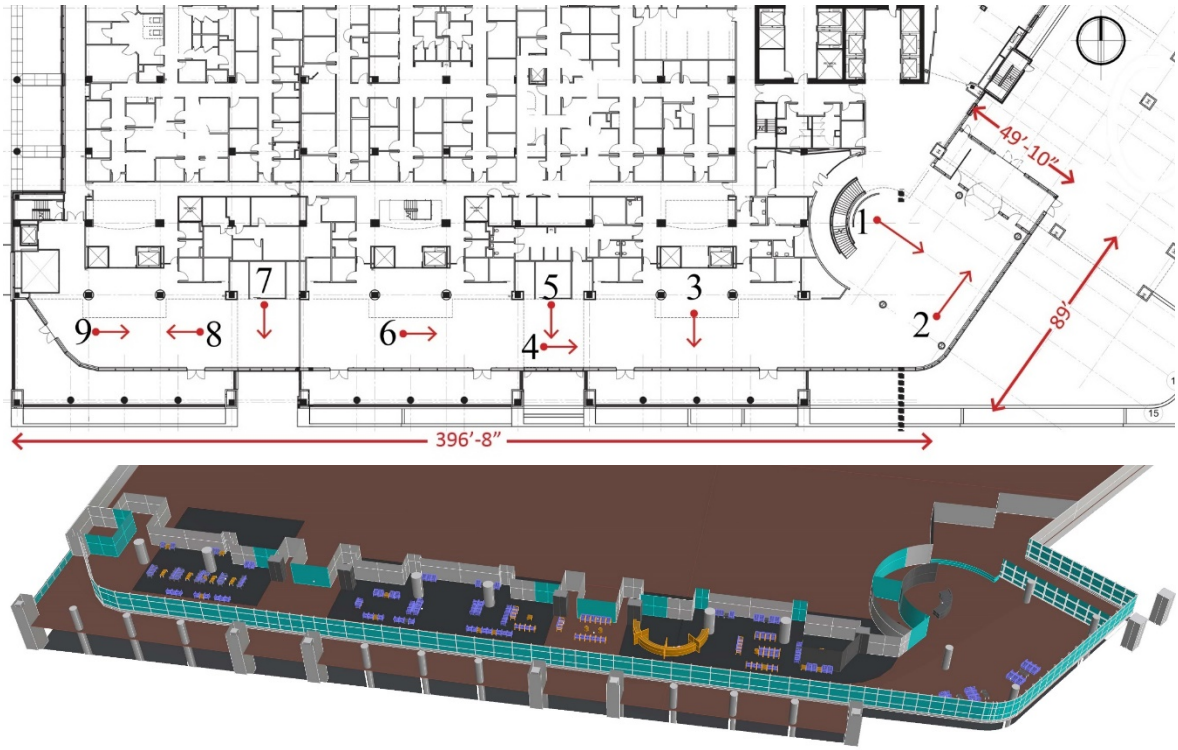

Figure 5.2: The layout and geometric model of the lobby and common spaces at CSM

5.3.2.1 Building Geometry

In order to guarantee the accuracy of a simulation model, onsite measurement and construction documents of a studied space are recommended. The objects that play important roles in interior lighting distributions, like tables, monitors, window frames, and shading devices, should be built in a model. Figure 5.2 (top) shows CSM's layout and Figure 5.2 (bottom) shows the interior perspective of the model. Figures 5.3 to 5.5 show the layouts and perspectives of Office 326, Office 422, and Office 479 at AUP. These perspectives were exported from the Rhino models as an example to show the modelling details. The red arrows on the layouts illustrate the occupants' position in the spaces, where the HDR images and simulated luminance maps were generated. These spaces include diverse orientations from east, south, to southwest.

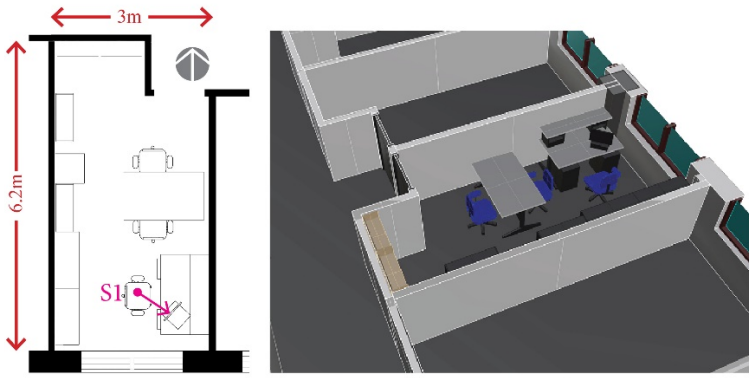

Figure 5.3: The layout and geometric model of Office 326 at AUP

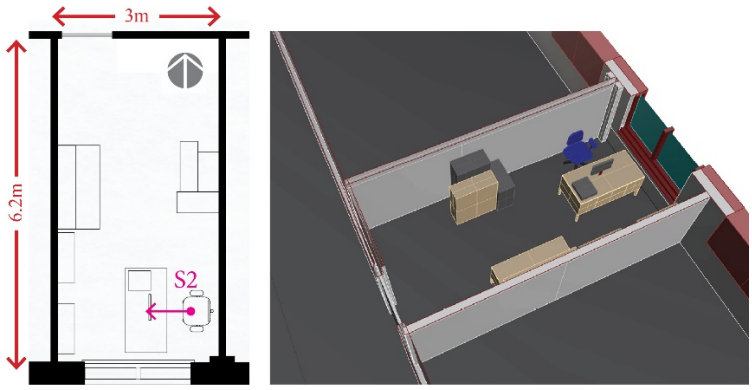

Figure 5.4: The layout and geometric model of Office 422 at AUP

5.3.2.2 Material Properties

Material properties should be measured on site. Throughout this research, the luminance meter, Gossen Starlite 2 was used to measure the reflected light from both an unknown material and an 18%

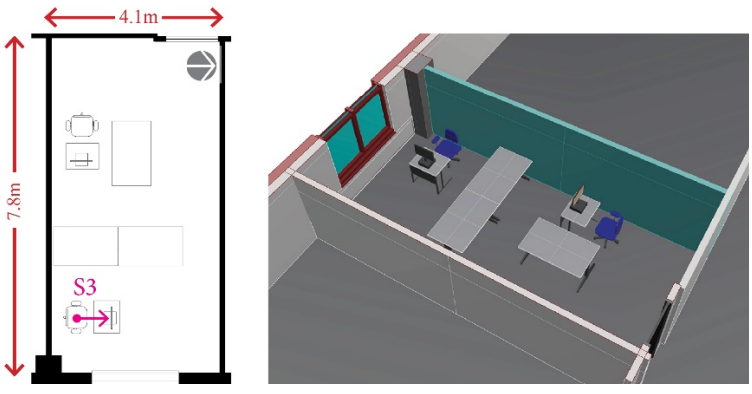

Figure 5.5: The layout and geometric model of Office 479 at AUP

grey card under consistent lighting environments. Then this unknown material's reflectance was calculated in Equation 5.1 (M. Dubois, 2001):

$$Ref_{material} = 0.18 \text{ x } \frac{L_{material}}{L_{grey\ card}} \quad Equation\ 5.1$$

where $L_{material}$ represents the measured luminance value from an unknown material, $L_{grey\ card}$ represents the measured luminance value from an 18% grey card, and $Ref_{material}$ indicates the unknown material's reflectance. In order to minimize the discrepancy caused by manual measurement, all the materials' reflectance were the averages of four or five measurements. The transmittance of the glazing in the three buildings were obtained from the construction documents and manufactories. The material properties are listed in Table 5.1.

Table 5.1: Select Radiance material definitions at CSM and AUP

Building	Material	Radiance material
CSM	Glazing	void glass glazing 0 0 3 0.73 0.73 0.73
	Mullion	void metal mullion 0 0 5 0.28 0.28 0.28 0.667 0.01
	Light floor	void plastic light_floor 0 0 5 0.475 0. 475 0. 475 0.05 0.01
	Dark floor	void plastic dark_floor 0 0 5 0.19 0.19 0.19 0 0.1
	Column & ceiling	void plastic column 0 0 5 0.72 0.72 0.72 0 0.1
	Sofa	void plastic column 0 0 5 0.07 0.07 0.07 0 0.15
	Dark wall	void plastic dark_wall 0 0 5 0.157 0.157 0.157 0 0.08
	Light wall	void plastic light_wall 0 0 5 0.22 0.22 0.22 0.02 0.05
	Wooden partition	void plastic partition 0 0 5 0.295 0.295 0.295 0 0.05
AUP	Black cabinet	void metal black_steel 0 0 5 0.025 0.025 0.025 0.667 0.15
	Glazing	void glass glazing 0 0 3 0.80 0.80 0.80
	Door	void plastic door 0 0 5 0.037 0.037 0.037 0.067 0.08
	Carpet	void plastic carpet 0 0 5 0.055 0.055 0.055 0 0.2
	Ceiling & wall	void plastic ceiling 0 0 5 0.721 0.721 0.721 0.005 0.08
	Column	void plastic column 0 0 5 0.445 0.445 0.445 0.0 0.1
	Bookshelf	void plastic bookshelf 0 0 5 0.229 0.229 0.229 0.05 0.1
	Blue wall in Office 479	void plastic bluewall 0 0 5 0.546 0.546 0.546 0.01 0.1
	Window frame	void metal black 0 0 5 0.55 0.55 0.55 0.7 0
	Outside ground	void plastic OutsideGround 0 0 5 0.1 0.1 0.1 0 0
	Surrounding buildings	void plastic OutsideBuilding 0 0 5 0.2 0.2 0.2 0 0

5.3.2.3 Sky Model

Both generic CIE sky models and the Perez all-weather sky model were employed in this chapter. Of the 15 CIE sky models, only six types are available in gensky (Ward, n.d.-b). By selecting a location, entering a date and time, and selecting a sky condition, a CIE sky can be generated as a lighting source in daylight simulations. The Perez all-weather sky model

requires either solar irradiance or illuminance as the input. CIE sky models are commonly used in daylight simulations by novice users and practitioners (Cauwerts et al., 2012) due to its simple input. Based on the sky conditions when the HDR images were taken at CSM, CIE sunny and overcast skies were used in simulations. Additionally, a weather station on the roof of UWM's Golda Meir Library recorded global horizontal solar irradiance at fifteen-minute intervals (Figure 5.6 (left)) when the HDR images were taken at CSM. The global horizontal solar irradiance was split into direct normal and diffuse horizontal solar irradiance in gen_reindl by Walkenhorst et al (Reindl, Beckman, Reindl, & Duffle, 1990), which follows Reindl et al's method (Reindl et al., 1990). Then gendaylit was used to generate Perez skies.

When the HDR images were taken in the three offices at AUP, another weather station was set on the library's roof to record global horizontal solar irradiance at 30-second intervals (Figure 5.6 (right)). Then Perez skies were generated following the same steps as CSM.

Figure 5.6: The weather station collecting data for CSM simulations (left) (taken by Jing Hong) and the weather station collecting data for AUP simulations (right)

5.3.3 Data Analysis

Although it is easy to compare an HDR image to a simulated luminance map pixel-by-pixel in terms of luminance ratio, a discrepancy can easily happen because of geometric misalignments between high-contrast objects (Jones & Reinhart, 2016; Rushmeier, Ward,

Piatko, Sanders, & Rust, 1995). Hence, several steps of data analysis were utilized. First, both the HDR images and simulated luminance maps at CSM and AUP were entered in evalglare (Wienold, 2015) to calculate DGP results and E_v. Then, the comparison between HDR images and simulated luminance maps at CSM and AUP utilized two methods due to the applications of different sky models. To test the accuracy of simulated luminance maps under CIE and Perez skies at CSM, a two-tailed t-test (Box, Hunter, & Hunter, 2005) was performed to examine whether there was statistically significant difference between the two groups of DGP results obtained from the HDR images and simulated luminance maps. To test the accuracy of simulated luminance maps at AUP, the relative mean bias errors (MBE_{rel}) and relative root mean squared errors ($RMSE_{rel}$) were calculated (C. F. Reinhart & Walkenhorst, 2001). MBE_{rel} demonstrates the percent of underestimation or overestimation of simulated results that are compared with measurements. $RMSE_{rel}$ offers a deviation percent measured from the simulated results in relation to the values of HDR images. The equations are as follows (Fakra, Boyer, Miranville, & Bigot, 2011):

$$MBE_{rel} = \frac{1}{N}\sum_{i=1}^{N}\frac{X_{HDR,i} - X_{simulation,i}}{x_{HDR,i}} \quad Equation\ 5.2$$

$$RMSE_{rel} = \frac{1}{X_{HDRmean}}\sqrt{\frac{\sum_{i=1}^{N}\left(X_{HDR,i} - X_{simulation,i}\right)^2}{N}} \quad Equation\ 5.3$$

where $X_{simulation,i}$ represents the E_v calculated from the i^{th} simulated luminance map, $X_{HDR,i}$ represents the E_v calculated from the i^{th} HDR image, and $X_{HDRmean}$ represents the mean E_v of all the HDR images. Although the E_v derived from the HDR images taken at CSM failed to accurately reflect the measured E_v on site, they were used as a reference for the simulation results.

5.4 RESULT

5.4.1 Validation of vertical eye illuminance

Figure 5.7 shows the scatter plot of E_v from HDR images taken in Office 326 ($E_{v\text{-}HDR}$) against measured E_v ($E_{v\text{-}mea}$). The MBE_{rel} and $RMSE_{rel}$ between $E_{v\text{-}mea}$ and $E_{v\text{-}HDR}$ were -6.5% and 9.5%, respectively. The results demonstrate that E_v calculated from interior HDR images can accurately represent E_v measured on site and lay the foundation of using E_v as the primary metric for comparison.

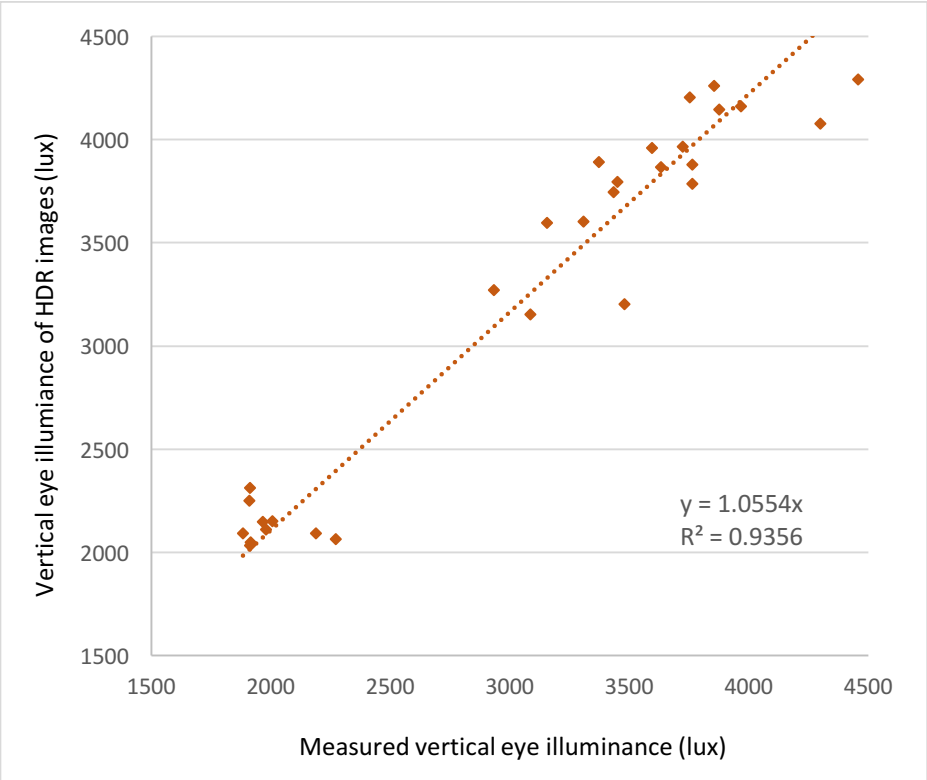

Figure 5.7: The scatter plot of vertical eye illuminance from HDR images against the measured vertical eye illuminance.

5.4.2 CSM Simulations under CIE and Perez Skies

Figure 5.8 shows the falsecolor images of HDR images and the simulated luminance maps of two scenes under the CIE and Perez skies. The comparisons between the HDR images and simulated luminance maps of the nine scenes are in Appendix A. Compared with the HDR images, both CIE and Perez sky models underestimated interior luminance maps. However, the Perez sky produced luminance maps that were closer to the HDR images under

both sunny and overcast sky conditions. Table 5.2 lists the DGP values of nine scenes from the HDR images and simulations. A paired comparison design (Box et al., 2005) was run between the DGP of the HDR images and simulations for both sky models. Table 5.3 lists the results of the t-test. With n=9, df=8, and a critical value of t(8)=3.355 for a two-tailed test with α=.01, any t statistic below 3.355 fails to prove that the two groups of statistics are

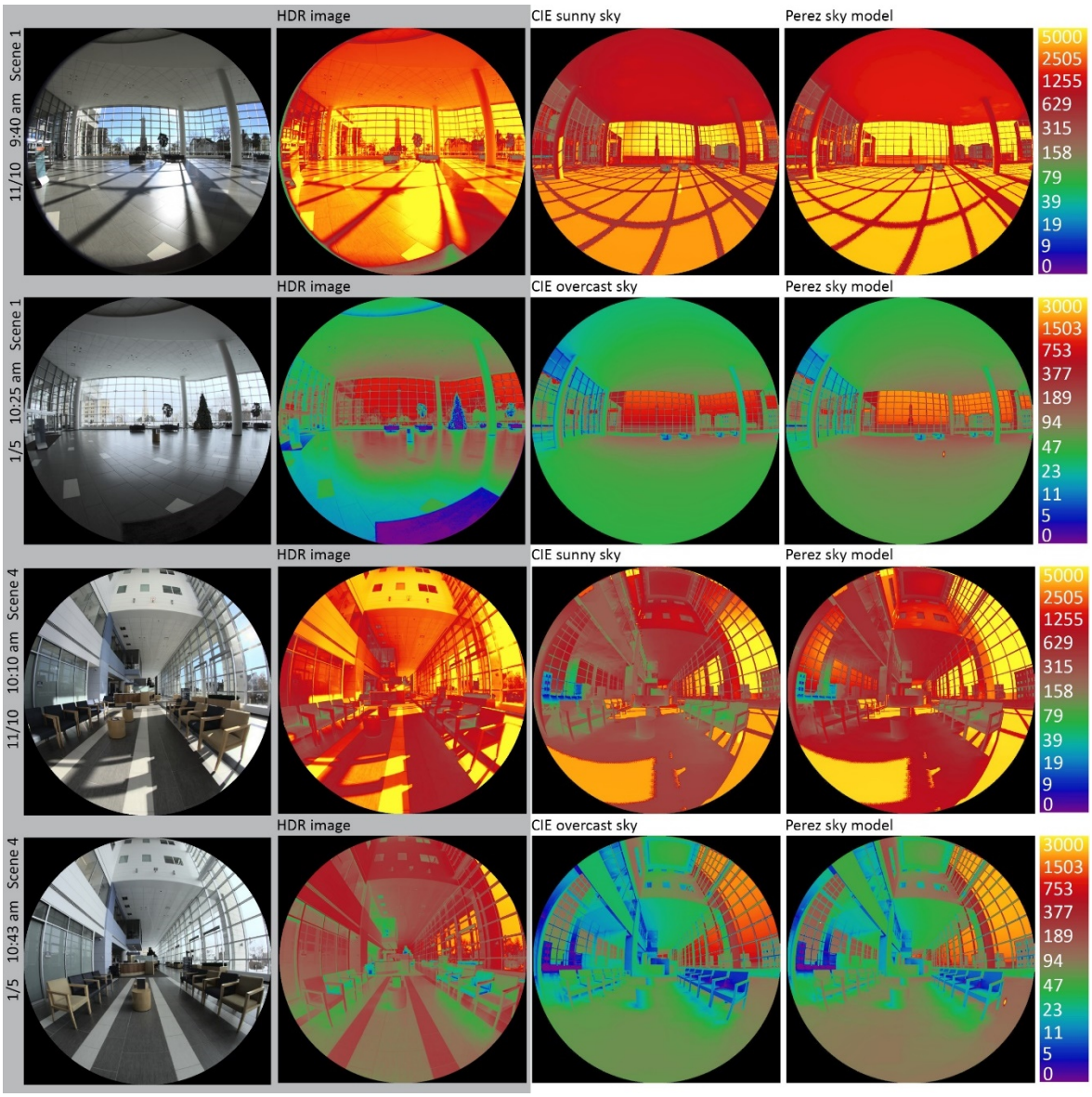

Figure 5.8: Falsecolor images of the HDR images and simulated luminance maps under CIE and Perez skies at CSM

significantly different (Kong et al., 2015). Therefore, the DGP values of the HDR images and the simulations under both CIE and Perez skies were comparable. However, compared with the HDR images, the CIE sunny sky underestimated Scene 8 with imperceptible glare (0.33),

while the Perez sky overestimated Scene 8 with intolerable glare (0.51). Figure 5.9 presents the E_v of the HDR images and simulated luminance maps. On the sunny day, both CIE and Perez sky models overestimated seven of nine scenes in terms of E_v. On the overcast day, both CIE and Perez sky models underestimated eight of nine scenes in terms of E_v.

Table 5.2: DGP results of the HDR images and simulations

Scene	HDR sunny	CIE sunny	Perez	HDR overcast	CIE overcast	Perez
Scene 1	0.97	0.67	1.00	0.21	0.19	0.25
Scene 2	0.68	0.50	0.65	0.17	0.19	0.20
Scene 3	1.00	1.00	1.00	0.32	0.19	0.33
Scene 4	0.58	1.00	1.00	0.20	0.17	0.24
Scene 5	0.81	0.76	1.00	0.33	0.20	0.22
Scene 6	0.55	1.00	1.00	0.19	0.12	0.17
Scene 7	1.00	1.00	1.00	0.24	0.20	0.33
Scene 8	0.44	0.33	0.51	0.22	0.17	0.19
Scene 9	0.60	1.00	1.00	0.19	0.18	0.23

Table 5.3: T-test results between the DGP of the HDR images and simulations

Group	T value	Group	T value
HDR & CIE sunny	0.474	HDR & CIE overcast	0.008
HDR & Perez sunny	0.048	HDR & Perez overcast	0.670

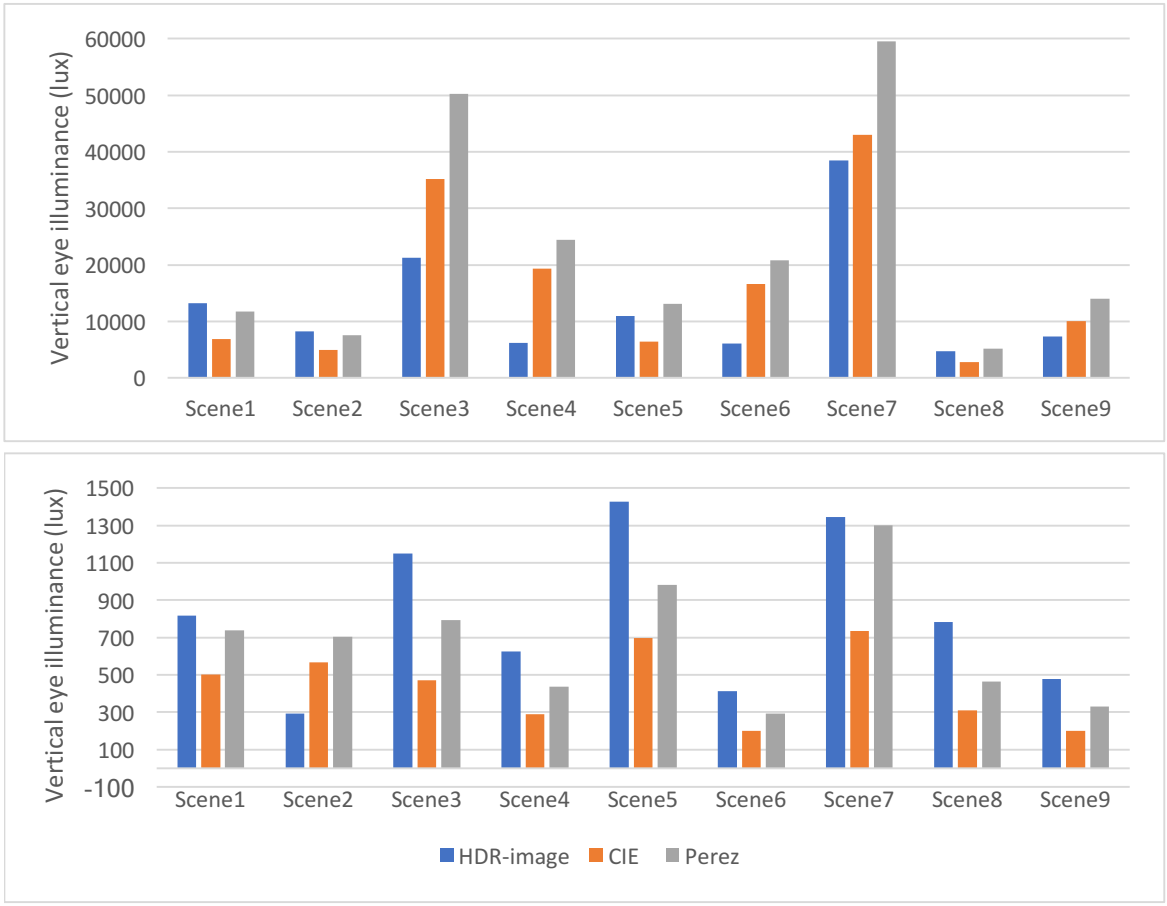

Figure 5.9: E_v comparison under the sunny (top) and overcast skies (bottom)

5.4.3 AUP Simulations under Perez Skies

Figure 5.10 shows the HDR images and the simulations under the Perez sky model within the three offices. The HDR images of Offices 326 and 422 were taken at 20-minute intervals, and the HDR images of Office 479 were taken at 30-minute intervals. Sixty-five groups of luminance maps were compared. The falsecolor images demonstrated comparable luminance distributions between the HDR images and the simulated luminance maps. Figures 5.11 to 5.13 present the DGP values of HDR images and the simulated luminance maps. The DGP results under the Perez sky model were lower than the DGP results of the HDR images.

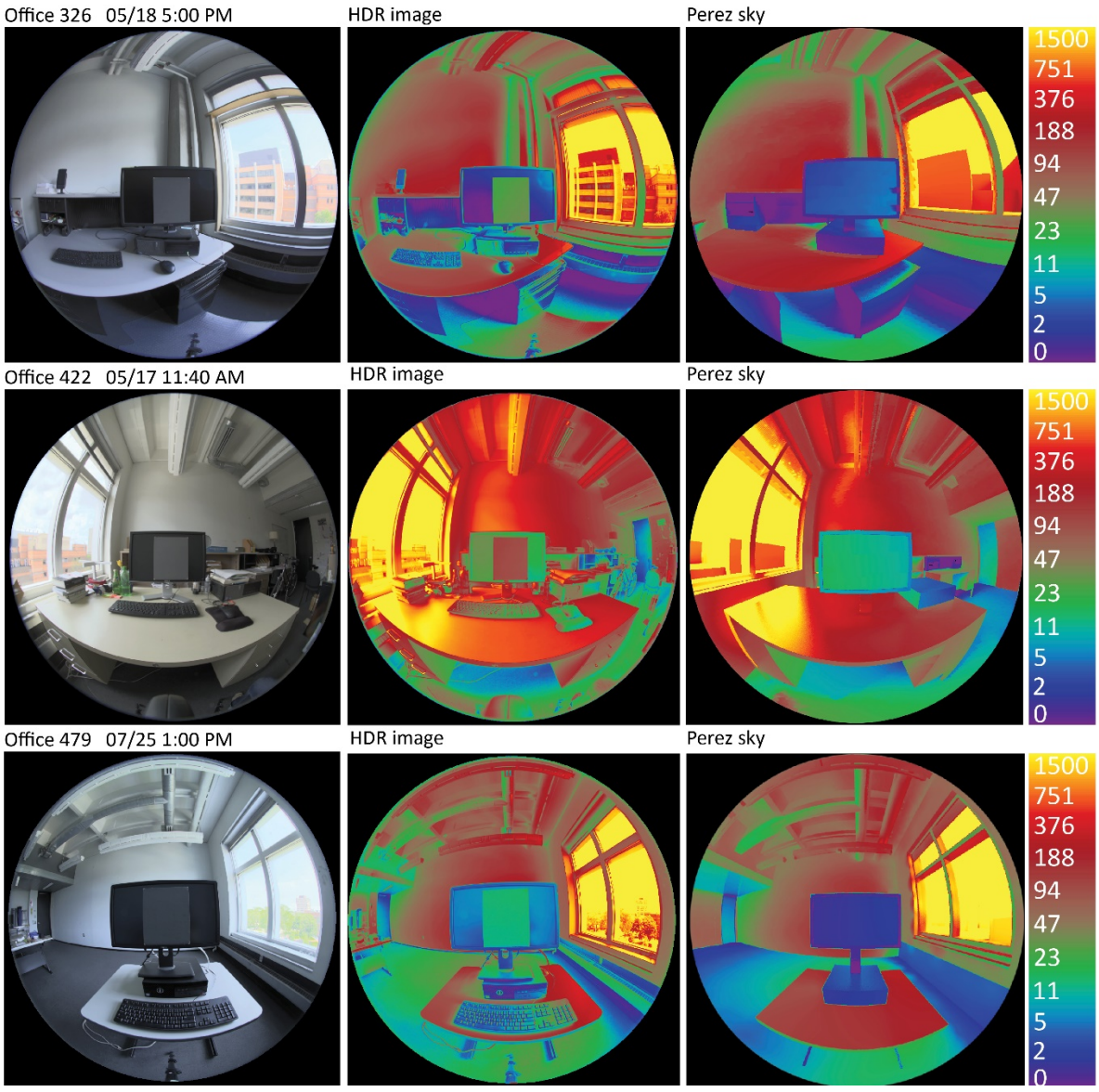

Figure 5.10: Falsecolor images of the HDR images and simulated luminance maps under Perez sky models at AUP

When Office 422 had perceptible glare at 1 p.m. and 4 p.m., the simulated luminance maps presented imperceptible glare. However, within the three offices, the Perez sky model predicted DGP levels with 94% accuracy. Table 5.3 lists the sky condition, the MBE_{rel} and $RMSE_{rel}$ of E_v for each office. The values lower than 20% are in bold. The negative MBE_{rel} values greater than -20% demonstrated the underestimation of the Perez sky model in all three offices. In both Offices 326 and 422, intermediate sky conditions resulted in greater $RMSE_{rel}$, 27.8% and 22.8% respectively. The $RMSE_{rel}$ of Office 479 on the sunny day was smaller than the intermediate conditions.

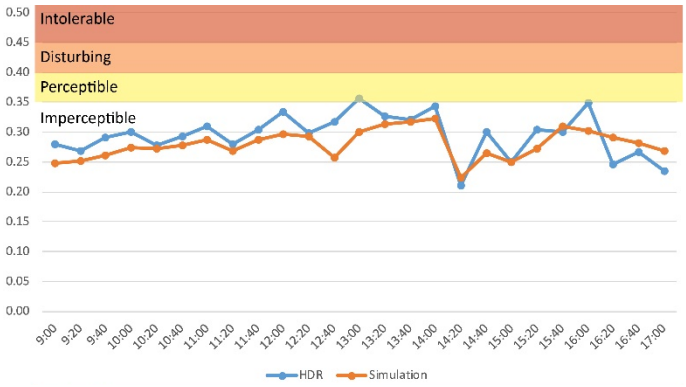

Figure 5.11: DGP results of the HDR images and simulated luminance maps in Office 326

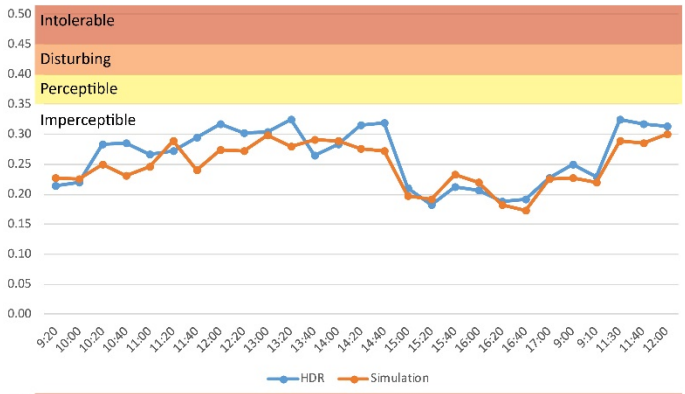

Figure 5.12: DGP results of the HDR images and simulated luminance maps in Office 422

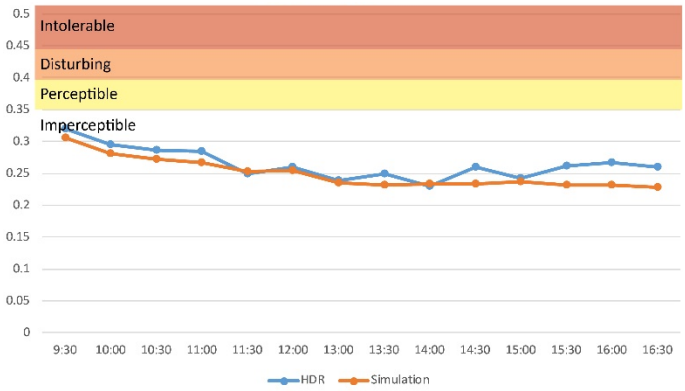

Figure 5.13: DGP results of the HDR images and simulated luminance maps in Office 479

5.5 DISCUSSION

Humans' visual perception is proportional to a logarithm of the actual lighting intensity (Fechner, 1966). In other words, subtle changes of illuminance or luminance values are not human perceptible. Additionally, it is neither possible nor practical to build a simulation model that exactly matches the reality. Therefore, researchers agree that the lighting simulation results with the MBE_{rel} and $RMSE_{rel}$

below 20% are accurate to represent real lighting environments (Jones & Reinhart, 2016; Mardaljevic, 1995; C. F. Reinhart & Walkenhorst, 2001).

Table 5.4: Relative MBE and RMSE of Ev within three offices at AUP

E_v	Data collection time	Sky Type	Count	MBE (%)	RMSE (%)
Office 326	May 18th, 2017, from 9 a.m. to 5 p.m. July 28th, 2017, from 9 a.m. to 1 p.m.	Intermediate & Cloudy Sunny	26	**-4.7**	27.8
Office 422	May 17th, 2017, from 9 a.m. to 5 p.m. July 28th, 2017, from 9 a.m. to 1 p.m.	Intermediate & Cloudy Sunny	25	**-8.3**	22.8
Office 479	July 25th, 2017, from 9 a.m. to 4:30 p.m.	Intermediate & Sunny	14	**-14.5**	20.1

5.5.1 Application and Limitations of CIE Skies

The results demonstrated the ability of CIE sunny and overcast sky models in terms of generating comparable DGP results ($t(8)=0.474$ for the sunny sky and $t(8)=0.008$ for the overcast sky). However, compared with the falsecolor images of real daylighting distributions, the simulated luminance maps under CIE sunny and overcast skies presented noticeable lower luminance. The conclusion that CIE sky models underestimated simulation results is in line with other studies (M. Inanici & Hashemloo, 2016; Kong, Utzinger, & Li, 2016). Despite their underestimation, CIE sky models are still commonly used in point-in-time daylight simulations by novice users and practitioners (Cauwerts & Piderit, 2018). CIE sky models can be employed by architects and researchers to obtain a rough understanding of the daylighting performance or compare the performance of design alternatives within a space. Nonetheless, architects and lighting designers should notice the underestimation characteristic of CIE sunny and overcast skies when interpreting the simulation results.

5.5.2 Accuracy and Limitations of Perez Skies

As the Perez sky model relies on onsite measured solar irradiance or illuminance (Perez et al., 1993), it generates accurate sky models for daylight simulations. However, in this study, two aspects of collected weather data influenced the accuracy of creating Perez skies. One was the distance between the weather stations and the studied space, and the other was the time interval at which the weather stations recorded the data. Since the weather

station was around 2.4 kilometers away from CSM, the recorded solar irradiance failed to accurately reflect the micro-climate at CSM. Hence, the Perez skies with the solar irradiance measured 2.4 kilometers away from CSM led to deviations with regards to simulated luminance maps. Solar radiations measured at 15-minute intervals easily averaged out the peak and bottom solar radiations that occurred within 15 minutes. Hence, shorter interval was required to record the actual sky conditions when interior HDR images were taken. In order to improve the research quality and minimize the discrepancies caused by weather data, the research conducted at AUP placed the pyranometer onsite. The pyranometer measured global horizontal solar irradiance at 10-second intervals so that the instantaneous data were extracted for accurate simulations.

5.5.3 Causes of Simulation Discrepancies

Besides sky models that resulted in discrepancies between simulated luminance maps and real daylighting conditions, there were two extra factors accounting for simulation discrepancies. First, material properties have a great impact on the simulation accuracy. The simulation accuracy obtained in this research showed an example of using a relatively simple method of measuring material reflectance, as introduced in 5.2.3. This method ignores the RGB values of an unknown material. Researchers need to make close assumptions about a material's specularity and roughness. To obtain more accurate simulation results, sophisticated and expensive equipment, such as a spectrophotometer, is recommended to measure materials' RGB values and specularity. Goniophotometer provides materials' roughness data in addition to the other lighting properties.

Second, discrepancies also occurred due to simplified modeling details. Small objects, such as books, keyboards, and phones, are usually omitted in daylighting modeling. The geometric and material properties of furniture, like tables and bookshelves, are also simplified in modeling. Researchers agree that the procedures of omitting small objects and

simplifying complex objects can result in accurate simulation results to represent real lighting environments. In other words, RME and RMSE within 20% of simulation results are acceptable (Jones & Reinhart, 2016). Following the same principles of modeling details, this study provides an example of demonstrating how accurate these modeling principles can be.

Building an exact match model as a real condition both prolongs the modeling process and increases simulation time. However, to date, no systematic study has proposed comprehensive suggestions concerning modeling details to strike a balance between the modeling complexity and result accuracy. LM-83 (Illuminating Engineering Society, 2013) proposed the guidelines for lighting simulations, although the recommendations of modeling external environments resulted in an average of 22.8% error on illuminance simulations (Nahrkhalaji & Mistrick, 2016). Further studies are required to clarify the relationship between modeling details and maximizing simulation accuracy.

5.6 CONCLUSION

This chapter presented the daylight simulations at CSM and AUP under CIE and Perez sky models. Although CIE sunny and overcast skies are capable of predicting comparable DGP results to the HDR images, they underestimate luminance distributions. The Perez sky model simulates more accurate luminance maps with the solar irradiance measured onsite. Using three offices at AUP as an example, the simulated E_v under the Perez sky presented relative MBE varying between -4.7% and -14.5% and relative RMSE varying between 20.1% and 27.8%. Due to the algorithm of the Perez all-weather sky model, it cannot present subtle luminance variations and cloud distributions. Therefore, the following chapter explores the HPR sky model which is able to capture and include detailed sky luminance variations.

6 EVALUATION OF SKY MODEL ACCURACY

As discussed in the previous chapter, neither Generic CIE sky models nor the Perez all-weather model includes cloud distributions in lighting simulations. This chapter explores the accuracy of a horizontal hybrid photo-radiometer (HPR) sky model, which combines modelled physical descriptions of the sun and HDR sky images. The primary aim is to build on and enrich the findings of a previous study (Humann & Mcneil, 2017) that reported this sky model using a physical scale model. To keep examples consistent, this chapter utilizes AUP, HGA, and ALF as the example to compare the simulated luminance maps with the HDR images, which have been analyzed in Chapter Four.

6.1 RESEARCH OBJECTIVES

This chapter has three primary aims. The first aim is to validate the horizontal HPR sky through field measurements under diverse sky conditions. The second aim is to enrich the application of the horizontal HPR sky model to diverse interior spaces covering different orientations, spatial organizations, and façade configurations. The third aim is to reveal the problems in the vertical HPR sky model in terms of simulating luminance maps.

6.2 RESEARCH QUESTION

This chapter mainly answers this question: compared with the Perez all-weather sky model, how accurate is the horizontal HPR sky model in terms of simulating luminance maps?

6.3 METHODOLOGY

6.3.1 Interior daylight luminance distributions

The HDR images analysed in Chapter Four were continuously used in this chapter. The pink arrows in Figures 6.2, 6.3, and 6.4 illustrate from where the HDR images were taken. Each scene was taken based on an occupant's perspective. E_v of all the HDR images was calculated to check the occurrence of luminous overflow as illuminance values at the lens opening were

not taken before and after taking the HDR images. Eight out of 125 interior HDR images with E_v over 5,000 lux were excluded from the data analysis due to luminous overflow.

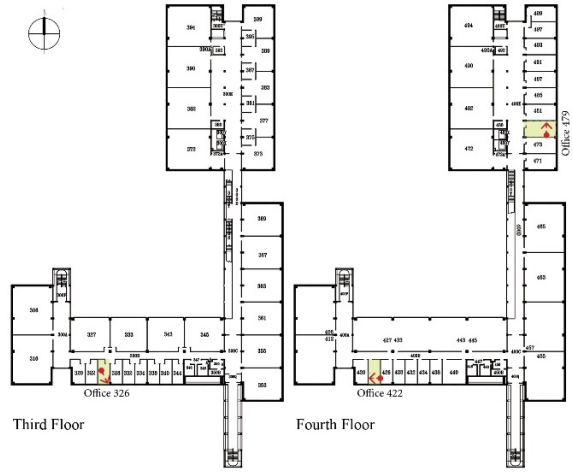

Figure 6.1: Three offices' locations at AUP

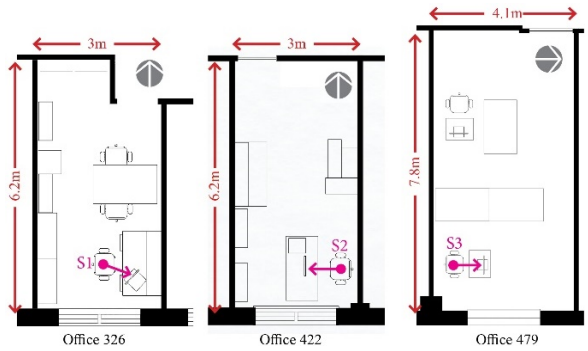

Figure 6.2: Three select offices' layouts

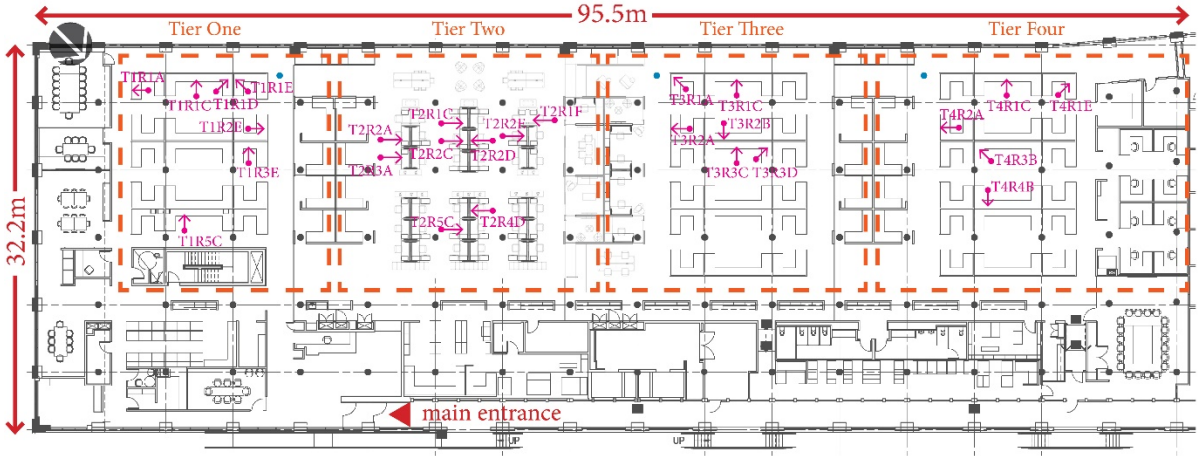

Figure 6.3: Select workstations at HGA where HDR images were taken

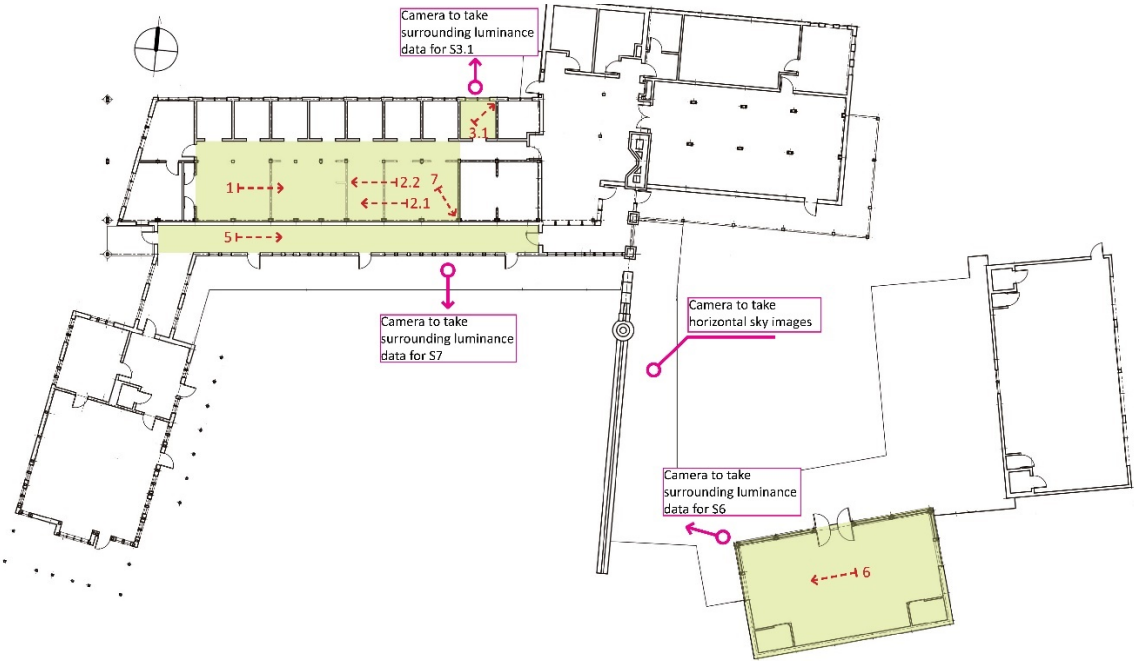

Figure 6.4: The scenes at ALF where HDR images were taken

6.3.2 Exterior sky luminance distribution

6.3.2.1 Calibration and validation procedure

The HPR sky model combines the modelled physical descriptions of the sun and calibrated HDR sky images. In order to extract an accurate calibration factor, a calibration and validation study of the horizontal HPR sky was carried out in advance. Exterior HDR images were taken by a Canon 5D II at f/11 at five-minute intervals over three overcast days (May 22nd, June 6th and 30th) on the roof of the library. Simultaneously, global horizontal illuminance (GHI) was recorded for calibration. The LDR images were assembled in hdrgen, and the vignetting correction was applied. The GHI of HDR images was calculated in pcomb. The average ratio between the measured and calculated GHI was applied as the calibration factor to the camera response curve for assembling HDR sky images in the future. Consequently, a study to validate the calibration factor of HDR sky images was conducted. Exterior HDR images of skies were captured under a clear sky and an intermediate sky, respectively. Two shading disks were assembled on the camera and the photometric sensor to block the direct sunlight from the camera's sensor and the photometric sensor (Thanachareonkit, Fernandes, & Papamichael, 2010). Figure 6.5 shows the equipment to validate the calibration factor.

Figure 6.5: The camera and photometric sensor assembled with the shading disks

6.3.2.2 Acquisition of exterior sky distribution

When interior HDR images were taken at AUP, a Canon 5D II with a SIGMA f/3.5 fisheye lens was placed on the roof of UWM's Golda Meir Library, 170 meters away from AUP, for collecting simultaneous sky data. LDR images of skies were taken at f/11 with the shutter speed varying between 4s and 1/8000s. Global horizontal solar irradiance was recorded by a HOBO pyranometer, and global horizontal illuminance was recorded by a LI-210R photometric sensor. At HGA, the equipment for collecting sky data was positioned on the roof of the building. At ALF, both horizontal sky and vertical luminance environments of a scene were captured separately. As shown in Figure 6.4, the Canon 5D II to capture horizontal sky images was placed in the center of the courtyard. Then, the camera was placed vertically to capture the surrounding luminance data of S3.1, S6, and S7 while the interior HDR images were taken. Table 1 lists the calendar for data collection. Figure 6.6 displays the equipment to collect both interior and exterior luminance distributions.

Table 6.1: Data collection calendar across the three buildings

Date	Sky condition	Studied space	Spatial orientation	Notes
05/17/2017	Intermediate & cloudy	Office 422	South	Both interior and exterior HDR images were taken at 20-minute intervals from 8 a.m. to 5 p.m.
05/18/2017	Intermediate & cloudy	Office 326	South	Both interior and exterior HDR images were taken at 20-minute intervals from 8 a.m. to 5 p.m.
05/22/2017	Sunny	ALF	North and south	Both interior and exterior HDR images were taken concurrently.
05/27/2017	Sunny & Intermediate	HGA	Southwest	Both interior and exterior HDR images were taken at 10-minute intervals from 10 a.m. to 5 p.m.
07/25/2017	Intermediate & Sunny	Office 479	East	Both interior and exterior HDR images were taken at 30-minute intervals from 8 a.m. to 5 p.m.
07/28/2017	Cloudy & Sunny	Offices 326 & 422	South	Both interior and exterior HDR images were taken at 20-minute intervals from 8 a.m. to 12 p.m.
07/29/2017	Sunny	HGA	Southwest	Exterior HDR images were taken at 10-minute intervals from 2 p.m. to 6 p.m.

Figure 6.6: Data collection equipment

6.3.2.3 Exterior data post-processing

The interior and exterior HDR images were taken at local times, and the corresponding solar times were calculated with the method introduced by Duffie and Beckman (Duffie & Beckman, 2013). The sun's altitude and azimuth angles were calculated in PyEphem (Rhodes, n.d.). A 5^{o} solid angle (WMO, 2010) disc was modelled to mask the sun and its circumsolar region in all HDR images, unless the sun was occluded by clouds (Humann & Mcneil, 2017). For the horizontal HPR sky, diffuse horizontal illuminance was calculated from the assembled HDR images of skies after applying the masking disc. Direct normal illuminance was calculated in Equation 6.1 (Humann & Mcneil, 2017):

$$DN_{Illum} = (GH_{Illum} - DH_{Illum})/\sin\theta \qquad Equation\ 6.1$$

where DN_{Illum} represents direct normal illuminance, GH_{Illum} represents global horizontal illuminance measured by LI-210R, DH_{Illum} represents diffuse horizontal illuminance obtained from the calibrated HDR images of skies, and θ represents the sun's altitude angle above horizon.

For the vertical HPR sky, diffuse horizontal illuminance was also calculated from the masked HDR sky images. Direct normal illuminance was calculated in Equation 6.2 (Humann & Mcneil, 2017):

$$DN_{Illum} = (GV_{Illum} - DV_{Illum}) / \cos\theta \cos\varphi \qquad Equation\ 6.2$$

where DN_{Illum} represents direct normal illuminance, DV_{Illum} represents global vertical illuminance measured by LI-210R, DV_{Illum} represents diffuse horizontal illuminance obtained from the calibrated HDR images of surrounding environments, θ represents the sun's altitude angle above horizon, and φ represents the sun's azimuth angle.

The inputs of generating the Perez sky in Chapter 5 were direct normal and diffuse horizontal solar irradiance. As the camera sensor cannot record the light spectrum outside of the visible range (400-700nm), illuminance (lux) values for the direct and diffuse sky components rather than full spectrum irradiance (W/m^2) values were used in the HPR sky model (Humann & Mcneil, 2017). In this Chapter, DN_{Illum} and DH_{Illum} (or DV_{Illum}) were used to generate both Perez skies and the solar component for both the horizontal and vertical HPR skies. The procedure of creating the horizontal HPR sky model is illustrated in Figure 6.7.

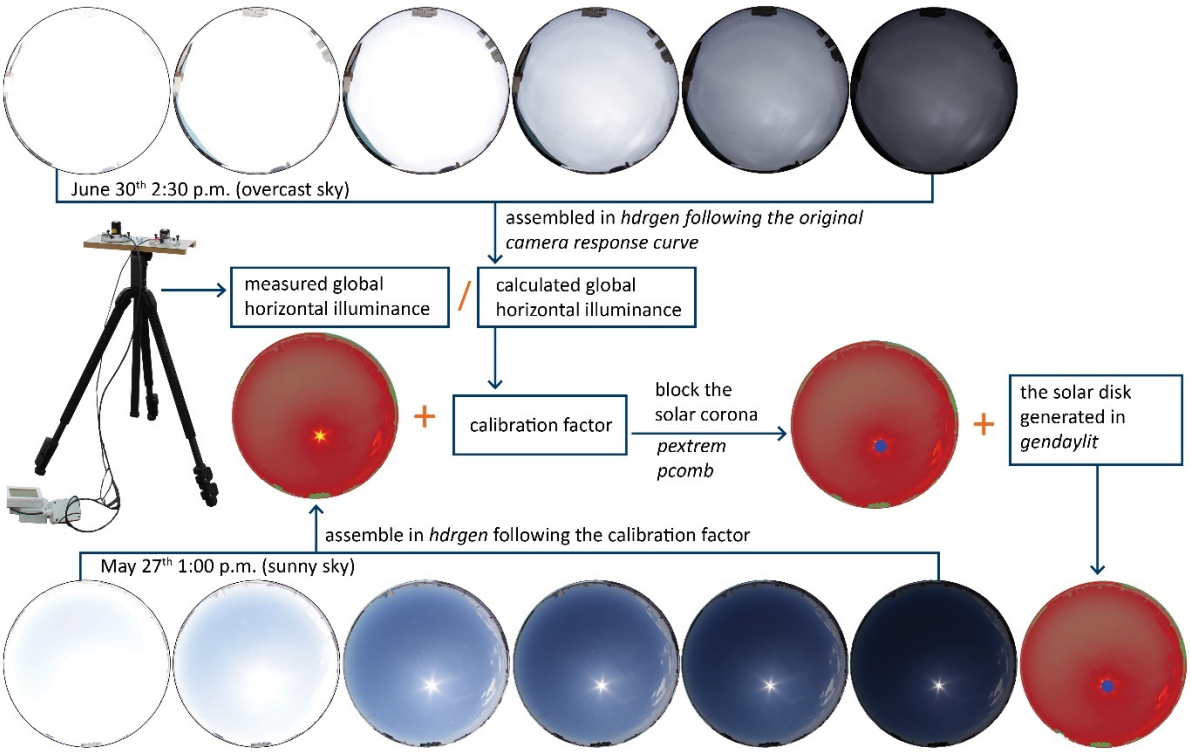

Figure 6.7: The procedures of generating the HPR sky model

6.3.3 Simulation

AUP, HGA, and ALF's models were established in Rhino ("Rhinoceros," n.d.) based on the construction documents and onsite measurements. The material properties are listed in Table 6.2.

Table 6.2: Select Radiance material definitions at AUP, HGA, and ALF

Building	Material	Radiance material
AUP	Black cabinet	void metal blacksteel 0 0 5 0.025 0.025 0.025 0.667 0.15
	Glazing	void glass glazing 0 0 3 0.80 0.80 0.80
	Door	void plastic door 0 0 5 0.037 0.037 0.037 0.067 0.08
	Carpet	void plastic carpet 0 0 5 0.055 0.055 0.055 0 0.2
	Ceiling & wall	void plastic ceiling 0 0 5 0.721 0.721 0.721 0.005 0.08
	Column	void plastic column 0 0 5 0.445 0.445 0.445 0.0 0.1
	Bookshelf	void plastic bookshelf 0 0 5 0.229 0.229 0.229 0.05 0.1
	Blue wall in Office 479	void plastic bluewall 0 0 5 0.546 0.546 0.546 0.01 0.1
	Window frame	void metal frame 0 0 5 0.55 0.55 0.55 0.7 0
	Outside ground	void plastic OutsideGround 0 0 5 0.1 0.1 0.1 0 0
	Surrounding buildings	void plastic OutsideBuilding 0 0 5 0.2 0.2 0.2 0 0
HGA	Turned-off monitor	void plastic BlackScreen 0 0 5 0.03 0.03 0.03 0 0
	Monitor plastic	void plastic MonBlack 0 0 5 0.054 0.054 0.062 0.013 0.05
	White table	void plastic Tablewhite67 0 0 5 0.677 0.677 0.677 0.005 0.005
	Wooden cabinet	void plastic HAGSheflwood 0 0 5 0.512 0.512 0.512 0.07 0.1
	Fabric partition	void plastic Partgrey 0 0 5 0.378 0.378 0.378 0.001 0.05
	Gray interior wall	void plastic Wallgrey 0 0 5 0.274 0.274 0.274 0.01 0.02
	Gray table	void plastic Tablegrey 0 0 5 0.23 0.23 0.23 0.0 0.05
	White wall	void plastic Wallwhite 0 0 5 0.713 0.713 0.713 0 0.02
	Column	void plastic Column 0 0 5 0.377 0.377 0.377 0 0.25
	Carpet	void plastic Carpet 0 0 5 0.151 0.151 0.151 0 0.25
	External glazing	void glass exglazing 0 0 3 0.78459 0.78459 0.78459
	Metal shelf	void metal Shelfblack 0 0 5 0.035 0.035 0.035 0.7 0
	External overhang	void metal SheetMetal 0 0 5 .9 .9 .9 .8 0
	Internal glazing	void glass GlazingInter 0 0 3 0.71 0.71 0.71
	Outside ground	void plastic OutsideGround 0 0 5 0.1 0.1 0.1 0 0
	Surrounding buildings	void plastic OutsideBuilding 0 0 5 0.2 0.2 0.2 0 0
	River	void dielectric Watersurface 0 0 5 0.8695 0.8695 0.8695 1.33 0
ALF	Wooden table	void plastic WoodTable 0 0 5 0.31 0.31 0.31 0.01 0.03
	Gray partition	void plastic GrayWall 0 0 5 0.475 0.475 0.475 0 0
	Wooden wall	void plastic WoodWall 0 0 5 0.38 0.38 0.38 0 0
	White plastic table	void plastic WhiteTable 0 0 5 0.387 0.387 0.387 0 0
	Brown floor	void plastic BrownFloor 0 0 5 0.121 0.121 0.121 0.01 0.04
	Gray floor	void plastic GrayFloor 0 0 5 0.228 0.228 0.228 0.01 0.04
	Wooden beam	void plastic DarkBeam 0 0 5 0.228 0.228 0.228 0 0.1
	Steel connections	void plastic Steel 0 0 5 0.0460 0.0456 0.0463 0.0052 0.0
	Turned-off monitor	void plastic BlackScreen 0 0 5 0.03 0.03 0.03 0 0
	Glazing	void glass SouthGlass 0 0 3 0.491 0.491 0.491
	Outside ground	void plastic OutsideGround 0 0 5 0.35 0.35 0.35 0 0

6.3.4 Data Analysis

6.3.4.1 Visual discomfort metrics

Building models for lighting simulations indicates that simplification occurs during the process. It is impossible to build an exact model that matches the reality. Small objects are often excluded, and furniture is usually simplified. Since it is neither possible nor necessary to compare the pixel-by-pixel luminance values between an HDR image and a simulated luminance map (Rushmeier et al., 1995), several visual discomfort metrics were employed for comparison. This study employed DGP (Wienold & Christoffersen, 2006) as the glare index since it outperforms other glare indices with its robust and consistent results under daylighting conditions when large regions of lighting sources exist (Jakubiec & Reinhart, 2012). E_v was also chosen due to its ability to predict people's visual perception (K. Van Den Wymelenberg, 2012) and easy calculation in evalglare (Wienold & Andersen, n.d.).

Furthermore, previous studies have independently demonstrated the effectiveness of a 40^o horizontal band in terms of predicting subjective visual perception (K. Konis, 2013; Mahić et al., 2017; K. Van Den Wymelenberg, 2012). Being view independent, a 40^o horizontal band is applicable to scenes with diverse spatial configurations. In order to examine the variations of simulated luminance maps associated with HDR images, the coefficient of variance (COV) of a 40^o horizontal band was calculated from both HDR images and simulated luminance maps. Figure 6.8 shows two scenes where the 40^o bands were applied, the two images on the left are S1 in Office 326, and the two images on the right are T1R1A at HGA.

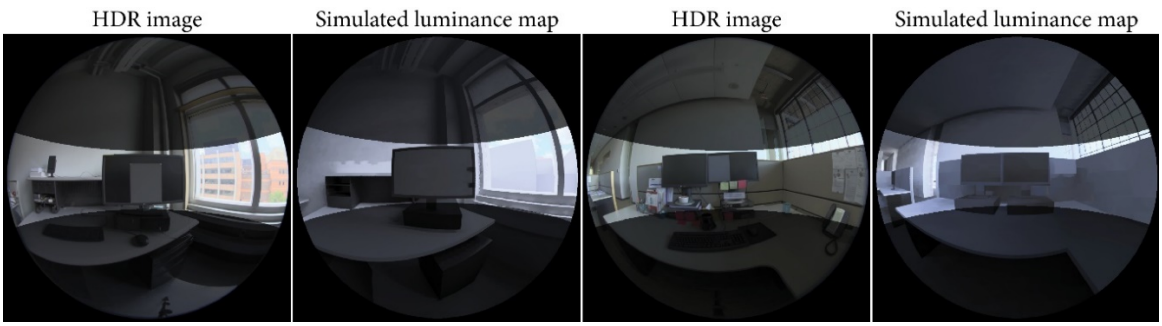

Figure 6.8: A 40^o horizontal band on the HDR images and simulations within Office 326 (two left) and HGA (two right)

6.3.4.2 Statistical analysis

First, the Linear Regression was run between the measured global horizontal illuminance and the simulated global horizontal illuminance under both sky models as a quick test. Then, interior HDR images and simulated luminance maps were analyzed and compared. Each groups of comparison included data from three sources: an HDR image taken onsite, a simulated luminance map under the horizontal HPR sky, and a simulated luminance map under the Perez sky. Instead of using absolute errors that greatly vary based on lighting intensities, the relative bias errors (BE_{rel}), the relative mean bias errors (MBE_{rel}) and relative root mean squared errors ($RMSE_{rel}$) were calculated (Jones & Reinhart, 2016). BE_{rel} (Equation 6.2) demonstrates the percent of underestimation or overestimation of simulated results compared to actual measurements. MBE_{rel} (Equation 5.1) shows an average deviation percent of simulated results compared to the values of HDR images, while $RMSE_{rel}$ (Equation 5.2) offers an absolute average deviation percent of simulated results in relation to the values of HDR images (Fakra et al., 2011).

$$BE_{rel} = \frac{X_{simulation,i} - X_{HDR,i}}{X_{HDR,i}} 100\% \quad Equation\ 6.2$$

where $X_{simulation,i}$ represents the E_v calculated from the i^{th} simulated luminance map and $X_{HDR,i}$ represents the E_v calculated from the i^{th} HDR image.

6.4 RESULTS OF HORIZONTAL HPR SKIES

6.4.1 Validation of diffuse sky components

Figure 6.9 demonstrates the two sky conditions under which the method of generating the diffuse sky component was validated. Figure 6.10 shows the measured diffuse horizontal illuminance (DHI_{mea}) in blue dashed lines and the diffuse horizontal illuminance calculated from HDR sky images (DHI_{HDR}) in red dots. On the clear day, the HDR sky images tended to overestimate diffuse horizontal illuminance with -9.7% MBE_{rel} and 9.8% $RMSE_{rel}$. On the intermediate day, the HDR sky images generated more accurate diffuse horizontal

illuminance with -0.6% MBE_{rel} and 5.6% $RMSE_{rel}$. The MBE_{rel} and $RMSE_{rel}$ under both sky conditions indicate the accuracy of the HPR sky model in terms of capturing the diffuse sky component.

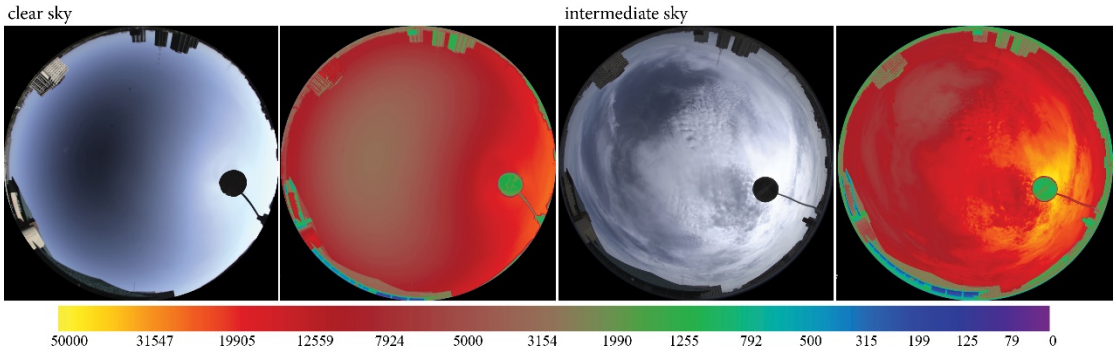

Figure 6.9: HDR sky images for the validation study

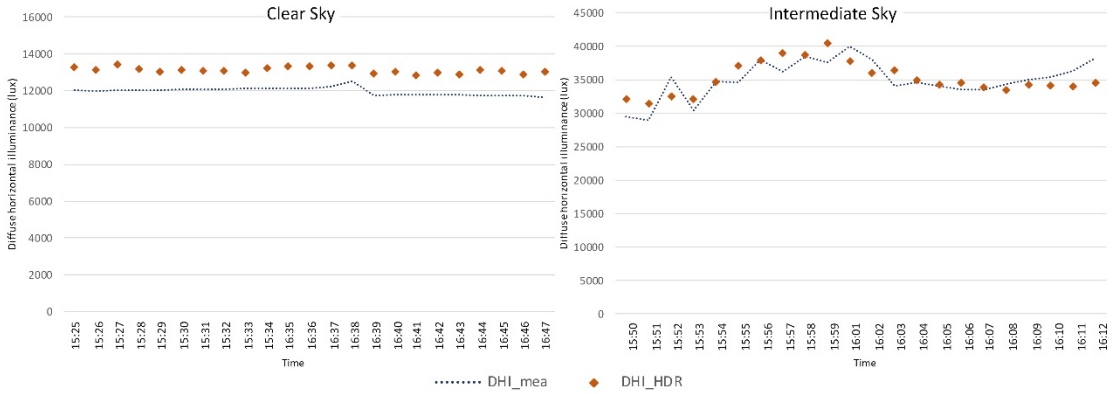

Figure 6.10: Diffuse horizontal illuminance of measurements and HDR sky images

6.4.2 Global Horizontal Illuminance

Figure 6.11 demonstrates the profiles of global horizontal illuminance on May 17th and July 25th, respectively. Most of the measured global horizontal illuminance (GHI_{meas}) and simulated global horizontal illuminance (GHI_{HPR} and GHI_{Perez} represent the simulated results under HPR and Perez skies, respectively) were identical. Both sky models slightly overestimated GHI on July 25th between 3 p.m. and 4:30 p.m. Table 6.3 lists the MBE_{rel} and $RMSE_{rel}$ under Perez and HPR skies over all seven days. On the sunny days of June 6th and July 29th, the GHI under both HPR and Perez skies resulted in MBE_{rel} and $RMSE_{rel}$ below 1%. On May 27th, July 25th, and July 28th, all involving partial sunny days, both the HPR and Perez sky models generated GHI with MBE_{rel} and $RMSE_{rel}$ equal to or less than 4%. However, when the sky conditions were intermediate and cloudy, deviations between the

measured GHI and simulated GHI increased. For example, on May 18th, the Perez sky model resulted in 26.23% $RMSE_{rel}$, while the HPR sky model resulted in the $RMSE_{rel}$ of 27.58%. One primary factor led to greater deviations between the measured GHI and simulated GHI was the sky condition. It rained shortly in the morning time under extremely cloudy conditions, which resulted in dynamic discrepancies.

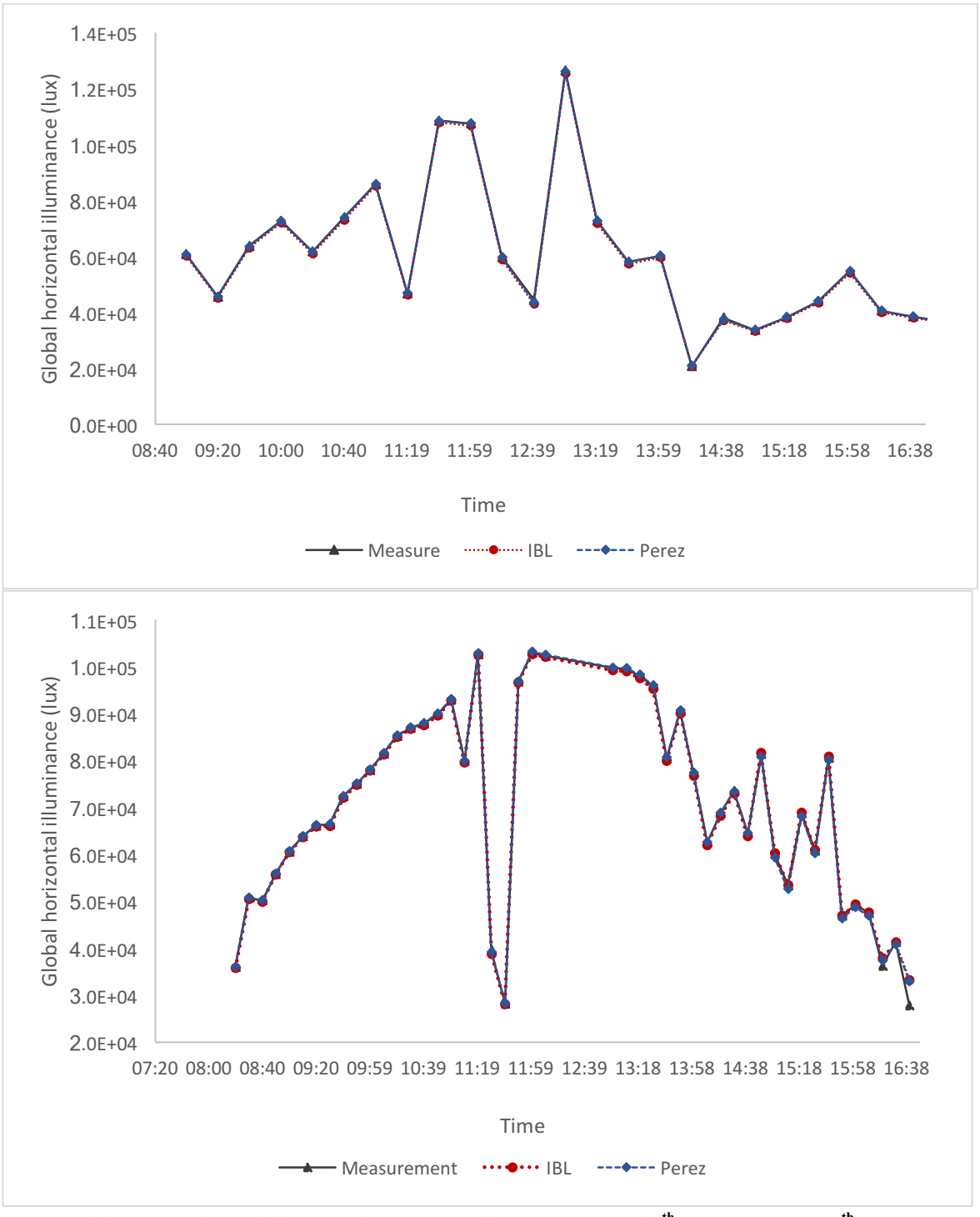

Figure 6.11: The profiles of GHI_{meas}, GHI_{HPR}, and GHI_{Perez} on May 17th (top) and July 25th (bottom)

Table 6.3: MBE_{rel} and $RMSE_{rel}$ under HPR and Perez skies

Date	05/17/2017	05/18/2017	05/27/2017	06/06/2017	07/25/2017	07/28/2017	07/29/2017
Sky condition	Intermediate & cloudy	Intermediate & cloudy	Sunny & Intermediate	Sunny	Intermediate & Sunny	Cloudy & Sunny	Sunny
HPR MBE_{rel}	0.03%	-27.17%	0.13%	-0.1%	-0.65%	1.9%	0.8%
Perez MBE_{rel}	1.04%	-23.95%	0.55%	-0.4%	0.11%	0.7%	0.4%
HPR $RMSE_{rel}$	3.30%	27.58%	0.15%	0.1%	1.15%	2.2%	0.7%
Perez $RMSE_{rel}$	1.33%	26.23%	0.53%	0.4%	1.17%	2.2%	0.4%

Figure 6.12 shows the scatter plots of GHI_{HPR} against GHI_{meas} in red, along with GHI_{Perez} against GHI_{meas} in blue. The Linear Regression was run between the two groups of data with the y-intercept fixed at zero. For the HPR sky model, the linear fit had a slope of 1.0011 with R^2 equal to 0.9963. For the Perez sky model, the linear fit had a slope of 0.9985 with R^2 equal to 0.9963. The average MBE_{rel} and $RMSE_{rel}$ of the GHI_{HPR} were 1.29% and 2.26%, respectively. The average MBE_{rel} and $RMSE_{rel}$ of the GHI_{Perez} were 0.74% and 2.26%, respectively. The results demonstrate that both the HPR sky model and the Perez sky model result in comparable and equally accurate GHI.

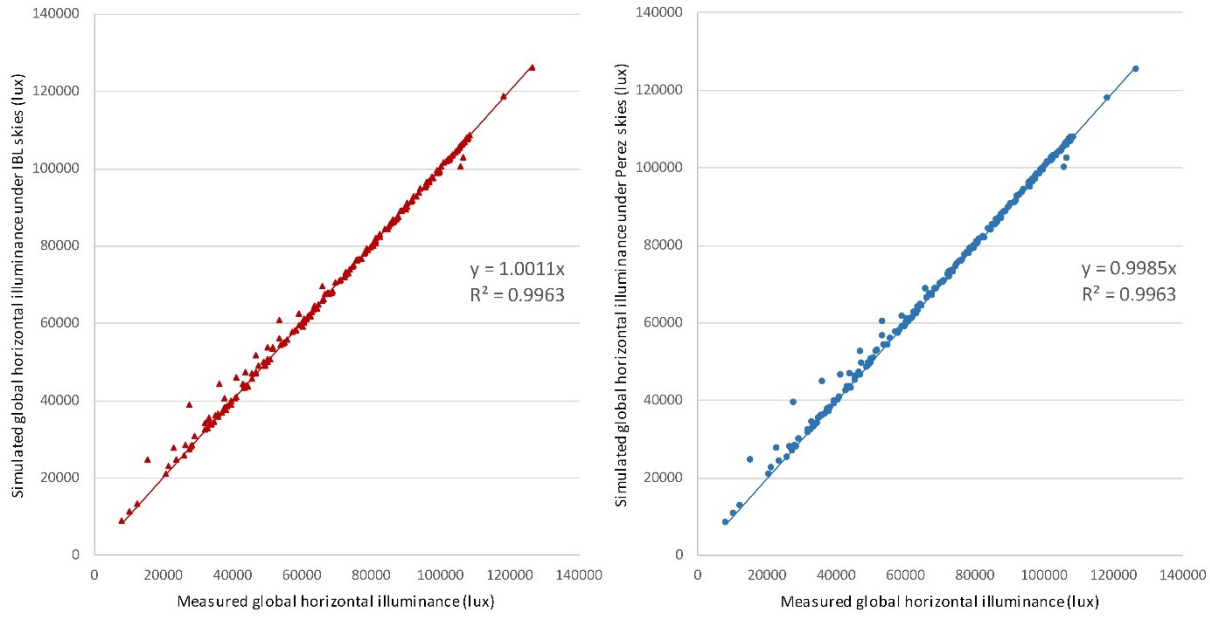

Figure 6.12: The scatter plot of GHI_{HPR} against GHI_{meas} (left) and the scatter plot of GHI_{Perez} against GHI_{meas} (right)

6.4.3 Visual Comparison of Skies and Interior Daylight Distributions

Table 6.4 presents the falsecolor images of HPR and Perez skies, along with interior HDR images and simulated luminance maps under two sky models. The falsecolor images of skies show comparable luminance distributions between the HPR and Perez skies. However, without cloud distributions, the Perez sky model failed to provide the subtle luminance variations as the HPR model did. Take S2 (May 17th at 2:20 p.m.) as an example. The cloud distributions and luminance variations of the HPR sky were smoothed by the Perez sky. Yet, both the HPR and Perez sky models generated comparable interior luminance maps.

Table 6.4: Falsecolor images of horizontal HPR skies, interior HDR images, and simulated luminance maps across three buildings

Scene	HPR skies	Perez skies	HDR image	Simulations under HPR skies	Simulations under Perez skies
S1 05/18 5:00 p.m.	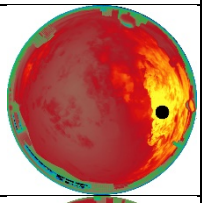	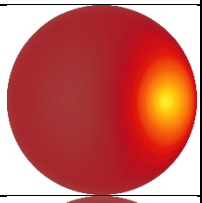	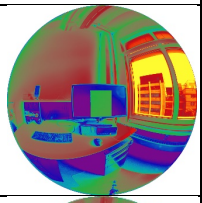	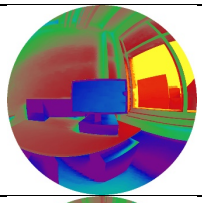	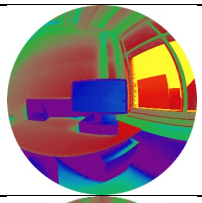
S2 05/17 2:20 p.m.	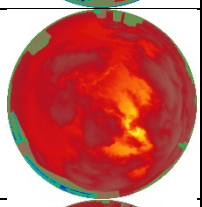	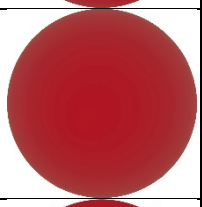	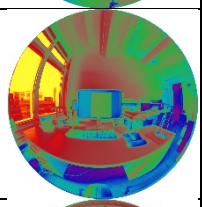	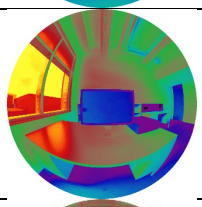	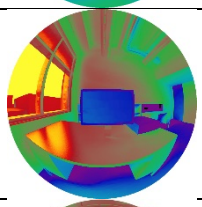
S3 07/25 2:00 p.m.	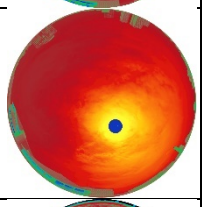	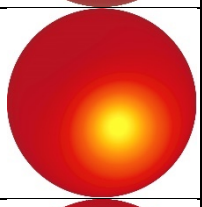	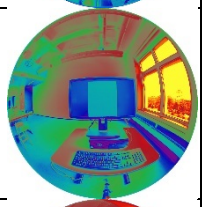	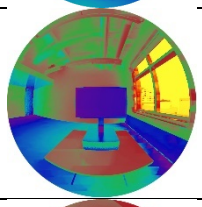	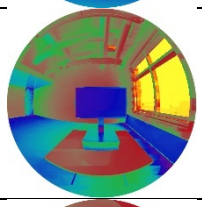
T1R1E 05/27 3:10 p.m.	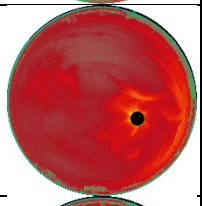	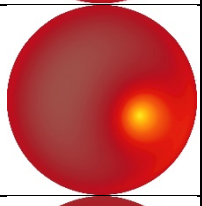	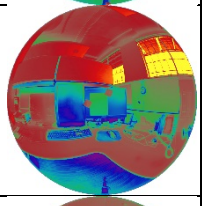	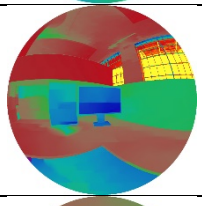	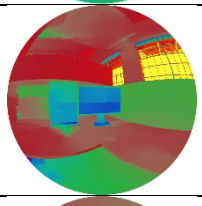
T1R2E 05/27 3:00 p.m.	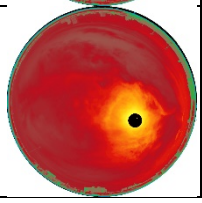	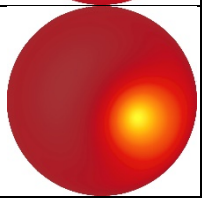	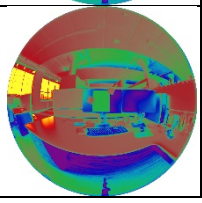	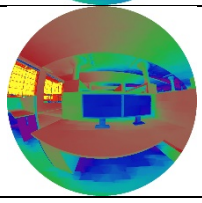	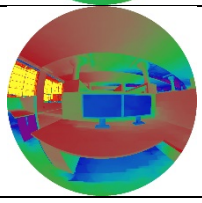

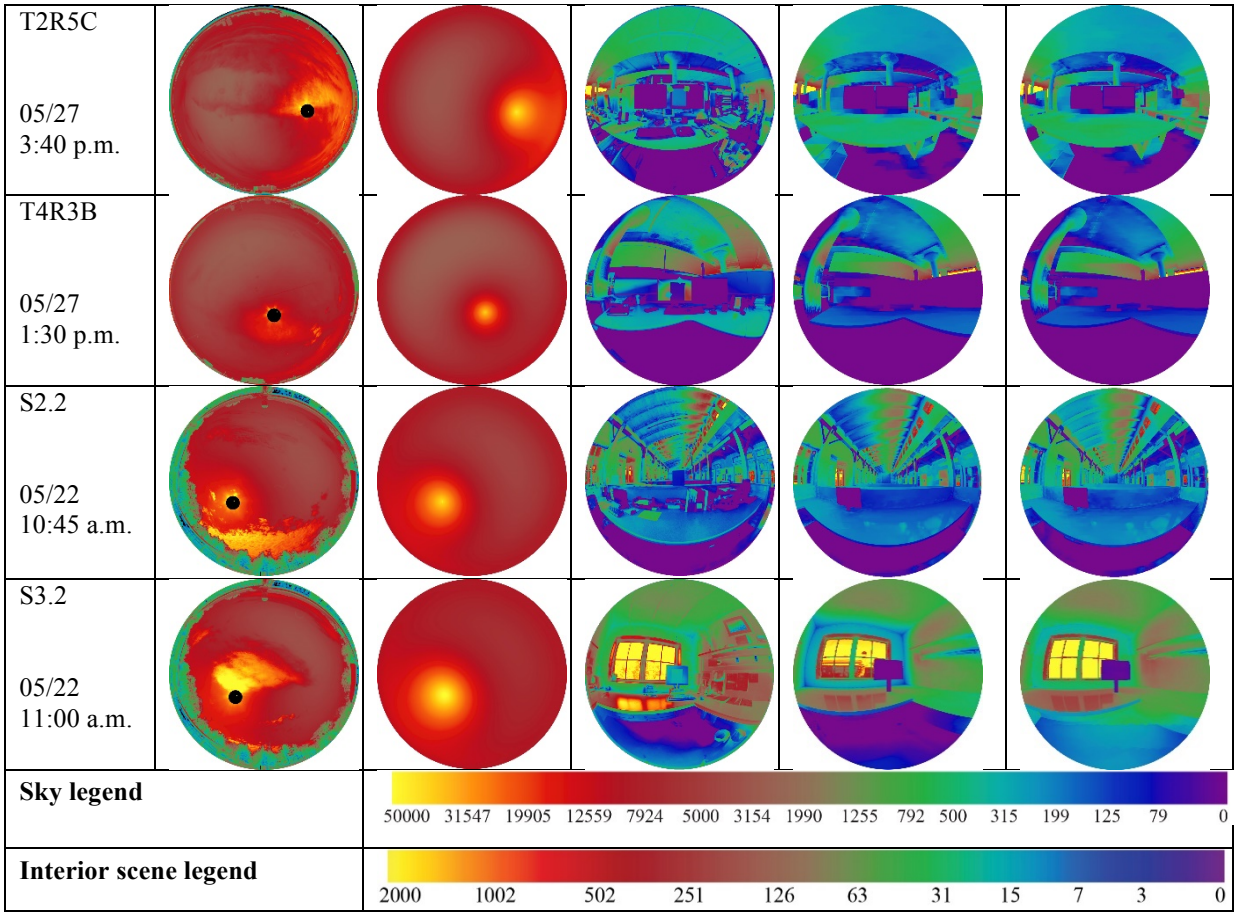

6.4.4 Comparison of Visual Discomfort Metrics

6.4.4.1 Vertical eye illuminance and DGP results

Figure 6.13 shows the E_v profiles of the HDR images ($E_{v\text{-}HDR}$) and the simulated luminance maps under HPR skies ($E_{v\text{-}HPR}$) and Perez skies ($E_{v\text{-}Perez}$). On May 17th and 25th, both $E_{v\text{-}HPR}$ (the red continuous line) and $E_{v\text{-}Perez}$ (the blue continuous line) underestimated $E_{v\text{-}HDR}$ (the gray dashed line), although $E_{v\text{-}HPR}$ was closer to $E_{v\text{-}HDR}$. On the remaining four days, $E_{v\text{-}HDR}$, $E_{v\text{-}HPR}$, and $E_{v\text{-}Perez}$ intersected with each other. The three scenes at AUP were near the windows and led to greater absolute errors between the simulated E_v and E_v from HDR images. On the contrary, the scenes at HGA with varying distances from the southwest windows presented smaller absolute errors between the simulated E_v and E_v from HDR images.

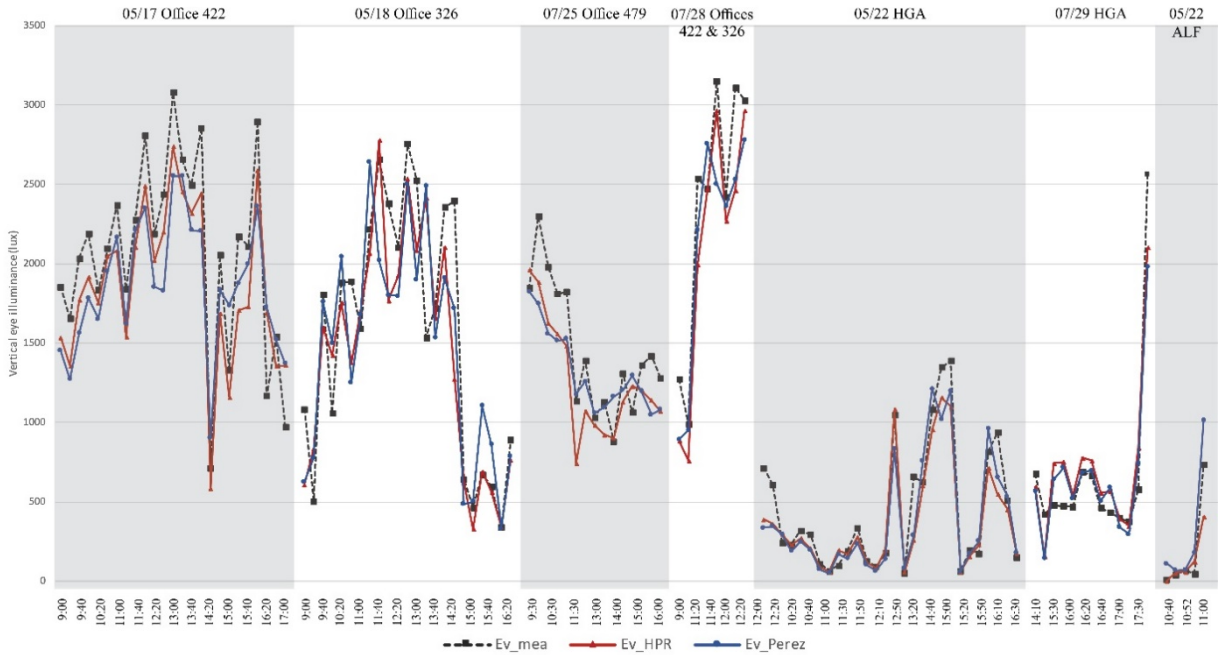

Figure 6.13: E_v profiles of HDR images and simulated luminance maps under HPR and Perez skies

Table 6.5 summarizes the numeric E_v errors between the simulated luminance maps and the HDR images. Compared with the Perez sky, the simulated results under the HPR sky model were slightly closer to $E_{v\text{-}HDR}$. Both the HPR and Perez sky models simulated more accurate luminance maps on sunny days than on intermediate or cloudy days. The simulated E_v under both sky models at HGA presented greater $RMSE_{rel}$ than at AUP. The simulated E_v at ALF demonstrated the lowest accuracy. Given that HGA is a large open-plan office with more complex spatial variations and material properties, more uncontrollable factors were attributed to greater $RMSE_{rel}$. Concerning DGP prediction, the frequency of accurate glare prediction under HPR skies varied between 87.5% and 100.0%, while the frequency under the Perez sky varied between 75.0% and 100.0%.

Excluding the results at ALF due to the inaccurate simulation model, the paired t-test (Box et al., 2005) was run between $RMSE_{rel}$ and the frequency of accurate glare prediction under two sky models. With n=6, df=5, and a critical value of t(5)=4.032 for a two-tailed test with α=.01, any t statistic falling between -4.032 and 4.032 fails to prove that the two groups of statistics are significantly different. As shown in Table 6, both t-test results failed to demonstrate any statistically significant difference between the two sky models in terms of

simulating luminance maps, which indicates that the horizontal HPR and Perez sky models simulated luminance maps at the same level of accuracy.

Table 6.5: Statistical comparison between HPR and Perez skies

Studied space	Date	Sky condition	$RMSE_{rel}$ of E_v under HPR skies	$RMSE_{rel}$ of E_v under Perez skies	Frequency of accurate glare prediction under HPR skies	Frequency of accurate glare prediction under Perez skies
Office 422	05/17	Intermediate & cloudy	14.3%	18.0%	92.0%	92.0%
Office 326	05/18	Intermediate & cloudy	25.3%	27.5%	100.0%	100.0%
Offices 422 & 326	07/28	Sunny & intermediate	14.8%	16.0%	87.5%	75.0%
Office 479	07/25	Intermediate & sunny	17.8%	18.0%	100.0%	100.0%
HGA	05/27	Cloudy & sunny	34.0%	35.4%	92.0%	92.0%
	07/29	Sunny	31.8%	32.8%	95.0%	95.0%
ALF	05/22	Sunny	83.2%	80.1%	85.7%	85.7%

Table 6.6: T-test results between HPR and Perez skies

Group	t value	Group	t value
$RMSE_{rel}$ of Ev	-3.280	Frequency of accurate glare prediction	1.000

6.4.4.2 COV of 40 horizontal band

Figure 6.14 shows the scatter plots between the COV under HPR skies (COV_{HPR}) against the COV of HDR images (COV_{HDR}) in red and the COV under Perez skies (COV_{Perez}) against COV_{HDR} in blue. The Linear Regression was run between the two groups of data with the y-intercept fixed at zero. For the HPR sky model, the linear fit had a slope of 0.8794 with R^2 equal to 0.8942. For the Perez sky model, the linear fit had a slope of 0.8417 with R^2 equal to 0.8278. The COV comparison confirmed the conclusion derived from the E_v and DGP comparisons that the horizontal HPR and Perez sky models are equally accurate.

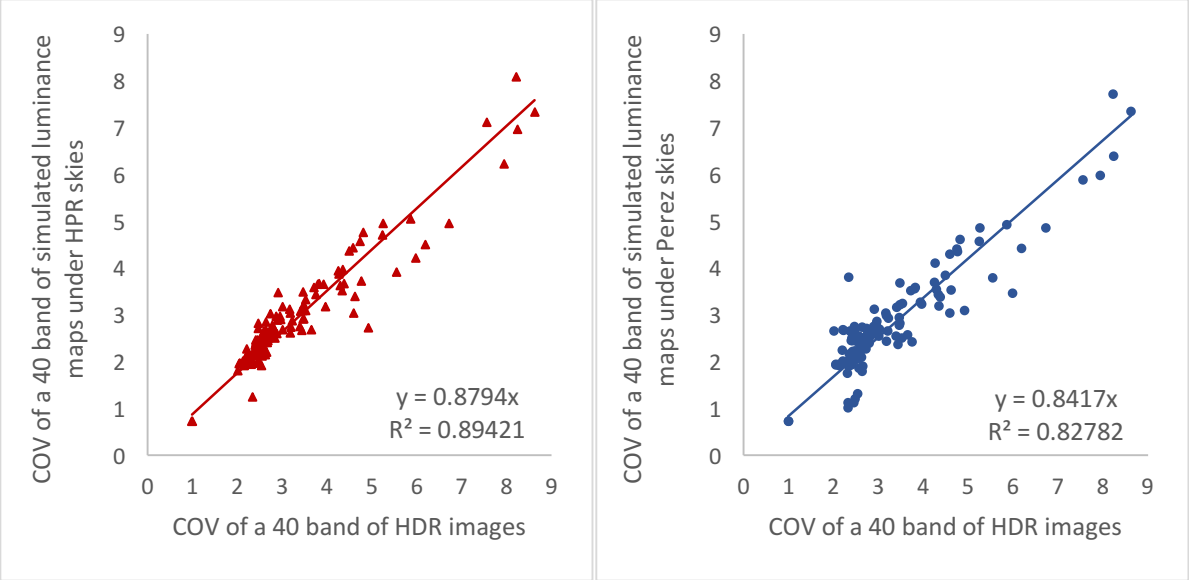

Figure 6.14: The scatter plot of COV_{HPR} against COV_{HDR} (left) and the scatter plot of COV_{Perez} against COV_{HDR} (right)

6.5 RESULTS OF VERTICAL HPR SKIES

Limited by the facilities, vertical luminance data of surrounding environments were only collected at ALF. Figure 6.15 shows the simulation results under vertical HPR skies. Compared with the HDR image, the simulated luminance map of S3.1 slightly underestimated luminance distributions. The results of S7 demonstrated the lack of sky data by capturing a hemispherical vertical sky image. The white circles on the simulated luminance maps highlight the boundary of the hemispherical HDR sky image. Unlike S3.1 with the window on one side, S7 with windows on three elevations revealed the missing luminance data of the hemispherical sky image. As the position of the outside camera failed to match exactly the vertical luminance environments of the interior camera, misalignments of exterior environments also occurred at S7. Although a spherical vertical HDR image can provide a complete lighting luminance of a scene, it is applicable in unconstructed sites rather than existing buildings. Additionally, a caution is required when only vertical HDR skies are employed in simulations. Due to its lack of surrounding geometric models, no shadows will be cast into a studied space from surrounding environments (Jones & Reinhart, 2016).

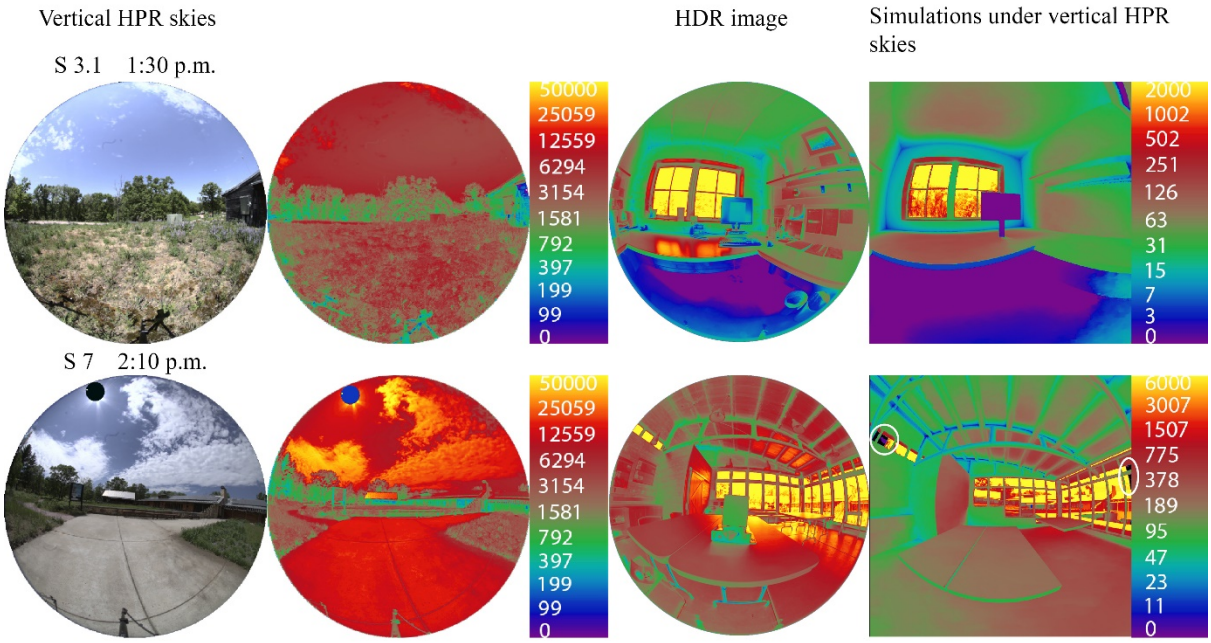

Figure 6.15: Falsecolor images of vertical HPR skies, interior HDR images, and simulated luminance maps at ALF

6.6 DISCUSSION

Compared with the simulated luminance maps of three offices at AUP, the simulations at HGA presented more scattered distributions of BE_{rel} and greater $RMSE_{rel}$. In other words, AUP's simulation results were more accurate than HGA's. It was reasonable to expect greater deviations of lighting simulations in a larger open-plan office with more furniture and a complex layout. This discussion section explored the view settings in simulations and its impact on simulation results.

As the E_v calculation was dependent on and sensitive to view settings, one primary cause that decreased the accuracy of simulated luminance maps at HGA was the larger misalignment errors between HDR images and simulated luminance maps. Unlike the fixed, daily camera positions for taking HDR images at AUP, the position of the camera at HAG slightly changed at each workstation at different times or on different days. Given the challenge of matching the exact position of a camera in the reality, a test of investigating the impact of image misalignments on deviation magnitudes of E_v was conducted. Three scenes, T1R2E, T2R5C, and T3R1C, were selected to include different portions of window areas

related to an entire scene. Based on the camera's positions in the real world, the simulated camera's heights were adjusted 2.5 centimeters (1 inch) higher and lower than the original heights (Figure 6.16 (right)). The camera's orientations were also rotated three steps clockwise and three steps counter-clockwise at 2.5-centimeter (1 inch) chord increments (Figure 6.12 (left)). Based on the changes of view settings in the simulation, the BE_{rel} of E_v varied between -13.4% and 24.0%, and the $RMSE_{rel}$ of E_v varied between 6.2% and 31.3% within the three scenes. The variations of BE_{rel} and $RMSE_{rel}$ partially explained the more scattered distributions of BE_{rel} and greater $RMSE_{rel}$ at HGA.

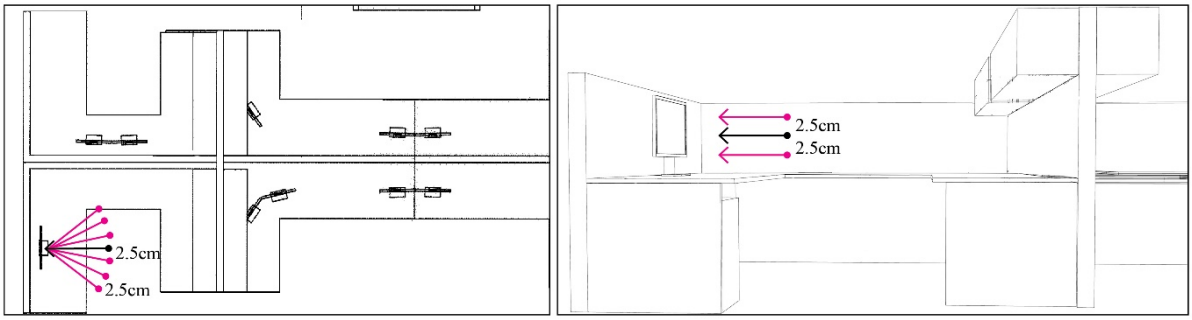

Figure 6.16: Various positions of camera settings in simulations in plan (left) and section (right)

In addition to the impact of the view settings in simulations, another cause of misalignments was the different degrees of control over the studied spaces. Under controlled environments, like the three offices at AUP, the BE_{rel} and $RMSE_{rel}$ were mostly below 20%. The offices were cleaned and reorganized before data collection. However, under uncontrollable environments, like HGA and ALF, since the researcher was not allowed to reorganize interior spaces, the BE_{rel} and $RMSE_{rel}$ of E_v were greater. Most of these uncontrollable factors that caused deviations in daylight simulations were deductive but quantitatively unpredictable. Therefore, a daylighting model with the RME and RMSE below 20% is capable of accurately representing lighting conditions in the real world (Jones & Reinhart, 2016).

The greater BE_{rel}, MBE_{rel} and $RMSE_{rel}$ at ALF were attributed to other reasons. One visit to ALF was insufficient to generate an accurately calibrated daylighting model. Second,

the camera for capturing sky models was placed in the courtyard. The camera's low position resulted in the HDR images of the skies with larger portions of surrounding environments, the buildings and trees, and smaller portions of sky. In that case, the HPR sky model underestimated most of the luminance maps, as shown in Table 6.4.

6.7 CONCLUSION

This chapter compared the accuracy of a hybrid photo-radiometer sky model with the Perez all-weather sky model by simulating luminance maps of real environments. The research employed the HPR sky model across three buildings, which varied in spatial organization, façade configuration, and material properties. Excluding the results at ALF due to the inaccurate simulation model, the $RMSE_{rel}$ of E_v under HPR skies and Perez skies were 21.2% and 23.7%, respectively. Although the simulated luminance maps under the horizontal HPR sky were closer to HDR images than the simulated luminance maps under the Perez sky, the difference in accuracy was insignificant. The results indicate that the horizontal HPR sky and the Perez sky generate comparable luminance maps, which result in E_v and glare predictions at the same level of accuracy. This paper recommends the Perez sky model for daylight simulations not only for its abundant weather data, but also for its ease of use in generating both point-in-time and annual simulation. Given this chapter only presented limited results of hemispherical vertical HPR skies, it recommends a future study of utilizing two cameras to capture the entire spherical scenes rather than half of a scene as the vertical HPR environmental model.

7 A POE STUDY OF DAYLIGHTING QUALITIES

The previous chapters demonstrate the effectiveness of two commonly used research tools, HDR image techniques and simulations, in terms of collecting and generating physical lighting data. This chapter explores the last research tool, questionnaire surveys, and explores occupant subjective evaluations concerning daylighting qualities at HGA. Occupant assessments of daylighting experiences are collected by interviews and questionnaires. The causes of visual discomfort are revealed. The office environmental variations that result in visual discomfort are discussed. Finally, the calibrated simulation model presents annual DGP profiles at select workstations to confirm the subjective evaluations.

7.1 RESEARCH OBJECTIVES

This chapter has three objectives. First, daylighting qualities at HGA are evaluated from occupants' perspectives to reveal individual variability and environmental variations that result in visual discomfort. Second, the renovated layout in Tier Two is analyzed in terms of glare reduction. Third, annual DGP profiles of select workstations are simulated and analyzed to confirm occupants' subjective assessments.

7.2 RESEARCH QUESTIONS

This chapter mainly solves the two questions below:

1. What are the environmental factors that have great impact on occupants' daylighting experience?

2. How effective is the renovated Tier Two in terms of daylight glare reduction?

7.3 METHODOLOGY

7.3.1 Interview

The methods of collecting subjective evaluations include interviews and questionnaires. First, 23 employees were interviewed to discover the main daylighting issues in the office. Interviews were conducted before the online survey for two purposes: 1) to

provide comprehensive understandings of lighting qualities in the office from occupants' perspectives; 2) to create an effective online questionnaire based on HGA's contexts. Table 7.1 shows the number of occupants and interviewees in each tier. Table 7.2 lists all the interview questions. The questions and orders were adjusted based on an interviewee's reaction. For instance, IQ2 was skipped if an interviewee was satisfied with lighting environments and did not experience visual discomfort. Each interviewee's responses were recorded and written down during the interview. The interviews were analyzed to determine the common issues regarding daylighting qualities and shading systems. The categorized themes were designed as questions with the detailed information as the options. The Institutional Review Board (IRB) Approval is in Appendix B.

Table 7.1: Count of the occupants and interviewees in the office

Tier	Occupants count	Percent of occupants in each tier	Count of interviewees	Percent of interviewees in each tier
Tier One	28	19.3	5	17.9
Tier Two	40	27.6	7	17.5
Tier Three	36	24.8	7	19.4
Tier Four	41	28.3	4	9.8

Table 7.2: Interview questions

IQ1	How do you feel about the lighting environments in the office, especially the daylighting aspect?
IQ2	What are the reasons that cause visual discomfort?
IQ3	How do you modify yourself or your workstation to solve visual discomfort?
IQ4	How do you feel about the river view outside?
IQ5	When do you normally experience visual discomfort in the office in a day and in a year?
IQ6	Do you think the interior mechoshades solve the visual discomfort? If not, what kinds of issues do you experience when the mechoshades are in operation?

7.3.2 Questionnaire

Before distributing the questionnaire to the entire office, a pilot study was carried out by distributing the questionnaire to 30 participants. According to their answers and comments, the questionnaire was modified to effectively reveal the issues relative to interior daylighting qualities. Then, the online questionnaire was distributed to the entire office on April 17th, 2017 and opened to the entire office for three weeks. As shown in Appendix C, the questionnaire consisted of two sections: daylighting evaluation and demographic information.

The daylighting evaluation section was comprised of seven-scale Likert questions, multiple-choice questions, and open-ended questions. Table 7.3 includes the numeric scales for the Likert questions. The daylighting evaluation section asked participants to rate their levels of satisfaction with the lighting and workstation environments, degrees of visual discomfort based on daily and seasonal occurrence, and levels of agreement on five statements that were extracted from the interviews. The degrees of visual discomfort on the bright side was employed (Osterhaus & Bailey, 1992), from imperceptible (comfortable), perceptible (slightly uncomfortable), disturbing, to intolerable. The participants who reported experience of visual discomfort were asked to select frequencies of nine adaptive behaviors, which were also summarized according to the interviews. This section also listed the issues related to the mechoshade systems as a multiple-choice question. The demographic section included gender, age, working hours per week, and locations of participants' workstations.

Table 7.3: Numeric values for 7-scale Likert questions

Question	**Likert scale**						
Q1. Satisfaction levels with lighting factors and workstation	Very satisfied	Moderately satisfied	Slightly satisfied	Neutral	Slightly dissatisfied	Moderately dissatisfied	Very dissatisfied
	+1	+2	+3	+4	+5	+6	+7
Q2 & Q3. Visual discomfort degree	NA/None	Comfortable	Perceptible	Disturbing	Intolerable		
	0	+4	+5	+6	+7		
Q7. Frequency of adaptive behavior	Never	Rarely	Occasionally	Sometimes	Frequently	Usually	Every time/always
	+1	+2	+3	+4	+5	+6	+7
Q9. Statement agreement	Strongly agreed	Agree	Somewhat agree	Neither agree or disagree	Somewhat disagree	Disagree	Strongly disagree
	+1	+2	+3	+4	+5	+6	+7

7.3.3 Participants

The questionnaire was distributed to all 145 employees through the internal HGA email system. From the 106 responses, 88 were valid, which resulted in a 60.7% response rate. The characteristics of the 88 participants are in Table 7.4. Of the 88 participants, 57

were males (64.8%) and 31 were females (35.2%). Over 80% of the participants were between 20 and 49 years old. Seventy-seven participants (87.5%) had been working in the office more than one year, and 67 participants (76.1%) spent more than 30 hours in the office per week. The high percent of the participants who had stayed in the office over one year and their long weekly working duration indicate their comprehensive understandings of the lighting environments. Seventy-four participants (84.1%) spent 61% or more of their time working on computers per week, which demonstrates the important role that computer-based work plays in the office.

Table 7.4: Participant information

	Measure	**Count of occupants**	**Percent of total**		**Measure**	**Count of occupants**	**Percent of total**
Gender	Male	57	64.8	**Weekly working hours at your workstation**	Less than 20 hours	5	5.7
	Female	31	35.2		20-30 hours	16	18.2
Age	20-29	25	28.4		30-40 hours	50	56.8
	30-39	28	31.8		Over 40 hours	17	19.3
	40-49	18	20.5	**Percent of using computer weekly**	Less than 20%	2	2.3
	50-59	13	14.8		21-40%	1	1.1
	60-69	4	4.5		41-60%	11	12.5
Years of working in the office	Less than 1 year	11	12.5		61-80%	20	22.7
	1-2 years	16	18.2		Over 81 %	54	61.4
	2-5 years	28	31.8				
	5-10 years	10	11.4				
	Over 10 years	23	26.1				

7.3.4 Annual Glare Simulations

In order to test occupants' subjective evaluations, annual glare profiles of select workstations were calculated. The calibrated simulation model from Chapter 6 was employed with the same material properties (Table 6.2). Comparing with the 78 valid HDR images taken on site, the simulated luminance maps presented 92% of accurate glare prediction (Table 6.5). This result also agreed with Jones and Reinhart's conclusion (Jones & Reinhart, 2016). As the calibrated model was capable of accurately representing the real lighting environments in terms of visual discomfort prediction, 14 representative workstations were selected to present their annual DGP profiles. In annual DGP simulations, when sunlight

penetration was perceived by the indoor sensors on the floor (the blue dots near the windows in Figure 7.1), the mechoshades were dropped to the pre-set positions. According to the pre-set positions in reality, the percent of windows covered by the mechoshade in Tier One, Tier Two and Tier Three, and Tier Four were 80%, 87.5%, and 77.5%, respectively.

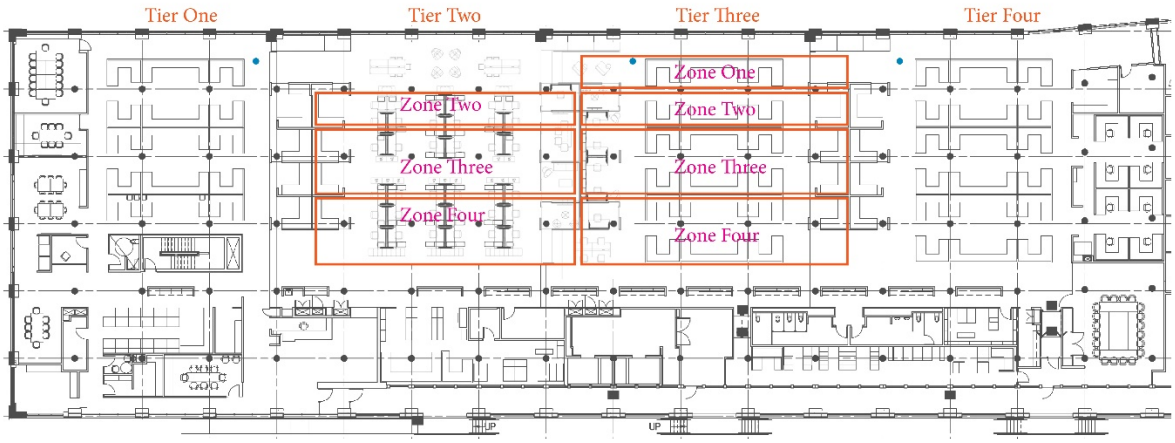

Figure 7.1: Spatial factors on the office layout

7.3.5 Data Analysis

The control, independent, and dependent variables are summarized in Table 7.5. The data was classified in accordance with the environmental characteristics: tier, zone, and seating orientations. As shown in Figure 7.1, the office had four tiers. Based on the distance between a workstation and the southwest facade, the office was divided into four zones (Figure 7.1). The eight seating orientations were divided into three groups based on their relations to the southwest windows. Table 7.6 displays the occupant count in each group.

Table 7.5: Independent and dependent variables

Independent variables	Environment variations: tiers, zones, and seating orientations Personal attitudes towards daylight & outside views Demographic differences: Gender and age
Dependent variables	Satisfaction levels with lighting environments, degrees of visual discomfort, frequencies of adaptive behaviors

All the participants' feedback was coded and exported to SPSS. Then the distribution of the data was tested for normality. The p values for all groups of responses were less than 0.05, therefore, the distribution failed to match the normality. The statistical methods that aim to analyze non-parametric data as the prerequisite were selected:

Table 7.6: Grouped data based on the environmental factors

Tier	Count	**Zone**	Boundary	Distance	Count	**Seating Orientation**	Seating orientation	Count
One	24	One	0 - 4.7 meters	4.7m	12	Towards windows	Southwest & South & West	28
Two	23	Two	4.7 - 7.5 meters	2.8m	12	Parallel windows	Southeast & Northwest	34
Three	17	Three	7.5 - 13.1 meters	5.6m	33	Away from windows	East & Northeast & North	26
Four	24	Four	13.1 - 18.7 meters	5.6m	31			

The Spearman Correlation evaluates the strength and direction of association between participant satisfaction levels with lighting environments, like artificial light, natural light, and overall light. The associations of participants' attitudes towards daylight, outside views, and the effectiveness of modified behaviors were also examined by the Spearman Correlation.

The Mann-Whiteny U Test determines if the two dependent samples, like males' and females' opinions of lighting environmental elements, have the same distributions. The Kruskal-Wallis Test compares three or more groups of independent samples and determines whether these samples stem from the same distribution. According to the office's environmental variations, four tiers, four zones, and three groups of seating orientations were categorized for analysis. After the Kruskal-Wallis Test reveals statistically significant differences among each dependent variable, the Dunn-Bonferroni post hoc method was employed to identify statistical differences between two or more groups.

7.4 RESULTS

7.4.1 Interviews Summary

As shown in Appendix D, six themes were derived from 23 interviewees' comments: causes of visual discomfort, visual discomfort occurrence schedule, individuals' adaptive behaviors due to visual discomfort, individuals' attitudes towards daylight and outside views, the issues related to mechoshade systems, and the problems related to artificial light. Of the 23 interviewees, eight reported no visual discomfort experience, while 15 reported different

degrees and causes of visual discomfort. Further interpretation of interviewees' responses was analyzed together with the results of the questionnaire in the discussion section.

7.4.2 Descriptive Data

Figure 7.2 shows the participants' rating of visual discomfort based on daily occurrence. Most participants (83.9%) indicated that they were comfortable with the lighting environment between 8 a.m. and 2 p.m. However, 34.4% of the participants experienced disturbing or greater visual discomfort between two and four in the afternoon, and 33.3% of the participants experienced disturbing or greater visual discomfort between 4 and 6 in the afternoon. After excluding the participants who reported no visual discomfort, the mean degree of visual discomfort between 2 and 4 p.m. was 5.17, and the mean between 4 and 6 p.m. was 5.01. Values greater than 5 demonstrate the occurrence of perceptible or greater visual discomfort. The larger the value, the more severe the degree of visual discomfort. The results indicated that visual discomfort often occurred in the afternoon.

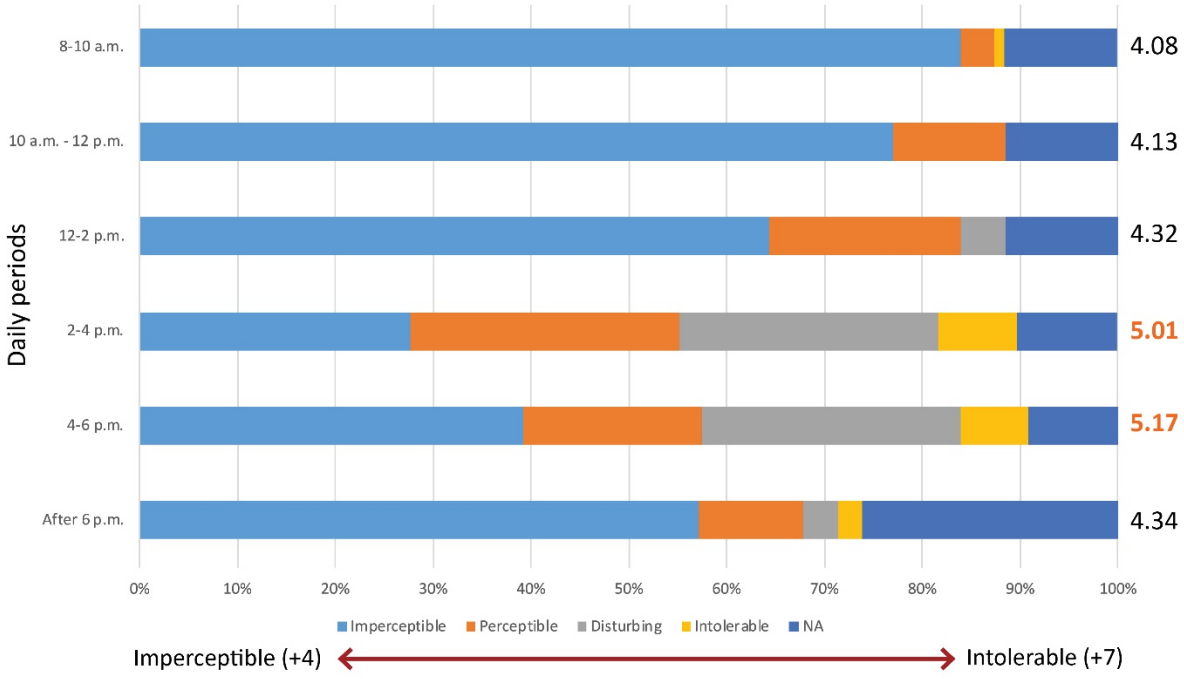

Figure 7.2: Participants' ratings of daily visual discomfort

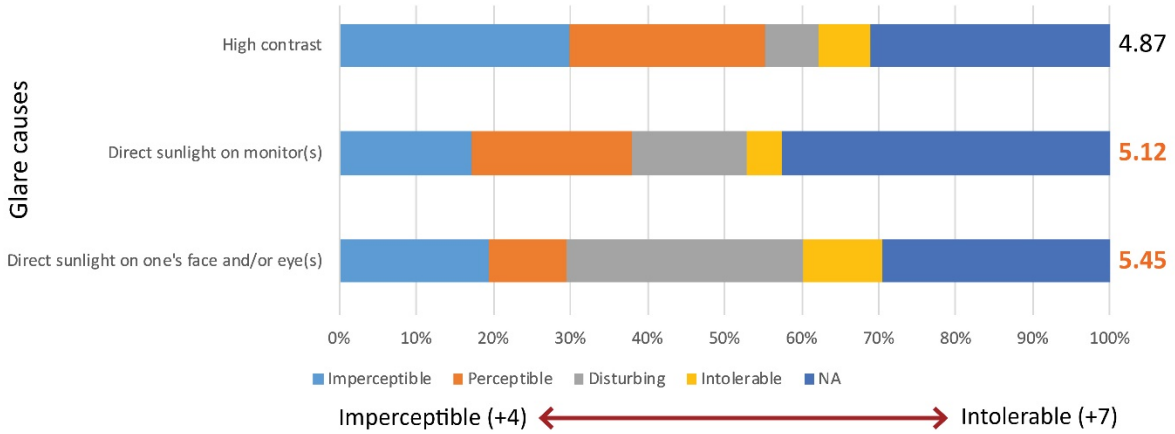

Figure 7.3: Participants' ratings of three causes of visual discomfort

Figure 7.3 demonstrates the participants' ratings of visual discomfort based on three causes: direct sunlight on faces and/or eyes, sunlight on monitors, and high contrasts between monitors and backgrounds. Over forty percent of the participants experienced direct sunlight on their faces and/or eyes and ranked this experience disturbing or greater. Nineteen-point-five percent of the participants considered direct sunlight on their monitors as disturbing or greater. Only 13.8% of the participants suffered from disturbing or intolerable degrees of high contrasts between their monitors and backgrounds. After excluding the participants who reported no visual discomfort, the mean degrees of direct sunlight on people's face and/or eyes, direct sunlight on monitors, and high contrasts were 5.45, 5.12, and 4.87, respectively. The results indicated that direct sunlight on people's faces and/or eyes was the most severe cause of visual discomfort in the office.

Figure 7.4 demonstrates the sky conditions (right) and the seasons (right) when visual discomfort frequently occurred. Selected by 77.5% of participants, clear/sunny skies were the sky condition when visual discomfort happened most frequently. Of the 19 participants who selected "other", 11 clarified that they did not access natural light or experience visual discomfort. Fifty-three participants (60.5%) selected winter as the season when visual discomfort occurred most frequently.

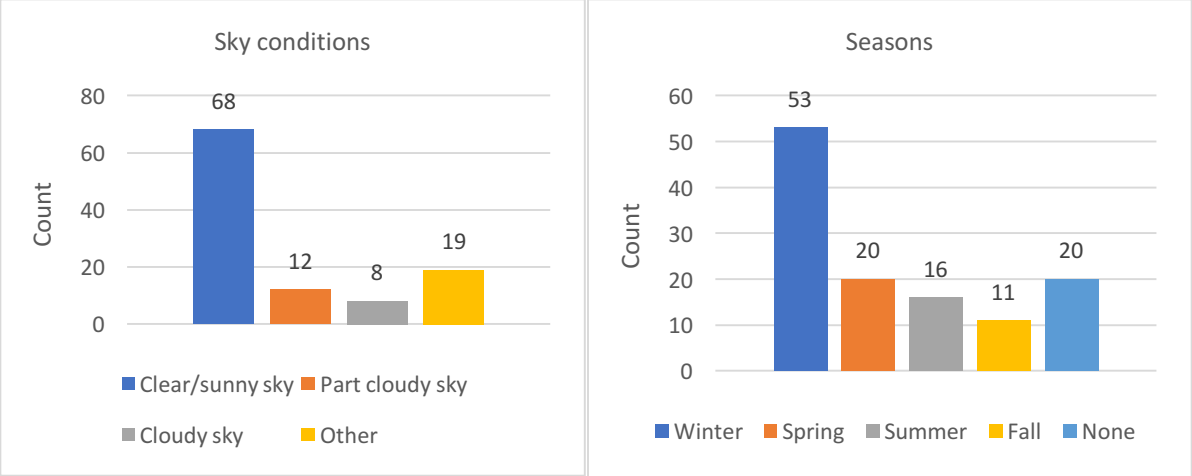

Figure 7.4: Sky conditions (left) and seasonal effects (right) on visual discomfort occurrence

7.4.3 Individual Different Attitudes

7.4.3.1 Attitudes towards Daylight and Outside Views

Table 7.7 presents the correlation coefficients between participant satisfaction levels with the five environmental items, natural lighting environments, artificial lighting environments, mechoshade systems, overall lighting environments, and workstation environments. Artificial lighting satisfaction was moderately correlated with overall lighting satisfaction (r^2=0.650, $p<0.01$), while the correlation between natural lighting satisfaction and overall lighting satisfaction was relatively weaker (r^2=0.447, $p<0.01$). The higher correlation coefficient between artificial lighting and overall lighting satisfaction indicated that artificial light played a more important role in participants' lighting experience. The remaining correlations were weak. The mechoshade satisfaction was correlated with the other four items. Although the correlation between mechoshade and overall lighting satisfaction (r^2=0.340, $p<0.01$) along with the correlation between mechoshade and workstation satisfaction (r^2=0.311, $p<0.01$) were weak, they demonstrated the statistically significant role that mechoshade systems played in occupants' satisfaction with lighting and workstation environments. Concerning the satisfaction with workstation environments, overall lighting satisfaction (r^2=0.374, $p<0.01$), artificial lighting satisfaction (r^2=0.244, $p<0.05$), and natural lighting satisfaction (r^2=0.213, $p<0.01$) all presented weak correlations.

Table 7.7: Correlations between lighting environmental items

Satisfaction level with	Artificial light	Natural light	Mechoshade	Overall Light	Workstation
Artificial light		.126	.217*	.650**	.244*
Natural light	.126		.258*	.447**	.213*
Mechoshade	.217*	.258*		.340**	.311**
Overall Light	.650**	.447**	.340**		.374**
Workstation	.244*	.213*	.311**	.374**	

** Correlation is significant at the 0.01 level (2-tailed)
* Correlation is significant at the 0.05 level (2-tailed)

Table 7.8 demonstrates the Spearman Correlation results for Question 9 (Q9). Q9 asked the participants to rate their levels of agreement with the five statements: 1) daylight is important; 2) the outside view is important; 3) natural light does not interfere with my work; 4) modified activities reduce visual discomfort; and 5) well-designed boards are necessary to block sunlight. Participants' attitudes towards daylight and outside views were strongly correlated (r^2=0.849, p<0.01), which confirmed interviewees' responses, whoever liked outside views also liked natural light, and vice versa. The correlations between Q9.4 and Q9.5 (r^2=0.330, p<0.01) indicated that erecting foam core boards was one type of participants' adaptive behaviors to resume their visual comfort. The correlations between Q9.1 and Q9.4 (r^2=0.292, p<0.05), along with Q9.2 and Q9.4 (r^2=0.243, p<0.05), demonstrated that participants who liked daylight and outside views were prone to adjust themselves and/or their workstations to resume visual comfort.

Table 7.8: Correlations between participants attitudes towards lighting environmental factors

	9.1. Daylight is important.	9.2. The outside view is important.	9.3. Natural light doesn't interfere my work.	9.4. Modified activities to reduce visual discomfort.	9.5. Well-designed boards to block sunlight.
9.1. Daylight is important.		.849**	.296**	.292**	.072
9.2. The outside view is important.	.849**		.264*	.243*	.051
9.3. Natural light doesn't interfere my work.	.296*	.264*		.160	.037
9.4. Modified activities reduce visual discomfort.	.292**	.243*	.160		.330**
9.5. Well-designed boards to block sunlight.	.072	.051	.037	.330**	

** Correlation is significant at the 0.01 level (2-tailed)
* Correlation is significant at the 0.05 level (2-tailed)

7.4.3.2 Attitude Impacts on Lighting Satisfaction

The Mann-Whitney U test was run to examine whether participants' attitudes towards daylight and outside views impacted their levels of satisfaction with lighting environments. The participants were divided into two groups: the participants who agreed with the importance of daylight ($group_{agr}$) and outside views versus the participants who disagreed with or rated neutral attitudes towards the importance of daylight and outside views ($group_{disagr}$). As shown in Table 7.9, there was statistically significant difference between $group_{agr}$ and $group_{disagr}$ in terms of participant satisfaction with natural lighting environments and outside views. The participants who considered daylight important were more satisfied with their natural lighting environments, while the participants who considered daylight unimportant were less satisfied with natural lighting environments (U=1086.5, p=0.010). Likewise, participants who considered outside views important were more satisfied with their natural lighting environments (U=1124.5, p=0.000) than the participants who did not care about the outside views.

Table 7.9: The Mann-Whitney U test of satisfaction with natural light due to individual variability

Satisfaction with natural light	Group (count)	Mann-Whitney U	Mean rank	Sig.
Daylight is important	$group_{agr}$ (58)	1086.5	38.8	0.010**
	$group_{disagr}$ (28)		53.3	
Outside view is important	$group_{agr}$ (61)	1124.5	37.6	0.000***
	$group_{disagr}$ (25)		58.0	

Note: *p<0.05; **p<0.01; ***p<0.001.

7.4.3.3 Gender Difference

The Mann-Whitney U test discovered different evaluations between the male and female groups, and the Kruskal-Wallis test analyzed diverse attitudes among different age groups. Table 7.10 shows the gender impacts on occupant satisfaction with lighting environments and workstation environments, along with their different attitudes towards daylight. Compared with the female participants, the male participants were more satisfied with both artificial lighting and workstation environments. However, the female participants

considered daylight more important than the male participants. Finally, age groups had no statistically significant difference among the environmental factors.

Table 7.10: The Mann-Whitney U test of gender differences

Satisfaction	**Gender (Count)**	**Mann-Whitney U**	**Mean rank**	**Mean**	**SD**	**Sig.**
Satisfaction with artificial light	Male (57)	586.5	38.7	3.3	0.24	
	Female (31)		49.8	4.1	0.32	0.043*
Satisfaction with overall workstation	Male (57)	582.0	38.6	2.9	0.21	
	Female (31)		51.1	3.6	0.29	0.020*
Statement agreement	**Gender (Number)**	**Mann-Whitney U**	**Mean rank**	**Mean**	**SD**	**Sig.**
Daylight is important	Male (57)	570.0	45.94	3.167	0.217	
	Female (31)		34.66	2.379	0.296	0.037*

Note: *p<0.05; **p<0.01; ***p<0.001.

7.4.4 Environmental Variations

7.4.4.1 Tier variance

As shown in Table 7.11, three subjective attributes had statistically significant differences among the four tiers: participant satisfaction levels with natural light (H(3)=12.17, p=0.007), degrees of direct sunlight on people's faces and/or eyes (H(3)=9.48, p=0.024), and degrees of visual discomfort between 2 and 4 p.m. (H(3)=11.50, p=0.009). Figure 7.5 shows the results of the pairwise tests. There was a statistically significant difference between Tier One and Tier Four (Test Statistic=-21.81, Adj. Sig.=.012), along with a statistically significant difference between Tier Two and Tier Four (Test Statistic=-19.31, Adj. Sig.=.041). Tier One and Tier Four had statistically significant difference (Test Statistic=21.51, Adj. Sig.=.012) in terms of

Table 7.11: Kruskal-Wallis results among tier groups

Tier	**Satisfaction with natural light**			**Direct sunlight on people's faces and/or eyes**			**Visual discomfort levels between 2 and 4 p.m.**		
	Mean rank	Chi-square	Sig.	Mean rank	Chi-square	Sig.	Mean rank	Chi-square	Sig.
One	36.1	12.17	.007*	52.0	9.48	.024*	54.1	11.50	.009*
Two	33.6			47.9			46.6		
Three	47.5			40.1			35.8		
Four	53.4			32.0			32.6		

Note: *p<0.05; **p<0.01; ***p<0.001.

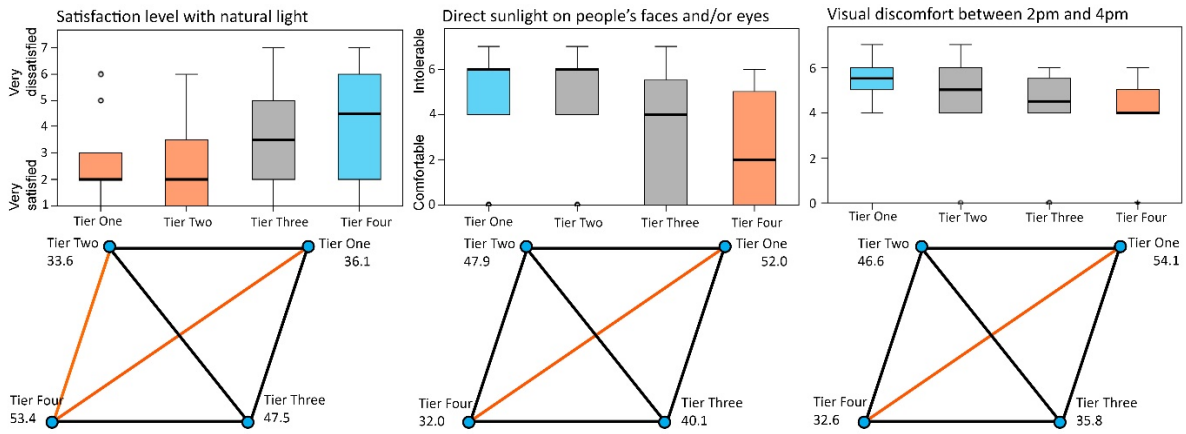

Figure 7.5: Pairwise tests of satisfaction levels with natural light (left), degree of direct sunlight on people's face and/or eyes (middle), and visual discomfort between 2 and 4 p.m. (right) among four tiers

degrees of visual discomfort between 2 and 4 p.m. Additionally, the results of the pairwise test displayed the greater degree of direct sunlight in Tier One than in Tier Four (Test Statistic=20.02, Adj. Sig.=.027). Compared with the participants in Tier Four, the participants in Tier One with the tallest windows were more satisfied with their natural lighting environments. However, the participants in Tier One also suffered greater degrees of direct sunlight on them, especially between 2 and 4 p.m.

7.4.4.2 Zone variance

Table 7.12 illustrates that all three causes of visual discomfort, direct sunlight on people's faces and/or eyes (H(3)=9.30, p=0.026), sunlight on monitors (H(3)=14.93, p=0.002), and high contrasts (H(3)=8.30, p=0.04), had statistically significant differences among the four zones. Figure 7.6 presents the results of the pairwise test of the three causes. Compared with Zone Three (Test Statistic=24.33, p=.019) and Zone Four (Test Statistic=21.86, p=.044), the participants in Zone One experienced more severe direct sunlight on their faces and/or eyes. Likewise, Zone One presented higher contrasts than Zone Three (Test Statistic=22.32, p=.032). The participants in Zone Two experienced more direct sunlight on their monitors than the participants in Zone Four (Test Statistic=27.92, p=.003).

Table 7.12: Kruskal-Wallis results for zone group

Zone	Direct sunlight on people's face/eye			Sunlight on monitors			High contrast		
	Mean rank	Chi-square	Sig.	Mean rank	Chi-square	Sig.	Mean rank	Chi-square	Sig.
One	61.4	9.30	.026*	52.0	14.93	.002*	59.6	8.30	.040*
Two	43.0			58.8			37.8		
Three	39.5			41.3			37.3		
Four	37.0			30.9			40.6		

Note: *p<0.05; **p<0.01; ***p<0.001.

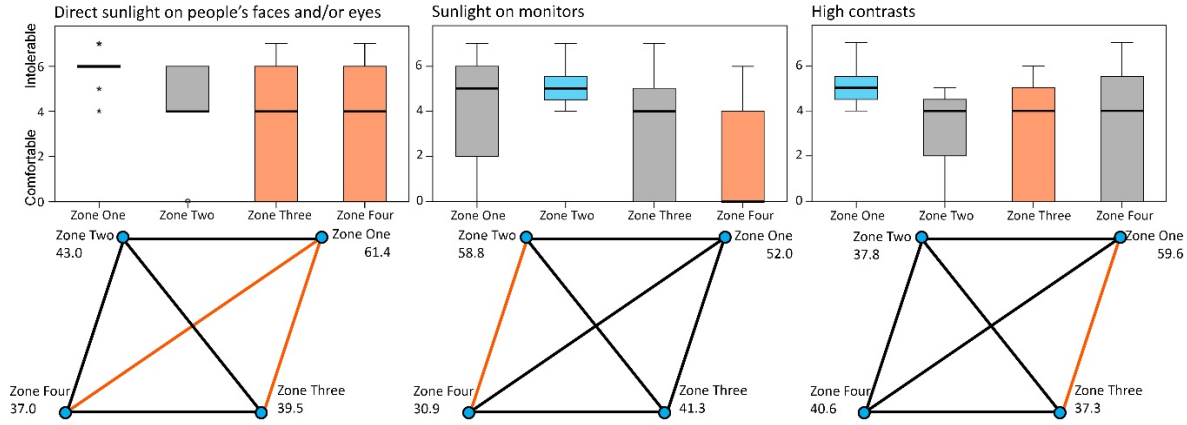

Figure 7.6: Pairwise tests of direct sunlight on people's face and/or eyes (left), high contrast (middle), and direct sunlight on monitors (right) among four zones.

7.4.4.3 Seating orientation variance

The results of the Kruskal-Wallis test demonstrated that the degrees of visual discomfort between 2 and 4 p.m. (H(2)=10.33, p=0.006) and direct sunlight on people's faces and/or eyes (H(2)=11.10, p=0.004) had statistically significant differences among three seating orientation groups (Table 7.13). As presented in Figure 7.7, compared with the participants facing away from the windows, the participants facing towards the windows suffered from greater visual discomfort between 2 and 4 p.m. (Test Statistic=20.74, p=.005) and direct sunlight on their faces and/or eyes (Test Statistic=22.01, p=.003).

Table 7.13: Kruskal-Wallis results for seating orientation group

Seating orientation	Degree of visual discomfort between 2 and 4 p.m.			Direct sunlight on people's face/eye		
	Mean rank	Chi-square	Sig.	Mean rank	Chi-square	Sig.
Towards windows	51.7	10.33	.006*	51.3	11.10	.004*
Parallel windows	38.7			40.0		
Away from windows	30.9			29.3		

Note: *p<0.05; **p<0.01; ***p<0.001.

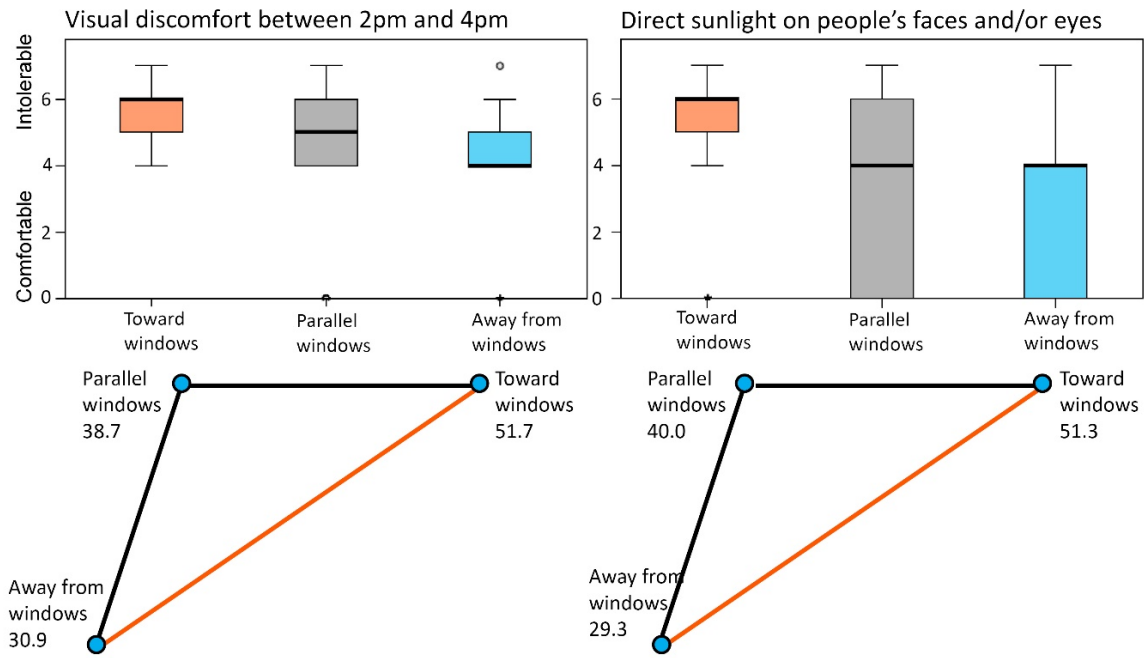

Figure 7.7: Pairwise tests of degrees of visual discomfort between 2 and 4 p.m. (left) and direct sunlight on peoples' faces and/or eyes (right) among three seating orientation groups.

7.4.5 Annul DGP Simulations

Fourteen workstations were selected to examine long-term visual discomfort. Figure 7.8 shows the annual DGP profiles at three of the select workstations. The horizontal axis represents 365 days per year, while the vertical axis represents daytime from 8 a.m. to 6 p.m. The red, orange, and yellow represent intolerable, disturbing, and perceptible glare, respectively. The green indicates imperceptible glare. Three workstations, T1R1C, T3R1C, and T4R1C, all faced towards the southwest façade with the same distance away from the façade. The DGP profiles demonstrated that visual discomfort occurred more frequently during the winter, especially in the afternoon after 2 p.m., which confirmed the conclusion of the questionnaire. Due to the tallest windows in Tier One, T1R1C had the longest duration of annual glare. As shown in Table 7.14, the annual disturbing and intolerable glare at T1R1C, T3R1C, and T4R1C lasted 315 hours, 246 hours, and 221 hours, respectively. The comparison of the annual DGP profiles at the three workstations demonstrated that the tallest windows in Tier One resulted in the longest annual glare duration.

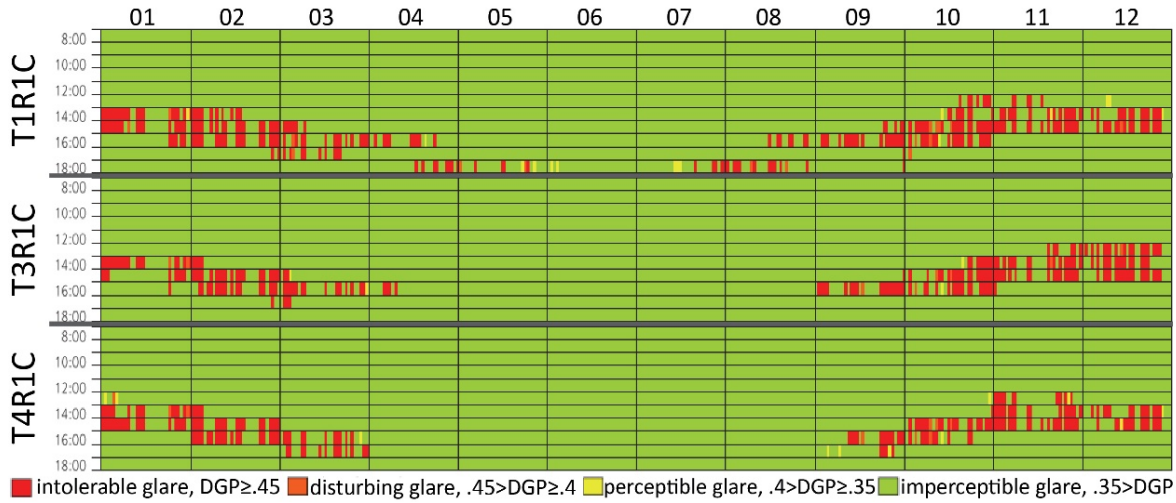

Figure 7.8: The variation in window heights with respect to annual DGP profiles

Figure 7.9 displays the annual DGP profiles at T3R2A, T2R1A, and T2R1F. All three workstations were the same distance from the façade, with the seating orientation parallel to the windows, and in the Tiers with the same window height. However, the original cubicle workstations (T3R2A) had no glare, while the more open workstations (T2R1A and T2R1F) had 30 hours of glare per year. The results showed the increase of annual glare duration caused by the more open workstations in the renovated layout.

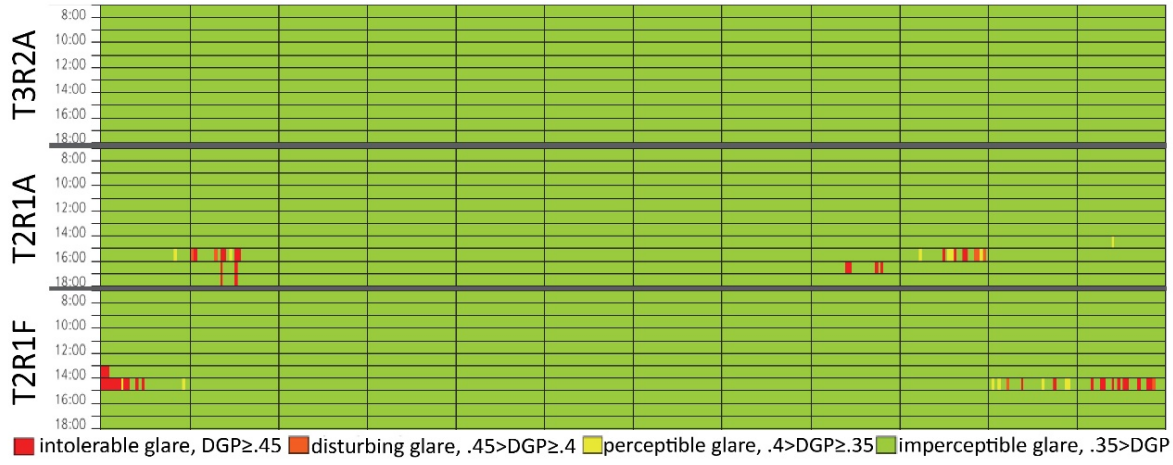

Figure 7.9: The variation in workstation enclosure with respect to annual DGP profiles

Figure 7.10 presents the annual DGP profiles at T1R1C, T1R3E, and T1R5C. All three workstations were in Tier One and directly faced the windows with varying distances away from the southwest windows. Compared with the 315 hours of disturbing and intolerable glare at T1R1C, T1R3E presented 84 hours of disturbing and intolerable glare, while T1R5C had no

glare. The DGP results indicated that the more distant a workstation from the windows, the shorter annual glare duration at that workstation, which confirmed the conclusion of the zone variation from the questionnaire analysis.

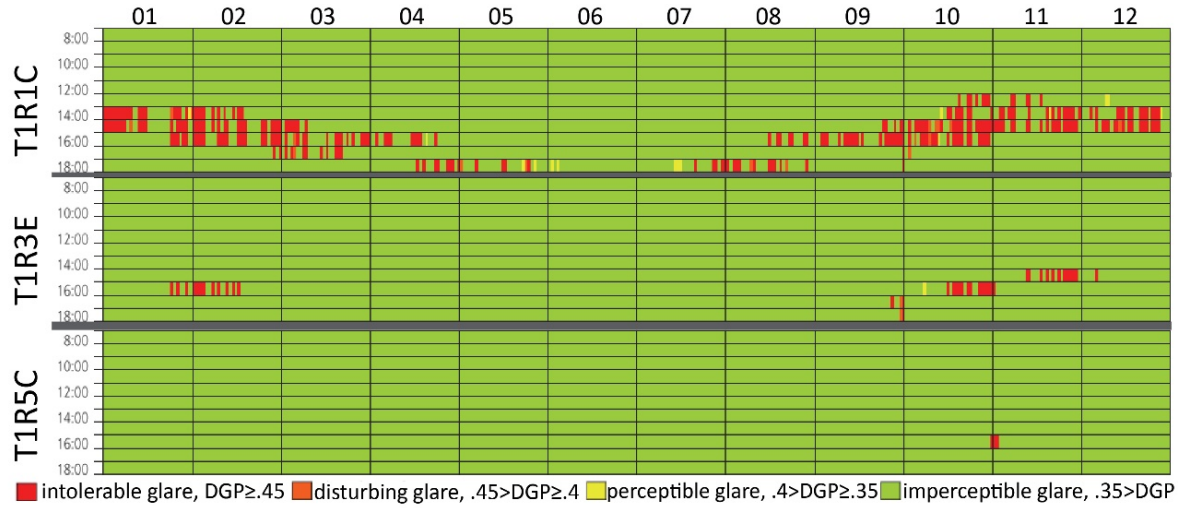

Figure 7.10: The variation in distance between workstation and the windows with respect to annual DGP profiles.

Table 7.14: Annual glare duration based on three degrees at 14 workstations.

Workstation	**T1R1C**	**T1R1E**	**T1R3E**	**T1R5C**	**T2R1A**	**T2R1F**	**T2R4C**
Intolerable	299	123	42	0	17	29	0
Disturbing	16	10	42	0	5	2	0
Perceptible	15	11	42	0	0	7	0
Workstation	**T2R4D**	**T3R1C**	**T3R2A**	**T3R4E**	**T4R1C**	**T4R1E**	**T4R3E**
Intolerable	0	238	0	0	212	61	0
Disturbing	0	8	0	0	9	17	0
Perceptible	0	4	0	0	12	10	0

Figure 7.11 demonstrates the annual DGP profiles at four workstations. Compared with T1R1C, T1R1E presented shorter annual glare duration due to the seating orientation. As shown in Table 7.14, T1R1E had 182 hours fewer annual glare duration. The same conclusion can be drawn from the comparison between T4R1C and T4R1E, one directly faced the windows while the other was at an oblique angle. The latter possessed 143 hours fewer annual glare than the former.

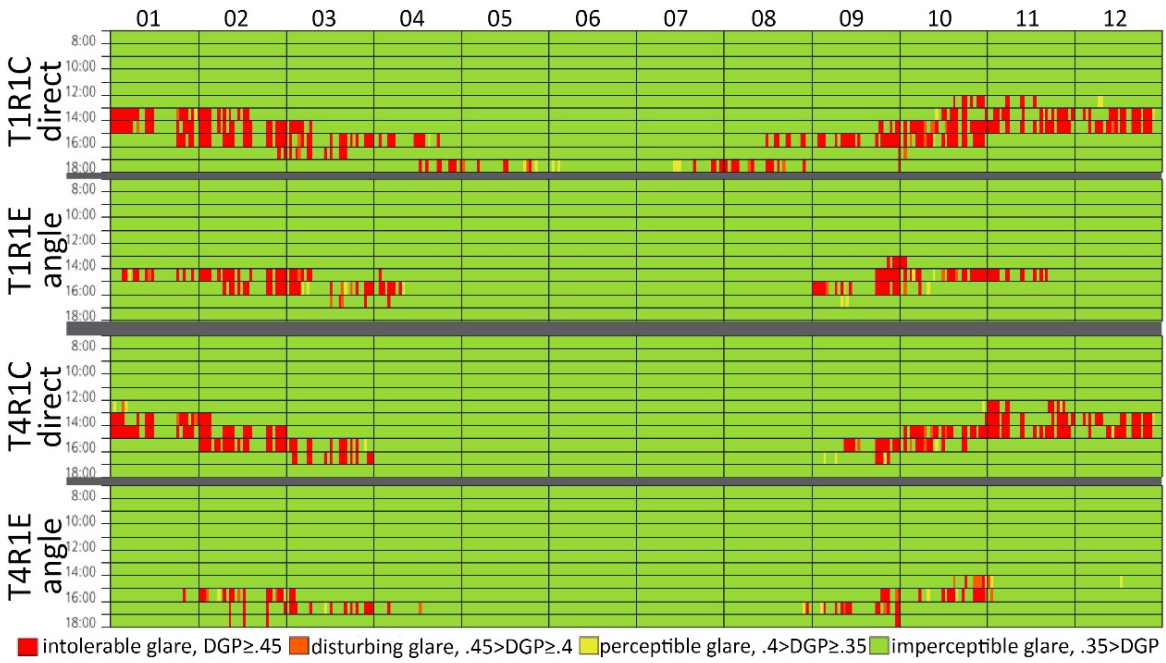

Figure 7.11: Effect of seating orientation on the annual DGP profiles at four workstations.

7.5 DISCUSSION

7.5.1 Individual Variability

Both the responses to the questionnaire and interview comments demonstrated the impacts of individual variabilities on participants' assessments of their lighting experience. It is reasonable to obtain a strong correlation between participants' attitudes towards daylight and outside views ((r^2=0.849, p<0.01). Participants' attitudes towards daylight and outside views also had positive influence on the levels of satisfaction with their natural lighting environments. The participants who considered daylight and outside views important were more likely to be satisfied with their daylighting environments. The interviewees who expressed their affection for outside views and daylight reported no visual discomfort experience. However, the interviewees who complained about visual discomfort expressed their indifferent attitudes towards views and daylight. These participants who held indifferent attitudes preferred comfortable lighting environments without glare disturbance so that they could concentrate on work. Furthermore, analysis results displayed statistically significant differences between the male and female participants in terms of satisfaction with daylighting

and workstation environments as well as attitudes towards daylight. Previous studies presented the similar conclusions that participants' gender has a significant influence on perceptual evaluations of office environments and female participants produced more negative reactions than male participants (Kim, de Dear, Cândido, Zhang, & Arens, 2013; Yildirim, Akalin-Baskaya, & Celebi, 2007). Substantial research proposed individual variability as one significant factor in relation to their lighting assessments (J. Alstan Jakubiec & Reinhart, 2016; Jin et al., 2017; K. Van Den Wymelenberg, 2012). Instead of randomly assigning staff members to workstations, providing staff members with the workstations based on their ambient preferences can reduce occupants' visual discomfort. In other words, positioning the occupants who prefer daylight and outside views near the windows and the ones who hold indifferent attitudes towards daylight and outside views further from the windows can take advantage of daylight (Heerwagen & Diamond, 1992).

7.5.2 Daylight Quality in Original Tiers

According to the analysis from both subjective and objective perspectives, the external and internal solar controls failed to provide comfortable lighting environments for most of the occupants in the office. Thirty-two-point nine percent of the participants were dissatisfied with their daylighting environments. Sixty-five-point nine percent of the participants reported that they experienced visual discomfort caused by daylight. The descriptive responses to the questionnaire revealed that the main cause of visual discomfort was direct sunlight on people's faces and/or eyes, which usually occurred on sunny days. Visual discomfort happened more frequently between 2 and 6 p.m., which can be explained by the office's southwest orientation. Additionally, neither exterior overhangs or interior mechoshade systems successfully blocked direct sunlight during the winter when the sun was low in the sky.

The results of the Kruskal-Wallis Test showed that Tier One, Zone One, and seating orientations toward the windows all presented high risk of visual discomfort. As shown in Figure 7.5, Tier One with the tallest windows (3.6m) led the occupants to longer periods of solar exposure. The tallest windows in Tier One resulted with the most severe visual discomfort between 2 and 4 p.m., as well as direct sunlight on people's faces and/or eyes. Although tall windows are encouraged in design strategies for deeper sunlight penetration (Baker & Steemers, 2002), architects need to provide controls for occupants to strike a balance between the amount of accessible daylight and visual discomfort.

Obviously, occupants who sat adjacent to windows or faced towards windows had a higher risk of experiencing visual discomfort. Although the original layout had a walkway functioning as a buffer zone between the southwest windows and the workstation areas, the spacing was insufficient for occupants to completely avoid direct sunlight. Another interesting finding revealed by the Zone variation was the high frequency of sunlight on the monitors in Zone Two. Given the fact that all occupants in Zone Two were either parallel or facing away from the windows, direct sunlight easily fell on the monitors rather than the occupants. Facing toward the windows also caused high contrasts between the bright windows and relatively dark monitors on cloudy days when the mechoshade systems were completely retracted.

7.5.3 Daylight Quality in Renovated Tier

The examination of objective lighting environments and occupant assessments between Tier Two and the remaining three tiers demonstrated that the renovation to Tier Two successfully improved its occupant satisfaction with their daylighting environments. The renovated design strategies were divided into two categories based on their influences on the interior daylighting environments, to reduce visual discomfort and to introduce positive impacts.

The design decisions that reduced occupants' visual discomfort included unifying workstations' seating orientations and enlarging the space between the windows and the working area. Compared with the original layout in the three tiers, all the workstations in Tier Two were arranged parallel to the windows. Therefore, all the monitors were perpendicular to the windows and the visual discomfort caused by facing towards the windows was solved. In other words, the solid angles between the glare source, the windows, and occupants' task views were effectively reduced. In addition to seating orientations, the whole working area was set half a bay, or 2.3 meters, further from the windows, which protected the occupants from most direct sunlight falling on them. Enlarging the spacing between the workstations and the windows resulted in an effective daylighting buffer zone in Tier Two. These two renovated design strategies reduced occupants' chances of experiencing visual discomfort and laid a foundation for the renovated layout.

Furthermore, the design decisions with positive impacts on lighting environments included the more open workstations and the flexible furniture. As shown in Figure 7.9, T2R1A and T2R1F had 30 hours of glare in a year, while T3R2A had no glare. Considering that Tier Two replaced the original enclosed workstations with the more open workstations, it was reasonable to expect more daylight penetration and longer visual discomfort. However, the renovated layout also provided more easily accessible outside views for the occupants, which had greater impact on occupants' satisfaction. As shown in Figure 7.12, the occupants in Tier Two were more satisfied with their natural lighting environments (mean satisfaction level = 2.61) than the occupants in Tier Three (mean satisfaction level = 3.56). As previous studies found that outside views containing interesting information, like the Milwaukee River and passing boats mentioned by the interviewees in Tier Two, can increase occupants' tolerance for visual discomfort (Shin et al., 2012; Tuaycharoen & Tregenza, 2007), this field study confirmed their conclusion.

Finally, the flexible furniture designs compensated for occupants' lack of control over their lighting environments. Although both the original and renovated workstations were adjustable in height, more occupants in Tier Two adjusted their desk heights than the occupants in the three original tiers. The responses to the questionnaire also showed that occupants in Tier Two adjusted themselves and/or their workstations more frequently to resume visual comfort. The flexible furniture encouraged occupants' adaptive behaviours (Heerwagen & Diamond, 1992) and increased their adaptation under the changing daylighting environments. This agrees with previous studies that easily reconfigurable office furniture has positive influence on occupant satisfaction with environments (Francis & Dressel, 1990; ONEILL, 1994).

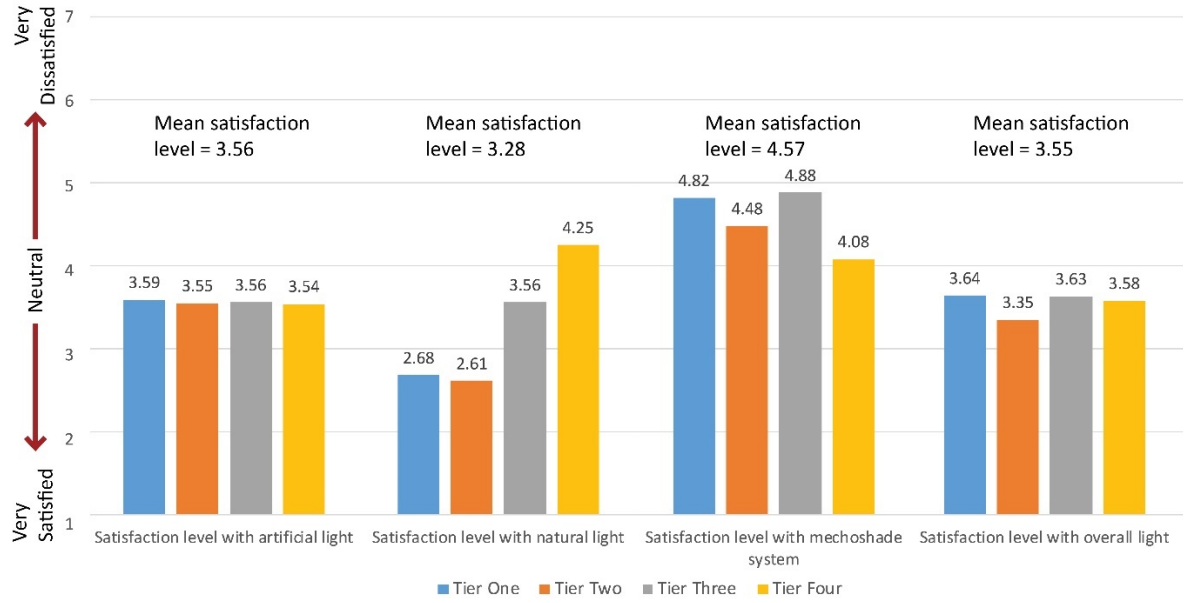

Figure 7.12: Mean satisfaction levels of the four tiers.

7.5.4 Benefits of Integrating Three Tools

This research demonstrates the advantages of pairing POE surveys with physical lighting environments. One advantage is to compensate for the weakness of one single method. Even though HDR image techniques can capture instantaneous daylighting distributions, it cannot capture direct sunlight on occupants. Without occupants' feedback about sunlight penetration, the primary cause of visual discomfort would be neglected. The simulation model calibrated by the HDR images presented annual visual discomfort outside

data collection periods. By combining both static HDR images taken onsite and dynamic visual discomfort simulations, a complete picture of interior lighting performance is presented.

The second advantage of utilizing multiple methods is to reveal the consistency between different data sources. For instance, both the field measurements and occupant assessments pointed out that the seating orientation toward the windows led to serious visual discomfort. Both the annual DGP results and occupants' responses to the questionnaire confirmed that visual discomfort occurred more frequently in the afternoon, especially during the winter. The problem of direct sunlight was mentioned during the interviews, reported in the questionnaire responses, and reflected from occupants' method of using the office. By combining the results of several methods, the internal validation of the research can be guaranteed. Therefore, the authors suggest collecting and analyzing data from multiple sources by utilizing different methods to efficiently decide research focuses.

7.6 CONCLUSION

This chapter evaluated the daylighting qualities at HGA from both subjective assessments and objective lighting data. The study showed that occupants' gender and attitude had statistically significant differences regarding their satisfaction with daylighting environments. The environmental variations, including window heights, distances between workstations and windows, and seating orientations, had significant impacts on occupant satisfaction with daylighting environments. By introducing positive environmental factors, like interesting outside views and flexible furniture, occupants' tolerance for visual discomfort was increased. The success of the renovated Tier Two in terms of visual discomfort reduction demonstrated the importance of integrating interior layout and furniture designs with building designs to achieve comfortable daylighting environments.

Furthermore, this paper showed the effectiveness of utilizing HDR image techniques as a tool to collect lighting data and calibrate simulation models. The calibrated models that can accurately predict visual discomfort provide future planers and design teams with more confidence to employ lighting simulations during the design stage. During the study, one important component revealed itself, occupants' adaptive behaviors caused by daylight glare. As introduced in Section 3.4, HGA provided a control-constrained environment where most of the occupants had no access to either shading controls or artificial lighting controls. Hence, when experiencing daylight glare, occupants developed their strategies to resume visual comfort. Although all the data was collected simultaneously, this topic was extracted and became an independent chapter presented below.

8 OCCUPANT ADAPTATION TO LIGHTING ENVIRONMENTS

This chapter presents the results concerning occupant adaptation towards daylight glare at HGA, an independent topic extracted from Chapter Seven. Occupants' responses to HGA's controlled environments and their adaptive behaviors are isolated. 23 interviewees' comments are interpreted. The HDR images and simulated luminance maps at select workstations demonstrate the luminance variations and glare reduction caused by occupants' adaptive behaviors.

8.1 RESEARCH OBJECTIVES

This chapter has three research objectives. First, occupants' adaptive behaviors to resume visual comfort are categorized and analyzed based on their types and frequency. Second, contextual factors that support or constrain adaptive behaviors are discussed. Finally, the magnitudes of visual discomfort reduction caused by adaptive behaviors are reflected from HDR images and simulated luminance maps.

8.2 RESEARCH QUESTIONS

This chapter mainly answers two questions concerning adaptive behaviors:

1. How effective are occupants' adaptive behaviors in terms of glare reduction?

2. What are the contextual factors that impact occupants' adaptive behaviors?

8.3 METHODOLOGY

8.3.1 Subjective Interview and Questionnaire

This chapter used interviews and questionnaires to explore occupant adaptation towards lighting environments at their workstations. First, 23 employees were interviewed to discover occupants' adaptive behaviors and main causes of visual discomfort. Table 7.1 demonstrates the count of interviewees in each tier, and Table 7.2 shows the interview questions. Then, the online questionnaire was distributed to the entire office and asked the participants (N=58) whoever experienced visual discomfort to rate their frequency of nine

adaptive behaviors, which were summarized based on 23 interviews. Table 7.3 displays the numeric values for the frequency questions. Participants' responses to two open-ended questions in the questionnaire were also interpreted.

8.3.2 Objective Lighting Distributions

Eight workstations were selected according to different types of adaptive behaviors. Two HDR images were taken at each workstation. The former recorded the lighting conditions without adaptive behaviors, while the latter recorded the lighting distributions with adaptive behaviors. Moreover, the luminance maps at five of these workstations were simulated by the calibrated Radiance model on the winter solstice between 9 a.m. and 5 p.m. at 20-minute intervals. The CIE sunny sky was employed in the simulation to reveal visual discomfort conditions. Based on the pre-set positions of mechoshades in real environments, Table 8.1 shows the percent of windows covered on the winter solstice. The winter solstice was selected due to its worst visual discomfort condition (Kong et al., 2018). E_v and DGP were calculated from the simulated luminance maps to reveal the visual discomfort reduction caused by adaptive behaviors.

Table 8.1: Percent of windows covered by mechoshades on the winter solstice

Time	9 – 10:40 a.m.	11:00 a.m.	11:20 a.m.	11:40 a.m. – 12:40 p.m.	1:00 – 5:00 p.m.
Tier One	0%	48.8%	48.8%	70.4%	79.9%
Tier Two & Tier Three	0%	46.5%	46.5%	67.4%	87.9%
Tier Four	0%	39.5%	77.1%	77.1%	77.1%

8.4 RESULTS & DISCUSSION

8.4.1 Descriptive Data

Heerwagen and Diamond categorized occupant adaptive behaviors into three types: environmental alterations, changes in behavior, and psychological processes (putting up with the problem) (Heerwagen & Diamond, 1992). According to 23 interviewees' responses, nine types of adaptive behaviors were summarized (Table 8.2), two types (monitor rotation and boards erection) of which belonged to the interactive adaptation and the remaining of which

belonged to the reactive adaptation (Nikolopoulou & Steemers, 2003). Participants were prone to alter their personal conditions rather than making changes to their workstations. Table 8.2 lists the percent of nine adaptive behaviors based on their frequency. The top three adaptive behaviors that participants did most frequently were: turning one's body (mean=4.12), using hands or objects to block sunlight (mean=3.62), and rotating monitors (mean=3.09). The three adaptive behaviors that participants did the least frequently were: using an umbrella (mean=1.12), wearing sunglasses (mean=1.46), and adjusting work schedule (mean=1.55). The frequencies of these adaptive behaviors indicated that the participants at HGA were more likely to turn their bodies, use hands or objects to temporarily block sunlight, or rotate their monitors. Although erecting boards had a great percent of "never" (62.1%) and low mean frequency (2.33), the percent of "every time/always" of erecting boards was 6.9%, the second greatest percent of all adaptive behaviors. This result confirmed the author's observation and interviews that putting up foam core boards along the barriers to block direct sunlight was likely a one-time and long-lasting behavior. Although all 58 participants who reported glare experience in the questionnaire undertook one or more adaptive behaviors, some interviewees who experienced daylight glare just withstood glare.

Table 8.2: Frequency of adaptive behaviors due to visual discomfort

Adaptive behaviors	Never (+1)	Rarely (+2)	Occasionally (+3)	Sometimes (+4)	Frequently (+5)	Usually (+6)	Every time/ Always (+7)	Mean	S.D.
Wear sunglasses	81.0%	10.3%	3.4%	1.7%	0.0%	1.7%	1.7%	1.41	1.14
Turn my body	12.1%	6.9%	17.2%	17.2%	19.0%	19.0%	8.6%	4.16	1.81
Use hands or objects to block sunlight	12.1%	6.9%	27.6%	25.9%	13.8%	8.6%	5.2%	3.69	1.59
Rotate monitors	31.0%	17.2%	12.1%	17.2%	10.3%	8.6%	3.4%	2.98	1.84
Adjust work schedule	72.4%	5.2%	13.8%	8.6%	0.0%	0.0%	0.0%	1.59	1.03
Leave my workstation for a break	25.9%	22.4%	13.8%	32.8%	3.4%	1.7%	0.0%	2.71	1.35
Move to another	48.3%	36.2%	6.9%	6.9%	1.7%	0.0%	0.0%	1.78	0.98

place to work									
Use an umbrella	94.8%	3.4%	0.0%	1.7%	0.0%	0.0%	0.0%	1.09	0.43
Erect boards	60.3%	8.6%	1.7%	12.1%	5.2%	5.2%	6.9%	2.36	2.01

8.4.2 Causes of Glare

Table 8.3 shows the correlations between participants' frequency of adaptive behaviors and the causes of visual discomfort. Three adaptive behaviors that were weakly correlated with direct sunlight on people's faces and/or eye(s) were: turning one's body (r^2=.299, p<0.05), using one's hand or object to block sunlight (r^2=.386, p<0.01), and erecting boards (r^2=.312, p<0.05). Four adaptive behaviors that were moderately or weakly correlated with direct sunlight on monitor(s) included: using one's hand(s) or objects to block sunlight (r^2=.388, p<0.05), rotating monitor(s) (r^2=.517, p<0.01), adjusting one's work schedule (r^2=.341, p<0.01), and leaving workstation for a break (r^2=.278, p<0.05). High contrast was weakly correlated with only one adaptive behavior, adjusting one's work schedule (r^2=.283, p<0.05). Furthermore, visual discomfort occurring between 2 and 4 p.m. was moderately correlated with two adaptive behaviors, using hands or objects to block sunlight (r^2=.444, p<0.01) and erecting boards (r^2=.439, p<0.01), and weakly correlated with turning one's body (r^2=.275, p<0.05).

Table 8.3: Correlations between the causes of visual discomfort and adaptive behaviors

	Direct sunlight on people	**Direct sunlight on monitors**	**High contrast**	**Visual discomfort between 2 and 4 p.m.**
Wear sunglasses	.183	.210	.171	-.230
Turn body	.299*	.148	.005	.275*
Use hands or an object to block sunlight	.386**	.388*	.168	.444**
Rotate monitors	.178	.517**	.036	.246
Adjust work schedule	.258	.341**	.283*	.237
Leave workstation	.184	.278*	.034	.167
Move to another place	.138	.143	.032	.223
Use an umbrella	.128	-.091	-.056	.016
Erect boards	.312*	-.061	.186	.439**

** Correlation is significant at the 0.01 level (2-tailed)
* Correlation is significant at the 0.05 level (2-tailed)

The correlations between adaptive behaviors and causes of visual discomfort indicated that different adaptive behaviors aimed to reduce different causes of visual discomfort. For example, occupants were more likely to rotate their monitors to protect their monitors from direct sunlight. Occupants were inclined to turn their bodies when direct sunlight fell on their faces and/or eyes. Occupants used hands or objects to temporarily block sunlight penetration that lasted for short periods.

8.4.3 Contextual Factors

HGA provided control-constrained environments with employees, where both mechoshade systems and artificial lights were automatically controlled. This section discusses HGA's contextual factors that influenced occupants' adaptive behaviors from both environmental and occupants' perspectives.

8.4.3.1 Personal Controls Over Lighting Environments

Since HGA was an open-plan office with over 150 workstations, both mechoshade systems and artificial lights were automatically controlled. The control systems were limited to only a few managers. According to the interviews and responses to open-ended questions in the questionnaire, participants were dissatisfied with the inaccessible and confusing control systems.

As shown in Figure 7.12, participants were slightly dissatisfied with the internal mechoshade systems (mean satisfaction level = 4.57) but slightly satisfied with the remaining four factors related to lighting environments. Figure 8.1 shows the number of participants who selected the problems relevant to the mechoshade systems. The failure of the control systems that sometimes occurred due to the updated control system was the top issue and selected by 50.0% of the participants. When the control systems failed to react, staff members were completely exposed to sunlight on sunny or part cloudy days. The second most frequently voted problem was the transparency of the fabrics, which was selected by 36.3%

of the participants. This issue resulted in views of the sun through the shades to the participants. The remaining issues were all relevant to the shading control system, like the delayed operations and the noises caused by the shade movement. Seven of the 17 participants who chose "others" explained that they had no access to the mechoshade systems. Participants' detailed responses concerning mechoshade systems are presented in Appendix E.

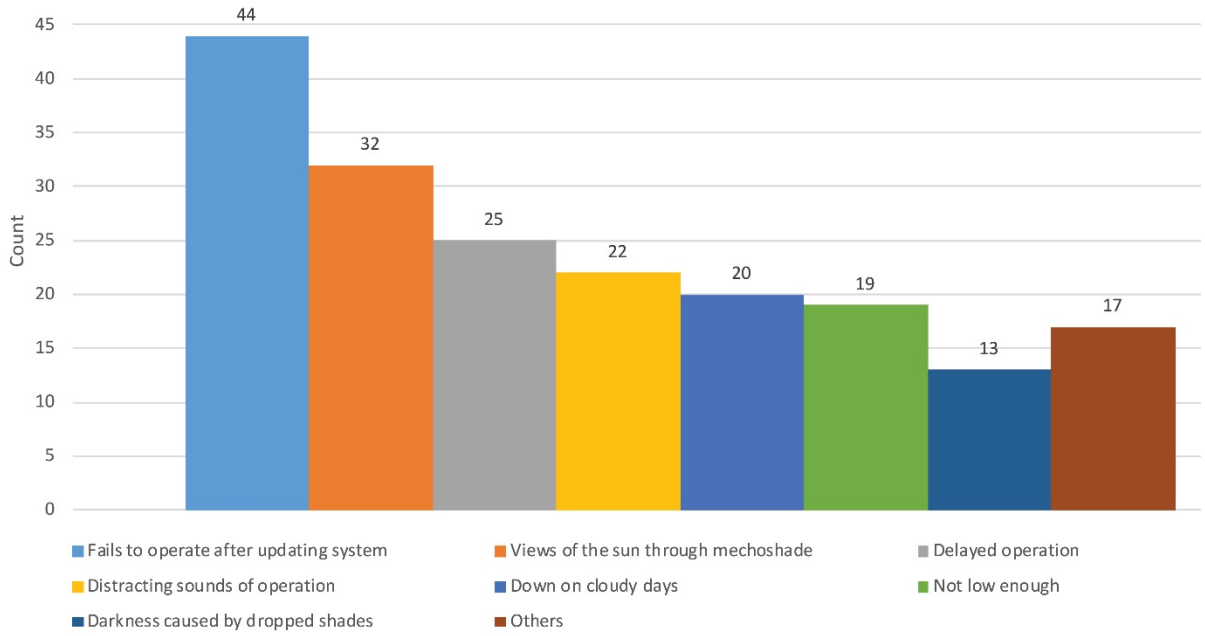

Figure 8.1: Problems related to the interior mechoshade system

Additionally, many participants complained about artificial lighting controls despite the focus of this study on daylighting qualities. As shown in Appendix E, six issues were extracted from participants' responses, three of them related to luminaires including personal preference, insufficient illuminance level, and types of luminaires, along with three others related to control systems including schedule of artificial lights, complexity of artificial control systems, and disconnections between mechoshade and artificial light control systems. As Nicol and Humphreys stated that "discomfort is increased if control is not provided, or if the controls are ineffective, inappropriate, or unusable" (Nicol & Humphreys, 2002), the lack of direct controls over their lighting environments both decreased occupant satisfaction with lighting environments and triggered diverse types of adaptive behaviors.

8.4.3.2 Views to and Connection with Outdoors

The importance of views to and connection with the outdoors was presented in Chapter Seven in terms of glare reduction. The more open design in Tier Two allowed outside views to more occupants, especially the ones sitting at the rear of Tier Two. As shown in Appendix E, some interviewees complained that shades blocked the beautiful river views outside. A balance is required between the amount of daylight penetration into a space and glare occurrence so that occupants would not sacrifice outside views for visual comfort.

8.4.3.3 Interior and Furniture Designs

The Kruskal-Wallis Test was run to test if there were significantly different frequencies of nine adaptive behaviors among tier, zone, and seating orientation groups. Table 8.4 showed that the frequency of rotating monitor(s) had statistically significant difference among four tiers (H(3)=9.30, p=0.026), and the frequency of erecting boards had statistically significant difference among four zones (H(3)=8.80, p=0.032). As shown in Figure 821, there were a statistically significant difference Tier Two and Tier Four (Test Statistic=16.98, Adj. Sig.=.022) in terms of rotating monitors and a statistically significant difference Zone One and Zone Three (Test Statistic=13.99, Adj. Sig.=.043) in terms of erecting boards.

Table 8.4: Kruskal-Wallis results among tier and zone groups

Tier	**Frequency of rotating monitor(s)**			**Zone**	**Frequency of erecting boards**		
	Mean rank	Chi-square	Sig.		Mean rank	Chi-square	Sig.
One	24.2	9.30	.026*	**One**	37.7	8.80	.032*
Two	36.8			**Two**	22.6		
Three	29.0			**Three**	23.7		
Four	19.8			**Four**	25.4		

Note: *p<0.05; **p<0.01; ***p<0.001.

Due to the flexible furniture designs, occupants in Tier Two were able to easily rotate their monitors. On the contrary, the enclosed cubicle workstations in the remaining original tiers were fixed design. In order words, more supportive a workstation, more frequently an occupant is likely to take adaptive behaviors. Since all the monitors were perpendicular to the

southwest windows, the occupants in Tier Two encountered more sunlight on their monitors, which also partially explained that the occupants in Tier Two rotated their monitors the most. As shown in Table 7.11 and Figure 7.5, the occupants in Zone One encountered the most severe direct sunlight on them, which resulted to more frequent board erection. On the other hand, with the barriers and bookshelves in Zone One, the occupants were easier to erect boards and block direct sunlight. Occupants in other zones also noticed this environmental support. Most of the interviewees who experienced visual discomfort indicated that they had no supportive environment to place boards. The results in this section demonstrate that not only the causes of visual discomfort but also the environments determine the types and frequencies of occupants' adaptive behaviors.

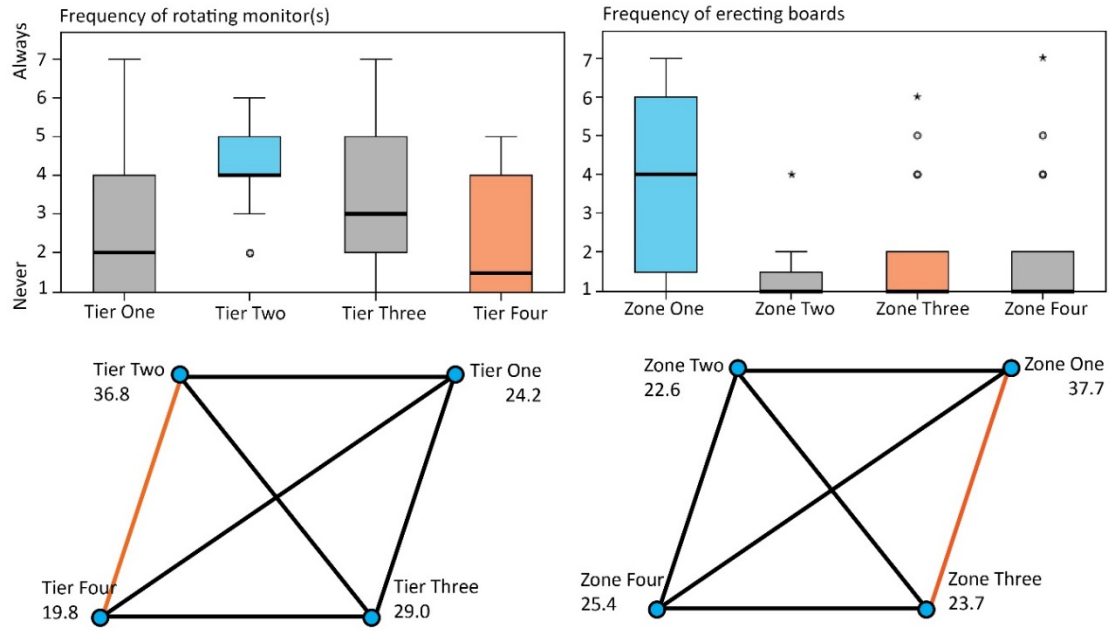

Figure 8.2: Pairwise tests of frequency of rotating monitor(s) between four tiers (left) and pairwise tests of frequency of erecting boards between four zones (right)

8.4.4 Effects of Adaptive Behaviors

8.4.4.1 Glare Reduction in Field Measurements

Figure 8.3 shows the falsecolor images of the HDR images taken on July 29th, 2017 at four workstations before and after applying the adaptive behaviors. The adaptive behavior at T1R5C was to lower one's body, as described by the occupant, to decrease high contrasts

between the monitors and backgrounds on cloudy days. Therefore, the luminance differences between the two upper left images demonstrate 7.6-centimeter (3-inch) height difference at the occupant's eye level. The remaining three groups of falsecolor images display the luminance variations before and after erecting foam core boards. The occupant at T1R1E complained about the direct sunlight that fell on his/her eyes and task areas. Table 8.5 lists the E_v variations caused by adaptive behaviors at eight workstations. Compared to the lighting conditions before the application of adaptive behaviors, the reduced percent of E_v varied between 28.2% and 91.0%. Figure 8.4 presents the DGP difference caused by adaptive behaviors at eight workstations. Although seven workstations had imperceptible glare before and after adaptive behaviors, the DGP at T3R1C decreased from a perceptible to an imperceptible degree. The analysis of HDR images demonstrates the effectiveness of adaptive behaviors in terms of visual discomfort reduction and visual comfort resumption.

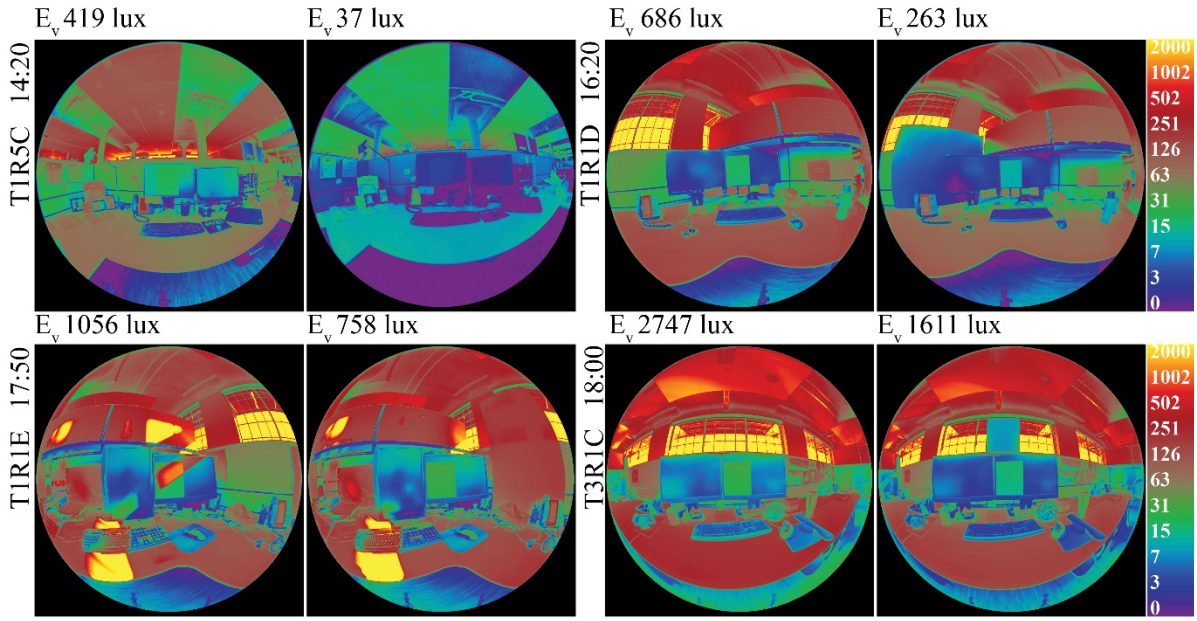

Figure 8.3: Luminance differences before and after including adaptive behaviors

Table 8.5: E_v variations before and after including adaptive behaviors

Workstation	T4R1E	T3R3C	T1R5C	T2R4C	T1R1D	T3R2C	T1R1E	T3R1C
$E_{v\text{-before}}$ (lux)	676	668	419	478	686	577	1,056	2,747
$E_{v\text{-after}}$ (lux)	381	276	38	271	263	304	758	1,611
E_v reduced percent	43.7%	58.7%	91.0%	43.3%	61.7%	47.3%	28.2%	41.4%

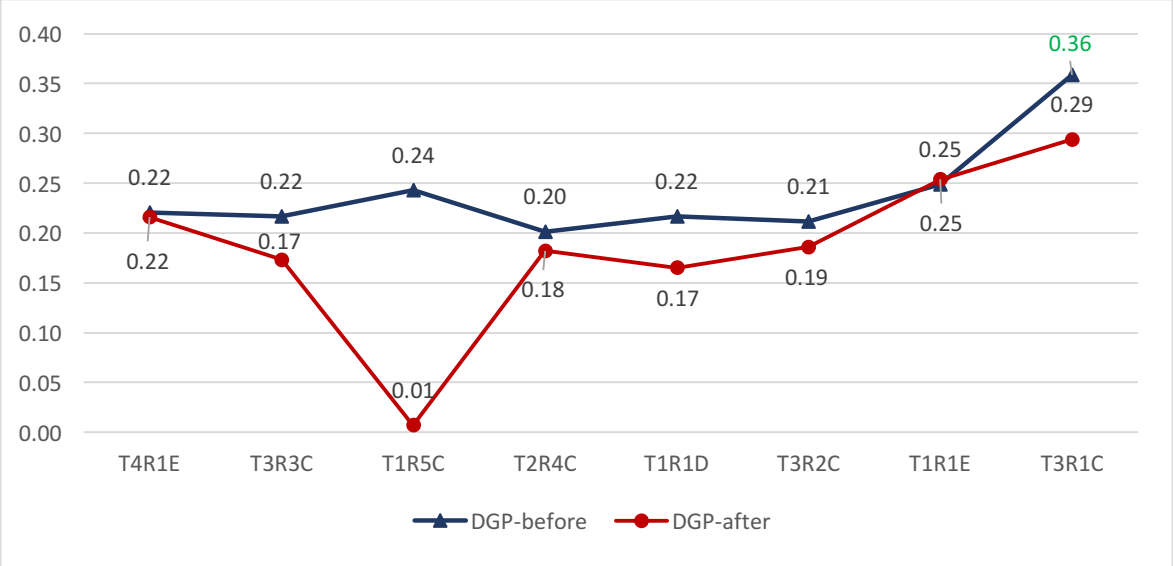

Figure 8.4: DGP differences caused by adaptive behaviors

8.4.4.2 Glare Reduction in Simulations

Figure 8.5 demonstrates the DGP variations at T1R1D, T1R1E, T2R4C, T3R1C, and T4R1E caused by the occupants' adaptive behaviors on the winter solstice from 9 a.m. to 5 p.m. The grey bars on each scene represent the mechoshade positions changing according to the control systems. Without adaptive behavior, each occupant experienced different degrees of visual discomfort on the winter solstice even with mechoshades down. The occupants at T1R1D, T1R1E, and T3R1C all erected foam core boards in different sizes to block direct sunlight. The DGP results at T1R1D and T1R1E at 12:20 and 12:40 p.m. were derived from a combination of two types of adaptive behaviors: erecting boards and lower one's body, since the foam core boards failed to create glare-free lighting environments. The similar severe glare also occurred at T3R1C at 1:00, 1:20, and 2:00 p.m. The reduced degrees of glare at the three workstations during these periods showed that occupants had to consistently adjust themselves and/or their workstations. Even though the occupants hid behind the boards, they still had a high chance of experiencing glare at noon, which indicates the transparency of mechoshade fabrics (5% openness factor) and the limitations of adaptive behaviors to reduce severe glare. The DGP variations at T2R4C presented visual discomfort reduction due to monitor rotations. The DGP variations at T4R1E were caused by lowering the table height,

since the occupant preferred to stand while working except for winter seasons. Due to the occupants' different adaptive behaviors, glare at these five workstations on the winter solstice reduced between 60% and 100%. Figure 8.6 demonstrates the reduced percent of E_v variations caused by adaptive behaviors at the five workstations. The percent of E_v reduction varied between -95% and -5%. The larger movement an adaptive behavior, the greater the range of E_v variation.

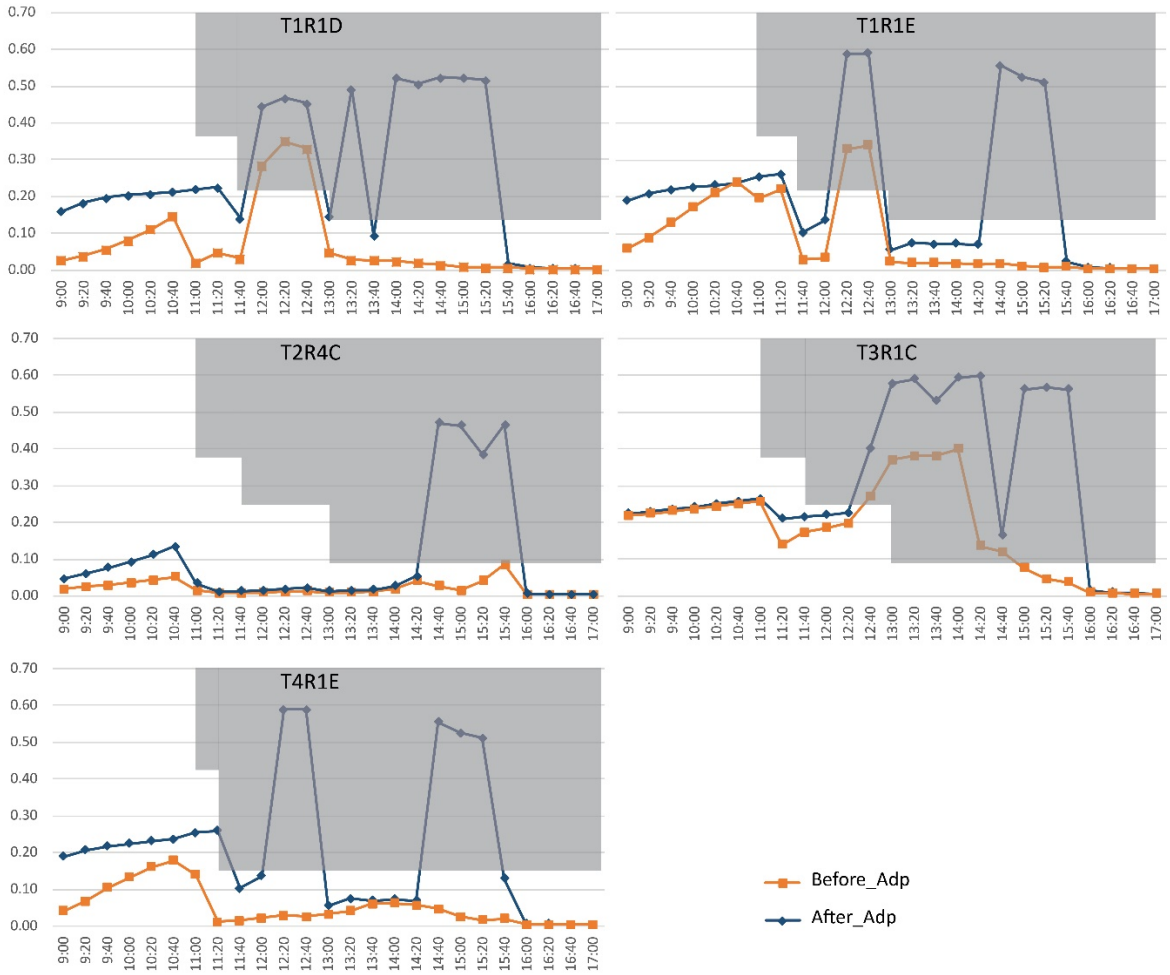

Figure 8.5: DGP profile variations caused by adaptive behaviors

Including adaptive behaviors in simulations has many difficulties. Although nine types of adaptive behaviors were summarized based on interviews, it is impossible to simulate all of them. For example, the behaviors like "wear sunglasses", "leave my workstation", and "change work schedule" were excluded from the simulations. Some detailed conditions in field, like various dimensions of foam core boards used by occupants,

add more difficulties to simulations. One method is to conceptualize several adaptive behaviors with similar effects on luminance distributions as one solution in simulations. Jakubiec and Reinhart created an adaptive zone of glare by enlarging an occupant's space about 315 to 45 degrees and 0.75m to the left or right of a rectangular desk (Jakubiec & Reinhart, 2012). Their model can cover several adaptive behaviors like rotating monitors, adjusting bodies, and adjusting workstations. Moreover, occupants presented some instantaneous reactions towards glare, like using a hand or small object to temporally block sunlight. Although the motivation to adaptive behaviors, daylight glare in this research, can be calculated in simulations, it is difficult to predict occupants' temporary reactions and simulate them in a quantitative way. Therefore, further research is required to conceptualize an adaptive behavior model before involving this important factor into daylight simulations.

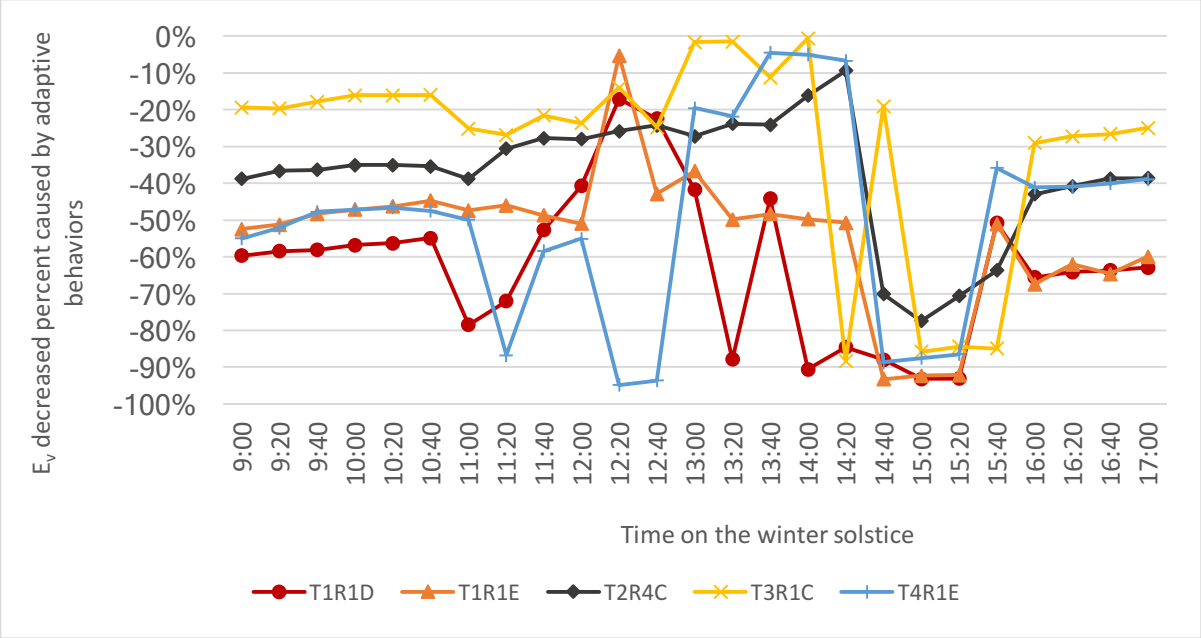

Figure 8.6: The percent of E_v variations caused by adaptive behaviors

8.5 CONCLUSION

This chapter presents occupants' nine types of adaptative behaviors caused by daylight glare. Occupants were more likely to adjust their bodies or use their hands and/or small objects to block direct sunlight. They were prone to rotate monitors or use their hands

and/or small objects to protect their monitors from direct sunlight. Select occupants were able to reduce glare experience varying between 60% and 100% on the winter solstice by combining several adaptive behaviors. Occupant adaptive behaviors were impacted by causes of glare and contextual factors including accessibility of control systems, views and connections with the outside, and interior and furniture designs. Although adaptive behaviors could enlarge occupants' visual comfort zones, the reliance on occupant adaptive behaviors to resolve glare was insufficient, especially under extremely severe glare conditions.

9 CONCLUSION

9.1 CONCLUSIONS

This dissertation investigated daylighting performance of multiple sidelit spaces across five buildings from subjective and objective perspectives. Chapter Three introduced the five buildings through the entire dissertation. Chapter Four presented the comparison of glare analysis results across the five buildings. The select glare indices based on the literature review of Chapter Two included DGI, DGP, UGP, and E_v. Over 200 HDR images were taken on site under various sky conditions. The results showed that DGI underestimated most of the scenes with intolerable glare, while UGP overestimated some scenes with imperceptible glare under both sunny and cloudy conditions. DGP performed consistently on the scenes with imperceptible and intolerable glare. In order to comprehensively identify daylight glare in sidelit spaces, Chapter Four recommended integrating DGP, DGI and E_v to analyze daylight glare. DGP is recommended to first detect daylight glare in sidelit spaces. DGI is recommended to verify the scenes with E_v over 1,000 lux and the existence of direct sunlight.

The following two chapters utilized the second tool of lighting studies, simulations. Chapters Five and Six validated simulated luminance maps generated by Radiance under CIE sunny and overcast skies, the Perez sky, and the horizontal HPR sky models. The HDR images taken within four of the five select buildings were utilized to validate the simulation results accordingly. Chapter Five compared the accuracy of glare prediction from simulated luminance maps under CIE skies and Perez skies. The results demonstrated that CIE sunny and overcast skies are able to produce accurate glare prediction. With solar irradiance measured on site, the Perez sky generated luminance maps with relative MBE varying between -4.7% and -14.5% and relative RMSE varying between 20.1% and 27.8%. Moreover, Chapter Six explored the accuracy of the horizontal HPR sky model, which included HDR images as the lighting source in simulations. The relative RMSE of E_v under

HPR skies and Perez skies were 21.2% and 23.7%, respectively. The frequencies of accurate glare prediction under HPR and Perez skies were 95.5% and 93.9%, respectively. The results indicated that both the horizontal HPR sky and the Perez sky simulate luminance maps at the same level of accuracy. Consequently, these two chapters recommended the Perez sky model for daylight simulations not only for its abundant weather data, but also for its ease of use in generating both point-in-time and annual simulation.

Chapters Seven and Eight integrated subjective occupant evaluations with the field measurements and simulations. The open-plan office with environmental variations in window height, seating orientation, distance between a workstation and windows, and layout design was selected. Occupants' assessments were integrated with both HDR images taken onsite and calibrated simulation results. Chapter Seven concluded that taller windows, proximity to windows, and facing towards windows led to severe daylight glare for occupants. By introducing positive environmental factors, like interesting outside views and flexible furniture designs, occupants' satisfaction with daylighting environments and tolerance for visual discomfort increased. The success of the renovated layout design in terms of glare reduction demonstrated the importance of integrating interior layout and furniture designs with building designs to achieve comfortable daylighting environments. Furthermore, Chapter Eight continued exploring occupants' adaptive behaviors. Nine types of adaptive behaviors were analyzed. The results demonstrated that occupants were more likely to adjust their bodies or use their hands and/or small objects to block direct sunlight on them. Select occupants were able to reduce glare experience varying between 60% and 100% on the winter solstice by combining several adaptive behaviors. However, a combination of several adaptive behaviors still failed to restore visual comfort under severe glare conditions.

The entire dissertation aimed to integrate three research tools, HDR image techniques, simulations, and questionnaire surveys, step by step. Figure 9.1 summarizes the structure of

the dissertation in terms of objective and method. Based on the primary objective, the three sub-aims were established as the supporting sections. Sequentially, the following section added one extra research tool to the previous section. The author recommends using these three tools together to efficiently investigate interior lighting environments. HDR image techniques can provide accurate field measurements, luminance distributions within existing spaces, for both visual discomfort analysis of instantaneous lighting environments and simulation model calibrations; calibrated Radiance models are capable of accurately generating both instantaneous and annual simulation results to extend lighting data outside of data collection periods; finally, questionnaire surveys reflect subjective occupant assessments that provides deep explanations. Integrating these three independent tools can compensate each other's weaknesses. In order words, utilizing these three tools simultaneously in lighting studies can reveal convergent results and discrepancies that might be neglected by employing a single tool.

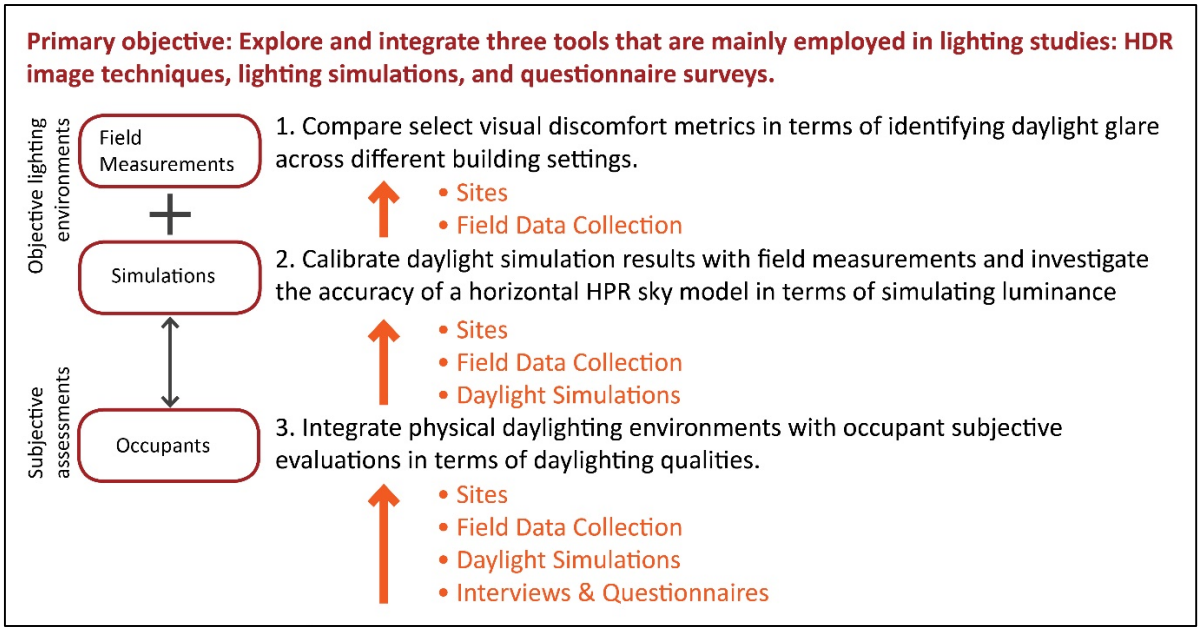

Figure 9.1: The objective and method structure of the dissertation

9.2 DISCUSSION

Based on the studies conducted across five buildings, this section discusses the design considerations to achieve visual comfortable environments. The two aspects associated with daylighting utilization include the spatial proportion and interior designs.

9.2.1 Spatial Proportion

As a rule of thumb, the daylighting zone is defined to be a depth of about two times the window head height (Robbins, 1986). Based on this guideline, architects are encouraged to design tall windows to introduce more daylight at the rear of a space (Baker & Steemers, 2002; IEA SHC, 2000). However, this guideline neglects the potential daylight glare that occupants sitting close to windows experience. As daylighting environments should be examined by both visual performance and comfort, a spatial proportion is proposed as a supplementary criterion for this guideline.

As concluded in Chapter 7, taller windows led to more severe daylight glare to occupants. CSM and HGA with similar glazing transmittances (0.70 and 0.71) and building orientations (south and southwest) were used as an example. 14 workstations at HGA and two locations at CSM were selected to calculate annual DGP results. In order to reflect the real lighting conditions, the mechoshade in 5% openness factor was down when glare occurred. Then, a ratio between the distance to windows and window head height to eye elevation, as illustrated in Figure 9.2, was used for a scatter plot. Figure 9.3 shows the scatter plot of this ratio of 14 workstations at HGA (red dots) and two locations at CSM (blue dots) against the annual glare duration at

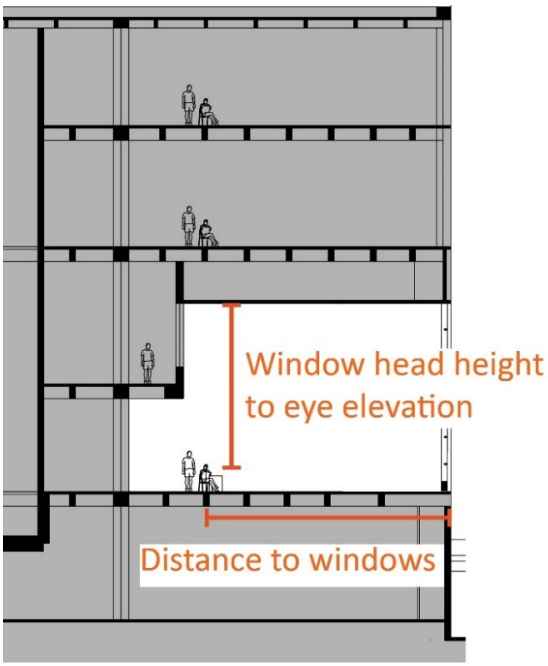

Figure 9.2: Spatial ratio using CSM as an example

each location accordingly. Although mechoshade systems were down when glare occurred, there were still seven locations at HGA with accumulated glare duration over 100 hours. At CSM, the two locations presented much longer glare duration, which was reasonable due to its curtain-wall elevations. Given annual 2,087 hours of office time (U.S. Office of Personnel Management, n.d.), 5% of allowable glare duration leads to 104 hours of allowable glare (Wienold, 2009). Under this specific building context, a ratio of 0.9 is recommended as the threshold to control annual glare duration. This ratio can be achieved in various aspects, like controlling window heights and incorporating interior design and layout.

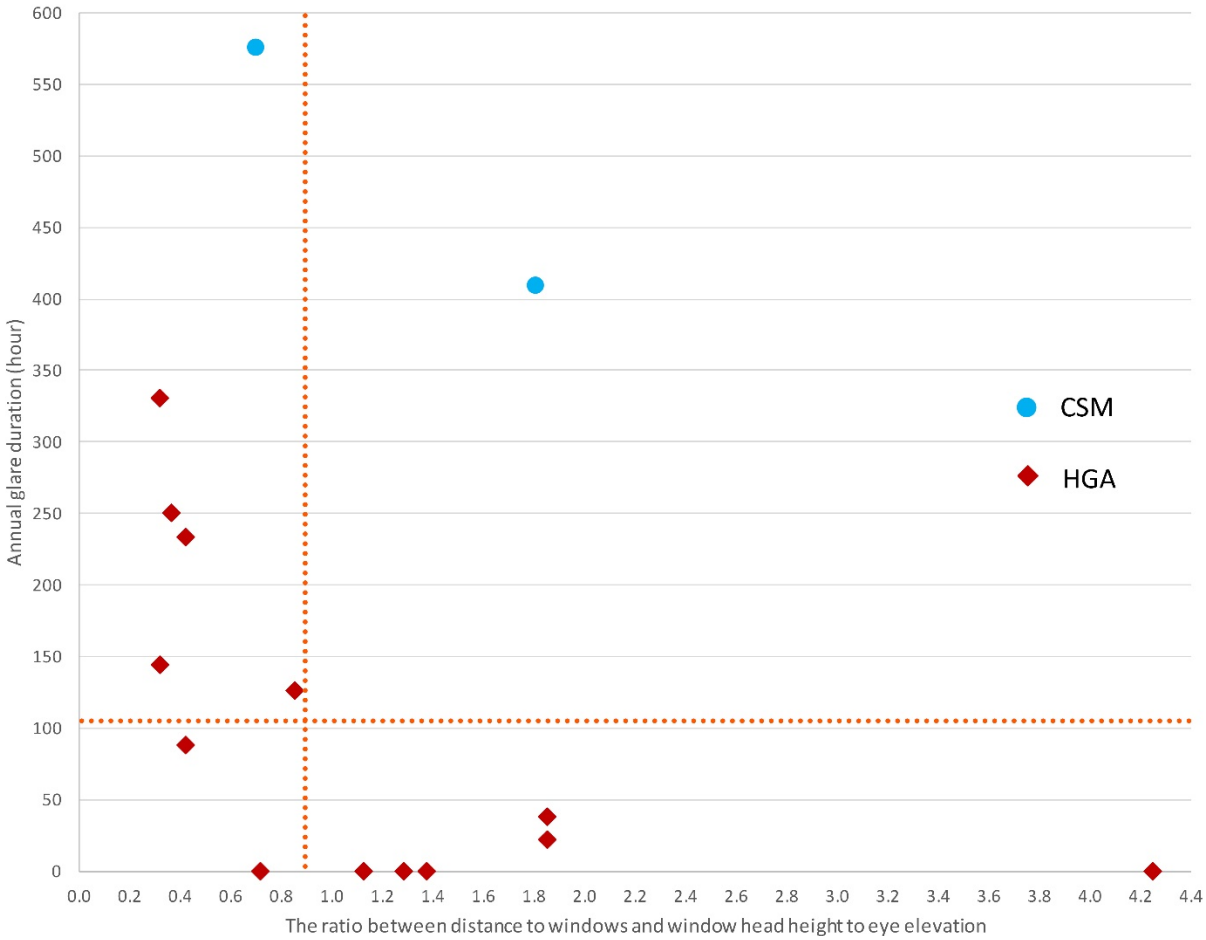

Figure 9.3: The scatter plot of the ratio against annual glare duration

9.2.2 Interior Design Incorporation

Chapter Seven concluded the importance of interior design and layout in terms of glare reduction. In order to emphasize the collaboration of interior designs, the following recommendations are proposed. These recommendations stem from a public open-plan office

where the controls of neither artificial light nor shading devices are available to most occupants.

1. Avoid the cubicle designs that have two or more sides of opaque partitions. Consider lowering partition heights and incorporating translucent materials to allow more daylight penetration and more outdoor views for the majority of the occupants.

2. Provide flexible furniture design like tables and chairs that are adjustable in height, and monitors that are easy to rotate.

3. Avoid orienting occupants towards the glazing in high transmittance. Seating orientations parallel to windows can strike a balance between visual discomfort and outdoor connection.

4. Predict sunlight penetration during the design stage. Simulations of sunlight penetration with shading devices need to be conducted during the design stage to guarantee that occupants are protected from direct sunlight throughout the day.

5. Consider the effectiveness of mechoshades in terms of blocking the solar disc within occupants' task views. Mechoshade systems in 5% openness factors cannot completely block the solar disc. Mechoshades in 2% and 3% openness factors are recommended.

6. Consider placing buffer zones between windows and working areas. Ensure sufficient depth of a buffer zone that can protect direct sunlight from occupants during the majority of their occupied hours. Buffer zones can be designed as circulations or public meeting spaces to increase occupants' connections with the outside.

7. Assign occupants to workstations based on their ambient preferences to daylight and outside views. The values of daylight and outside views can be maximized by the occupants who like them; glare disturbance can be minimized among the occupants who possess positive attitudes towards daylight and/or outside views.

9.3 FUTURE WORK

This dissertation offers several potential topics for future work.

9.3.1 Individual Variability in Glare Perception

Previous studies concluded that individual variability play an important role in visual discomfort perception (Kim et al., 2013; Yildirim et al., 2007). Kent et al. concluded that caffeine ingestions resulted in statistically significant difference in glare sensation (Kent et al., 2016). The great impacts of individual differences on glare evaluations are partially attributed to the low coefficient of determination (R^2) values for single visual discomfort metric in terms predicting subjective evaluations (Jakubiec et al., 2015; Van Den Wymelenberg, 2012). Chapter Seven revealed the statistically significant differences in daylighting satisfaction levels caused by participants' genders and attitudes. Although substantial studies mentioned the great impacts of individual differences on glare evaluations, most of them failed to systematically explore this aspect in more detail. Future studies are required to explore individual attributes in relation to glare sensation and quantify their impacts on glare sensation.

9.3.2 Dynamic Daylight Glare Prediction

Despite many studies that explored visual discomfort metrics to predict instantaneous glare, there is insufficient research that explores dynamic daylight glare prediction. Although Chapter 7 utilized annual DGP simulations (Wienold, 2009) to confirm subjective occupant assessments, no subjective study validates the annual DGP results. Additionally, the long-term visual discomfort model proposed by Jakubiec and Reinhart is specific to the participants and building contexts (J. Alstan Jakubiec & Reinhart, 2016). Like the concept of Useful Daylight Illuminances (Nabil & Mardaljevic, 2006) and Daylight Autonomy (C. F. Reinhart et al., n.d.; C. F. Reinhart & Walkenhorst, 2001), further research is required to propose a dynamic glare prediction metric that is validated by subjective studies.

9.3.3 Subjective Adaption towards Lighting Environments

As occupants constantly interact with and adapt themselves to their immediate environments (Yang et al., 2014), occupants' adaptive behaviors influence their visual sensation and satisfaction with lighting environments. Jakubiec and Reinhart concluded that involving occupant adaptive behaviors in simulations can greatly decrease intolerable discomfort (Jakubiec & Reinhart, 2012). However, no further subjective occupant study confirms the simulation results. Chapter Eight investigated occupants' adaptive behaviors caused by daylight glare. Since the research was based on 23 participants' interviews and 58 participants' responses to the questionnaire in an open-plan office, this chapter was also specific to the participant and office context. More studies are required to enrich building contexts and populations of participants to generate representative models of occupant adaptive behaviors, which can be employed in simulations.

REFERENCES

Aries, M. B. C., Veitch, J. A., & Newsham, G. R. (2010). Windows, view, and office characteristics predict physical and psychological discomfort. *Journal of Environmental Psychology*, *30*(4), 533–541. https://doi.org/10.1016/j.jenvp.2009.12.004

Ascension. (2010). Columbia St. Mary's - The New Columbia St. Mary's Hospital Milwaukee Will Transform the Patient Experience. Retrieved March 31, 2018, from http://www.columbia-stmarys.org/wtn/Page.asp?PageID=WTN000393

Baker, N., & Steemers, K. (2002). *Daylight design of buildings*. James & James Ltd.

Begemann, S. H. A., Beld, G. van den, & Tenner, J. A. D. (1997). Daylight, artificial light and people in an office environment, overview of visual and biological responses. *Industrial Ergonomics*, (20), 231–239.

Bhusal, P., Tetri, E., Halonen, L., Proceedings, A., Vries, D., Oseland, N., … Kim, K. S. (2014). Effects of realistic office daylighting and electric lighting conditions on visual comfort, alertness and mood. *Lighting Research and …*, *0*(4), 1–18. https://doi.org/10.1177/1477153514531518

Boubekri, M., Cheung, I. N., Reid, K. J., Wang, C. H., & Zee, P. C. (2014). Impact of Windows and Daylight Exposure on Overall Health and Sleep Quality of Offi ce Workers : *Journal of Clinical Sleep Medicine*, *10*(6), 603–11. https://doi.org/10.5664/jcsm.3780

Box, G. E. P., Hunter, J. S., & Hunter, W. G. (2005). *Statistics for Experimenters Design, Innovation, and Discovery* (Second Edi). New Jersey: Wiley-Interscience.

Boyce, P. (2014). Lighting for offices. In *Human factors in lighting* (Third Edit, pp. 233–283). Taylor & Francis Group, LLC.

Boyce, P., Hunter, C., & Howlett, O. (2003). The Benefits of Daylight through Windows. *Lighting Reasearch Center*, *1*(1), 1–88. https://doi.org/12180-3352

Brien, W. O., & Gunay, H. B. (2014). The contextual factors contributing to occupants ' adaptive comfort behaviors in of fi ces e A review and proposed modeling framework. *Building and Environment*, *77*, 77–87. https://doi.org/10.1016/j.buildenv.2014.03.024

British Standards Institution. (2002). *BS EN 12461-1: 2002 Light and Lighting: Lighting of workplaces: Indoor workplaces*. London, U.K.: BSI.

Cai, H. (2013). High Dynamic Range Photogrammetry for Light and Geometry Measurement. *AEI 2013: Building Solutions for Architectural Engineering*, 544–553. https://doi.org/10.1061/9780784412909.053

Carter, D. J. et al. (1994). The influence of luminance distribution on subjective impressions and performance within an non-uniformly lit office. In *Proceedings CIBSE National Lighting Conference* (pp. 61–74).

Cauwerts, C., Bodart, M., & Deneyer, A. (2012). Comparison of the vignetting effects of two identical fisheye lenses. *LEUKOS - Journal of Illuminating Engineering Society of North America*, *8*(3), 181–203. https://doi.org/10.1582/LEUKOS.2012.08.03.002

Cauwerts, C., & Piderit, M. (2018). Application of High-Dynamic Range Imaging Techniques in Architecture: A Step toward High-Quality Daylit Interiors? *Journal of*

Imaging, *4*(1), 19. https://doi.org/10.3390/jimaging4010019

Chiou, Y.-S., & Huang, P.-C. (2015). An HDRi-based data acquisition system for the exterior luminous environment in the daylight simulation model. *Solar Energy*, *111*, 104–117. https://doi.org/10.1016/j.solener.2014.10.032

Christopher Center Library Services: READ Posters: Index. (n.d.). Retrieved August 12, 2017, from https://library.valpo.edu/read/index.html

CIE/ISO. (2004a). *CIE Standard Overcast Sky and Clear Sky*. https://doi.org/ISO 15469:2004 (E)/CIE S 011/E:2003

CIE/ISO. (2004b). *Spatial distribution of daylight - CIE Standard General Sky*. https://doi.org/ISO 15469:2004(E)/CIE S 011/E:2003

CIE. (2014). *CIE standard general sky guide*. CIE Central Bureau.

Creswell, J. W. (2014). Mixed Methods Procedures. In *Research Design, Qualitative, Quantitative, and Mixed Methods Approaches* (Fourth Edi, pp. 215–239). SAGE PublicationsSage UK: London, England.

Debevec, P. (2002). Image-based lighting. *IEEE Computer Graphics and Applications*, *22*(2), 26–34. https://doi.org/10.1109/38.988744

Delaunay, J.-J., Wienold, J., Sprenger, W., & ISE, F. (n.d.). gendaylit. Retrieved May 3, 2018, from https://www.radiance-online.org/learning/documentation/manual-pages/pdfs/gendaylit.pdf

Dilaura, D. L., Houser, K. W., Mistrick, R. G., & Steffy, G. R. (2011). *The Lighting Handbook* (Tenth Edit). Illuminating Engineering Soceity.

DIVA for Rhino. (n.d.). Retrieved from http://diva4rhino.com/

DRI Design. (n.d.). COLUMBIA ST. MARY'S HOSPITAL - DRI-DESIGN PANELS SELECTED FOR MASSIVE CLADDING PROJECT - Dri-Design. Retrieved August 26, 2017, from http://www.dri-design.com/columbia-st-marys-hospital-dri-design-panels-selected-for-massive-cladding-project/

Dubois, M. (2001). *Impact of Shading Devices on Daylight Quality in Offices Simulations with Radiance*.

Dubois, M. C., & Blomsterberg, Å. (2011). Energy saving potential and strategies for electric lighting in future north european, low energy office buildings: A literature review. *Energy and Buildings*, *43*(10), 2572–2582. https://doi.org/10.1016/j.enbuild.2011.07.001

Duffie, J. A., & Beckman, W. A. (2013). *Solar Engineering of Thermal Processes* (Fourth Edi).

Einhorn, H. D. (1979). Discomfort glare: a formula to bridge differences. *Lighting Research & Technology*, *11*(2), 90–94. https://doi.org/10.1177/14771535790110020401

Elzeyadi, I. (2011). *Daylighting-Bias and Biophilia: Quantifying the Impact of Daylighting on Occupants Health*. *Greenbuild 2011*. Retrieved from http://www.usgbc.org/resources/daylighting-bias-and-biophilia

EnergyPlus. (n.d.). Weather Data Sources. Retrieved April 23, 2018, from

https://energyplus.net/weather/sources

Escuyer, S., & Fontoynont, M. (2001). Testing in situ of automatic ambient lighting plus manually controlled task lighting: office occupants reactions. In *Proceedings of the 9th European Lighting Conference (Lux Europa)* (pp. 70–75).

Fabi, V., Andersen, R. V., Corgnati, S., & Olesen, B. W. (2012). Occupants' window opening behaviour: A literature review of factors influencing occupant behaviour and models. *Building and Environment*, *58*, 188–198. https://doi.org/10.1016/j.buildenv.2012.07.009

Fakra, A. H., Boyer, H., Miranville, F., & Bigot, D. (2011). A simple evaluation of global and diffuse luminous efficacy for all sky conditions in tropical and humid climate. *Renewable Energy*, *36*(1), 298–306. https://doi.org/10.1016/j.renene.2010.06.042

Fechner, G. (1966). *Elements of Psychophysics*. (D. H. Howes, Ed.). Holt, Rinehart and Winston (1966).

Francis, J., & Dressel, D. L. (1990). Workspace influence on worker performance and satisfaction: an experimental field study. In *Promoting health and productivity in the computerized office* (pp. 3–16). Taylor & Francis/Hemisphere Bristol, PA, USA.

Galasiu, A. D., Newsham, G. R., Suvagau, C., & Sander, D. M. (2007). Energy saving lighting control systems for open-plan offices: A field study. *LEUKOS - Journal of Illuminating Engineering Society of North America*, *4*(1), 7–29. https://doi.org/10.1582/LEUKOS.2007.04.01.001

Galasiu, A. D., & Veitch, J. A. (2006). Occupant preferences and satisfaction with the luminous environment and control systems in daylit offices: a literature review. *Energy and Buildings*, *38*(7), 728–742. https://doi.org/10.1016/j.enbuild.2006.03.001

Guth, S. K. (1963). A method for the evaluation of discomfort glare. *Illuminating Engineering*, *5*(58), 351–364.

Guth, S., & K., S. (1966). Computing Visual Comfort Ratings For a Specific Interior Lighting Installation. *Illuminating Engineering*, 634–642.

Haldi, F., & Robinson, D. (2010). Adaptive actions on shading devices in response to local visual stimuli. *Journal of Building Performance Simulation*, *3*(2), 135–153.

Halonen, L., & Lehtovaara, J. (1995). Need of individual control to improve daylight utilization and user satisfaction in integrated lighting systems. In *Proceedings of the 23rd Session of the CIE* (pp. 200–203).

Heerwagen, J., & Diamond, R. C. (1992). Adaptations and Coping: Occupant Response to Discomfort in Energy Efficient Buildings. *1992 Summer Study on Energy Efficiency in Buildings*.

Hirning, M. B., Isoardi, G. L., & Cowling, I. (2014). Discomfort glare in open plan green buildings. *Energy and Buildings*, *70*, 427–440. https://doi.org/10.1016/j.enbuild.2013.11.053

Hirning, M. B., Isoardi, G. L., & Garcia-Hansen, V. R. (2017). Prediction of discomfort glare from windows under tropical skies. *Building and Environment*, *113*, 107–120. https://doi.org/10.1016/j.buildenv.2016.08.005

Hoes, P., Hensen, J. L. M., Loomans, M. G. L. C., Vries, B. De, & Bourgeois, D. (2009).

User behavior in whole building simulation. *Energy and Buildings*, *41*, 295–302. https://doi.org/10.1016/j.enbuild.2008.09.008

Hopkinson, R. G. (1972). Glare from daylighting in buildings. *Applied Ergonomics*, *3*(4), 206–215.

Huang, Y. C., & Wang, T. (2016). AUTOMATIC CALCULATION OF A NEW CHINA GLARE INDEX. In *Proceedings of Building Simulation & Optimization* (Vol. 5). Newcastle, UK.

Humann, C., & Mcneil, A. (2017). Using HDR Sky Luminance Maps to Improve Accuracy of Virtual Work Plane Illuminance Sensors, 1740–1748.

IEA SHC. (2000). Daylight in Buildings - a source book on daylighting systems and components. *IEA SHC Task 21 - ECBCS Anexo 29*, 262. https://doi.org/10.1016/j.ecoenv.2010.09.004

Illuminating Engineering Society. (2013). *IES LM-83-12*. Retrieved from https://www.techstreet.com/standards/ies-lm-83-12?product_id=1853773

Inanici, M., & Hashemloo, A. (2016). An investigation of the daylighting simulation techniques and sky modeling practices for occupant centric evaluations. *Building and Environment*, 1–12. https://doi.org/10.1016/j.buildenv.2016.09.022

Inanici, M., & Liu, Y. (2016). Robust sky modelling practices in daylighting simulations. In *PLEA 2016 Los Angeles*. Los Angeles.

Inanici, M. N. (2006). Evaluation of high dynamic range photography as a luminance data acquisition system. *Lighting Research & Technology*, *38*(2), 123. https://doi.org/10.1191/1365782806li164oa

Inanici, M. N. (2010). Evalution of High Dynamic Range Image-Based Sky Models in Lighting Simulation. *Journal of the Illuminating Engineering Society (IESNA)*, *7*(December), 69–84. https://doi.org/10.1582/LEUKOS.2010.07.02001

Inkarojrit, V. (2005). *Balancing Comfort: Occupants' control of window blinds in private offices*. University of California, Berkeley.

Jacobs, A. (2011). Camera Calibration. Retrieved January 26, 2018, from http://www.jaloxa.eu/webhdr/calibrate.shtml

Jakubiec, A., Van den Wymelenberg, K., Inanici, M., & Mahic, A. (2016). Accurate Measurement of Daylit Interior Scenes using HDR Photography (p. CIE (International Commission on Illumination) 201).

Jakubiec, J. A., Inanici, M., Van den Wymelenberg, K., & Mahic, A. (2016). Improving the Accuracy of Measurements in Daylit Interior Scenes Using High Dynamic Range Photography. In *PLEA 2016 Los Angeles*.

Jakubiec, J. A., & Reinhart, C. F. (2011). DIVA 2.0: Integrating daylight and thermal simulations using rhinoceros 3D, DAYSIM and EnergyPlus. In *Proceedings of Building Simulation 2011: 12th Conference of International Building Performance Simulation Association* (pp. 2202–2209). https://doi.org/10.1017/CBO9781107415324.004

Jakubiec, J. A., & Reinhart, C. F. (2013). Predicting visual comfort conditions in a large daylit space based on long-term occupant evaluations: A field study. In *Proceedings of*

Building Simulation 2013.

Jakubiec, J. A., & Reinhart, C. F. (2016). A Concept for Predicting Occupants' Long-Term Visual Comfort within Daylit Spaces. *LEUKOS - Journal of Illuminating Engineering Society of North America*, *12*(4), 185–202. https://doi.org/10.1080/15502724.2015.1090880

Jakubiec, J. A., Reinhart, C. F., & Van Den Wymelenberg, K. (2015). Towards an Integrated Framework for Predicting Visual Comfort Conditions from Luminance-based Metrics in Perimeter Daylit Spaces. In *14th Conference of International Building Performance Simulation Association* (pp. 1223–1230).

Jakubiec, J., & Reinhart, C. (2012). The "adaptive zone" - A concept for assessing discomfort glare throughout daylit spaces. *Lighting Research and Technology*, *44*(2), 149–170. https://doi.org/10.1177/1477153511420097

Jay, P. (1954). Visual comfort: letter to the editor. *Light and Lighting*, *47*, 354.

Jin, H., Li, X., Kang, J., & Kong, Z. (2017). An evaluation of the lighting environment in the public space of shopping centres. *Building and Environment*, *115*. https://doi.org/10.1016/j.buildenv.2017.01.008

Jones, N. L., & Reinhart, C. F. (2016). Experimental validation of ray tracing as a means of image-based visual discomfort prediction. *Building and Environment*. https://doi.org/10.1016/j.buildenv.2016.08.023

Kent, M. G., Altomonte, S., Tregenza, P. R., & Wilson, R. (2016). Temporal variables and personal factors in glare sensation. *Lighting Research and Technology*, *48*(6), 689–710. https://doi.org/10.1177/1477153515578310

Keyvanfar, A., Shafaghat, A., Abd Majid, M. Z., Bin Lamit, H., Warid Hussin, M., Binti Ali, K. N., & Dhafer Saad, A. (2014). User satisfaction adaptive behaviors for assessing energy efficient building indoor cooling and lighting environment. *Renewable and Sustainable Energy Reviews*, *39*, 277–295. https://doi.org/10.1016/j.rser.2014.07.094

Kim, J., de Dear, R., Cândido, C., Zhang, H., & Arens, E. (2013). Gender differences in office occupant perception of indoor environmental quality (IEQ). *Building and Environment*, *70*, 245–256. https://doi.org/10.1016/j.buildenv.2013.08.022

Kong, Z., Utzinger, D. M., Freihoefer, K., & Steege, T. (2018). The impact of interior design on visual discomfort reduction: A field study integrating lighting environments with POE survey. *Building and Environment*, *138*(April), 135–148. https://doi.org/10.1016/j.buildenv.2018.04.025

Kong, Z., Utzinger, M., & Li, X. (2016). Compare CIE sky models and Perez sky models to HDR images in vertical luminance modeling. In *Illuminating Engineering Society Annual Conference*.

Kong, Z., Utzinger, M., & Liu, L. (2015). SOLVING GLARE PROBLEMS IN ARCHITECTURE THROUGH INTEGRATION OF HDR IMAGE TECHNIQUE AND MODELING WITH DIVA. In *Building Simulation Conference*.

Konis, K. (2013). Evaluating daylighting effectiveness and occupant visual comfort in a side-lit open-plan office building in San Francisco, California. *Building and Environment*, *59*, 662–677. https://doi.org/10.1016/j.buildenv.2012.09.017

Konis, K. S. (2012). *Effective daylighting: Evaluating daylighting performance in the San Francisco Federal Building from the Perspective of Building Occupants*. *eScholarship*. https://doi.org/10.1080/09613218.2011.556008

Kosnik, W., Winslow, L., Kline, D., Rasinski, K., & Sekuler, R. (1998). Visual changes in daily life throughout adulthood. *Journal of Gerontology*, *43*(3), 63–70.

Lindelöf, D., & Morel, N. (2006). A field investigation of the intermediate light switching by users. *Energy and Buildings*, *38*(7), 790–801. https://doi.org/10.1016/j.enbuild.2006.03.003

Lindsay, C. R. T., & Littlefair, P. J. (1992). *Occupant use of Venetian blinds in offices*.

Loe, D. L., Mansfiedl, K. P., & Rowlands, E. (1994). Appearance of the lit environment and its relevance in lighting design: Experimental sutdy. *Lighting Research & Technology*, 119–133.

Mahić, A., Galicinao, K., & Van Den Wymelenberg, K. (2017). A pilot daylighting field study: Testing the usefulness of laboratory-derived luminance-based metrics for building design and control. *Building and Environment*, *113*, 78–91. https://doi.org/10.1016/j.buildenv.2016.11.024

Mardaljevic, J. (1995). Validation of a lighting simulation program under real sky conditions. *Lighting Research & Technology*, *27*(4).

Nabil, A., & Mardaljevic, J. (2006). Useful daylight illuminances: A replacement for daylight factors. *Energy and Buildings*, *38*(7), 905–913. https://doi.org/10.1016/j.enbuild.2006.03.013

Nahrkhalaji, R. S., & Mistrick, R. (2016). The impacts of different levels of exterior surround detail on daylight simulation results.

Newsham, G. R. (1994). Manual Control of Window Blinds and Electric Lighting: Implications for Comfort and Energy Consumption. *Indoor and Built Environment*, *3*(3), 135–144. https://doi.org/10.1177/1420326X9400300307

Nicol, J. F., & Humphreys, M. A. (1973). Thermal comfort as part of a self-regulating system. *Building Research and Practice*, *1*(3), 174–179. https://doi.org/10.1080/09613217308550237

Nicol, J. F., & Humphreys, M. A. (2002). Adaptive thermal comfort and sustainable thermal standards for buildings. *Energy and Buildings*, *34*(6), 563–572. https://doi.org/10.1016/S0378-7788(02)00006-3

Nikolopoulou, M., & Steemers, K. (2003). Thermal comfort and psychological adaptation as a guide for designing urban spaces. *Energy and Building*, *35*(1), 95–101. https://doi.org/Pii S0378-7788(02)00084-1\nDoi 10.1016/S0378-7788(02)00084-1

ONEILL, M. J. (1994). Work Space Adjustability, Storage, and Enclosure As Predictors of Employee Reactions and Performance. *Environment and Behavior*. https://doi.org/10.1177/001391659402600403

Osterhaus, W. K. E., & Bailey, I. L. (1992). Large area glare sources and their effect on visual discomfort and visual performance at computer workstations. *Conference Record - IAS Annual Meeting (IEEE Industry Applications Society)*, *1992–Janua*, 1825–1829. https://doi.org/10.1109/IAS.1992.244537

Painter, B., Fan, D., & Mardaljevic, J. (2009). Evidence-based daylight research: development of a new visual comfort monitoring method. In *Proceedings Lux Europa. 11th International Lighting Conference*. Istanbul, Turkey.

Parducci, A. (1965). Reviewed Work: Adaptation-Level Theory by Harry Helson Review by : Allen Parducci Source. *The American Journal of Psychology*, *78*(1), 158–159.

Perez, R., Seals, R., & Michalsky, J. (1993). All-weather model for sky luminance distribution-Preliminary configuration and validation. *Solar Energy*, *50*(3), 235–245. https://doi.org/10.1016/0038-092X(93)90017-I

Pierson, C., Wienold, J., & Bodart, M. (2017). Discomfort glare perception in daylighting: Influencing factors. *Energy Procedia*, *122*, 331–336. https://doi.org/10.1016/j.egypro.2017.07.332

Qarout, L. (2017). Reducing the Environmental Impacts of Building Materials: Embodied Energy Analysis of a High- performance Building. Retrieved from http://dc.uwm.edu/etd

Reindl, D. T., Beckman, W. A., Reindl, D. T., & Duffle, J. A. (1990). DIFFUSE FRACTION CORRELATIONS. *Solar Energy*, *45*, 1–7. https://doi.org/10.1016/0038-092X(90)90060-P

Reinhard, E., Heidrich, W., Debevec, P., Pattanaik, S., Ward, G. J., & Myszkowski, K. (2010). *High dynamic range imaging : acquisition, display, and image-based lighting*. Morgan Kaufmann/Elsevier.

Reinhart, C. (n.d.-a). Daysim. Retrieved June 6, 2018, from https://daysim.ning.com/

Reinhart, C. (n.d.-b). DAYSIM. Retrieved from https://daysim.ning.com/

Reinhart, C. F., & Andersen, M. (2006). Development and validation of a Radiance model for a translucent panel. *Energy and Buildings*, *38*(7), 890–904. https://doi.org/10.1016/J.ENBUILD.2006.03.006

Reinhart, C. F., Mardaljevic, J., & Rogers, Z. (n.d.). Dynamic Daylight Performance Metrics for Sustainable Building Design. https://doi.org/10.1582/LEUKOS.2006.03.01.001

Reinhart, C. F., & Walkenhorst, O. (2001). Validation of dynamic RADIANCE-based daylight simulations for a test office with external blinds. *Energy and Buildings*, *33*(7), 683–697. https://doi.org/10.1016/S0378-7788(01)00058-5

Reinhart, C., & Fitz, A. (2006). Findings from a survey on the current use of daylight simulations in building design. *Energy and Buildings*, *38*(7), 824–835. https://doi.org/10.1016/j.enbuild.2006.03.012

Rhinoceros. (n.d.). Retrieved February 20, 2018, from https://www.rhino3d.com/

Rhodes, B. C. (n.d.). PyEphem. Retrieved January 1, 2017, from http://rhodesmill.org/pyephem/

Robbins, C. L. (1986). *Daylighting : design and analysis*. Van Nostrand Reinhold.

Rushmeier, H., Ward, G., Piatko, C., Sanders, P., & Rust, B. (1995). Comparing Real and Synthetic Imags: Some Ideas About Metrics. In *6th Eurographics Workshop on Rendering*. Springer-Verlag, Dublin.

Sanati, L. (2014). *SUBDIVIDED WINDOWS WITH MIXED SHADING DEVICES : A DAYLIGHTING SOLUTION FOR EFFECTIVE INTEGRATION OF OCCUPANTS INTO THE BUILDING ENVIRONMENTAL CONTROL*.

Shin, J. Y., Yun, G. Y., & Kim, J. T. (2012). View types and luminance effects on discomfort glare assessment from windows. *Energy and Buildings*, *46*, 139–145. https://doi.org/10.1016/j.enbuild.2011.10.036

Society of Light and Lighting. (2009). *SLL Lighting Handbook*. London, U.K.: SLL.

Sonnenfeld, J. (1967). Environmental perception and adaptation levle in the Arctic. *Enviornmental Perception and Behavior*, *109*, 42–59.

Subova, A., Kittler, R., & MacGowan, D. (1991). Results of an ongoing experiments on subjective response discomfort glare. In *Conference of IEI*. Japan, Chiba.

Suk, J. Y., Schiler, M., & Kensek, K. (2017). Investigation of existing discomfort glare indices using human subject study data. *Building and Environment*, *113*, 121–130. https://doi.org/10.1016/j.buildenv.2016.09.018

Thanachareonkit, A., Fernandes, L. L., & Papamichael, K. (2010). Field Luminance Mapping of the Sky. *IES Annual Conference 2010*.

Tuaycharoen, N., & Tregenza, P. R. (2005). Discomfort glare from interesting images. *Lighting Research and Technology*, *37*(4), 329–341. https://doi.org/10.1191/1365782805li147oa

Tuaycharoen, N., & Tregenza, P. R. (2007). View and discomfort glare from windows. *Lighting Research & Technology*, *39*(2), 185–200. https://doi.org/10.1177/1365782807077193

U.S. Department of Energy. (2012). Buildings energy databook. *Energy Efficiency & Renewable Energy Department*, 286. Retrieved from http://buildingsdatabook.eren.doe.gov/DataBooks.aspx

U.S. Office of Personnel Management. (n.d.). Computing Hourly Rates of Pay Using the 2,087-Hour Divisor. Retrieved June 18, 2018, from https://www.opm.gov/policy-data-oversight/pay-leave/pay-administration/fact-sheets/computing-hourly-rates-of-pay-using-the-2087-hour-divisor/

Utzinger, M., & Wasley, J. (2013). *CASE STUDY The Aldo Leopold Legacy Center*. Milwaukee.

Van Den Wymelenberg, K. (2012). *Evaluating human visual preference and performance in an office environment using luminance-based metrics.* University of Washington Seattle.

Van Den Wymelenberg, K. G. (2014). Visual Comfort, Discomfort Glare, and Occupant Fenestration Control: Developing a Research Agenda. *Leukos*, *10*(4), 207–221. https://doi.org/10.1080/15502724.2014.939004

Van Den Wymelenberg, K., Inanici, M., & Johnson, P. (2010). The effect of luminance distribution patterns on occupant preference in a daylit office environment. *LEUKOS - Journal of Illuminating Engineering Society of North America*, *7*(2), 103–122. https://doi.org/10.1582/LEUKOS.2010.07.02003

Veitch, J. A. (2001). Psychological processes influencing lighting. *Journal of the Illuminating*

Engineering Society, *30*(1), 124–140. Retrieved from http://www.tandfonline.com/doi/pdf/10.1080/00994480.2001.10748341

Veitch, J. A., Farley, K. M. J., & Newsham, G. R. (2002). *Environmental Satisfaction in Open-Plan Environments : 1 . Scale Validation and Methods*. https://doi.org/IRC-IR-844

Ward, G. (n.d.-a). gensky. Retrieved May 3, 2018, from https://www.radiance-online.org/learning/documentation/manual-pages/pdfs/gensky.pdf

Ward, G. (n.d.-b). gensky. Retrieved from https://www.radiance-online.org/learning/documentation/manual-pages/pdfs/gensky.pdf

Ward, G. (n.d.-c). Learn — Radsite. Retrieved December 6, 2017, from https://www.radiance-online.org/learning

Ward, G. (n.d.-d). Mailing Lists — Radsite. Retrieved December 6, 2017, from https://www.radiance-online.org/community/mailing-lists

Wienold, J. (2009). Dynamic daylight glare evaluation. *Eleventh International IBPSA Conference: Building Simulation*, 944–951. https://doi.org/citeulike-article-id:11069372

Wienold, J. (2013). *Glare analysis and metrics*. *12th International Radiance Conference*. Retrieved from http://www.radiance-online.org/community/workshops/2013-golden-co/wienold_glare_rad_ws2013.pdf

Wienold, J. (2015). Evalglare. Retrieved from https://www.radiance-online.org/learning/documentation/manual-pages/pdfs/evalglare.pdf/view

Wienold, J., & Andersen, M. (n.d.). *Evalglare 2.0 – new features …. faster …. and more robust HDR-image evaluation*. Retrieved from https://www.radiance-online.org/community/workshops/2016-padua/presentations/211-Wienold-Evalgaare2.0.pdf

Wienold, J., & Christoffersen, J. (2006). Evaluation methods and development of a new glare prediction model for daylight environments with the use of CCD cameras. *Energy and Buildings*, *38*(7), 743–757. https://doi.org/10.1016/j.enbuild.2006.03.017

WMO. (2010). *Guide to Meteorological Instruments and Methods of observation*. *Guide to Meteorological Instruments and Methods of Observation* (Vol. I & II). https://doi.org/Guide to meteorological instrument and observing practices

Wohlwill, J. F. (1974). Human adaptation to levels of environmental stimulation. *Human Ecology*, *2*(2), 127–147. https://doi.org/10.1007/BF01558117

Yang, L., Yan, H., & Lam, J. (2014). Thermal comfort and building energy consumption implications - a review. *Applied Energy*, (115), 64–73.

Yildirim, K., Akalin-Baskaya, A., & Celebi, M. (2007). The effects of window proximity, partition height, and gender on perceptions of open-plan offices. *Journal of Environmental Psychology*, *27*(2), 154–165. https://doi.org/10.1016/j.jenvp.2007.01.004

APPENDICES

APPENDIX A: HDR images and simulated luminance maps at CSM

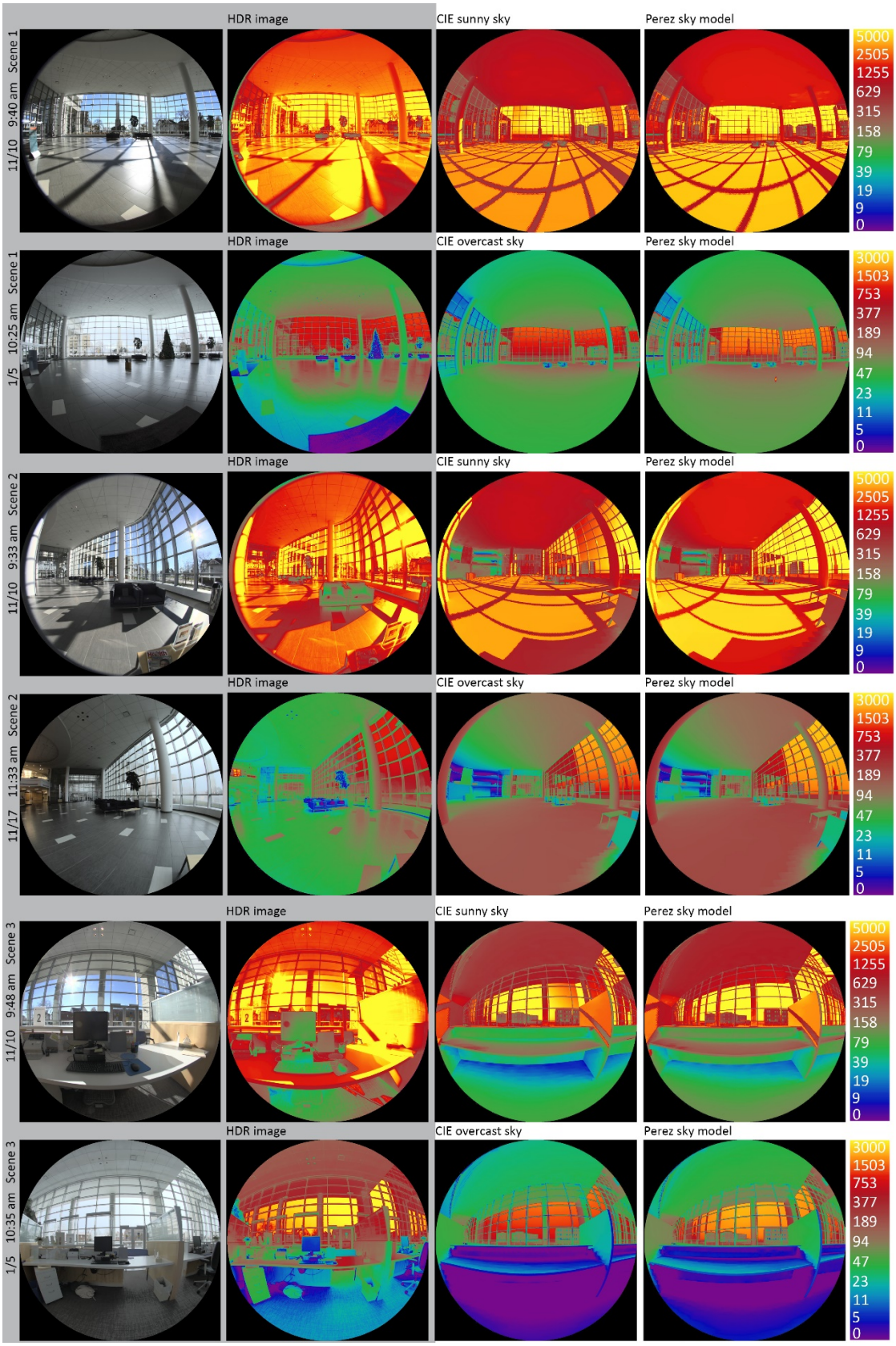

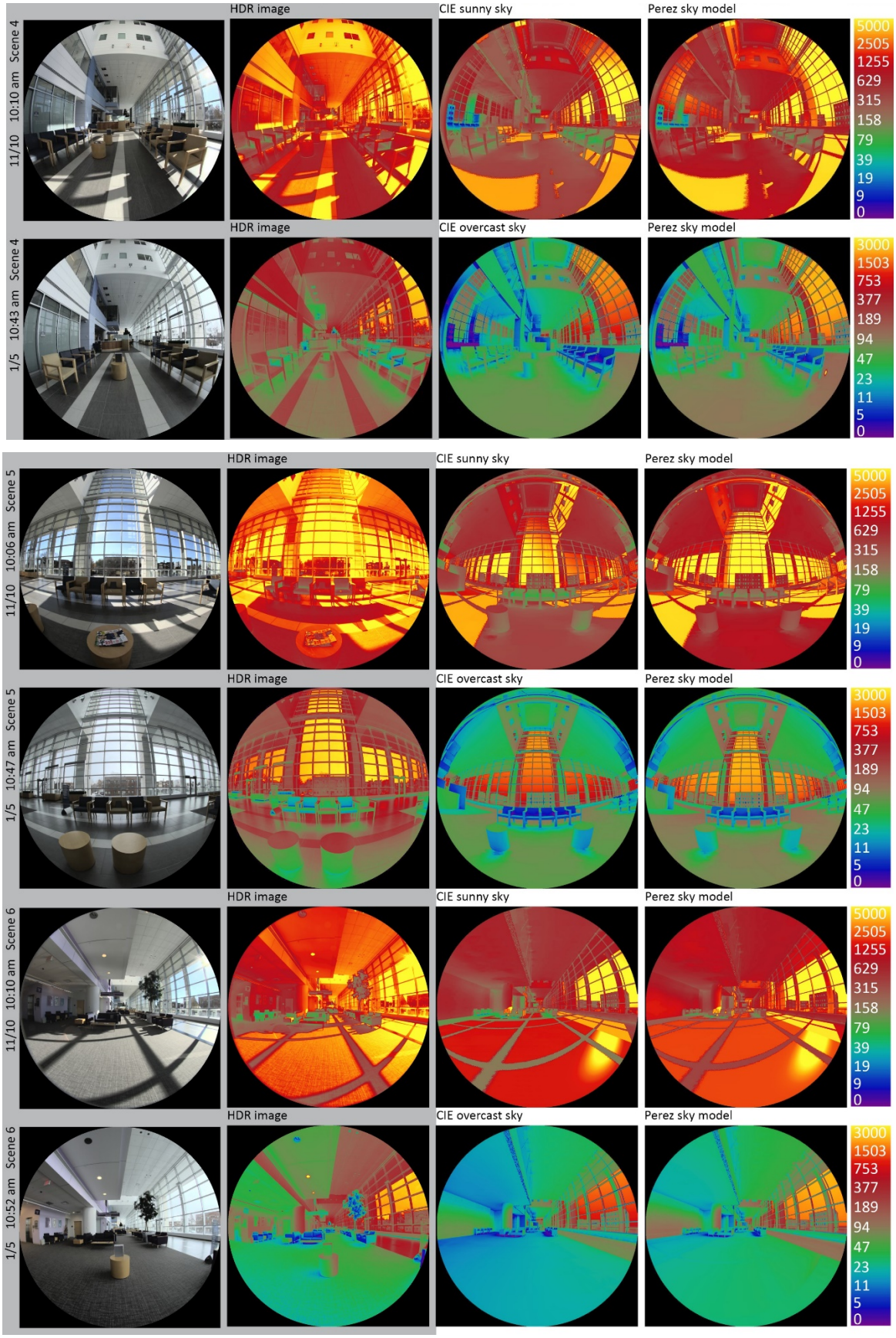
HDR image
CIE sunny sky
Perez sky model
11/10 10:10 am Scene 4
5000
2505
1255
629
315
158
79
39
19
9
0
HDR image
CIE overcast sky
Perez sky model
1/5 10:43 am Scene 4
3000
1503
753
377
189
94
47
23
11
5
0
HDR image
CIE sunny sky
Perez sky model
11/10 10:06 am Scene 5
5000
2505
1255
629
315
158
79
39
19
9
0
HDR image
CIE overcast sky
Perez sky model
1/5 10:47 am Scene 5
3000
1503
753
377
189
94
47
23
11
5
0
HDR image
CIE sunny sky
Perez sky model
11/10 10:10 am Scene 6
5000
2505
1255
629
315
158
79
39
19
9
0
HDR image
CIE overcast sky
Perez sky model
1/5 10:52 am Scene 6
3000
1503
753
377
189
94
47
23
11
5
0

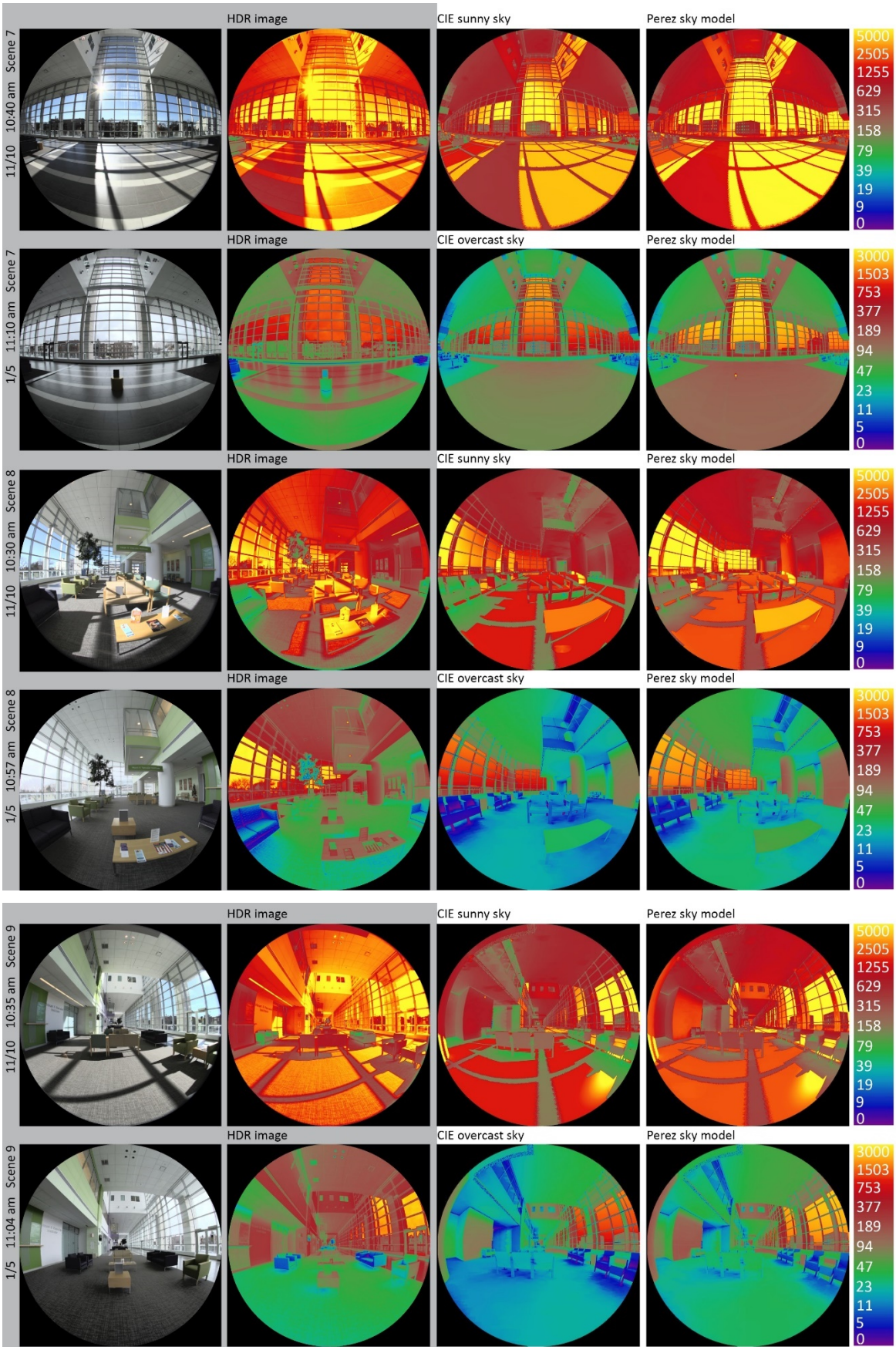
HDR image
CIE sunny sky
Perez sky model
Scene 7
10:40 am
11/10
5000
2505
1255
629
315
158
79
39
19
9
0
HDR image
CIE overcast sky
Perez sky model
Scene 7
11:10 am
1/5
3000
1503
753
377
189
94
47
23
11
5
0
HDR image
CIE sunny sky
Perez sky model
Scene 8
10:30 am
11/10
5000
2505
1255
629
315
158
79
39
19
9
0
HDR image
CIE overcast sky
Perez sky model
Scene 8
10:57 am
1/5
3000
1503
753
377
189
94
47
23
11
5
0
HDR image
CIE sunny sky
Perez sky model
Scene 9
10:35 am
11/10
5000
2505
1255
629
315
158
79
39
19
9
0
HDR image
CIE overcast sky
Perez sky model
Scene 9
11:04 am
1/5
3000
1503
753
377
189
94
47
23
11
5
0

APPENDIX B: Institutional Review Board Approvals

UNIVERSITY of WISCONSIN
UWMILWAUKEE

Department of University Safety & Assurances

Melody Harries
IRB Administrator
Institutional Review Board
Engelmann 270
P. O. Box 413
Milwaukee, WI 53201-0413
(414) 229-3182 *phone*
(414) 229-6729 *fax*

http://www.irb.uwm.edu
harries@uwm.edu

New Study - Notice of IRB Exempt Status

Date: April 12, 2017

To: Dennis Utzinger, PhD
Dept: Architecture and Urban Planning

CC: Zhe Kong

IRB#: 17.285
Title: Lighting Quality Evaluation in the HGA Milwaukee Office

After review of your research protocol by the University of Wisconsin – Milwaukee Institutional Review Board, your protocol has been granted Exempt Status under Category 2 as governed by 45 CFR 46.101(b). Your protocol has also been granted approval to waive documentation of informed consent for the survey portion of the research as governed by 45 CFR 46.117 (c).

This protocol has been approved as exempt for three years and IRB approval will expire on April 11, 2020. If you plan to continue any research related activities (e.g., enrollment of subjects, study interventions, data analysis, etc.) past the date of IRB expiration, please respond to the IRB's status request that will be sent by email approximately two weeks before the expiration date. If the study is closed or completed before the IRB expiration date, you may notify the IRB by sending an email to irbinfo@uwm.edu with the study number and the status, so we can keep our study records accurate.

Any proposed changes to the protocol must be reviewed by the IRB before implementation, unless the change is specifically necessary to eliminate apparent immediate hazards to the subjects. The principal investigator is responsible for adhering to the policies and guidelines set forth by the UWM IRB, maintaining proper documentation of study records and promptly reporting to the IRB any adverse events which require reporting. The principal investigator is also responsible for ensuring that all study staff receive appropriate training in the ethical guidelines of conducting human subjects research.

As Principal Investigator, it is also your responsibility to adhere to UWM and UW System Policies, and any applicable state and federal laws governing activities which are independent of IRB review/approval (e.g., FERPA, Radiation Safety, UWM Data Security, UW System policy on Prizes, Awards and Gifts, state gambling laws, etc.). When conducting research at institutions outside of UWM, be sure to obtain permission and/or approval as required by their policies.

Contact the IRB office if you have any further questions. Thank you for your cooperation, and best wishes for a successful project.

Respectfully,

Melody Harries
IRB Administrator

APPENDIX C: HGA Online Questionnaire

DAYLIGHTING EVALUATION SECTION

1.1 Please rate degree of satisfaction with the lighting at your workstation

	Very Dissatisfied	Moderately Dissatisfied	Slightly Dissatisfied	Neutral	Slightly Satisfied	Moderately Satisfied	Very Satisfied
Artificial light							
Natural light							
Interior mechoshade system							
Overall satisfaction with the lighting conditions at your workstation							
Overall satisfaction with the design of your workstation							

1.2 Please rate the visual discomfort issues caused by natural light.

	NA	Imperceptible	Slightly Uncomfortable/ Perceptible	Disturbing, bearable for 15 to 30 minutes	Intolerable
Direct sunlight on my face / eye(s)					
Direct sunlight on my monitor(s)					
High contrast ratios between my monitor(s) and the background					
Reflected light from the river					
Overall visual discomfort issues					
Other. Please describe and rate					

1.3 Please rate visual discomfort issues and when they occur (select all that apply).

	NA	Imperceptible	Slightly Uncomfortable/ Perceptible	Disturbing, bearable for 15 to 30 minutes	Intolerable
8:00 to 10:00 a.m.					
10:00 a.m. to 12:00 p.m.					
12:00 to 2:00 p.m.					
2:00 to 4:00 p.m.					
4:00 to 6:00 p.m.					
after 6:00 p.m.					

1.4 Under what kinds of weather/sky conditions is visual discomfort most often a problem (select all that apply)?

A) Clear / Sunny sky B) Part cloudy and part sunny C) Cloudy sky
D) Other. Please describe: _____

1.5 At what time of year are visual discomfort issues caused by natural light most often a problem (select all that apply)?

A) Winter B) Spring C) Summer D) Fall E) NA

1.6 When you experience visual discomfort issues, how do you handle it?

A) I do not experience visual discomfort issues. B) I experience visual discomfort issues.
Condition: I do not experience visual ... Is Selected. Skip To: Please select the visual discomfort i....Condition: I experience visual discomfort... Is Selected. Skip To: Please rate the frequency of your rea....

1.7 Please rate the frequency of your reaction(s) to modify visual discomfort (select all that apply).

	Never	Rarely	Occasionally	Sometimes	Frequently	Usually	Every time / Always
Wear sunglasses							
Turn or lower my body to avoid direct sunlight							
Use my hand or an object to block direct sunlight for a short time							
Rotate the monitor(s) to avoid direct sunlight on the screen							
Adjust working schedule to avoid times of day that are uncomfortable							

Leave my desk and take a break							
Move to another place and continue my work							
Use an umbrella							
Erect a board to block direct sunlight							

1.8 Please select the visual discomfort issues caused by mechoshade (select all that apply).

A) The view of the sun / sunlight through the mechoshade
B) The mechoshade is not low enough to block direct sunlight
C) The mechoshade system fails to work sometimes
D) The brightness caused by the delay between the occurrence of visual discomfort issues and the mechoshade operation.
E) The darkness caused by the delay between operating mechoshades and turning on artificial light.
F) The mechoshade is down on cloudy conditions
G) The automatic up-and-down control systems are distracting.
H) Other. Please describe_____

1.9 Please rate your level of agreement for the following statements

	Strongly disagree	Disagree	Somewhat disagree	Neither agree or disagree	Somewhat agree	Agree	Strongly agree
It is important for me to have enough daylight at my workstation so that I can feel connected with the outdoors.							
It is important for me to have a view to the outside so that I can feel connected with the outdoors.							
Overall, the natural light at my workstation does not interfere with my ability to get my work done.							
After some modified reactions, I have reduced the visual discomfort issues caused by natural light							
It is necessary to prepare well-designed shading boards for the purpose of blocking temporarily direct sunlight							

1.10 Please identify any other issues or sources of visual discomfort that was not addressed in this survey:

DEMOGRAPHIC SECTION

2.1 The practice group you work for

A) Structural B) Healthcare C) ACE D) Mechanical E) Corporate F) Administrative G) Electrical & Plumbing H) Interiors
I) Energy & Infrastructure J) Human Resources K) Other. Please describe:
_____

2.2 Your job title

A) Associate and Senior Associate B) Senior Leadership (AVP, VP) C) Hourly employee /intern
D) Staff E) Researcher F) Other. Please describes___

2.3 Your gender

A) Male B) Female C) Trans gender D) Prefer not to answer

2.4 Your age

A) under 20 B) 20-29 C) 30-39 D) 40-49 E) 50-59 F) 60-69 G) over 70

2.5 How long have you been working in this office?

A) less than 1 year B) 1 ~ 2 years C) 2 ~ 5 years D) 5 ~ 10 years E) over 10 years

2.6 How many hours do you work at your workstation in a typical week?

A) less than 20 hours B) 20 ~ 30 hours C) 30 ~ 40 hours D) over 40 hours

2.7 What percent of time per week do you work on the computer?

A) less than or equal to 20% B) 21% ~ 40% C) 41% ~ 60% D) 61% ~ 80% E) over 81%

2.8 Your workstation is in

A) Tier One B) Tier Two C) Tier Three D) Tier Four

Display This Question:

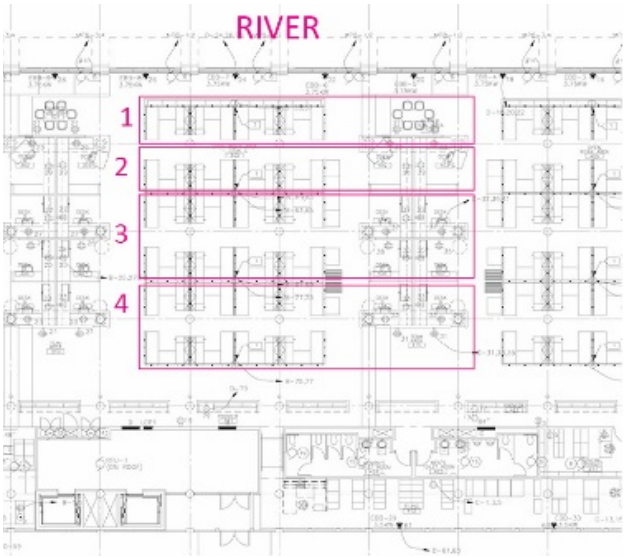

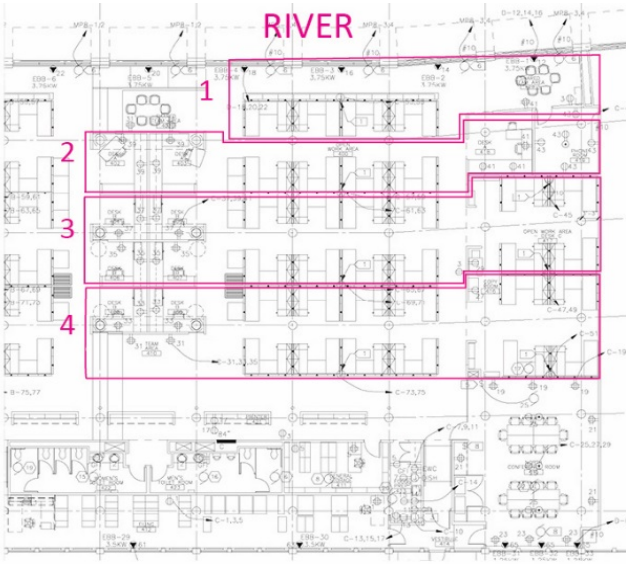

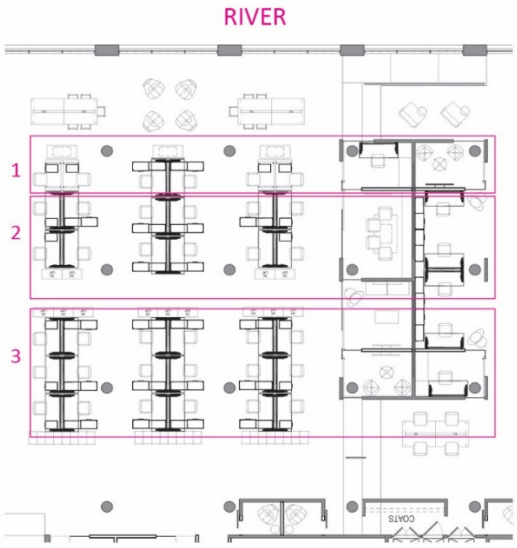

If Your workstation is in ❢ Tier One Is Selected
Or Your workstation is in ❢ Tier Three Is Selected

2.9 Your workstation is in zone (Figure 1)
A) Zone 1 B) Zone 2 C) Zone 3 D) Zone 4

2.10 When working on the computer, you are facing (based on the eight images above)
A) Towards window B) Back to Window C) Parallel with Window towards Larger Tier
D) Parallel with window toward smaller Tier
E) Towards south F) Towards West G) East F) North

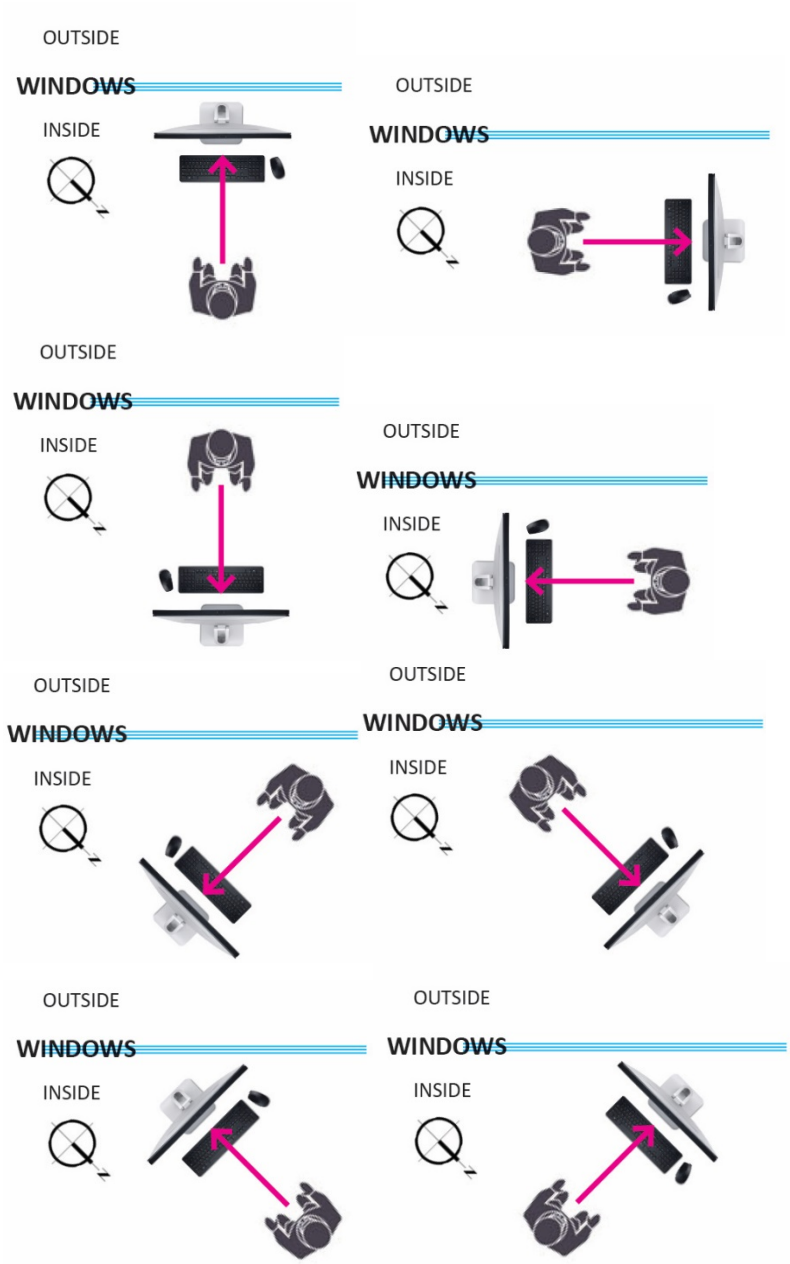

Display This Question:
If Answer YES to provide your consent and complete the questionnaire; NO Is Selected

This is the END of the questionnaire. Thank you for your time and participation.

APPENDIX D: Interview Responses Summary

	Causes of visual discomfort	Mechoshade systems	Artificial lighting controls	Adaptive behaviors	Glare	Attitudes towards daylight & views	Comments
1	Direct sunlight in winter, result in one of my eyes in the sunlight the other not.	When shade is down, really dark. The shade isn't low enough to block sunlight	The light up there (the first line) doesn't always turn on when the shade is down.	Put an umbrella; move my work to one of the conference rooms; Concerns about bad looking of foam core boards	Winter in the afternoon with direct sunlight		Parallel with windows don't work if too close to the windows; The only other improveme nt is the timing before the shade coming down and the light adjusted.
2	Not fun when the sun blinds you. Hard to focus. Direct sunlight bothers me the most. The higher sun penetrates through the board and hits me.	The sun through the shade also bothers me.		Change my gesture, change my body position to avoid direct sunlight. Erect a foam core board.	Most of the afternoon from 2 p.m. Winter is a lot worse.	I would rather see my work than the outside views. The outside views are too bright to adjust back to the screens.	
3	Very bright, one eye in bright and one eye in dark 1 to 2 p.m., direct sunlight, no sunshade (openings between the overhangs) Tall windows in Tier One causes the trouble. Tier Four has no such issue	Sunlight through the mechoshade is still bright Top portion of the window. The conference room has black shades on the top portion.		Erect foam core boards	After May, I don't notice sunlight on me or my desk	Don't care about the views. Would rather sit back to avoid direct sunlight	
4	Worse contrast issues on cloudy days	Shade resolves contrast issues		Lower my body	Winter low sun angles	River reflections on the ceiling, cool	
5	Direct sunlight hits me Between 3:30 and 4:00 p.m. in winter, last 5 minutes			Continue working Rotate my body or block direct sunlight with my hands			

6	I've noticed that, occasionally, sunlight on my laptop. There are sometimes there is a little bit of glare, but there is nothing that is not tolerable. The cubicles are darker to me.	Mechoshade certainly helps. It is typical when I notice a slight glare on my screen if they are not down.		I just rotate my laptop.	It happens in the afternoon. The sunlight in winter doesn't bother me.	I love natural light. I like the water. Just nice to be able to see the views outside.	
7	Direct sunlight on my eyes/face around 3 p.m. through the mechoshade systems Last around 10 to 15 minutes for one or two weeks in spring	Shade is old, see the sun through the shade		Take a break, but lose that amount of working time	Spring is the worst	Better view in Tier Two	Open layout (barriers removed) better sunlight penetration, seating orientation is better
8	Old setting (direct sunlight into my eyes)	It is dark when the shade drops Sometimes it shouldn't drop, sometimes it isn't on time. It blocks the views of the River.		Old setting (wear sunglasses)		Like lighting environments here; Like the views outside	Tier two is better in terms of visual discomfort; More access to the views; More connection to the outside; Enjoy the views while walking
9	Short time of direct sunlight, around 30 minutes Doesn't bother me that much; In spring, summer, and fall, sunlight doesn't reach low.	It is a shame to put anything on the views	More sensitive to artificial light Turn on lamps for book reading	Put a foam core board to block sunlight;		Take daylighting as much as I can; The views are great	
10	I don't have any issue with the amount of natural light. I never have a problem with being too bright or glare. If it is the evening hour, I wish it could be brighter.	Mechoshades are OK. Sometimes they'll go down at 5 o'clock, like the night. They must take some readings somewhere in the buildings and decide to drop the shades. That doesn't seem to correlate with the actual lighting conditions. When the sun is right there, they'll go up and there'll be lighter.	I'm not a big fun of fluorescent. The fact that I am so close to the glass offsets any need for task lighting.			I like it a lot. It is nice to have the view.	Just moved to my current location in January. Some colleagues complain about sunlight penetration in the evening.

11	Generally daylighting is good; direct sunlight is the main issue, no way to get away from it;	Mechoshade helps, but a little bit delay; doesn't happen on time; or no reaction. The sun through the mechoshade catches my eyes.		Turn my monitor; move my body; used to erect foam core boards	Spring & fall afternoon time, direct sunlight penetrates. Winter is the worst;		I like the flexibility; more cluttered with less space; don't notice any change in daylighting
12	The overall lighting is adequate. I found myself felt lighting levels from the direct and indirect fixtures and daylight was sufficient. My eyes got a little tired. I got eyestrain or eye fatigue. There were moments when you got a reflection from something surrounding outside (neighboring buildings or the river).	It is more relative to the control system. It needs fine tuning. It makes it darker, maybe on an overcast day. The control criteria are the trickiest.	I would turn on the task light if I was doing reading-based research, like code research.	The reflection isn't anything, and I don't need to move.	On winter solstice, the lowest solar angle, it was OK.	The river views are great. I like it. It has the effect of being pleasant.	The lighting in Tier Four was terrible (low windows). On overcast days, the shades go on to the point where you need supplement ed light because I wasn't able to see anything.
13	Bright in the afternoon when I need to face the glazing and talk to whoever standing there. Nothing with regard to computer. I don't experience any glare. But direct sunlight doesn't bother me.	The shades don't work. Sometimes they go do when it is not that sunny. Sometimes they don't do much to block it when it is really sunny.		Just adjust the position. I have the option of raising up my desk if I experience glare, but I never do.	Usually in the afternoon around 3 p.m., direct sunlight comes in.	I love the views. I have one of the best desk because I can see the river. I can see what's going on outside, the weather.	
14	Used to sit in Tier 4, too dark; direct sunlight in the afternoon;	The shade helps.		Continue working; put my body in the right direction to block my screen from the sun		Don't mind about no access to outside views; still see it when walking down.	
15	A little glare, reflections from my monitor	Sometimes the shade has no reaction	I rotate my monitor sometimes; continue working;	Wish to turn off artificial light;	Winter afternoon it happens a lot		
16	Direct sunlight; Contrast isn't an issue on overcast days.	Mechoshade helps a little, but it is still bright. I still have issues with sunlight through the shade.	Use a huge board to block the sunlight		Winter afternoon is bad, from 3 to 5 or 2:30 to 5 p.m.;		The orientation of the new workstation solves my problem; If

							I can parallel with the windows, there won't be direct sunlight hitting me.
17	I don't experience lighting issues at all. Direct sunlight comes this way affects me a little. If it is really strong, it is still doable.	The blinds help a lot. They make a big difference.	Work with it.			I like the lighting environments . I love the windows and lighting here. I love the sunlight, the more the better. I love the views of the river. My view is restricted by the cubicle.	
18	I always sit right facing the river, so direct sunlight comes right into my eyes.	Sometimes it doesn't work on days, or it doesn't go low enough. It is bothering when they move down a foot. Then 15 minutes later, they move down a foot again. It is kind of nice if they just brought it down like half way and full way. When the sun comes out, so it goes back up. Why don't you just stay down. It'll be better if we move it VS its automatically moving down.	I usually slouch my chair, just move my head to the right angle until my screen is safe.	Artificial light doesn't bother me.	During the afternoon time when the sun starts coming over the settings, you are distracted, probably from 1:30 to 6:30 p.m.	I like the river views. It is very comforting to have the water and activities there.	I've only been here for two months, so it's all about the same.
19	I never have problem with it. When the sun is west, just for like an hour or two, hitting my face. Probably a couple of times a month. I don't notice seasonal difference. If I stand up and look towards the windows, it bothers me.	Without any issue. It is not something I will complain about.					

20	The ambient light is not appropriate. It is not bright enough. When people come to my workstation like you did. I turned to them and it is so bright behind them. Two periods when direct sunlight comes in at different angles and hit me. It is relatively easy to handle.	It is either too bright or too dark. The timing on the mechoshade just doesn't seem accurate.	I thought about having a hat when I have visual discomfort, but I never did.	I do have an extra task light.	Late winter and early fall, two times a year.	Nice to have a view.	
21	I am satisfied the lighting environments at my workstation. It's with the direct sunlight and lots of contrasts, glare.	The screen, the mesh we have that coming down, is not effective when a particular condition is present. If anything, I would need, to be a black out curtain that would come down. It is funny, running bit of humor between the meter raised mechoshades, moving up and down. That's like all the sudden they go down.	The sensors we have up there for the artificial lights get confused. On a cloudy day there is no natural light, and even our lights go off. If it is cloudy, like here these lights are on and those lights are off.	I have to put something to block sunlight, but I look at it as a minor inconvenience. It doesn't inhibit my work. Small price to pay for a lot of light to coming in. I can stack boxes and material samples on top of the partition. I stand while working. I have my screen perpendicular to the windows, and that helps. In this condition, I can't stand and work. So, I am hiding behind those stone boxes.	They are some months out of the year are little tricky, especially December, November, and January in the late afternoon. The quality of the light from the other nice months out of the year is so much better. In the winter, the sun is about over that white building when it is going down, and it hits my eyes.	I am really appreciated with the amount of glass, the amount of natural light coming in. It makes our working environments pleasant. I love how, especially in the summer, the light bounced of the water, and you can see the shades of the river and the ceiling tiles.	I really like my workstation. It is one of the better office, better cubicles in the whole firm. You need to adapt It is funny that nobody really knows what's triggering it. Your eyes adapt to certain levels of conditions. And then all the sudden, just changes, the screens go down and the lights turn on. I'm in my 50th, so I need more foot-candles. We can't control the natural

22	Direct sunlight; contrast issues. My eyes have issues with adjusting to darkness.	Don't know how to predict the mechoshade; sometimes it doesn't react to direct sunlight; Once the shade is down, it is also dark. It is gloomy.	Get closer and lower to my computer to hide from direct sunlight; deal with direct sunlight. No foam core board to erect.		Direct sunlight in winter in the afternoon is the worst;		
23	Direct sunlight around 2:30 to 4:00 p.m. on my screen. Hard to see my screen. It lasts around 45 minutes, pretty long. My eyes easily get fatigue.	Mechoshade helps when it is down, but it doesn't catch sunlight on time.	I just bear with it. I can't place a foam core board. I can only rotate my screen, squint my eyes a little.		Winter is bad. Spring and fall also happen. Fall is the worst.	It doesn't matter to me since I can't access the outside views.	

APPENDIX E: Participants' Comments on Control Systems

Responses to artificial light controls	Problem summary
The lights turn off after 6pm on tier 2 even when I am still working and/or walking around when the lights on all of the other tiers are still on.	Schedules of artificial lights
After 7 pm, the "motion-sensored" lights shut off on a timer, even if you are moving around.	Schedules of artificial lights
Other than the few times a year where the sun is low and directly shining in. The work environment is relatively nice. I do feel it is on the darker side because I am closer to the windows the lights shut off, but then the mechoshades are down and it seems very dark. It would be nice if the lights are going to go off that the mechoshade stay up or put the shade down and leave the light on, losing both overhead light and natural light makes the station feel dark.	Disconnected control systems between the mechoshade and artificial lights
Overall lighting level of artificial light in office is low. I require a task light for morning or late afternoon (winter) times.	Insufficient artificial lighting levels
I don't have a problem with the natural light as I am as far away from the window as one can get. I have an issue with the artificial light at my workstation. I would like to have more light.	Insufficient artificial lighting levels
Finding and being able to operate light switches sometimes an issue. When I come in at night or early in the morning, sometimes I have trouble finding the light switches and then when I do find them, they are not very intuitive and sometimes tough to operate.	Complexity of artificial control systems
The use of any can or spot-type lighting in the office should be carefully considered. Back when the structural department was in the Annex, those spot lights were sometimes directly aimed at our faces. I would keep any of these types of lights away from new workstations.	Types of artificial lights
Honestly, really my only thing is that when you're in one of the enclosed cubes, the artificial lighting can be very dark... and when the shades go down and block the sun that makes it worse.	Disconnected control systems between the mechoshade and artificial lights
The light up there (the first line) doesn't always turn on when the shade is down.	Disconnected control systems between the mechoshade and artificial lights
I am more sensitive to artificial light. I usually need to turn on lamps for book reading.	Insufficient artificial lighting levels
I'm not a big fun of fluorescent. The fact that I am so close to the glass offsets any need for task lighting.	Personal preference
I would turn on the task light if I was doing reading-based research, like code research.	Insufficient artificial lighting levels
The sensors we have up there for the artificial lights get confused. On a cloudy day there is no natural light, and even our lights go off. If it is cloudy, like here these lights are on and those lights are off.	Disconnected control systems between the mechoshade and artificial lights

Responses to mechoshade controls	Problem summary
When shade is down, it is really dark. The shade isn't low enough to block sunlight	Darkness caused by dropped shades
The sun through the shade also bothers me.	Views of the sun through mechoshades
Sunlight through the mechoshade is still bright on the top portion of the window. The conference room has black shades on the top portion.	Views of the sun through mechoshades
Shade resolves contrast issues	Mechoshades work
Mechoshade certainly helps. It is typical when I notice a slight glare on my screen if they are not down.	Mechoshades work
Shade is old. I can see the sun through the shade.	Views of the sun through mechoshades
It is dark when the shade drops. Sometimes it shouldn't drop, sometimes it isn't on time. It blocks the views of the River.	Darkness caused by dropped shades; Views blocked by shades
It is a shame to put anything on the views	Views blocked by shades
Mechoshades are OK. Sometimes they'll go down at 5 o'clock, like the night. They must take some readings somewhere in the buildings and decide to drop the shades. That doesn't seem to correlate with the actual lighting conditions. When the sun is right there, they'll go up and there'll be lighter.	Darkness caused by dropped shades; Fails to react on sunny days
Mechoshade helps, but a little bit delay; doesn't happen on time; or no reaction. The sun through the mechoshade catches my eyes.	Delayed operation; Fails to react on sunny days; Views of the sun through mechoshades
It is more relative to the control system. It needs fine tuning. It makes it darker, maybe on an overcast day. The control criteria are the trickiest.	Darkness caused by dropped shades
The shades don't work. Sometimes they go do when it is not that sunny. Sometimes they don't do much to block it when it is really sunny.	Darkness caused by dropped shades; Fails to react on sunny days;
The shade helps.	Mechoshades work
Sometimes the shade has no reaction	Fails to react on sunny days
Mechoshade helps a little, but it is still bright. I still have issues with sunlight through the shade.	Views of the sun through mechoshades
The blinds help a lot. They make a big difference.	Mechoshades work
Sometimes it doesn't work on days, or it doesn't go low enough. It is bothering when they move down a foot. Then 15 minutes later, they move down a foot again. It is kind of nice if they just brought it down like half way and full way. When the sun comes out, so it goes back up. Why don't you just stay down. It'll be better if we move it VS its automatically moving down.	Not low enough to block sunlight; Unexpected movements
Without any issue. It is not something I will complain about.	Mechoshades work
It is either too bright or too dark. The timing on the mechoshade just doesn't seem accurate.	Darkness caused by dropped shades; Fails to react on sunny days
The screen, the mesh we have that coming down, is not effective when a particular condition is present. If anything, I would need, to be a black out curtain that would come down. It is funny, running bit of humor between the meter raised mechoshades, moving up and down. That's like all the sudden they go down.	Views of the sun or sunlight through mechoshades; Unexpected movements
Don't know how to predict the mechoshade; sometimes it doesn't react to direct sunlight; Once the shade is down, it is also dark. It is gloomy.	Unexpected movements; Delayed operation; Darkness caused by dropped shades
Mechoshade helps when it is down, but it doesn't catch sunlight on time.	Delayed operation

CURRICULUM VITAE

ZHE KONG

PhD (c) kongzhewode@gmail.com

Education

Ph.D. in Sustainability, Resources and Technology

September 2011 – August 2018 — University of Wisconsin-Milwaukee, School of Architecture and Urban Planning
Advisor: D. Michael Utzinger

Master of Architecture

September 2009 – January 2011 — Harbin Institute of Technology, China, School of Architecture
Advisor: Xiaopeng Bai, Yu Shao
Master Thesis: The Maternity Hospital Design Strategies under New Healthy Concept

Bachelor of Architecture

September 2004 – July 2009 — Harbin Institute of Technology, China, School of Architecture

Publications

Kong, Z., Utzinger, D.M., Humann, C., "Evaluation of a hybrid photo-radiometer sky model compared with the Perez sky model", Energy and Buildings, under the second revision

Kong, Z., Utzinger, D.M., Freihoefer, K., Steege, T., "The Impact of Interior Design on Visual Discomfort Reduction: A Field Study Integrating Lighting Environments with POE Survey", Building and Environment 138 (2018), pp. 135-148

Kong, Z. & Utzinger, D.M., "Solving Glare Problems in Architecture through Integration of HDRI Techniques and Modeling with DIVA", Building Simulation 2015, Proceedings of the 14th International Building Performance Simulation Association, 1213-1220.

Jin, H., Li, X., Kang, J., & **Kong, Z**., "An Evaluation of the Lighting Environment in the Public Space of Shopping Centers", Building and Environment 115 (2017), pp. 228-235

Sun, C., Liu, L. & **Kong, Z.** "Simplified Lighting Energy Consumption Prediction Model of Office Buildings in Northeast Severe Cold Region of China", Building Simulation 2015, Proceedings of the 14th International Building Performance Simulation Association, 1221-1228

Kong, Z. & Bai, X. "The Influence Analysis upon Environmental Pressure Perception due to Different Behavior Competence", Environment-Behavior Research Association, Proceedings of the 9th International Symposium on Environment-behavior Research, EBRA 2010

Kong, Z., Su, R. & Bai, X. "The Convert Mode of Long-span Public Buildings Function Response to Disaster", International Disaster and Risk Conference, IDRC DAVOS 2010

Presentation

HGA Daylighting Evaluation Presentation

July 2017 "Comprehensive Evaluations of Daylighting Environments in the HGA Milwaukee Office"
Milwaukee, WI, USA

ShenZhou Forum of International Young Scholars

December 2016 ''Illumination Design and Simulation of Architecture - Visual Discomfort Evaluation under Daylighting Environments''
Harbin Institute of Technology, Harbin, China

IES Annual Conference 2016

October 2016 ''Compare CIE Sky Models and Perez Sky Models to HDR Images in Vertical Luminance Modeling''
Orlando, Florida, USA

SBSE Retreat 2015

June 2015 ''A Replicable Method of Renovating Buildings to Reduce Glare''
Highlands, North Carolina, USA

IES Annual Conference 2015

November 2015 ''Comparing Point-in-Time and Annual DGP Glare Estimates''
Indianapolis, Indiana, USA

Teaching

Adjunct Faculty

Fall 2016 Arch. 520 Environmental system: Illumination & thermal comfort

Teaching Assistant

Fall 2014 Arch. 520 Environmental system: Illumination & thermal comfort
Fall 2013 Arch. 303 Architecture environmental response
Spring 2013 Arch. 302 Architecture & human behavior
Fall 2012 Arch. 303 Architecture environmental response
Spring 2012 Arch. 303 Architecture environmental response
Fall 2011 Arch. 301 Architecture structures & construction

Experience

Postdoctoral Research Fellow

August 2017 – December 2018 Architecture and Sustainable Design, Singapore University of Technology and Design, Singapore

Research Intern

March 2017 – July 2017 Hammel Green & Abrahamson Inc, Milwaukee, WI

Design Detailer

September 2015 – May 2016 Midwest Structure Engineering, Milwaukee, WI

Architectural Intern

January 2011 – February 2011 Werkhart International, Beijing, China

Architectural Intern

December 2008 – March 2009 Urban Development and Landscape Architecture Institute, Harbin, China

Architectural Intern

July 2008 – October 2008 SiFang Construction Engineering Design AC Demydn, Harbin, China

Professional Organizations

Student Membership Illuminating Engineering Society (IES)

Awards

Young Professionals Scholarship Recipient
November 2015 Illuminating Engineering Society
Gaylord Nelson/Moebius Award
Fall 2014 School of Architecture and Urban Planning, University of Wisconsin Milwaukee
Scholarship under China Scholarship Council
August 2011 China Scholarship Council
Nan Bo Second-class Scholarship
October 2010 Harbin Institute of Technology, Harbin, China
Special Grade Scholarship, Ranked first in Architectural Graduate Students
Fall 2010 School of Architecture, Harbin Institute of Technology, Harbin, China
Fall 2009 School of Architecture, Harbin Institute of Technology, Harbin, China
Excellent Graduate
Spring 2009 School of Architecture, Harbin Institute of Technology, Harbin, China
First-class of National Scholarship
Fall 2008 School of Architecture, Harbin Institute of Technology, Harbin, China

Reference

The University of Wisconsin Milwaukee	**D. Michael Utzinger, AIA – Associate Professor** utzinger@uwm.edu, (414)229-6073
The University of Wisconsin Milwaukee	**Brian Schermer, Associate Professor** bscherm@uwm.edu, (414)229-3815
Singapore University of Technology and Design	**J. Alstan Jakubiec, Assistant Professor** john_jakubiec@sutd.edu.sg, +65 6499 4530